Post Polymerization Modification of Poly(vinyl amine) with Functional Epoxides: Multifunctional, Antimicrobial, Protein-like Polymers

Von der Fakultät für Mathematik, Informatik und Naturwissenschaften
der RWTH Aachen University zur Erlangung des akademischen Grades einer
Doktorin der Naturwissenschaften genehmigte Dissertation

vorgelegt von

Diplom-Chemikerin, Diplom-Wirtschaftschemikerin

Angela Schmalen, geb. Plum

aus Aachen

Berichter: Universitätsprofessor Dr. Dr. h. c. Martin Möller

Universitätsprofessor Dr. Andrij Pich

Tag der mündlichen Prüfung: 02.09.2014

ACKNOWLEDGMENT

The present work was carried out at the Institute of Technical and Macromolecular Chemistry and the DWI - Leibniz-Institut für Interaktive Materialien at RWTH Aachen University under the supervision of Prof. Dr. Martin Möller. I would like to take the opportunity to thank the people who contributed to the success of this work.

At first, I want to thank Prof. Dr. Martin Möller for giving me the opportunity to be part of his research group and for giving me a large freedom in the organization of my work.

I am deeply grateful to Dr. Helmut Keul for his never ending scientific support, the many discussions we had and the critical revision of this thesis. I enjoyed being part of his group.

Additionally, I had the opportunity to collaborate with Dr. Elisabeth Heine and I want to thank her for the critical revision of parts of this thesis, and together with her co-workers for carrying out the antimicrobial and hemolytic tests, as well as the permeabilization experiments and their constant willingness to discuss the obtained results.

During my PhD I had the chance to be part of the EU project *Nanobond*. I would like to thank all co-operation partners for the fruitful collaborations and for sharing their ideas with me. Especially, I would like to thank Prof. Dr. Éva Kiss and her co-workers for carrying out the Langmuir film experiments.

I have to thank Rainer Haas for his constant cooperativeness and help regarding any question or technical problem. Many thanks also to my research students Bianca Stöckel and Janine Broda who contributed to this work.

Many thanks go to my lab mates Marc Hans, Sascha Pargen, Michael Scharpf, and Jens Köhler and all the other people from AK Keul and DWI for providing an enjoyable atmosphere and a pleasant working environment and for all the interesting discussions we had. Thinking about other colleagues at the DWI and ITMC, many thanks go also to Alex, Anika, Dragos, Huihui, Kalle, Marc, Melanie, and Ramona for many great hours inside and outside the institute.

Finally, special thanks belong to my parents, my sister, my brother, and the rest of my family for their never-ending support over the years. Dear Laurent, thank you for all your love, support and constant patience.

KURZFASSUNG

Durch die zunehmende Resistenz von Bakterien gegenüber gebräuchlichen antimikrobiellen Mitteln besteht ein erheblicher Bedarf an neuen antimikrobiellen Wirkstoffen. In diesem Zusammenhang befasst sich die vorliegende Arbeit mit der Herstellung und Charakterisierung neuartiger multifunktioneller Poly(vinyl amine). Poly(vinyl amin) wurde erfolgreich mit quaternären Ammoniumgruppen und Alkylgruppen funktionalisiert, mit dem Ziel, natürliche antimikrobielle Peptide nachzuahmen und so Zugang zu neuen antimikrobiellen Substanzen zu erhalten. Als vielseitiger Ansatz um hydrophile und hydrophobe Reste in das Polymer einzubringen, wurde die polymeranaloge Reaktion mit funktionellen Epoxiden gewählt. Der Funktionalisierungsgrad kann über das Verhältnis von funktionellen Epoxiden zu Aminogruppen einfach eingestellt werden, wodurch eine Vielzahl an unterschiedlichen Polymeren herstellbar ist. Die neuen multifunktionellen Poly(vinyl amine) wurden mit Hinblick auf den Einfluss der hydrophilen/hydrophoben Balance auf verschiedenste Eigenschaften in Lösung und als Oberflächenbeschichtung charakterisiert. Der Einfluss der hydrophilen/hydrophoben Balance auf die antimikrobielle Wirksamkeit, die kritische Aggregationskonzentration und die Fähigkeit, in Membranmodelle einzudringen, wurde untersucht. In funktionellen Polymeren mit gleicher chemischer Zusammensetzung und gleichem Molekulargewicht wurden erfolgreich unterschiedliche Mikrostrukturen erzeugt. Der Einfluss dieser Mikrostrukturen wurde auf die oben genannten Eigenschaften und zusätzlich auf die Viskosität, die Fähigkeit in die äußere/innere Membran von *E. coli* einzudringen und die hämolytische Wirksamkeit der Polymere, untersucht. Die erhaltenen multifunktionellen Polymere lassen sich z.B. als antimikrobielle Mittel für Oberflächenbeschichtungen oder Textilausrüstungen einsetzen.

ABSTRACT

The increasing resistance of bacteria towards common antimicrobial agents causes a significant need for new antimicrobial compounds. In this context, the present thesis deals with the preparation and characterization of novel multifunctional poly(vinyl amine)s. Poly(vinyl amine) was successfully functionalized with quaternary ammonium groups and alkyl groups with the goal to mimic natural antimicrobial peptides and give access to novel antimicrobial agents. The post polymerization modification with functional epoxides was chosen as a versatile approach to introduce hydrophobic and hydrophilic functionalities into the polymer. The degree of functionalization can easily be adjusted by the ratio of functional epoxides to amine groups giving access to a high variety of polymers. The novel multifunctional poly(vinyl amine)s were characterized in detail with regard to the influence of the hydrophilic/hydrophobic balance on several properties in aqueous solution and coated on surfaces. The influence of the hydrophilic/hydrophobic balance on the antimicrobial activity, the critical aggregation concentration, and the penetration ability into model membranes was thoroughly investigated. Different microstructures were successfully introduced into functional polymers having an identical chemical composition and molecular weight. The influence of these microstructures on the antimicrobial effect, the critical aggregation concentration, the viscosity, the ability to penetrate into a model DPPC membrane, the ability to penetrate into the outer/inner membrane of *E. coli*, and the hemolytic activity of the polymers was determined. The resulting multifunctional polymers can, e.g., be used as antimicrobial agents for surface coatings or textile finishings.

CONTENTS

ABBREVIATIONS

a. D.	after dialysis
AFM	atomic force microscopy
aq.	aqueous
br	broad
°C	degree Celsius
CAC	critical aggregation concentration
cf.	confer
cfu	colony forming unit
cm	centimeter
d	days
DH	degree of hydrolysis
dist.	distilled
DNA	deoxyribonucleic acid
DOW	superwetting agent Q2-5211 from DOW Chemicals
DPPC	dipalmitoylphosphatidylcholine
DPPG	dipalmitoylphosphatidylglycerol
DSMZ	Deutsche Sammlung von Mikroorganismen und Zellkulturen
EA8	1,2-epoxyoctane
EA10	1,2-epoxydecane
EA12	1,2-epoxydodecane

EA14	1,2-epoxytetradecane
EA16	1,2-epoxyhexadecane
EA18	1,2-epoxyoctadecane
EC	effective concentration
e.g.	for example
EG	ethyleneglycole
EQ	glycidyltrimethylammonium chloride
eq	equivalents
et al.	et alii (and others)
etc.	et cetera
g	gram
GPC	gel permeation chromatography
h	hour
kDa	kilodalton
L	liter
$\overline{M}$	averaged molecular weight of the repeating units calculated from the ^{1}H NMR spectrum
M	molar mass
m	multiplet
m	meter
mbar	millibar
meq	milliequivalents
mg	milligram
MHz	megahertz
MIC	minimum inhibitory concentration

min	minutes
mL	milliliter
mm	millimeter
mN	millinewton
MP	membrane permeabilization of *E. coli*
MW	molecular weight
mW	milliwatt
NL1	nutrient solution
NMR	nuclear magnetic resonance
nm	nanometer
NVF	N-vinyl formamide
OD	optical density
ONP	*o*-nitrophenol
ONPG	o-nitrophenyl-β-D-galactopyranosid
p. a.	pro analysi
PAM	poly(acrylamide)
PBS	phosphate-buffered saline
PEI	poly(ethylene imine)
PNVF	poly(N-vinyl formamide)
POM	polyoxymethylene
ppm	parts per million
PVAm	poly(vinyl amine)
RBC	red blood cells
Rh	Rhesus factor
rH	relative humidity

RNA	ribonucleic acid
rpm	revolutions per minute
RT	room temperature
s	singlet
sec	seconds
sf	salt free
t	time
THF	tetrahydrofuran
wt%	weight percent
µL	microliter
µS	microsiemens

CHAPTER 1

INTRODUCTION

The antimicrobial resistance of bacteria towards antibiotics increased dramatically in the last decades and the number of new antibiotic approvals is declining.[1,2,3,4,5,6,7,8] Therefore, the development of new antimicrobially active agents which are not prone to resistance mechanisms is of high interest.[9,10] In this context, the focus of research activities since the 1980s has been on host defense peptides and synthetic polymer disinfectants, two classes of novel antimicrobials.[9] Host defense peptides are very effective antimicrobial agents. They act as broad-spectrum, fast-killing antibiotics and are not sensible to bacterial resistances.[11] However, they have the drawback of high manufacturing cost, susceptibility to proteolysis, and poorly understood pharmacokinetics hindering their application.[12] In contrast, synthetic polymeric antimicrobials have the advantage of low manufacturing cost, large-scale synthesis, and diversity of synthesizable chemical structures. And as opposed to low molecular weight agents, antimicrobial polymers have the advantage that the formation of antimicrobial resistances is unlikely due to their mode of action.[13] Furthermore, antimicrobial polymers possess a higher efficiency against bacteria in comparison to their monomeric equivalents.[14] However, the drawback of polymeric antimicrobial materials is that they are often toxic to human cells[15] or the toxicities are not well studied.

The combination of the design principles of host defense peptides with the simple and inexpensive methods of polymer science can combine the advantages of both fields and thereby give access to affordable and biocompatible antimicrobials.[9,16] A lot of research is currently going on to obtain peptide-mimicking antimicrobial polymers with potent

antimicrobial activities and minimal or no hemolytic activity by optimization of the polymeric structure.[9,17,18,19,20,21,22,23,24,25,26,27,28,29] Peptides containing cationic and hydrophobic amino acid residues are known to be antimicrobially active.[9] However, the antimicrobial mode of action is not completely understood to this date and several models for the antimicrobial interaction have been proposed.[9,27,30,31,32,33,34,35] The investigation of structure-properties relations in polymers bearing cationic and hydrophobic groups is therefore of interest to gain insights in the mode of operation of antimicrobial agents.

This thesis deals with the preparation and characterization of multifunctional, antimicrobial, protein-like polymers. Poly(vinyl amine) was functionalized with quaternary ammonium groups and alkyl groups with the goal to mimic natural antimicrobial peptides and to give access to novel antimicrobial agents. The post polymerization modification with functional epoxides was chosen as a versatile approach to introduce hydrophobic and hydrophilic functionalities into the polymer. The influence of the hydrophilic/hydrophobic balance on several polymer properties in aqueous solution and coated on surfaces was studied. Furthermore, the formation of different microstructures within polymers having an identical chemical composition and molecular weight and the effect of these microstructures on different polymer properties were investigated.

1.1 Poly(vinyl amine)

1.1.1 Synthesis

Poly(vinyl amine) (PVAm) is a linear, weak, cationic polyelectrolyte. The direct polymerization of vinylamine as a precursor to PVAm is not possible, due to the enamine-imine tautomerism (Scheme 1)[36].

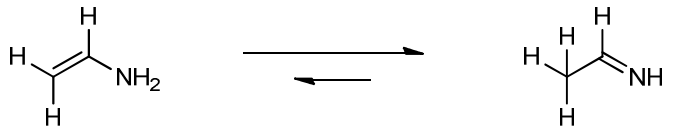

vinylamine (enamine) ethylidenamine (imin)

Scheme 1. Schematic illustration of the enamine-imine tautomerism of vinylamine.

Therefore it is only possible to prepare poly(vinyl amine) indirectly via post polymerization modification. Several routes of synthesis have been developed since the 1940's. Already in 1944 Jones *et al.* prepared poly(vinyl amine) as a side product in a reaction of ethanol amine, phthalic anhydride, and acetic anhydride. Further syntheses wherein N-substituted monomers are polymerized and afterwards hydrolyzed to give PVAm are known[36,37,38,39,40,41,42,43,44,45]. Some examples are given in Scheme 2. Modifications as shown in Scheme 2 are always complicated and expensive, because several steps are required to obtain the final pure product. Another disadvantage of such syntheses is the need for drastic reaction conditions for the hydrolysis of poly(N-vinyl amide)s (e.g. reaction under acidic conditions with excess of hydrochloric acid or under basic conditions at high temperatures).

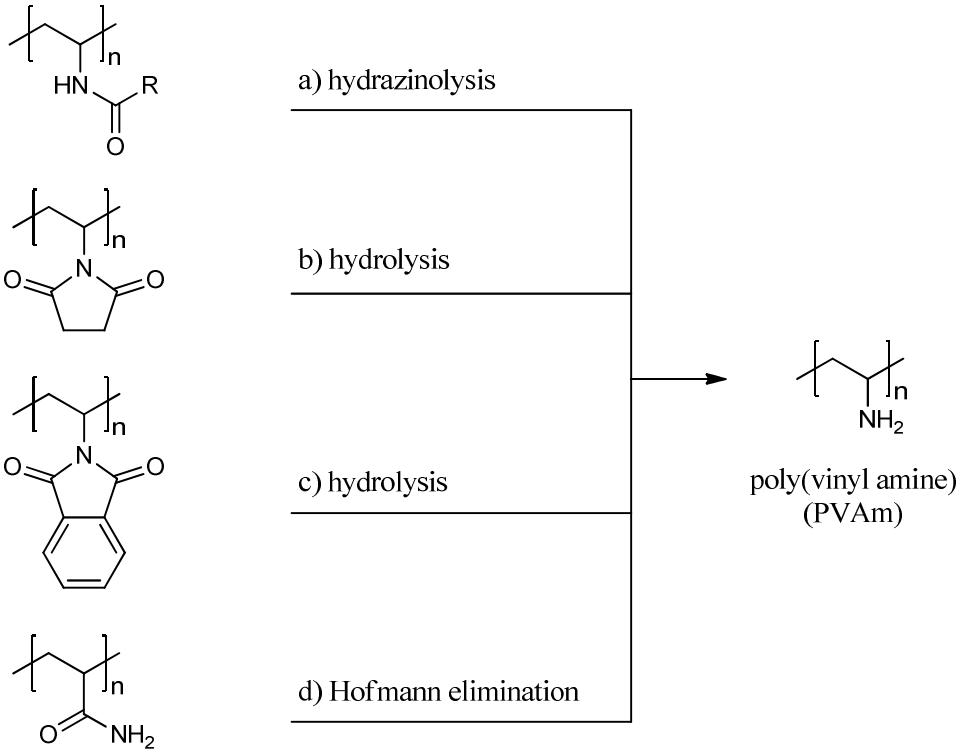

Scheme 2. Synthesis of poly(vinyl amine) by post polymerization modification. a) hydrazinolysis of poly(*N*-vinyl carboxamide)s[42,43,44,45], b) hydrolysis of poly(*N*-vinyl succinimide)[39], c) hydrolysis of poly(*N*-vinyl phthalimide)[39,40], d) Hofmann elimination of poly(acrylamide)[41].

N-Vinylformamide (NVF) was developed as a precursor to PVAm to allow a simple, economic synthesis. It has been commercially available since 1999. NVF as a precursor to high molecular weight polyamides and polyamines shows a high reactivity both in radical polymerization and copolymerization as well as in the hydrolysis of the amide groups. The first successful synthesis of NVF has been carried out more than 40 years ago[46]. Since that time, several synthesis routes to NVF have been reported[47]. One route developed in 1993 starts with two simple chemicals (acetaldehyde and formamide) to prepare ethylideneformamide, a precursor of NVF. After the condensation of acetaldehyde and

formamide to ethylidenformamide, the latter is isomerized to NVF through heating in presence of a catalyst[48] (Scheme 3).

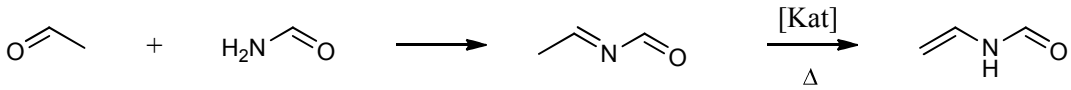

acetaldehyde formamide ethylidenformamide *N*-vinylformamide

Scheme 3. Synthesis of *N*-vinylformamide (NVF).

This synthesis route is commercially attractive and renewed the industrial and academic interest in NVF and its polymers. Poly(*N*-vinyl formamide) (PNVF) is prepared by radical polymerization using oil- or water-soluble azocompounds as initiatior. It is attractive due to its low toxicity. Functional polyelectrolytes with high molecular weight are easily obtained. Because of these reasons, PNVF possesses great potential to replace poly(acrylamide) (PAM) in many applications. Poly(acrylamide) and poly(N-vinyl formamide) are structural isomers with similar properties (Scheme 4).

PNVF PAM

Scheme 4. Structures of poly(*N*-vinyl formamide) (PNVF) and poly(acrylamide) (PAM).

Poly(*N*-vinyl formamide) can easily be hydrolyzed to PVAm under moderate conditions both in acidic and in basic solutions. Cationic polymers are available through acidic hydrolysis, whereas polymers with free amine groups are available through alkaline hydrolysis. Usually the alkaline hydrolysis is the more effective method with almost 100% conversion[49]. Acidic

hydrolysis only allows up to 80% conversion due to the electrostatic repulsion between ammonium groups and protons. One disadvantage of the basic hydrolysis with sodium hydroxide is the generation of sodium formate as byproduct. It has to be removed via dialysis or ultrafiltration. In contrast, the acidic hydrolysis in a methanol/water-mixture generates methylformate as byproduct, which can be removed by distillation. An alternative approach, which was developed in 1996, is the catalytic thermic hydrolysis[50]. The different synthetic routes to PVAm via alkaline and acidic hydrolysis of PNVF are shown in Scheme 5.

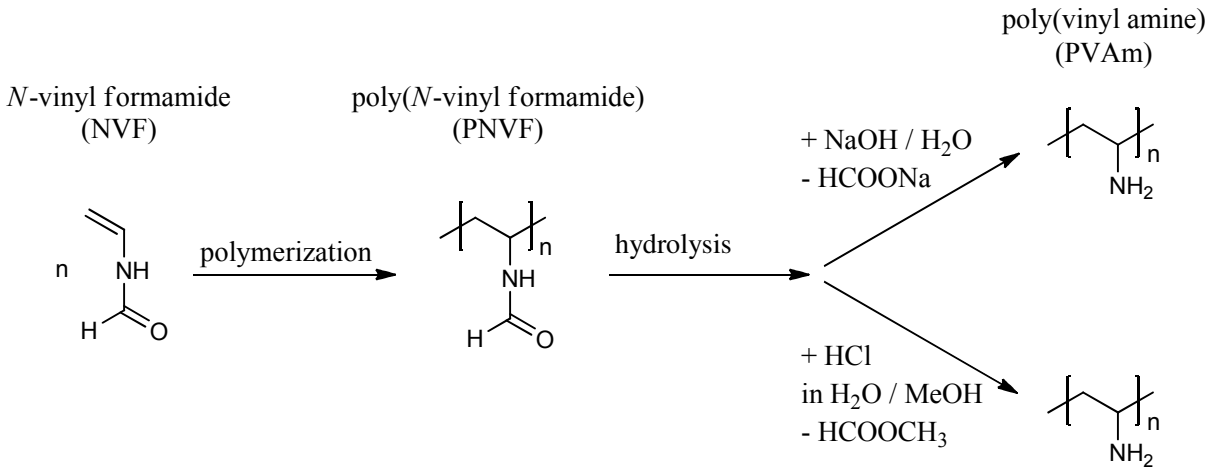

Scheme 5. Synthetic routes to poly(vinyl amine) (PVAm) starting with *N*-vinyl formamide (NVF).

The degree of hydrolysis and thereby the charge density of the polymer backbone can be adjusted by the choice of the hydrolysis conditions like temperature, reaction time, and concentration of the acid or the base[47,51,52,53,54,55]. PVAm is produced in industrial scale by BASF AG and is commercially available.

1.1.2 Solution Properties and Charge Density

Poly(vinyl amine) is a cationic polyelectrolyte and its primary amine groups are protonated under acidic conditions. The degree of dissociation of the ionic groups of PVAm and thereby the charge density along the polymer backbone is a function of the pH-value. This means PVAm is a weak polyelectrolyte. The difference in charge density with varying pH-value leads to a change in the conformation of the polymer chains (Scheme 6). Under strong basic conditions there are almost no protonated groups. The charge density along the polymer backbone is low and the conformation of the polymer is mainly coiled. With decreasing pH-value, more groups are protonated and due to the repulsion of the positive charges the coil conformation is expanded. Under strong acidic conditions, the polymer has an extended chain conformation due to the high charge density[56,57]. Besides the pH, the ionic strength of the solution largely influences the polymer conformation (Scheme 6). At low ionic strengths, the counter ions can shield the charges at the polymer backbone only insufficiently and the polymer has an extended chain conformation due to electrostatic repulsion. With increasing ionic strength, the ability of the counter ions to shield the charges increases and the conformation of the polymer becomes more and more coiled. The pH-value, salt-content, and degree of hydrolysis additionally influence the surface tension and viscosity of poly(vinyl amine) in aqueous systems[58,59].

Due to its positive charge, PVAm shows an excellent adhesion behaviour to glass[60] and metal surfaces as well as to negatively charged cellulose surfaces[61,62]. With 23 milliequivalents per gram (meq/g) polymer, it possesses the highest currently known charge density for a technical polymer. The highest practically as well as theoretically achievable charge density in a vinylogous polyamine can be found in poly(methylene amine). It was successfully prepared in laboratory scale at the Max-Planck-Institut in Mainz by radical polymerization of 1,3-diacetyl-1,4-imidazoline-2-one followed by hydrolysis[63] (Scheme 7).

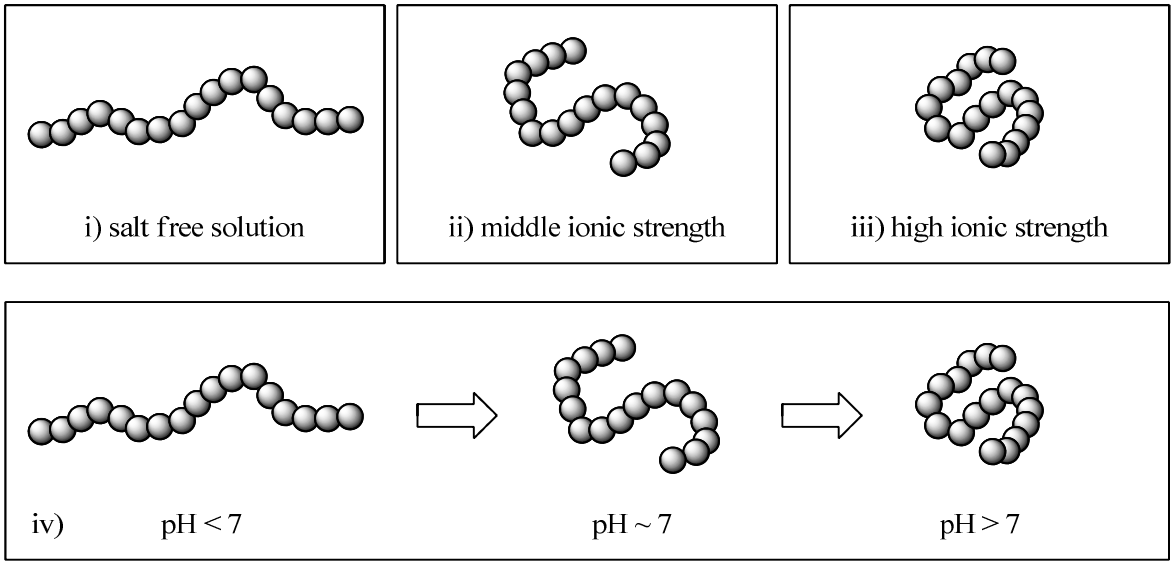

Scheme 6. Conformational changes of polyelectrolytes: i) in salt free solution with low ionic strength, ii) increasing salt concentration, middle ionic strength, iii) high salt concentration, high ionic strength, and iv) conformational change of weak cationic polyelectrolytes with increasing pH values.

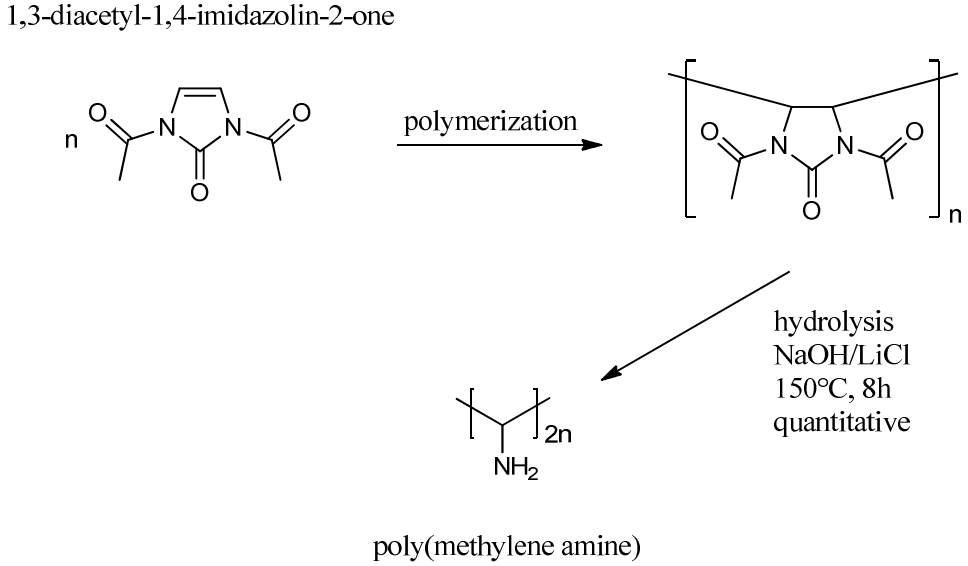

Scheme 7. Synthesis of poly(methylene amine) starting with 1,3-Diacetyl-1,4-imidazoline-2-one.

With increasing pH-values and decreasing degrees of hydrolysis, the charge density of PVAm also decreases. It is interesting to note that even at relatively high pH-values (8-9), there is a significant charge density of 6 meq/g[64]. Due to a pK_a value of 8.49, PVAm has still a relatively high degree of protonation, even at higher pH-values[65].

1.1.3 Reactions

Reactions of the primary amine groups of PVAm with electrophiles have been mentioned in several publications[66,67,68,69,70,64,71]. The theoretically possible reactions with typical electrophiles, like epoxides, anhydrides, isocyanates, etc., are shown in Scheme 8. With its free amine groups acting as Lewis bases, PVAm can complex heavy metal ions[72,73]. This fact is used during the polymerization of methyl methacrylate wherein a copper(II)-poly(vinyl amine) complex in the presence of sodiumsulfit is used as a catalyst for crosslinking[74]. High molecular weight PVAm is only soluble in very polar solvents like water, ethyleneglycole (EG), or methanol and mixtures thereof with THF. Therefore a later derivatization is interfered and mostly limited to reactants soluble in these solvents. Spange *et al.* successfully reacted PVAm with 4-fluoronitrobenzol and its derivatives, mediated by β-cyclodextrine[70]. They further derivatized PVAm such that it can be used in nanotechnology as a functional polyelectrolyte layer (thickness ca. 0.5 nm), e.g., as coating on silica gel particles. As a possible application, they propose the use of the resulting insoluble hybrid material as a biocompatible material for implants in medicine. Furthermore, PVAm was modified to yield polymer surfactants[75], and to mimic natural enzymes[88]. The aforementioned examples show that it is possible to synthesize tailor-made polymers from PVAm with various possible applications.

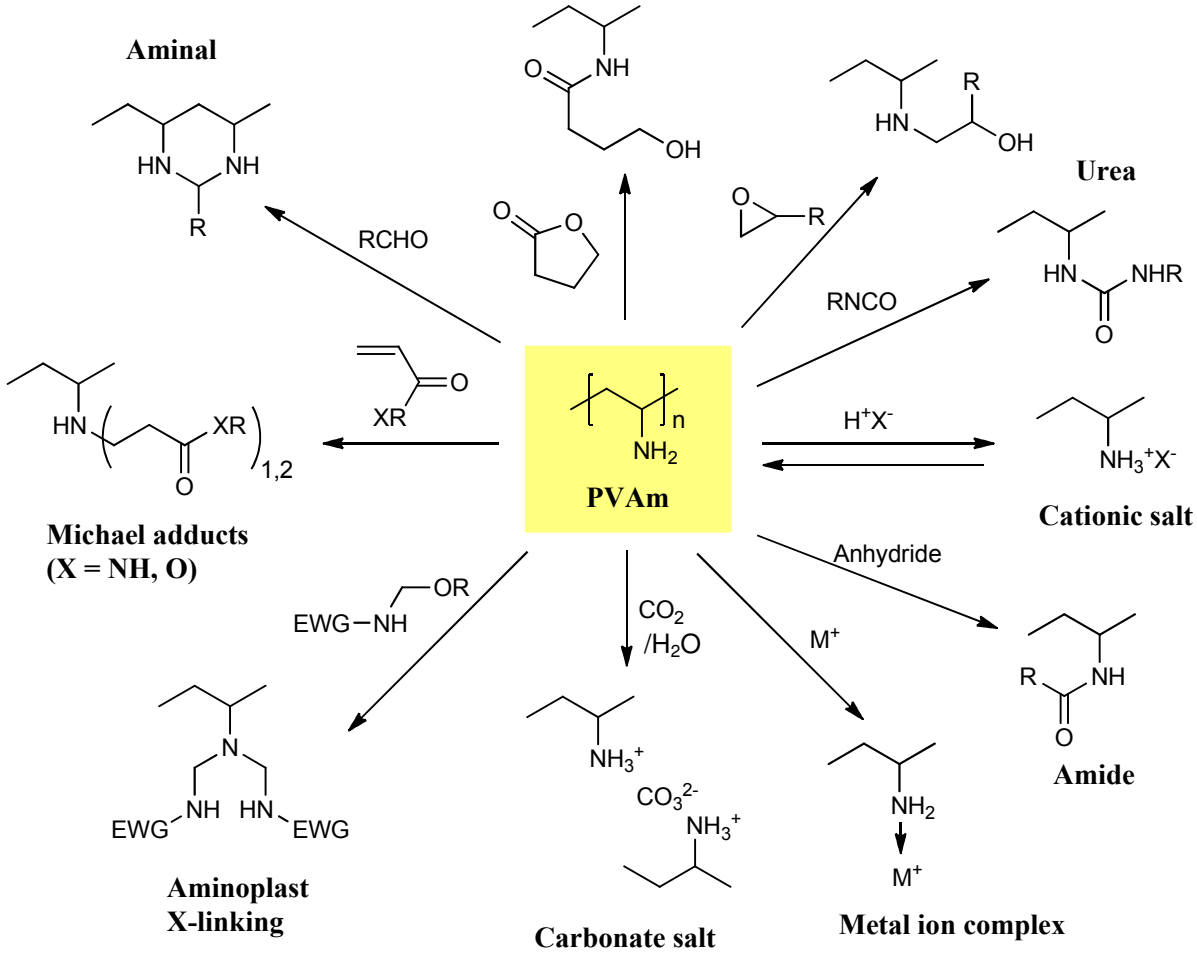

Scheme 8. Schematic illustration of possible post polymerization modifications of PVAm.[67] EWG = electron withdrawing group.

1.1.4 Fields of Application

One important field of application for poly(vinyl amine) and partly hydrolyzed poly(*N*-vinyl formamide) is the paper and pulp industry where it is used to improve the printability, fixation and retention of the paper[76,77,78]. Furthermore, PVAm is used as flocculant for wastewater treatment[79], in oil production[48,80,81,82,83,84,85] , as protective colloid for polymer dispersions[86,87], for catalysis[88] and chelation[65], and as super absorber[89,90,91,92]. Due to their high charge density, poly(vinyl amine)s are also suitable for surface modifications at higher pH values, e.g. hydrophilization, cationization, corrosion protection, or improvement of compatibility[93,94].

PVAm can be used as a non-viral gentransfer system in biological systems, in the same way as Chitosan. It builds a genvector-complex and infiltrates DNA into animal cells[95]. In this work, the possibility to react amines with epoxides is used for the post polymerization modification of PVAm.

1.2 Post Polymerization Modification

There are several approaches to synthesize functional polymers described in literature. These approaches follow one of the three main concepts: i) the direct copolymerization of functional monomers, ii) the copolymerization of protected monomers followed by selective deprotection, and iii) the post polymerization modification of reactive groups bearing polymers.[96]

The first two concepts show some disadvantages[96]: Concept i), the direct copolymerization of functional monomers, is still not possible for a broad range of side chain functionalities due to the occurrence of side reactions at these functionalities. Concept ii), the copolymerization of protected monomers followed by selective deprotection, needs an additional deprotection step. The difficulty with this deprotection step is that it may affect the structural integrity of the polymer backbone and, in addition, that it may not proceed quantitatively. In contrast to these two first concepts, Concept iii), the post polymerization modification of reactive groups bearing polymers, overcomes the aforementioned disadvantages.[96] It is possible to obtain excellent conversions under mild conditions, the reactions have got an excellent functional group tolerance, and they are orthogonal. Thereby it is possible to obtain polymers which cannot be prepared by direct polymerization of the corresponding functional monomers. Another exceptionally important point is the possibility to obtain a library of functional polymers. Taking one single reactive polymer precursor as starting material the resulting

functional polymers possess identical average chain length and chain length distributions and are thereby ideally suitable for studying structure-property relationships.

1.3 Bacteria Constitution and Antimicrobial Agents

The following sections closely follow the presentation of the topics given in reference 97 (bacteria composition) and 98 (antimicrobial agents). Bacteria belong to the group of prokaryotes and they appear with a wide range of shapes, from spheres to rods to spirals. Although one individual microbe is very small, their total amount and thereby their collective mass on earth is immense. They can be found almost everywhere where free liquid water is present. Their total biomass has been estimated to be nearly as large as that of all living plants, or even larger. Bacteria reproduce by cell division. In the laboratory, some bacteria can divide once every 20 minutes and others can divide even faster, but there are also some that divide more slowly, e.g., once every 24 hours (*Mycobacterium tuberculosis*). Despite the fact that the number of existing bacteria is so large, some diseases are caused by interacting with only very few of them.

The anatomy and the surface components of bacteria are adapted to their special needs and often determine whether an organism is able to survive in a particular environment or not. Bacteria have to face nutritionally varied conditions, withstand physical and chemical challenges, and often need the ability to attach to surfaces. The microbial cells are therefore surrounded by different envelope layers and bear appendages to protect the cell against hostile environments like, e.g., extreme osmolarity, harsh chemicals, and antibiotics.

Each bacterium is surrounded by a cell membrane which usually consists of a lipid bilayer. This membrane is the boundary between the cell interior and the environment. It consists of phospholipids and of more than 200 different kinds of proteins, which make up more than 70% of the mass of the membrane. Like all other membranes, the bacterial membrane is

sensitive to detergents and other amphipathic agents and it has to resist intracellular osmotic pressures. To protect the membrane, the bacteria surround it with tough, bag-like structures. These structures are different for the various kinds of bacteria. In general, one can divide between four main groups of bacteria: i) Gram positive, ii) Gram negative, iii) acid-fast, and iv) mycoplasmas. Most of the bacteria can be divided into Gram positive and Gram negative bacteria, whereof the Gram negative species appears in higher quantities. The name originates from an early Danish microbiologist (Hans Christian Joachim Gram), who developed a method to stain bacteria. The Gram positive bacteria can be stained and retain a complex of a purple dye (crystal violet) and iodine after a brief alcohol wash, whereas the Gram negative bacteria lose the complex and thereby the colour; afterwards they can be stained red (safranin). This different stainability shows the fundamental differences between the cellular envelopes of the two kinds of bacteria. In what follows, the cell structure of Gram positive and Gram negative bacteria is described in more detail. The acid fast and mycoplasmas cell structure will not be described in detail because only few bacteria belong to these groups.

1.3.1 Gram Positive Bacteria

To protect the cell membrane against osmotic pressure, Gram positive bacteria are surrounded by a thick cell wall (Scheme 9). This cell wall consists mainly of murein (Scheme 10), a peptidoglycan (complex polymer of sugars and amino acids). The murein builds several layers and is responsible for the bacteria's shape and rigidity. The phosphates, sugars (polysaccharides), and charged amino acids contained in the murein layers are highly polar and build a hydrophilic barrier to damaging hydrophobic agents. In addition, some other unique polymers like teichoic acids (chains of sugar alcohol) and lipoteichoic acids are linked to the cell wall by phosphodiester bonds.

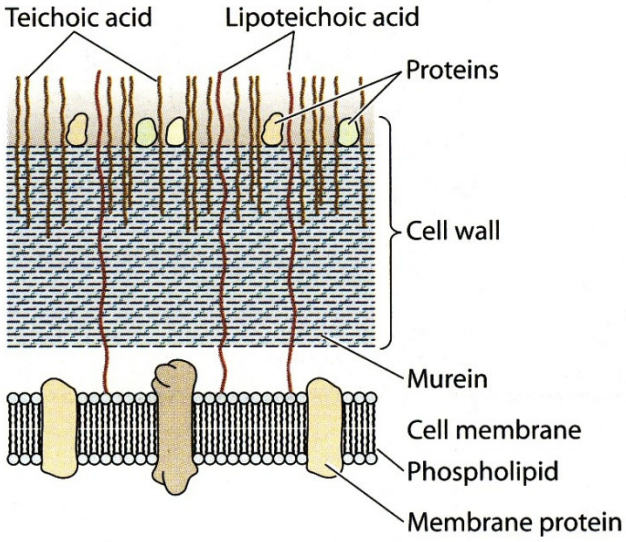

Scheme 9. Envelope of Gram positive bacteria (Picture from reference[97], ©2006 American Society for Microbiology. Used with permission. No further reproduction or distribution is permitted without the prior written permission of American Society for Microbiology).

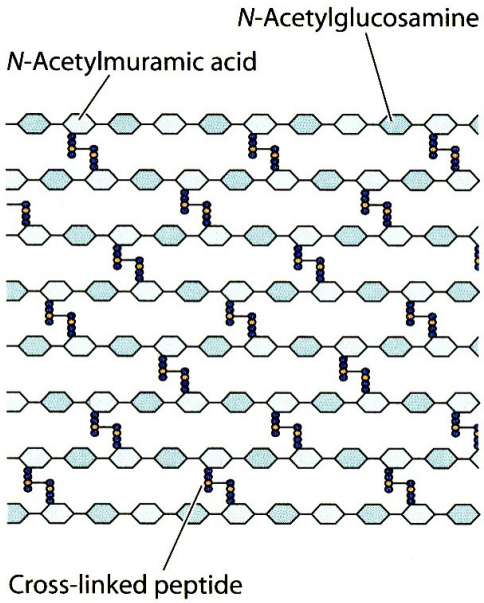

Scheme 10. Structure of murein (Picture from reference[97], ©2006 American Society for Microbiology. Used with permission. No further reproduction or distribution is permitted without the prior written permission of American Society for Microbiology).

1.3.2 Gram Negative Bacteria

Gram negative bacteria follow a different strategy to protect their cell membrane (Scheme 11). They only possess a thin cell wall of murein (Scheme 10). This thin layer is surrounded by an outer membrane protecting the cell agains harmful chemicals. This membrane has got a bilayered structure: its outer layer contains a lipopolysaccharide and its inner layer consists of phospholipids. The hydrophilic polysaccharides in the outer membrane build a hydrophilic barrier to hydrophobic agents like in the murein layer of Gram positive bacteria. To allow the transport of nutrients into the cell, the outer membrane contains special channel proteins (porins). The area between the outer and the inner membrane, which contains the thin murein layer, is called periplasm. Besides murein precursors and proteins that assist in the nutrition, it also contains enzymes which are active against antibiotics. Gram positive bacteria do not have a periplasm but they release similarly active enzymes into their environment.

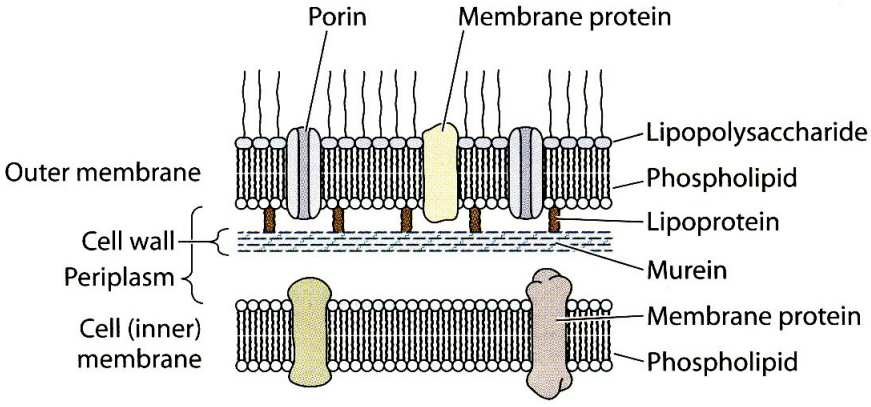

Scheme 11. Envelope of Gram negative bacteria (Picture from reference[97], ©2006 American Society for Microbiology. Used with permission. No further reproduction or distribution is permitted without the prior written permission of American Society for Microbiology).

In addition to the walls and membranes, some bacteria possess other external structures like capsules (for defense), flagella (enabling the cell to move actively), and pili (diverse functions, e.g. enabling the cell to attach to surfaces). These modifications are adaptions to special living conditions and vary from bacteria to bacteria.

1.3.3 Antimicrobial Interaction

Several theories and models exist in literature about how an antimicrobial polymer interacts with and how it kills bacteria. Bacterial cells carry negative charges on their surfaces with mostly bivalent ions like Mg^{2+} and Ca^{2+} as counter ions. The cell walls and the peptidoglycan layer (murein layer) of Gram positive bacteria contain teichoic acids and polysaccharides. The outer membranes of Gram negative bacteria as well as the cytoplasmic membranes (inner membranes) of both, Gram positive and Gram negative bacteria, contain anionic lipids like phosphatidylglycerol and its dimer. As a first step of interaction, all theories consistently describe the adsorption of the cationic antimicrobial agent onto the bacterial cell caused by electrostatic interaction. The subsequent steps leading to the destruction of the bacterium vary for the different theories.[99] Some theories explain the destruction of the bacteria cells by electrostatic interaction only, whereas others contain an active disruption of the bacterial cytoplasmic membrane by functional groups of the antimicrobial agent. This disruption leads to the death of the bacterium by leaching of intracellular components like K^+, PO_4^{3-}, DNA, RNA, and other cytoplasmic components from its interior.

1.3.4 Systems Acting by Electrostatic Interaction

The easiest theory described, e.g., by Chen *et al.*[99] is based on the idea that negatively charged lipids are extracted from the bacterial membrane and are bound to the cationic functionality of the antimicrobial agent. Hereby, the membrane is damaged and finally destroyed. Ikeda *et al.*

describe the same effect[100]. They analyzed polycationic substances with biguanidine hydrochloride groups and were able to show the formation of complexes with the anionic phosphatidylglycerol of the membrane. In contrast, no complexes with neutral lipids were built. According to the authors this complexation of anionic lipids leads to a destabilization and finally to the destruction of the membrane.

Another theory discusses the rearrangement of the anionic lipids within the bacterial membrane caused by the cationic antimicrobial agent. The lipids can freely move within (lateral diffusion) and in-between (transversal diffusion) the phospholipid bilayers of the membrane.[101] If the antimicrobial agent comes close to the bacterium, a rearrangement of the anionic lipids within the bacterial membrane is caused. The anionic lipids move towards the contrarily charged surface and neutral lipids replace them in the inner layer. This essentially disturbs the identification and the metabolism activities because these activities depend on the specific arrangement of the lipids. This causes the death of the bacterial cell[102].

1.3.5 Systems Acting by Active Disruption of the Bacterial Cytoplasmic Membrane by, e.g., Functional Groups of the Antimicrobial Agent

Besides the mechanisms based on electrostatic interaction, there is evidence for other mechanisms which include an active disruption of the cytoplasmic membrane as crucial step. The prerequisite for these mechanisms is that the active components of the antimicrobial agent reach the membrane. Franklin *et al.* proposed a concept consisting of six steps for such a mode of action in 1981.[103]

The six steps are:

1) Adsorption onto the bacterial cell due to electrostatic interaction.

2) Diffusion through the cell wall

3) Binding or rather adsorption to the cytoplasmic membrane

4) Disruption of the cytoplasmic membrane

5) Release of K^+ ions and other constituents of the cytoplasmic membrane

6) Death of the cell

By comparing monomeric and polymeric antimicrobial agents, the first difference in behaviour can be observed in the initial step. Here the adsorption of the polycation to the negatively charged bacterial cell takes place more strongly and to a greater extent than that of the monomeric agent. This is due to the higher charge density within the polycation. After a successful diffusion through the cell wall, the hydrophobic or lipophilic moieties of the antimicrobial agent bind to the cytoplasmic membrane and disrupt it. The longer/bigger the hydrophobic moieties are, the more hindered is the diffusion. A careful adjustment of the hydrophilic/hydrophobic balance is therefore of great importance.

1.3.6 Antimicrobial Surfaces

If the antimicrobial agent is bound to a surface, the chain length of the polymer is important for the activity. The chains need to have a certain length to be able to penetrate through the approximately 30 nm thick cell wall and to reach the cytoplasmic membrane.[104] Surface bound antimicrobial agents, so called contact systems, show some advantages: The agent is not released to the environment and thereby the concentration of the compound on the surface is constant. After one bacterium has been killed, the agent is not consumed and available for the next bacterium. Therefore, the surface has got an enduring activity against bacteria. A

drawback of contact systems is that destroyed bacteria and impurities from the surrounding medium can stick to the surface and contaminate it. The antimicrobial surface is then covert and not active against bacteria anymore. For this reason, the surfaces have to be regularly cleaned and have to be resistant to this cleaning step.

In this work, quaternary ammomium groups bearing polymers were developed. This kind of polymers is known to be more active against Gram positive bacteria than against Gram negative bacteria due to differences in the cell wall composition.[103] The developed polymers were tested both in solution and bound to surfaces for their antimicrobial activity.

1.4 Content of this Thesis

This thesis deals with the preparation and characterization of multifunctional, antimicrobial, protein-like poly(vinyl amine)s. The polymers were characterized with regard to the influence of the hydrophilic/hydrophobic balance on several properties in aqueous solution and coated on surfaces. The influence of different microstructures within polymers of the same chemical composition and molecular weight on these properties was investigated.

Chapter 1 (present block) gives an introduction on the used polymer poly(vinyl amine), the post polymerisation modification technique, as well as the constitution of bacteria and modes of action of antimicrobial agents.

Chapter 2 presents the synthesis of multifunctional polymers starting from poly(vinyl amine) by post polymerization modification with different functional epoxides to introduce quaternary ammonium groups and alkyl chains into the polymer. Kinetic studies and fractionation experiments to prove a homogenous modification were performed.

Chapter 3 deals with the ability of functional poly(vinyl amine)s to form micelle-like aggregates in aqueous solution. The critical aggregation concentrations were determined depending on the chain length and on the concentration of the introduced alkyl chains.

In **Chapter 4,** the antimicrobial activity of the developed polymers was determined in solution and coated on substrates. The influence of the hydrophilic/hydrophobic balance on the antimicrobial activity and on the ability to penetrate into lipid monolayers was studied.

Chapter 5 shows the synthesis of polymers with different microstructures but having the same chemical composition and molecular weight. The influence of the microstructures on different properties like antimicrobial effect, critical aggregation concentration, hemolytic activity, penetration ability into membranes, and viscosity was investigated. The effect of annealing on the antimicrobial activity of polymer coated surfaces was studied.

Appendix A provides the proliferation curves of *E. coli* after exposure on surfaces coated with the tested polymers, as supplementary material to Chapter 4.

1.6 Literature

[1] Infectious Diseases Society of America (IDSA), *Clin. Infect. Dis.* **2012**, *55* (*8*), 1031-1046.

[2] M. E. Falagas, I. A. Bliziotis, *Int. J. Antimicrob. Agents* **2007**, *29*, 630–636.

[3] M. E. Falagas, P. I. Rafailidis, D. K. Matthaiou, S. Virtzili, D. Nikita, A. Michalopoulos, *Int. J. Antimicrob. Agents* **2008**, *32*, 450–454.

[4] R. Valencia, L. A. Arroyo, M. Conde, *Infect. Control. Hosp. Epidemiol.* **2009**, *30*, 257–263.

[5] M. S. Hoffmann, M. R. Eber, R. Laxminarayan, *Infect. Control Hosp. Epidemiol.* **2010**, *31*, 196–197.

[6] M. D. Adams, G. C. Nickel, S. Bajaksouzian, *Antimicrob. Agents Chemother.* **2009**, *53*, 3628–3634.

[7] E. Lautenbach, M. Synnestvedt, M. G. Weiner, *Infect. Control Hosp. Epidemiol.* **2009**, *30*, 1186–1192.

[8] S. Navon-Venezia, A. Leavitt, Y. Carmeli, *J. Antimicrob. Chemother.* **2007**, *59*, 772–774.

[9] E. F. Palermo, K. Kuroda, *Appl Microbiol Biotechnol* **2010,** *87*, 1605–1615.

[10] H. W. Boucher, G. H. Talbot, J. S. Bradley, J. E. Edwards, D. Gilbert, L. B. Rice, M. Scheld, B. Spellberg, J. Bartlett, *Clin. Infect. Dis.* **2009**, *48*, 1–12.

[11] R. E. W. Hancock, R. Lehrer, *Trends Biotechnol.* **1998**, *16*, 82–88.

[12] A. K. Marr, W. J. Gooderham, R. E. W. Hancock, *Curr. Opin. Pharmacol.* **2006**, *6*, 468–472.

[13] A. Klibanov, *J. Mater. Chem.* **2007**, *17*, 2479–2482

[14] T. Tashiro, *Macromol. Mater. Eng*. **2001**, *286*, 63-87.

[15] M. A. Gelman, B. Weisblum, D. M. Lynn, S. H. Gellman, *Org. Lett.* **2004**, *6*, 557–560.

[16] G. J. Gabriel, A. Som, A. E. Madkour, T. Eren, G. N. Tew, *Mater. Sci. Eng. R. Rep.* **2007** *57*, 28–64.

[17] G. N. Tew, R. W. Scott, M. L. Klein, W. F. Degrado, *Acc. Chem. Res.* **2010** *43*, 30–39.

[18] C. Z. S. Chen, S. L. Cooper, *Adv Mater* **2000**, *12*, 843–846.

[19] M. F. Ilker, K. Nusslein, G. N. Tew, E. B. Coughlin, *J. Am. Chem. Soc.* **2004**, *126*, 15870–15875.

[20] K. Kuroda, G. A. Caputo, W. F. DeGrado, *Chem. Eur. J.* **2009**, *15*, 1123–1133.

[21] B. P. Mowery, S. E. Lee, D. A. Kissounko, R. F. Epand, R. M. Epand, B. Weisblum, S. S. Stahl, S. H. Gellman, *J. Am. Chem. Soc.* **2007**, *129*, 15474.

[22] B. P. Mowery, A. H. Lindner, B. Weisblum, S. S. Stahl, S. H. Gellman, *J. Am. Chem. Soc.* **2009**, *131*, 9735–9745.

[23] E. F. Palermo, K. Kuroda, *Biomacromolecules* **2009**, *10*, 1416–1428.

[24] E. F. Palermo, I. Sovadinova, K. Kuroda, *Biomacromolecules* **2009**, *10*, 3098–3107.

[25] P. H. Sellenet, B. Allison, B. M. Applegate, J. P. Youngblood, *Biomacromolecules* **2007**, *8*, 19–23.

[26] T. R. Stratton, J. L. Rickus, J. P. Youngblood, *Biomacromolecules* **2009**, *10*, 2550–2555.

[27] N. Pasquier, H. Keul, E. Heine, M. Moeller, B. Angelov, S. Linser, R. Willumeit, *Macromol. Biosci.* **2008**, *8*, 903–915.

[28] É. Kiss, E. T. Heine, K. Hill, Y-C. He, N. Keusgen, Cs. B. Pénzes, D. Schnöller, G. Gyulai, A. Mendrek, H. Keul, M. Möller, *Macromolecular Bioscience* **2012**, *12 (9)*, 1181–1189.

[29] Y. He, E. Heine, N. Keusgen, H. Keul, M. Möller, *Biomacromolecules* **2012**, *13* (*3*), 612–623.

[30] L. Silvestro, J. N. Weiser, P. H. Axelsen, *Antimicrob. Agents Chemother.* **2000**, *44* (*3*), 602–607.

[31] M. Zasloff, *Nature* **2002**, *415*, 389.

[32] O. Toke, L. Cegelski, J. Schaefer, *Biochim. Biophys. Acta* **2006**, *1758*, 1314.

[33] H. Sato, J. B. Feix, *Biochim. Biophys. Acta* **2006**, *1758*, 1245.

[34] Y. Shai, *Biopolymers* **2002**, *66*, 236.

[35] D. I. Chan, E. J. Prenner, H. J. Vogel, *Biochim. Biophys. Acta* **2006**, *1758*, 1184.

[36] *CD Römpp Chemielexikon, Version 1.0*, Georg Thieme Verlag, Stuttgart/New York **1995**.

[37] S. Zhang, J. Yang, Z. Hu, *Journal of Dalian University of Technology* 46, **2002**, 2, 659-662.

[38] E. Parzich, *GIT Labor-Fachzeitschrift* 2 **2005**, 133-135.

[39] W. E. Hanford, H. B. Stevenson, *Patent* **1944**, US 2365340.

[40] D. D. Reynolds, W. O. Kenyon, *J. Am. Chem. Soc.* **1947**, *69*, 911-915.

[41] H. J. Tanaka, *J. Polym. Sci. Part B* **1978**, 16, 87-89.

[42] D. J. Dawson, R. D. Gless, R. E. Wingard Jr., *J. Am. Chem. Soc.* **1976**, *98*, 5996–6000.

[43] R. W. Stackman, R. H. Summerville, *Ind. Eng. Chem. Prod. Res. Dev.* **1985**, *24*, 242–246.

[44] C. G. Overberger, S. J. Kikiyotani, *Polym. Sci. Chem. Ed.* **1983**, *21*, 525–540.

[45] D. J. Dawson, P. J. Brock, *Patent* **1983**, US 4393174.

[46] P. Kurtz, H. Disselnkoetter, *Patents* **1966**, DE 1228246 and DE 1224304.

[47] R. K. Pinschmidt Jr., D. J. Sagl, *Polymeric Materials Encyclopedia*; Ed.: Salamone, J. C.; CRC Press New York **1996**, 7095 ff.

[48] S. Stinson, *Chem. Eng. News* **1993**, 71 (36), 32.

[49] R. J. Badesso, R. K. Pinschmidt Jr., D. J. Sagl, *Proc. Am. Chem. Soc., Div. Polym. Mat. Sci. Eng.* **1993**, 69, 251.

R. J. Badesso, A. F. Nordquist, R. K. Pinschmidt Jr., D. J. Sagl, In: *Hydrophilic Polymers: Performance with Environmental Acceptance*; E. Glass, Ed.; American Chemical Society: Washington, D.C., **1995**; 489

[50] M. Ford, J. N. Armor, *Patent* **1996**, US 5491199.

[51] Technisches Merkblatt *N-Vinylformamid*, Mitsubishi Kasai, Japan, **1997**.

[52] L. Gu, S. Zhu, A. N. Hrymak, R. H. Pelton, *Polymer* **2001**, *42*, 3077–3086.

[53] L. Gu, S. Zhu, A. N. Hrymak, *J. Appl. Polym. Sci.* **2002**, *86*, 3412–3419.

[54] M. Kröner, J. Dupuis, M. Winter, *J. Prakt. Chem.* **2000**, *342*, 115–131.

[55] Produkt-Informationsbroschüre zu Lupaminen®, BASF AG, Ludwigshafen, **2000**.

[56] H.-G. Elias, *Makromoleküle: Struktur-Eigenschaften-Synthesen Stoffe*, 2. Edition., Hüthig & Wepf Verlag, Basel, Heidelberg **1972**, 271–275.

[57] L. J. Kirwan, G. Papastavrou, M. Borkovec, *Nano Lett.* **2004**, *4*, 149–152.

[58] R. Pelton, J. Hong, *Colloid Polymer Science 280* **2002**, 203-205.

[59] S. Zhang, J. Yang, Y. Chen, Z. Hu, *Journal of Applied Polymer Science 89* **2003**, 3889-3893.

[60] E. Poptoshev, M. W. Rutland, P. M. Claesson, *Langmuir* **2000**, *16*, 1987–1992.

[61] A. Shulga, J. Widmaier, E. Pefferkorn, S. Champ, H. Auweter, *Journal of Colloid and Interface Science* **2003**, 258, 219–227.

[62] A. Shulga, J. Widmaier, E. Pefferkorn, S. Champ, H. Auweter, *Journal of Colloid and Interface Science* **2003**, 258, 228–234.

[63] C. Hamaciuc, R. Dyllick-Brenzinger, K. Müllen, M. Klapper, *Angewandte Chemie* **2003**, 115, 4835-4838.

[64] Polyvinylamin, BASF AG, *Firmen-Information* **2004**.

[65] S. Kobayashi, K.-D. Suh, Y. Shirokura, *Macromolecules* **1989**, *22*, 2363.

[66] R. J. Badesso, A. F. Nordquist, R. K. Pinschmidt Jr., D. J. Sagl, *Adv. Chem. Ser.* **1996**, 248, 489-504.

[67] W. E. Caroll, N. Chen, J. Drescher, A. F. Nordquist, R. K. Pinschmidt Jr.; W. L. Renz, K. J. Yacoub, *Macromol. Sci., Pure Appl. Chem*. **1997**, A34, 1885 – 1905.

[68] I. Voigt, F. Simon, H. Komber, H. J. Jacobasch, S. Spange, *Colloid Polym. Sc*i. **2000**, *278*, 48-56.

[69] B. J. Haupt, J. Ennis, E. M. Sevick, *Langmuir* **1999**, *15*, 3886-3892.

[70] I. Roth, S. Spange, *Macromol. Rapid Commun*. **2001**, *22*, 1288-1291.

[71] W. Renz Jr., W. E. Carroll, K. Yacoub, J. Drescher, A. Nordquist, N. Cheng, R. K. Pinschmidt, *Pure Applied Chemistry A 34* **1997**, *10*, 1885-1905.

[72] G. V. Seguel, K. E. Geckeler, B. L. Rivas, *Angewandte Makromolekulare Chemie* **1997**, *251*, 97-106.

[73] A. Rether, Entwicklung und Charakterisierung wasserlöslicher Benzoylthioharnstoff-funktionalisierter Polymere zur selektiven Abtrennung von Schwermetallionen aus Abwässern und Prozesslösungen. In: *Dissertation*, München **2002**.

[74] Z. Zhang, X. Xuewei, L. Wang, X. Zhu, J. Lu, *Journal of Molecular Catalysis A: Chemical* **2004**, *207*, 204-214.

[75] Y. Qui, T. Zang, M. Ruegsegger, R. E. Marchant *Macromolecules* **1998**, *31*, 165–171.

[76] F. Linhart, W. Auhorn, *Das Papier* **1992**, *10A*, V38–V45.

[77] U. Riebeling, A. De Clercq, A. Stange, N. Sendhoff, C. Nilz, M. Kröner, *Patent* **1993**, EP 553135.

[78] F. Wang, H. Tanaka *J. Appl. Polym. Sci.* **2000**, *78*, 1805–1810.

[79] F. Brunnmueller, R. Schneider, M. Kroener, H. Mueller, F. Linhart, H. Burkert, K.-H. Beyer, Patent **1982**, EP 071050.

[80] R. K Pinschmidt Jr, B. R. Vijayendran, Ta.-W. Lai, *Patent* **1992**, US 5085787.

[81] Jr. R.K. Pinschmidt, T. Lai, *Patent* **1990**, US 4931194.

[82] P. Shu, *Patent* **1992**, US 5134*17*6.

[83] D. Monech, H. Hartmann, E. Freudenberg, A. Stange, *Patent* **1993**, US 5262008; W. Auhorn, F. Linhart, P. Lorencak, M. Kroener, N. Sendhoff, W. Deninger, H. Hartmann, *Patent* **1992**, US 5145559; S. Pfohl, M. Kroener, H. Hartmann, W. Denzinger, *Patents* **1989**, US 4978427, US 4880497 and **1988**, US 4774285.

[84] H. Burkert, F. Brunnmueller, K. Beyer, M. Kroener, H. Mueller, *Patent* **1984**, US 4444667.

[85] D. Monech, H. Hartmann, K. Buechner, *Patent* **1993**, US 5225088.

[86] W. E. Lenney, D. Sagl, *Patent* **1995**, US 5470903.

[87] I. Cabrera, *Patent* **1997**, EP 894809.

[88] B. Martel, A. Pollet, M. Morcellet, *Macromolecules* **1994**, *27*, 5258–5262.

[89] T. Beihoffer, M. Mitchell, L. T. Truzpek, J. W. Darlington, M. Anderson, *Patent* **2001**, US 6194631.

[90] T. Beihoffer, M. Mitchell, J. W. Darlington, M. Anderson, *Patent* **1997**, WO 99/25745.

[91] T. Beihoffer, M. Mitchell, *Patent* **2000**, US 6159591.

[92] T. Beihoffer, M. Mitchell, *Patent* **2001**, US 6235965.

[93] H. Keller, G. Hoffmann, W. Denzinger, R. Fässler, *Patent* **1994**, EP 672467.

[94] A. Schrell, B. Huber, *Patent* **1994**, EP 692559.

[95] S. Gersting, Einfluss Extrazellulärer Faktoren auf Struktur und Funktion viraler Genvektoren. In: *Dissertation*, Ludwig-Maximilians-Universität München **2003**.

[96] M. A. Gauthier, M. I. Gibson, H-A. Klok, *Angew. Chem. Int. Ed.* **2009**, *48*, 48-58.

[97] M. Schaechter, J. L. Ingraham, F. C. Neidhardt, *Microbe – Das Original mit Übersetzungshilfen*, 1. Ed., Elsevier GmbH, München, **2007**, 3ff.

[98] A. M. Bieser, Oberflächenmodifizierung durch Hydrogelierung und durch Beschichtung mit antimikrobiellen Cellulosederivaten. In: *Dissertation*, Freiburg im Breisgau **2007**.

[99] C.Z. Chen, S. L. Cooper, *Biomaterials* **2002**, *23*, 3359-3368.

[100] T. Ikeda, S. Tazuke, M. Watanabe, *Biochim. Biophys. Acta* **1983**, *735*, 380.

[101] S. J. Singer, G. L. Nicolson, *Science* **1972**, *175*, 720.

[102] A. A. Yaroslavov, N. S. Melik-Nubarov, F. M. Menger, *Acc. Chem. Res*., **2006**, *39*, 702.

[103] T. Tashiro, *Macromol. Mater. Eng.* **2001**, *286*, 63-87.

With reference to: T. J. Franklin, G. A. Snow, Eds., *"Biochemistry of Antimicrobial Action, Antiseptics, Antibiotics, and the Cell Membrane"*, Chapman & Hall, Ltd., London **1981**, p. 58–78.

[104] J. C. Tiller, C-J. Liao, K. Lewis, A. M. Klibanov *Proc. Nat. Acad. Sci. U.S.A.* **2001**, *98*, 5981.

CHAPTER 2

SYNTHESIS OF AMPHIPHILIC POLYMERS FROM POLY(VINYL AMINE)

2.1 Introduction

Functional polymers are a field of increasing interest in polymer chemistry and several approaches for their synthesis have been developed: i) direct copolymerization of functional monomers, ii) copolymerization of protected monomers followed by selective deprotection, and iii) post polymerization modification of polymers bearing reactive groups.[1] Although new controlled "living" radical polymerization techniques have been developed and there have been advances in catalytic polymerization expanding the functional group tolerance, the direct copolymerization of functional monomers is still not possible for a broad range of side chain functionalities.[1] The copolymerization of protected monomers has the disadvantage of an additional deprotection step which may affect the structural integrity of the polymer backbone and which may not proceed quantitatively in addition. In contrast, the post polymerization modification (also called polymer analogous reaction) is a very attractive approach to synthesize functional polymers. It overcomes the limited functional group tolerance of many controlled "living" polymerization techniques.[1] In a first step, monomers with functional and reactive groups that are inert towards the polymerization conditions are polymerized. In the second step, the conversion of the reactive side groups with suitable reagents leads to new functionalities. The main advantages of the post polymerization modification are excellent conversions under mild conditions, the excellent functional group tolerance and the orthogonality of the reactions. The post polymerization modification gives access to

functional polymers which cannot be prepared by direct polymerization of the corresponding functional monomers. It is furthermore possible to synthesize a library of functional polymers starting from one single reactive polymer precursor. All resulting functional polymers possess identical average chain lengths and identical chain length distributions so that the investigation of structure-property relationships becomes possible.

In this chapter, the post polymerization modification of poly(vinyl amine) (PVAm) as single reactive polymer precursor is presented. As described in Chapter 1, PVAm is a linear, weak, cationic polyelectrolyte with up to 100 % free primary amine groups, one per repeating unit. Its direct synthesis from vinylamine is not possible due to the enamine-imine tautomerism. Therefore, PVAm is nowadays prepared from poly(N-vinyl formamide) (PNVF) by hydrolysis under moderate conditions both in acidic and in alkaline media. PNVF is prepared by radical polymerization using oil- or water-soluble azocompounds as initiatior. Functional polyelectrolytes with high molecular weights are easily obtained. Alkaline hydrolysis of PNVF yields almost 100 % conversion of the functional groups to free amine groups, whereas acidic hydrolysis allows only up to 80 % conversion due to electrostatic repulsion[2]. The degree of hydrolysis and thereby the charge density of the polymer backbone can be adjusted by the choice of the hydrolysis conditions like temperature, reaction time, and amount of acid or base.[3,4,5,6,7,8]

Post polymerization modification of the free primary amine groups of PVAm with functional epoxides is presented in this chapter and the resulting functional polymers are characterized. By this approach, different functionalities (cationic and hydrophobic groups) were introduced as side groups within the polymer. The resulting polymers are potential candidates for antimicrobial finishings or coatings because the combination of these functionalities is known to be antimicrobially active.[9,10,11,12]

2.2 Experimental Part

Poly(vinyl amine) is composed of different repeating units: vinyl amine and residual vinyl formamide. The ratio of these repeating units can be determined by ^{1}H NMR spectroscopy. In what follows, $\overline{M}$ denotes the averaged molecular weight of the repeating units calculated from the ^{1}H NMR spectrum.

2.2.1 Materials

Starting materials were used as received: 1,2-epoxyoctane (**EA8**) (Alfa Aesar, 97 %), 1,2-epoxydecane (**EA10**) (Alfa Aesar, 97 %), 1,2-epoxydodecane (**EA12**) (Alfa Aesar, 96 %) and glycidyltrimethylammonium chloride (**EQ**) (Aldrich, 75-80 % in water; since the oxirane degrades in time, the active content is determined just before use by NMR spectroscopy). Three different poly(vinyl amine)s (PVAm) have been supplied by BASF: Lupamin 9095 (supplier information: molecular weight = 340.000 g/mol), Lupamin 1595 (supplier information: molecular weight = 10.000 g/mol), explorative material: salt free PVAm (supplier information: purified by ultra filtration, molecular weight = 340.000 g/mol). Lupamin 9095 and Lupamin 1595 are technical polymer solutions with up to 70 % salt-content. PVAm was freeze-dried before use. The dialysis tubings of regenerated cellulose had a molecular weight cut off of 25 kDa and 50 kDa (CelluSep). The analytical data of the PVAm charges are summarized in Table 1.

Table 1. Analysis of the different poly(vinyl amine) charges.

Polymer	MW [a)] [g/mol]	DH [a)] [%]	DH [b)] [%]	Salt content [b)] [%]	$\overline{M}$ (repeating unit) [c)] [g/mol]
PVAm (salt free)	340.000	100	99	1	43.60
Lupamin 9095	340.000	95	83	67	47.83
Lupamin 1595	10.000	> 90	78	70	49.23

DH = Degree of hydrolysis, [a)] supplier information, [b)] determined by NMR, [c)] $\overline{M}$ = averaged molecular weight per repeating unit calculated from NMR.

2.2.2 Measurements

^{1}H and ^{13}C NMR spectra were recorded on a Bruker AV 400 FT-NMR spectrometer at 400 MHz (^{1}H) and 100 MHz (^{13}C), respectively, and on a Bruker AV-600 FT-NMR spectrometer at 600 MHz (^{1}H) and 150 MHz (^{13}C), respectively. Deuterated methanol (MeOD) or deuterium oxide (D_2O) were used as solvents and the solvents residual peaks were used as internal standards.

For the kinetic measurements, the ^{1}H and ^{13}C NMR spectra were recorded on a Bruker DPX-300 FT-NMR spectrometer at 300 MHz (^{1}H) and 75 MHz (^{13}C), respectively. Deuterated methanol (MeOD) and deuterium oxide (D_2O) were used as solvents and the solvents residual peaks were used as internal standards.

The Raman spectra were recorded at room temperature on a Bruker RFS 100S spectrometer with a Nd: YAG-Laser (1064 nm, 400 mW) at a spectral resolution of 4 cm^{-1} with 1000 scans.

2.2.3 Name of Prepared Products

Polymers are named using a threefold expression: The first part of this expression denotes the used poly(vinyl amine). The second and the third part denote the used epoxides and the corresponding indices show the degrees of functionalization based on the total amount of amino groups. The used abbreviations are given in Table 2.

Table 2. Abbreviations for the denotation of the products.

Unit	Correlation
PVAm	salt free PVAm, MW [a)] = 340.000 g/mol
L9095	Lupamin 9095, technical charge of PVAm, MW [a)] = 340.000 g/mol
L1595	Lupamin 1595, technical charge of PVAm, MW [a)] = 10.000 g/mol
EQ	glycidyltrimethylammonium chloride
EA8	epoxyoctane
EA10	epoxydecane
EA12	epoxydodecane

[a)] supplier information

For example, PVAm-EQ_{15}-$EA12_{10}$ stands for the functionalization of salt free PVAm with 15 % EQ and 10 % EA12.

2.2.4 Syntheses

To study the reaction of PVAm with functional epoxides, the salt free solution was chosen to avoid influences of the salt on the conversion. The optimized procedure for the reaction of PVAm with functional epoxides is described in what follows.

General Procedure for the Functionalization of PVAm with Functional Epoxides

To a solution of freeze-dried salt free PVAm (200 mg) in dist. water/methanol (p.a.) (2 mL/4 mL) at 60 °C, a solution of the desired functional epoxides in methanol (p.a., 8 mL) was added. The solution was stirred at 60 °C for 2 d. The resulting solution was then dialysed against dist. water to remove impurities that originate from the educts (especially from EQ). The water was exchanged several times. The product was then isolated by freeze-drying. The freeze-dried products were all soluble in methanol, in some cases swellable in water and in some cases soluble in water. The reaction of PVAm with the functional epoxides EQ and EA12 is shown in Scheme 1.

Along this route, PVAms with different ratios of long alkyl chains and quaternary ammonium groups were prepared.

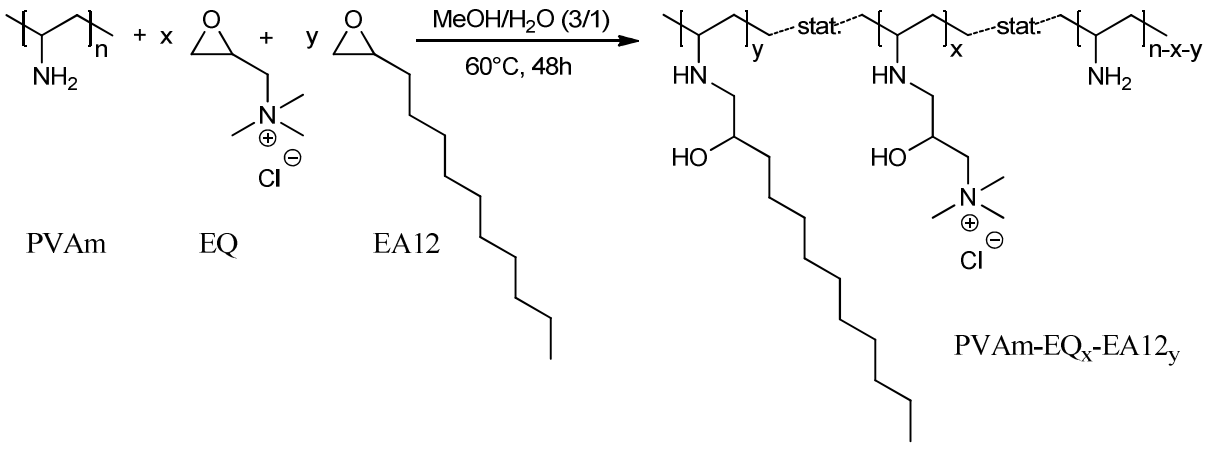

Scheme 1. Reaction of PVAm with functional epoxides EQ and EA12.

General Procedure for the Synthesis of PVAm-EQ$_x$ Using the Example of PVAm-EQ$_{40}$

To a solution of freeze-dried salt free PVAm (0.200 g, $\overline{M}$ (repeating unit) = 43.60 g/mol, 0.004587 mol repeating units) in dist. water/methanol (p.a.) (4 mL/8 mL) at 60 °C, a solution of glycidyltrimethylammonium chloride (EQ, 54 %, 0.644 g, M = 151.63 g/mol, 0.002293 mol) in methanol (p.a.) (8 mL) was added. The solution was stirred at 60 °C for 2 d and then dialyzed against dist. water. The water was exchanged several times. The product was isolated by freeze-drying as a colorless solid. The freeze-dried product was soluble in methanol and in water. The product was characterized by NMR and Raman spectroscopy to verify the full conversion of the epoxides. The degree of functionalization was determined by ^{1}H NMR spectroscopy.

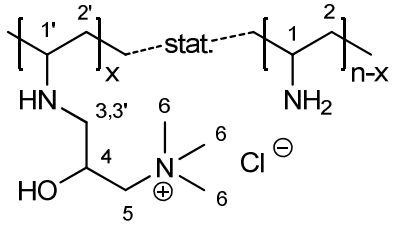

PVAm-EQ$_x$

Yield: 0.454 g, 82 %, degree of functionalization x = 40 %. ^{1}H NMR (MeOD-*d*$_4$): δ (ppm) = 1.17 – 1.88 (m, CH(NHR)C**H$_2$**, H$^{2,2'}$), 2.57 – 2.81 (m, R$_2$CHNHC**H$_2$**, H$^{3,3'}$), 2.81 – 3.19 (m, C**H**(NHR)CH$_2$, H$^{1,1'}$), 3.19 – 3.32 (s, br, CH$_2$N(C**H$_3$**)$_3$, H^6), 3.36 – 3.58 (m, CH(OH)C**H$_2$**N(CH$_3$)$_3$, H^5), 3.58 – 3.90 (s, br, CHO**H**), 4.15 – 4.36 (m, CH$_2$C**H**(OH)CH$_2$, H^4). ^{13}C NMR (MeOD-*d*$_4$): δ = 41.80 – 48.60 (m, **C**H**C**H$_2$, C$^{1,1'}$, C$^{2,2'}$, backbone), 50.30 – 51.80 (br, **C**H$_2$CH(OH)CH$_2$N(**C**H$_3$)$_3$, C^3), 55.08 (s, br, CH$_2$N(**C**H$_3$)$_3$, C^6), 66.30 – 67.30 (br, CH$_2$**C**H(OH)CH$_2$, C^4), 70.40 – 71.20 (br, CH(OH)**C**H$_2$N(CH$_3$)$_3$, C^5), the signals of **C**H**C**H$_2$ (C$^{1,1'}$, C$^{2,2'}$, backbone) and **C**H$_2$CH(OH)CH$_2$N(**C**H$_3$)$_3$ (C^3) are only distinguishable from the baseline noise in quantitative ^{13}C measurements on a 600 MHz spectrometer.

General Procedure for the Synthesis of PVAm-EA12$_y$ Using the Example of PVAm-EA12$_{41}$

To a solution of freeze-dried salt free PVAm (0.200 g, $\overline{M}$(repeating unit) = 43.60 g/mol, 0.004588 mol repeating units) in dist. water/methanol (p.a.) (4 mL/8 mL) at 60 °C, a solution of 1,2-epoxydodecane (EA12, 96 %, 0.349 g, M = 184.32 g/mol, 0.001817 mol) in methanol (p.a.) (10 mL) was added. The solution was stirred at 60 °C for 2 d and then dialyzed first against methanol and second against dist. water. The methanol and the water were exchanged several times. The product was isolated by freeze-drying as a colorless solid. The freeze-dried product was soluble in methanol. The product was characterized by NMR and Raman spectroscopy to verify a full conversion of the epoxides. The degree of functionalization was determined by ^{1}H NMR spectroscopy.

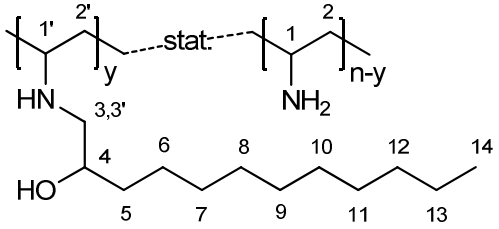

PVAm-EA12$_y$

Yield: 0.449 g, 82 %, degree of functionalization y = 41 %. ^{1}H NMR (MeOD-*d*$_4$): δ (ppm) = 0.84 – 0.98 (m, CH(OH)(CH$_2$)$_9$C**H$_3$**, H^{14}), 1.17 – 1.88 (m, CH(OH)(C**H$_2$**)$_9$CH$_3$, H$^{5\text{-}13}$, CH(NHR)C**H$_2$**, H$^{2,2'}$), 2.35 – 2.57 (m, 1H, R$_2$CHNHC**H$_2$**CH(OH), H$^{3'}$), 2.60 – 2.80 (m, 1H, R$_2$CHNHC**H$_2$**CH(OH), H^3), 2.80 – 3.19 (m, C**H**(NHR)CH$_2$, H$^{1,1'}$), 3.58 – 3.73 (m, CH$_2$C**H**(OH)(CH$_2$)$_9$, H^4), 3.73 – 3.90 (s, br, CHO**H**).

^{13}C NMR (MeOD-*d*$_4$): δ (ppm) = 14.80 (br, (CH$_2$)$_9$**C**H$_3$, C^{14}), 23.82 (br, (CH$_2$)$_8$**C**H$_2$CH$_3$, C^{13}), 27.01 (br, CH$_2$CH(OH)CH$_2$**C**H$_2$(CH$_2$)$_7$CH$_3$, C^6), 30.22 – 31.61 (m, (CH$_2$)$_2$(**C**H$_2$)$_5$(CH$_2$)$_2$CH$_3$, C$^{7\text{-}11}$), 33.21 (br, (CH$_2$)$_7$**C**H$_2$CH$_2$CH$_3$, C^{12}), 36.79 (br, CH$_2$CH(OH)**C**H$_2$(CH$_2$)$_8$CH$_3$, C^5), 41.80 – 48.60 (m, **C**H**C**H$_2$, C$^{1,1'}$, C$^{2,2'}$, backbone), 51.80 – 54.50 (br, **C**H$_2$CH(OH)(CH$_2$)$_9$CH$_3$, C^3),

70.40 – 71.20 (br, $CH_2\mathbf{C}H(OH)(CH_2)_9CH_3$, C^4), the signals of $\mathbf{C}H\mathbf{C}H_2$ ($C^{1,1'}$, $C^{2,2'}$, backbone) and $\mathbf{C}H_2\mathbf{C}H(OH)(CH_2)_9CH_3$ (C^3 and C^4) are only distinguishable from the baseline noise in quantitative ^{13}C measurements on a 600 MHz spectrometer.

General Procedure for the Synthesis of PVAm-EQ$_x$-EA12$_y$ Using the Example of PVAm-EQ$_{16}$-EA12$_{11}$

To a solution of freeze-dried salt free PVAm (0.565 g, $\overline{M}$ (repeating unit) = 43.60 g/mol, 0.012959 mol repeating units) in dist. water/methanol (p.a.) (10 mL/20 mL) at 60 °C, a solution of glycidyltrimethylammonium chloride (EQ, 69 %, 0.564 g, M = 151.63 g/mol, 0.002566 mol) and 1,2-epoxydodecane (EA12, 96 %, 0.246 g, M = 184.32 g/mol, 0.001336 mol) in methanol (p.a.) (10 mL) was added. The solution was stirred at 60 °C for 2 d and then dialyzed against dist. water. The water was exchanged several times. The product was isolated by freeze-drying as a colorless solid. The freeze-dried product was soluble in methanol and in water. The product was characterized by NMR and Raman spectroscopy to verify a full conversion of the epoxides. The degree of functionalization was determined by ^1H NMR spectroscopy.

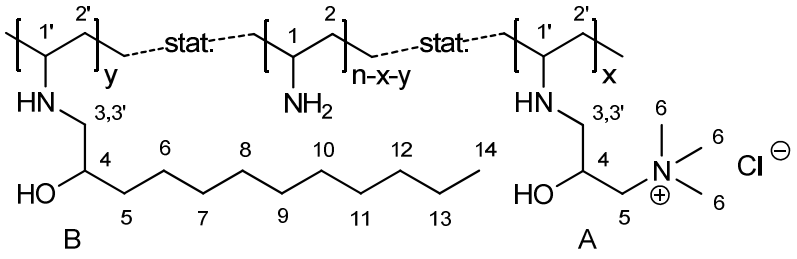

PVAm-EQ$_x$-EA12$_y$

Yield: 0.936 g, 79 %, degree of functionalization y = 11 % and x = 16 %. ^1H NMR (MeOD-d_4): δ (ppm) = 0.84 – 0.98 (m, $CH(OH)(CH_2)_9C\mathbf{H_3}$, H^{14B}), 1.17 – 1.88 (m, $CH(OH)(C\mathbf{H_2})_9CH_3$, $H^{5\text{-}13B}$, $CH(NHR)C\mathbf{H_2}$, $H^{2,2'}$), 2.35 – 2.57 (m, 1H, $R_2CHNHC\mathbf{H_2}CH(OH)$, $H^{3'B}$), 2.57 – 2.81 (m, 3H, $R_2CHNHC\mathbf{H_2}CH(OH)$, $H^{3B,3A,3'A}$), 2.81 –

3.19 (m, C**H**(NHR)CH_2, $H^{1,1'}$), 3.19 – 3.32 (s, br, $CH_2N(C\mathbf{H_3})_3$, H^{6A}), 3.36 – 3.58 (m, $CH(OH)C\mathbf{H_2}N(CH_3)_3$, H^{5A}), 3.58 – 3.73 (m, $CH_2C\mathbf{H}(OH)(CH_2)_9$, H^{4B}), 3.73 – 3.90 (s, br, CHO**H**), 4.15 – 4.36 (m, $CH_2C\mathbf{H}(OH)CH_2$, H^{4A}).

^{13}C NMR (MeOD-d_4): δ (ppm) = 14.80 (br, $CH_2CH(OH)(CH_2)_9\mathbf{C}H_3$, C^{14B}), 23.82 (br, $CH_2CH(OH)(CH_2)_8\mathbf{C}H_2CH_3$, C^{13B}), 27.01 (br, $CH_2CH(OH)CH_2\mathbf{C}H_2(CH_2)_7CH_3$, C^{6B}), 30.22 – 31.61 (m, $CH_2CH(OH)(CH_2)_2(\mathbf{C}H_2)_5(CH_2)_2CH_3$, $C^{7\text{-}11B}$), 33.21 (br, $(CH_2)_7\mathbf{C}H_2CH_2CH_3$, C^{12B}), 36.79 (br, $CH_2CH(OH)\mathbf{C}H_2(CH_2)_8CH_3$, C^{5B}), 41.80 – 48.60 (m, **C**H**C**H_2, $C^{1,1'}$, $C^{2,2'}$, backbone), 50.30 – 51.80 (br, $\mathbf{C}H_2CH(OH)CH_2N(\mathbf{C}H_3)_3$, C^{3A}), 51.80 – 54.50 (br, $\mathbf{C}H_2CH(OH)(CH_2)_9CH_3$, C^{3B}), 55.08 (s, br, $CH_2CH(OH)CH_2N(\mathbf{C}H_3)_3$, C^{6A}), 66.30 – 67.30 (br, $CH_2\mathbf{C}H(OH)CH_2N(CH_3)_3$, C^{4A}), 70.40 – 71.20 (m, $CH_2CH(OH)\mathbf{C}H_2N(CH_3)_3$, C^{5A} and $CH_2\mathbf{C}H(OH)(CH_2)_9CH_3$, C^{4B}), the signals of **C**H**C**H_2 ($C^{1,1'}$, $C^{2,2'}$, backbone), $\mathbf{C}H_2CH(OH)CH_2N(\mathbf{C}H_3)_3$ (C^{3A}) and $\mathbf{C}H_2\mathbf{C}H(OH)(CH_2)_9CH_3$ (C^{3B} and C^{4B}) are only distinguishable from the baseline noise in quantitative ^{13}C measurements on a 600 MHz spectrometer.

Reaction Kinetics

^{13}C NMR spectroscopy was used to study the kinetics of the reaction of 1 eq PVAm (salt free) (0.150 g, $\overline{M}$ (repeating unit) = 43.60 g/mol, 0.003441 mol repeating units) with 0.27 eq EA12 (96 %, 0.176 g, M = 184.32 g/mol, 0.000956 mol). The reaction was carried out in a mixture of deuterated methanol and deuterium oxide following the above described general procedure (60 °C). Samples of each 0.5 mL were taken after every hour starting at t = 0 h and ending at t = 9 h. The samples were cooled down with crashed ice and measured immediately. To study the kinetics at a higher temperature (80 °C), the reaction was carried out in a mixture of deuterated ethanol and deuterium oxide. Besides this, the same procedure as described above had been followed. Samples were taken every hour from t = 0 h until t = 8 h.

^{1}H NMR spectroscopy was used to study the kinetics of the reaction of 1 eq PVAm (salt free) (0.435 g, $\overline{M}$ (repeating unit) = 43.60 g/mol, 0.009978 mol repeating units) with 0.27 eq EQ (60 %, 0.672 g, M = 151.63 g/mol, 0.002661 mol). The reaction was carried out in a mixture of deuterated methanol and deuterium oxide following the above described general procedure (60 °C). Samples of each 0.5 mL were taken every 30 minutes starting at t = 0 min and ending at t = 7 h.

General Procedure for the Synthesis of L9095-EQ$_x$-EA12$_y$ and L1595-EQ$_x$-EA12$_y$ Using the Example of L9095-EQ$_{11}$-EA12$_{12}$

First, a solution of freeze-dried Lupamin 9095 (0.505 g, 33 %, $\overline{M}$ (repeating unit) = 47.83 g/mol, 0.003484 mol repeating units) in dist. water/methanol (p.a.) (10 mL/ 20 mL) was prepared. For dissolving the PVAm, the solution was stirred at least one night. The pH of the solution was adjusted to pH = 13 with conc. NaOH (aq.). A solution of EQ (54 %, 0.1202 g, M = 151.63 g/mol, 0.000428 mol) and EA12 (96 %, 0.0825 g, M = 184.32 g/mol, 0.000430 mol) in MeOH (p.a.) (10 mL) was added at once. The solution was stirred for 5 days at 60 °C and then dialyzed against dist. water. The water was exchanged several times. The product was isolated by freeze-drying. The freeze-dried product was soluble in methanol and had a degree of functionalization of 12 % EA12 and 11 % EQ. The degree of functionalization was obtained from the NMR spectra.

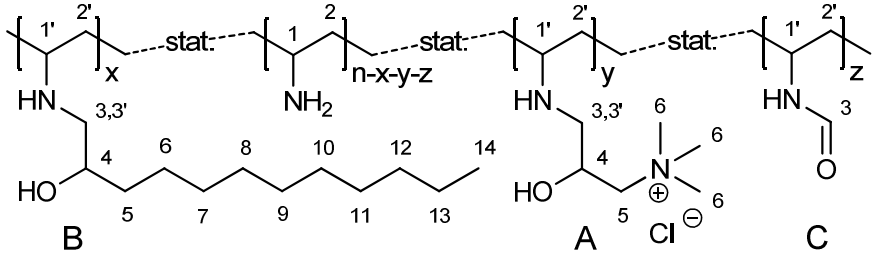

Yield: 0.275 g, 89 %, degree of functionalization x = 12 % and y = 11 %.

^{1}H NMR (MeOD-d_4): δ (ppm) = 0.84 – 0.98 (m, CH(OH)$(CH_2)_9$C**H$_3$**, H^{14B}), 1.17 – 2.35 (m, CH(OH)(C**H$_2$**)$_9$$CH_3$, $H^{5\text{-}13B}$, CH(NHR)C**H$_2$**, $H^{2,2'}$), 2.35 – 2.57 (m, 1H, R_2CHNHC**H$_2$**CH(OH), $H^{3'B}$), 2.57 – 2.81 (m, 3H, R_2CHNHC**H$_2$**CH(OH), $H^{3B,3A,3'A}$), 2.81 – 3.19 (m, C**H**(NHR)CH_2, $H^{1,1'}$), 3.19 – 3.32 (s, br, CH_2N(C**H$_3$**)$_3$, H^{6A}), 3.36 – 3.58 (m, CH(OH)C**H$_2$**$N(CH_3)_3$, H^{5A}), 3.58 – 3.73 (m, CH_2C**H**(OH)$(CH_2)_9$, H^{4B}), 3.73 – 3.90 (s, br, CHO**H**), 4.15 – 4.36 (m, CH_2C**H**(OH)CH_2, H^{4A}), 7.10 – 7.60 (NHC**H**O, H^{3C}, formamide), 8.54 (OC**H**ONa, sodium formate).

Fractionation of Functional Polymers

Fractionation of PVAm-EQ$_{40}$

To a solution of PVAm-EQ_{40} (250 mg) in methanol (p.a., 15 mL), diethyl ether (p.a.) was slowly added until an opalescent solution was obtained. The precipitate was not settling down and was therefore isolated by centrifugation of the solution for 30 min at 3500 rpm. To the centrifugate, diethyl ether (p.a.) was added until the solution became opalescent again and the precipitate was isolated by centrifugation. This was repeated several times and afterwards, the rest of the solution was evaporated to obtain the last fraction of isolated polymer. All in all six different fractions were obtained in this way. The fractions were dried by vacuum distillation (15 mbar) (Table 3).

Table 3. Fractions obtained from PVAm-EQ_{40}.

Fraction	Et_2O [mL] [a]	Solid [mg] [b]
1	15	44
2	2	73
3	1	34
4	1.5	37
5	10	12
6	-	52
		Σ252

[a] mL of diethyl ether used for precipitation, [b] some samples contain small amounts of solvent.

Fractionation of PVAm-$EA12_{41}$

To a solution of PVAm-$EA12_{41}$ (300 mg) in methanol (p.a., 15 mL), diethyl ether (p.a.) was slowly added. After the addition of 50 mL diethyl ether, still no precipitate or opalescent solution was obtained. The addition of acetone, dichloromethane, or water instead of diethyl ether also led to a clear solution.

Fractionation of PVAm-$EA12_{10}$

To a solution of PVAm-$EA12_{10}$ (45 mg) in methanol (p.a., 2 mL) diethyl ether (p.a.) was slowly added. An opalescent solution was obtained. The precipitate was not settling down and was therefore isolated by centrifugation of the solution for 30 min at 3500 rpm. Diethyl ether (p.a.) was added to the centrifugate until the solution became opalescent again, followed by centrifugation to isolate the precipitate. Afterwards, the rest of the solution was evaporated to

obtain the last fraction of isolated polymer. All in all 3 different fractions were obtained in this way. The fractions were dried by vacuum distillation (15 mbar). They are summarized in Table 4.

Table 4. Fractions obtained from PVAm-EA12$_{10}$.

Fraction	Et_2O [mL] [a)]	Solid [mg] [b)]
1	7	13
2	5	20
3	-	8
		Σ41

[a)] mL of diethyl ether used for precipitation, [b)] some samples contain small amounts of solvent.

Fractionation of PVAm-EQ$_{14}$-EA12$_{11}$

To a solution of PVAm-EQ$_{14}$-EA12$_{11}$ (194 mg) in methanol (p.a., 10 mL), diethyl ether (p.a.) was slowly added until an opalescent solution was obtained. The precipitate was not settling down and therefore isolated by centrifugation of the solution for 30 min at 3500 rpm. To the centrifugate, diethyl ether (p.a.) was added until the solution became opalescent again, followed by centrifugation to isolate the precipitate. This was repeated several times and afterwards, the rest of the solution was evaporated to obtain the last fraction of isolated polymer. All in all, six different fractions were obtained in this way. The fractions were dried by vacuum distillation (15 mbar). They are summarized in Table 5.

Table 5. Fractions obtained from PVAm-EQ_{14}-$EA12_{11}$.

Fraction	Et_2O [mL] [a]	Solid [mg] [b]
1	25	29
2	4	59
3	4	52
4	4	24
5	4	12
6	-	38
		Σ214

[a] mL of diethyl ether used for precipitation, [b] some samples contain small amounts of solvent.

2.3 Results and Discussion

The goal of this study was the preparation of multifunctional polymers from PVAm, e.g., for surface coating.

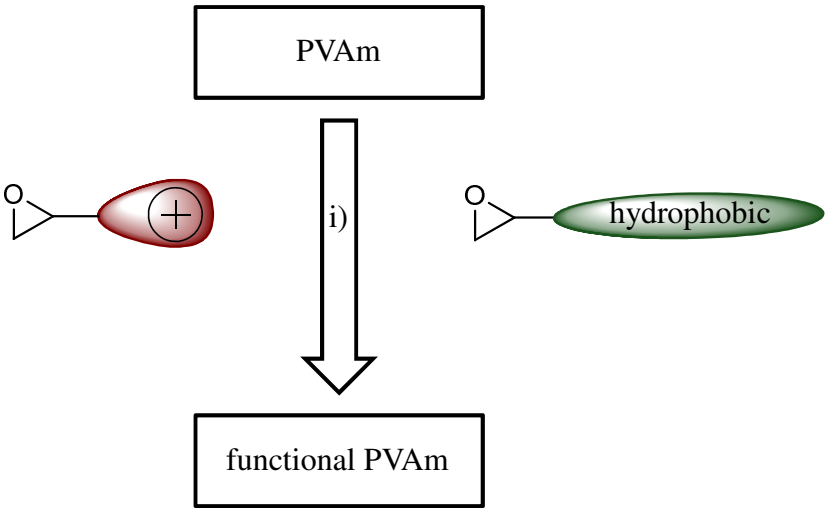

Figure 1. Synthesis concept. i) Post polymerization modification of PVAm with functional epoxides.

The polymers should contain hydrophilic, cationic, and hydrophobic groups to achieve an antimicrobial activity. In addition, the cationic groups can be used for surface binding. PVAm provides up to 100 % primary amine groups (one in each repeating unit) which can be used for functionalization. Different functional epoxides were converted with the primary amine groups of PVAm to introduce different functionalities into the polymer (Figure 1).

2.3.1 Synthesis and Characterization of Amphiphilic PVAm

Synthesis and Characterization of PVAm-EAX$_y$

The reaction of PVAm (salt free) with the epoxyalkanes EA12, EA10, and EA8 was studied (Scheme 2).

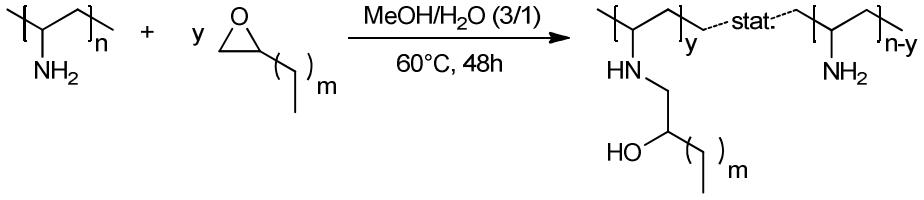

PVAm EAX PVAm-EAX$_y$

m(EA8) = 4
m(EA10) = 6
m(EA12) = 8

Scheme 2. Reaction of PVAm with epoxyalkanes EA8, EA10 and EA12.

PVAm was reacted with the functional epoxide in a water/methanol mixture at 60°C for 2d. The obtained products were purified by dialysis first against methanol and second against water. The methanol and the water were exchanged several times. It was found that a dialysis against water was sufficient to remove all impurities. Table 6 shows the expected and obtained degrees of functionalization for different ratios of EA12, EA10, and EA8 with respect to the primary amine groups of PVAm.

Table 6. Results for the reaction of PVAm with three different epoxyalkanes.

	n [%]*	Degree of functionalization y [%]	
Name	**PVAm**	**Expected**	**Obtained****
PVAm-EA12$_{10}$	100	10	10
PVAm-EA12$_{21}$	100	20	21
PVAm-EA12$_{32}$	100	30	32
PVAm-EA12$_{41}$	100	40	41
PVAm-EA12$_{42}$	100	52	42
PVAm-EA10$_{18}$	100	15	18
PVAm-EA10$_{28}$	100	30	28
PVAm-EA10$_{49}$	100	45	49
PVAm-EA10$_{54}$	100	60	54
PVAm-EA8$_{21}$	100	16	21
PVAm-EA8$_{29}$	100	31	29
PVAm-EA8$_{40}$	100	46	40
PVAm-EA8$_{45}$	100	61	45

* Amount of repeating units in %, ** calculated from ^{1}H NMR spectroscopy.

Under the reaction conditions described above, equivalent and reproducible conversions were obtained. The amine group can open the oxirane ring by performing a nucleophilic attack at two different positions of the ring. The reactivity depends on the basicity of the amine nucleophile and on the steric hindrance at the epoxy ring due to substituents. According to the ^{1}H NMR spectroscopy data, only the sterically less hindered side of the ring is attacked yielding only a single constitutional isomer. A complete conversion has been proven by Raman spectroscopy where no unreacted epoxide was found (see below). Comparing the

expected and obtained degrees of functionalization, there seems to be a limit for the degree of functionalization at around 50 % (cf. Table 6). This limit seems to stem from the occurrence of sterical hindrance.

The freshly prepared products were soluble in methanol and some of the products were as well soluble in water. They have been characterized by NMR spectroscopy. Figure 2 shows the ^{1}H NMR spectra of the educts. The spectrum of PVAm shows the expected peaks for the polymer backbone. It shows a multiplet with a maximum at $\delta = 1.33$ ppm which belongs to the protons of the aliphatic CH_2 groups and a multiplet with two maxima ($\delta = 2.92$ ppm and $\delta = 3.00$ ppm) which can be assigned to the protons of the CH groups. As expected, the integral ratio of the two multiplets is two (CH_2) to one (CH). The occurrence of multiplets for the protons of the backbone is on the one hand due to the high molecular weight of the polymer – whereby the protons in one position are not chemically equivalent – and on the other hand it can be a hint for an atactic polymer. At $\delta = 7.50$ ppm, one more multiplet occurs which can be assigned to residual formamide groups in the PVAm (cf. Chapter 1). From this signal, the degree of hydrolysis can be calculated. The singlet at $\delta = 8.50$ ppm belongs to the proton of sodium formate, which is generated during the hydrolysis of PNVF to PVAm and can be used to calculate the amount of sodium formate contamination of the polymer. The spectrum of EA12 shows the typical signals for the epoxy ring a, a' and b at around $\delta = 2.40 – 3.00$ ppm. The signals for the alkyl chain appear as multiplet between $\delta = 1.20 – 1.65$ ppm and the signal for the terminal CH_3 group appears at $\delta = 0.90$ ppm.

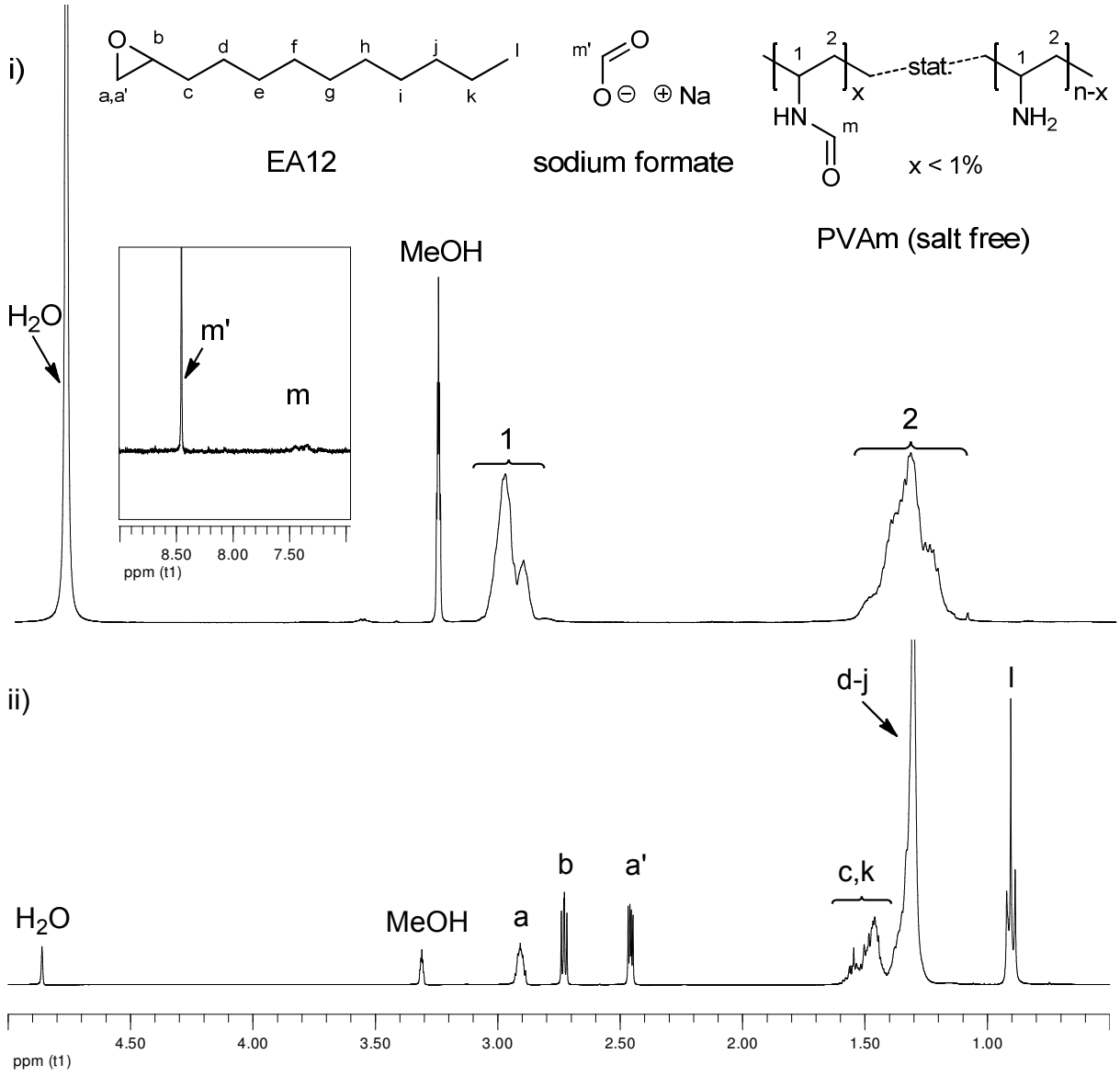

Figure 2. ^{1}H NMR spectra in MeOD of the educts. i) PVAm (salt free) ii) EA12.

The ^{1}H NMR spectra of the conversion of PVAm (salt free) with EA12 after i) 0 h, ii) 22.5 h, and iii) the end product after purification via dialysis are shown in Figure 3. It can be observed that the signals a, a' and b of the epoxyalkane decrease over time and are completely missing in the end product. In addition, new signals 3, 3' and 4 are appearing and increasing over time, showing the formation of the desired product.

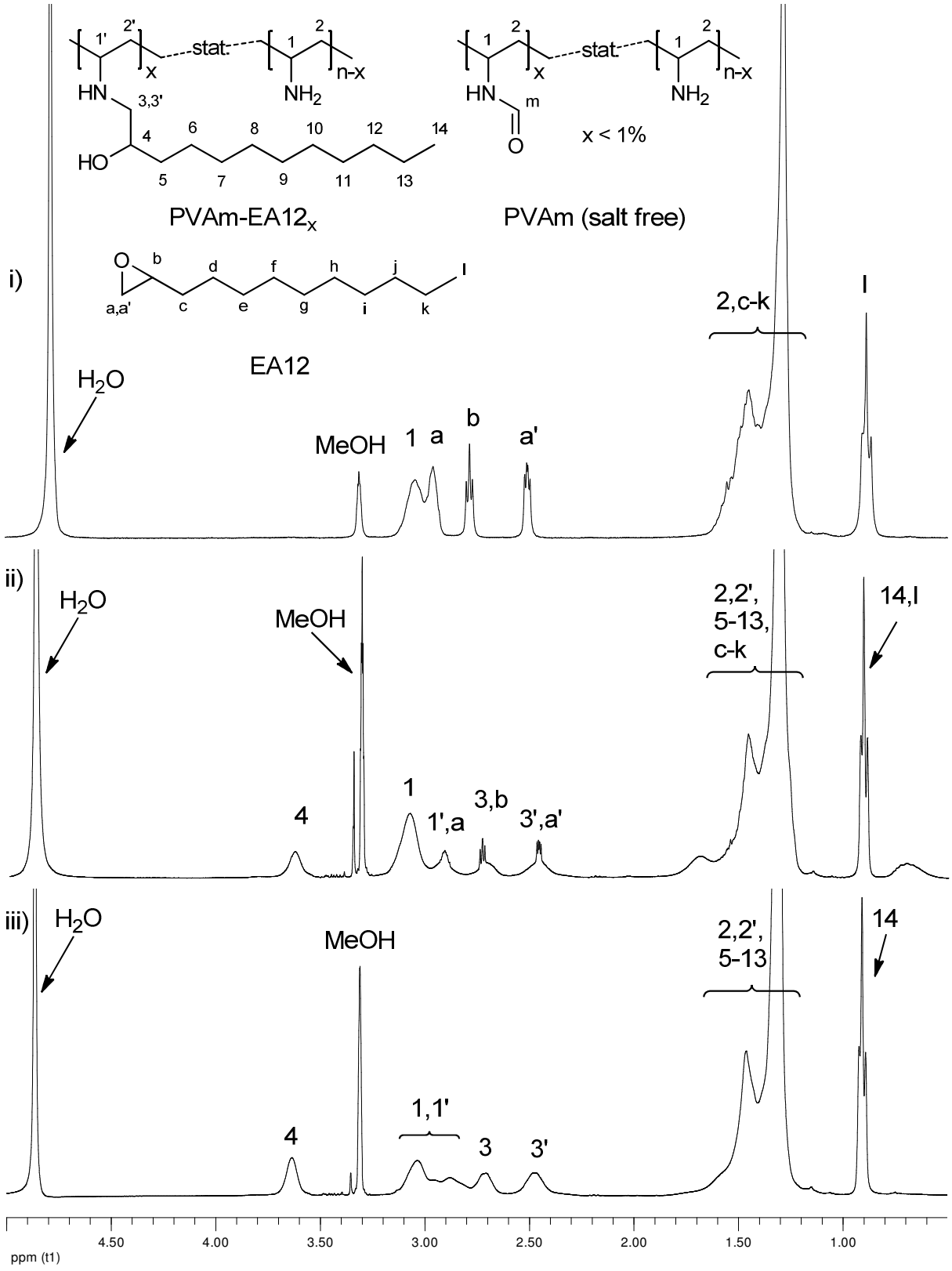

Figure 3. ^{1}H NMR spectra in MeOD of the conversion of PVAm (salt free) with EA12. i) 0 h, ii) 22.5 h, iii) end product after purification via dialysis.

The degree of functionalization can be calculated from the ^{1}H NMR spectrum by comparing the integral of the signal for the protons in position 14 to the integral of the signal for the protons in position 2 and 2' of the polymer backbone. The signal of the protons in position 2 and 2' is overlapping with the signal of the protons in position 5-13. The integral for the signal of the protons in position 5-13 can be calculated from the integral for the signal of the protons in position 14. To calculate the integral for the signal of the protons in position 2 and 2' the integral of the signal for the protons in position 5-13 is subtracted from the whole integral for the combined signal of 2, 2' and 5-13.

The ^{13}C NMR spectra of the educts are shown in Figure 4. The carbon atoms of the polymer backbone (signal 1, 2) give broad signals at around $\delta = 45.0 - 50.0$ ppm which are overlapping with the solvent signal of methanol and are often not distinguishable from the baseline noise. This is again, as for the proton NMR, a hint for an atactic polymer. The spectrum of EA12 shows the signals a and b of the epoxy ring and all expected signals for the alkyl chain (c – l).

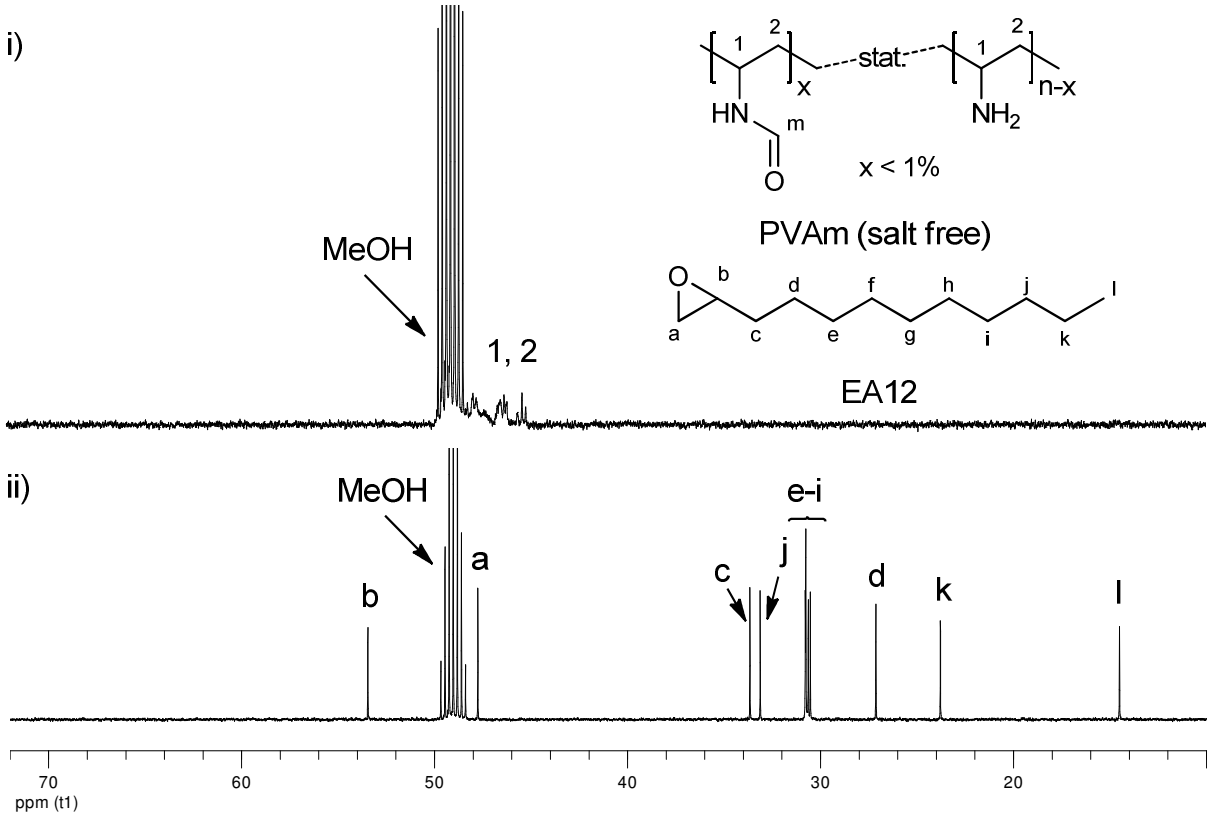

Figure 4. ^{13}C NMR spectra in MeOD of the educts. i) PVAm (salt free) ii) EA12.

The ^{13}C NMR spectra of the conversion of PVAm (salt free) with EA12 after i) 0 h, ii) 22.5 h, and iii) the end product after purification via dialysis are shown in Figure 5. It can be observed that the signals a and b of the epoxy ring decrease over time and can not be detected any more in the end product. Signal c, belonging to the CH_2 group adjacent to the epoxy ring, is shifted to lower fields and appears as new signal 5, showing the formation of the desired product.

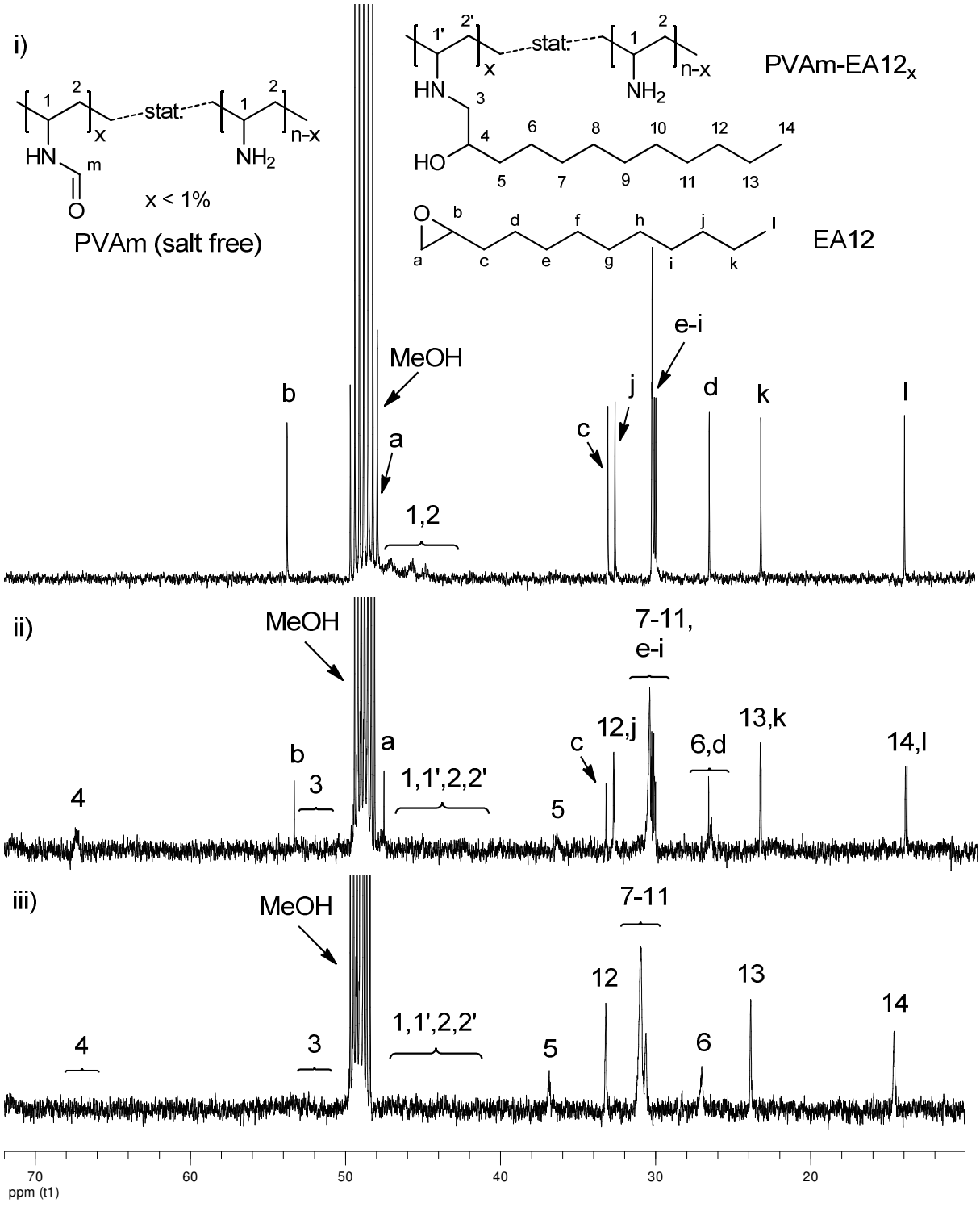

Figure 5. ^{13}C NMR spectra in MeOD of the conversion of PVAm (salt free) with EA12. i) 0 h, ii) 22.5 h, iii) end product after purification via dialysis.

Synthesis and Characterization of PVAm-EQ$_x$

The reaction of PVAm with a quaternary ammonium group bearing epoxide (EQ) was studied (Scheme 3).

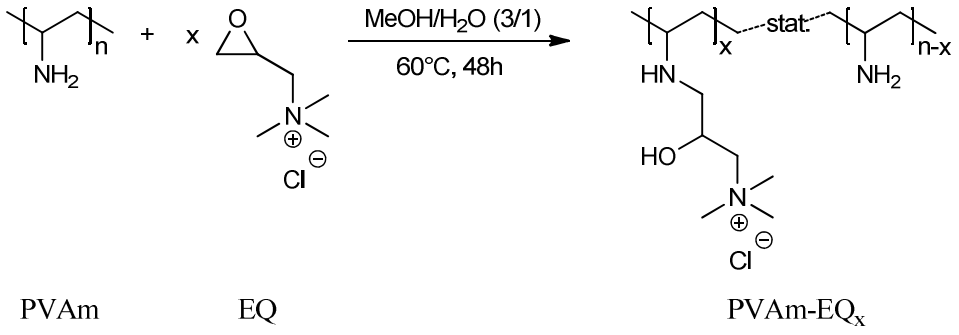

Scheme 3. Reaction of PVAm with cationic epoxide EQ.

PVAm was reacted with EQ in a water/methanol mixture at 60 °C for 2d. The obtained products were purified by dialysis against water to remove impurities originating from the educt EQ. Table **7** shows the expected and obtained degrees of functionalization for different ratios of EQ to the primary amine groups of PVAm. Again, as for the reaction of PVAm with EA12, equivalent and reproducible results were found under the above mentioned reaction conditions. As explained for the reaction with EA12 the oxirane ring is only opened at the sterically less hindered side of the ring and only one constitutional isomer is obtained. Degrees of functionalization of up to about 70 % were reached. Higher conversions cannot be reached due to the electrostatic repulsion of the cationic groups and due to sterical hindrance. The expected and obtained degrees of functionalization match quite well for $x \leq 30$ %. This is not the case for $x > 30$ %, here the obtained degrees of functionalization are lower than the expected ones.

Table 7. Results for the reaction of PVAm with EQ.

Name	n [%]* PVAm	Degree of functionalization x [%]	
		Expected	Obtained**
PVAm-EQ$_{12}$	100	10	12
PVAm-EQ$_{20}$	100	20	20
PVAm-EQ$_{28}$	100	30	28
PVAm-EQ$_{34}$	100	40	34
PVAm-EQ$_{23}$	100	30	23
PVAm-EQ$_{40}$	100	40	30
PVAm-EQ$_{73}$	100	100	73

* Amount of repeating units in %, ** calculated from ^{1}H NMR spectroscopy.

The complete conversion of the epoxide has been proven by Raman spectroscopy (see below). The products were soluble in methanol and in water and they have been characterized by NMR spectroscopy. The ^{1}H NMR spectra of the educts are shown in Figure 6. For a detailed description of the spectrum of PVAm please see the paragraph "Synthesis and characterization of PVAm-EAX$_y$" on page 42. The spectrum of EQ shows the typical signals a and a' for the epoxy ring at around $\delta = 2.75 - 3.10$ ppm. Signal b of the epoxy ring is overlapping with the solvent signal of methanol and signal d of the quaternary amine group at $\delta = 3.25 - 3.40$ ppm. The signal for the protons in position c/c' is appearing isolated as a doublet of a doublet at $\delta = 4.05$ ppm and was used for the determination of the monomer conversion (see below). EQ is sold as aqueous solution with 75-80 % solid content. According to the supplier, 90 % of this solid is EQ and the rest are impurities. Since the oxirane degrades over time, the active content is determined just before use by NMR spectroscopy. The signals of the hydrolysis product of EQ can be seen in the spectrum (*).

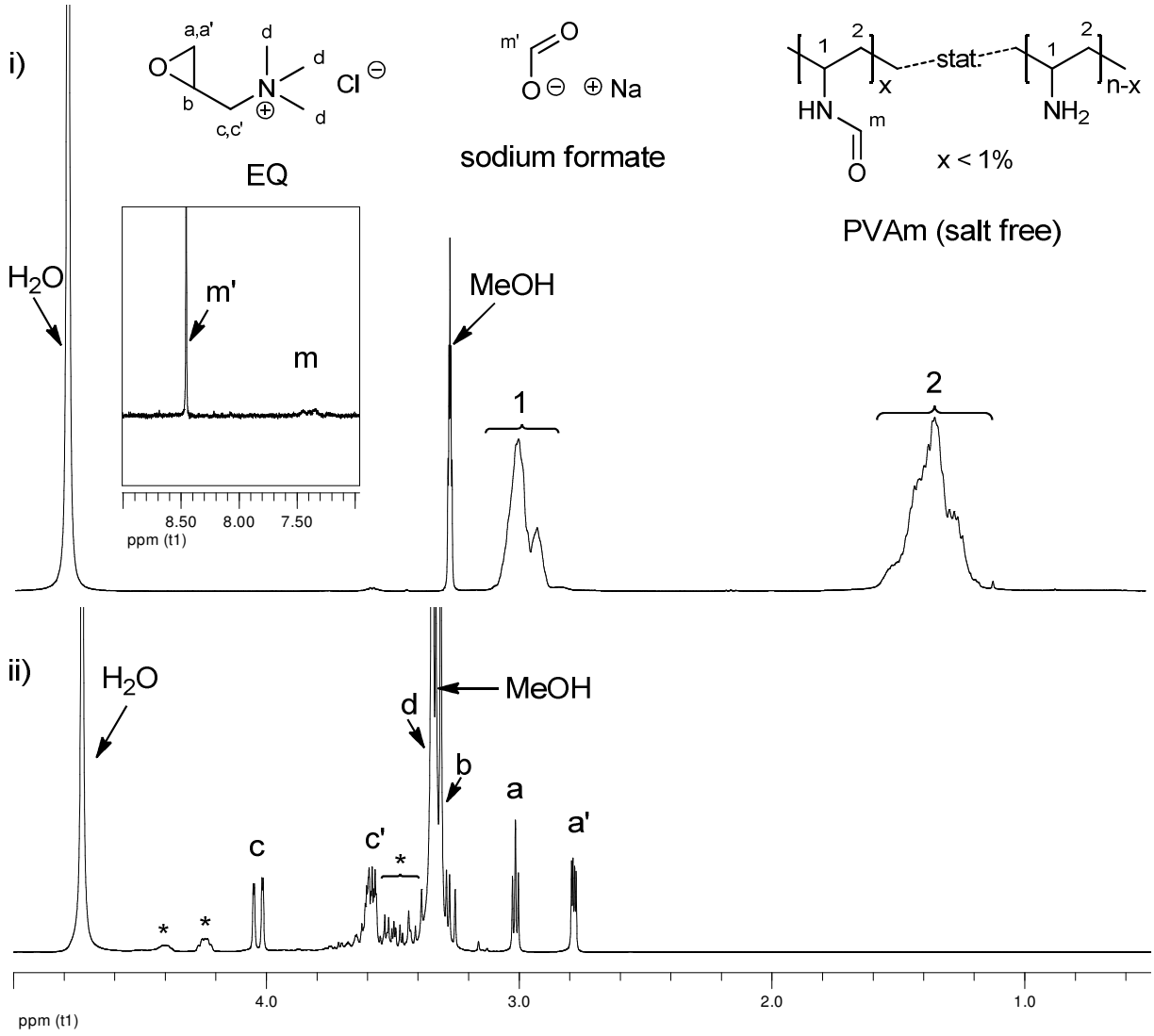

Figure 6. ^{1}H NMR spectra in MeOD of the educts. i) PVAm (salt free), ii) EQ. * hydrolysis product of EQ

The ^{1}H NMR spectra of the conversion of PVAm (salt free) with EQ after i) 0 h, ii) 3 h, and iii) the end product after purification via dialysis are shown in Figure 7. The signals a, a', and c of the epoxide decrease over time and are absent in the end product. In addition, new signals 3, 3', 4, and 5 are arising over time showing the formation of the desired product.

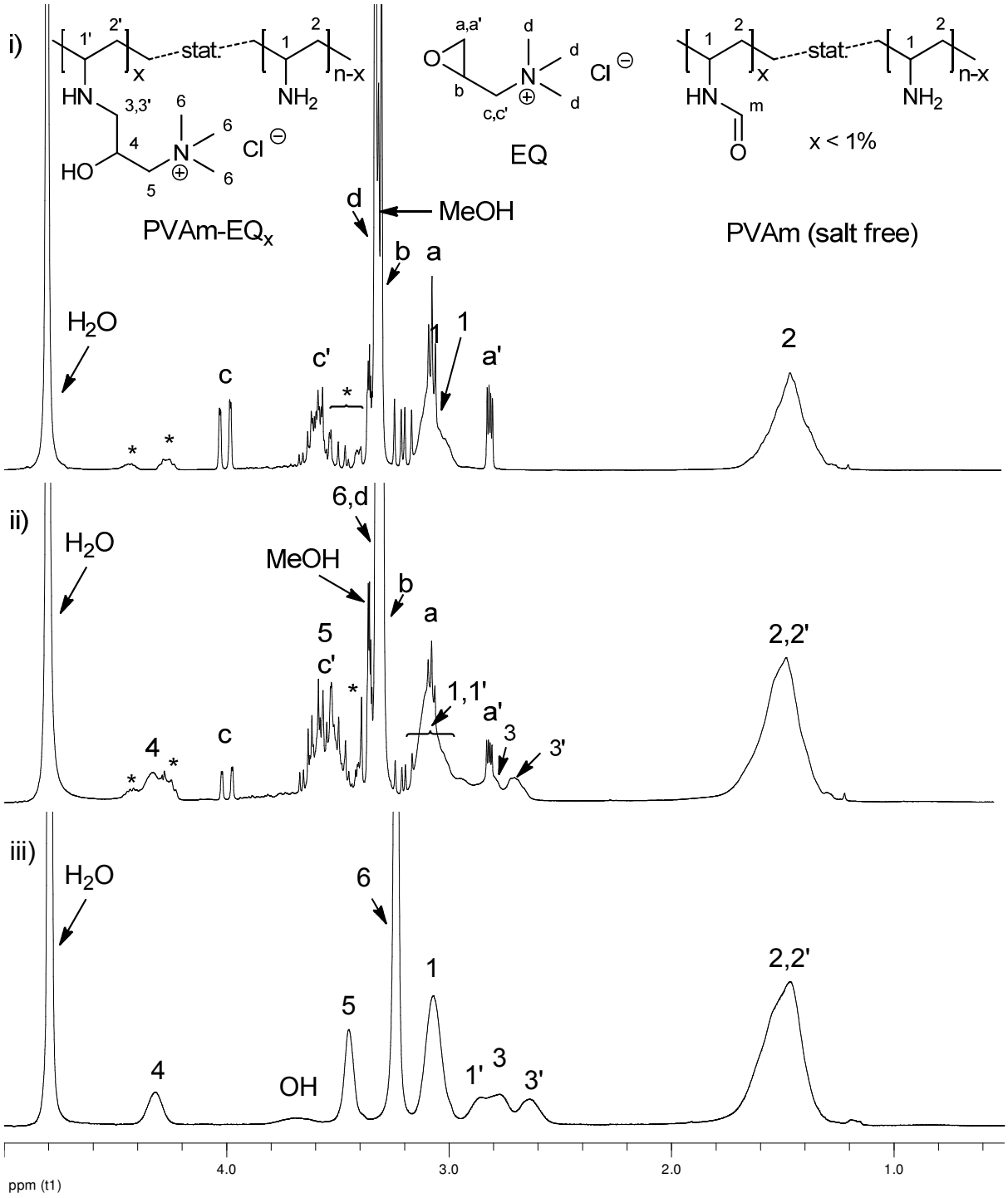

Figure 7. ^{1}H NMR spectra in MeOD of the conversion of PVAm (salt free) with EQ. i) 0 h, ii) 3 h, iii) end product after purification via dialysis in D_2O. * hydrolysis product of EQ.

The degree of functionalization can be calculated from the spectrum by comparing the integral of the signal for the protons in position 4 with the integral of the signal for the protons in position 2 and 2' of the polymer backbone.

The ^{13}C NMR spectra of the educts PVAm (salt free) and EQ are shown in Figure 8. As already described in the paragraph "Synthesis and characterization of PVAm-EAX_y" on page 42, the carbons of the polymer backbone (signals 1, 2) give very broad signals around $\delta = 45.0 - 50.0$ ppm, overlapping with the solvent signal of methanol. They are often indistinguishable from the baseline noise.

The spectrum of EQ shows the signals a and b of the epoxy ring. Signals d (quaternary ammonium group of EQ) and d* (quaternary ammonium group of the hydrolysis product of EQ) can be used to calculate the active content of EQ from a quantitative ^{13}C NMR measurement.

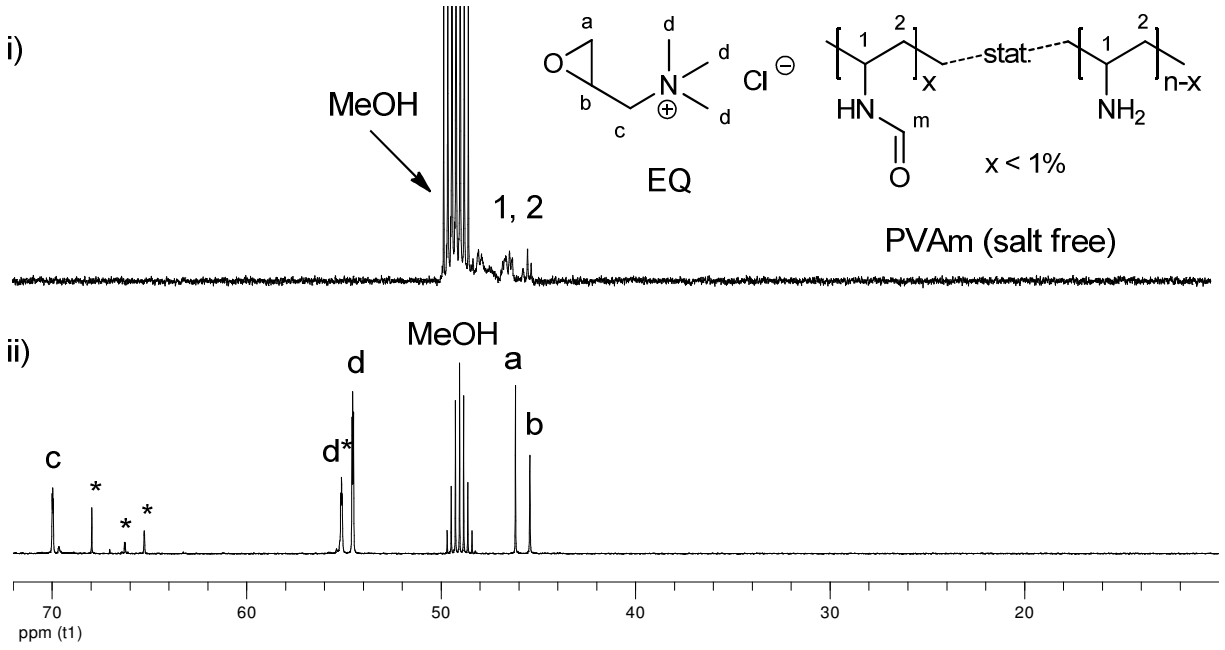

Figure 8. ^{13}C NMR spectra in MeOD of the educts. i) PVAm (salt free), ii) EQ. * hydrolysis product of EQ.

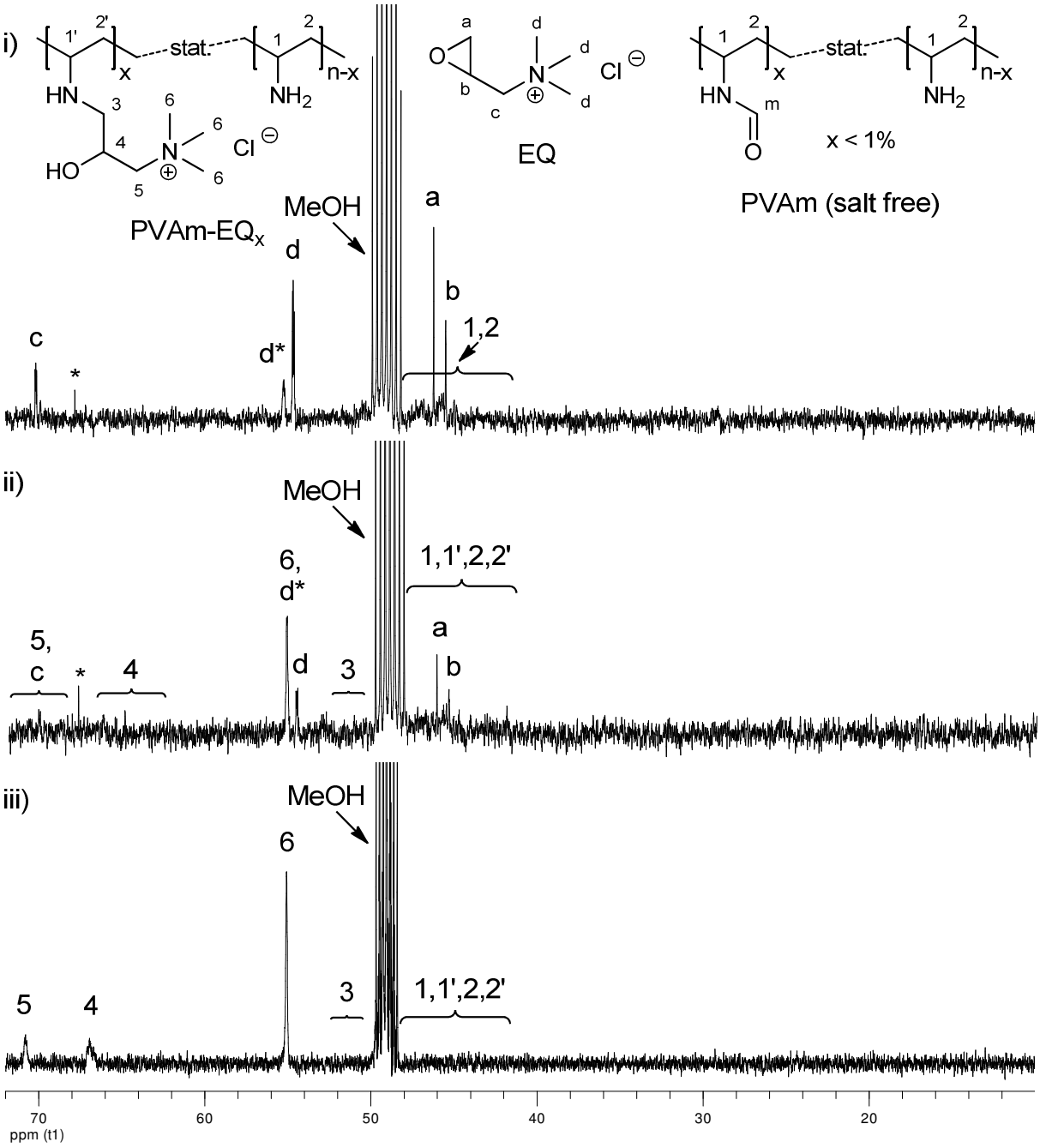

Figure 9. ^{13}C NMR spectra in MeOD of the conversion of PVAm (salt free) with EQ. i) 0 h, ii) 3 h, iii) end product after purification via dialysis. * hydrolysis product of EQ.

The ^{13}C NMR spectra of the conversion of PVAm (salt free) with EQ after i) 0 h, ii) 3 h, and iii) the end product after purification via dialysis are shown in Figure 9. The signals a, b, and d of the epoxyalkane vanish over time and are not present in the end product anymore. The

other signals broaden and new signals 4, 5, and 6 are appearing and increasing over time, showing the formation of the desired product.

Synthesis and Characterization of PVAm-EQ$_x$-EA12$_y$

The reaction of PVAm with a mixture of EA12 and EQ was studied (Scheme 4).

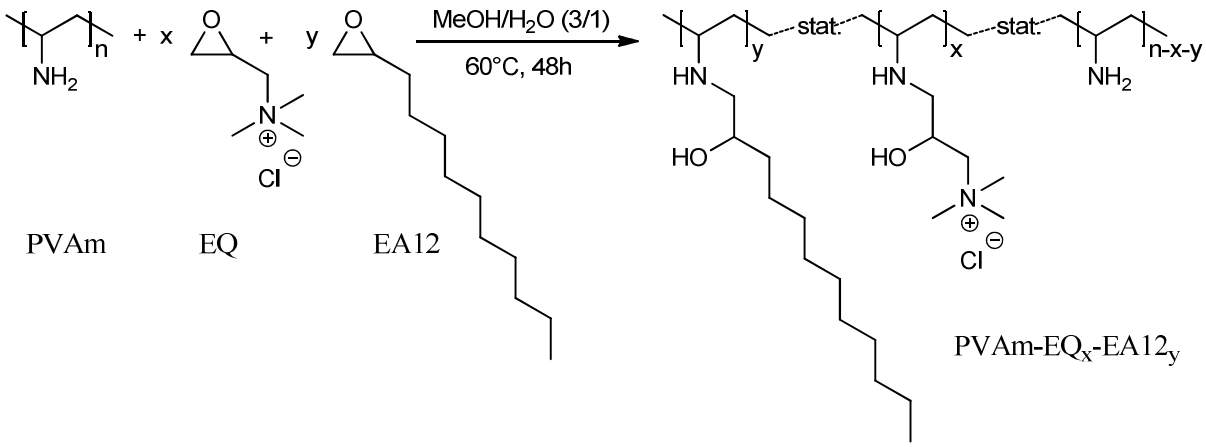

Scheme 4. Reaction of PVAm with cationic epoxide EQ and epoxyalkane EA12.

PVAm was reacted with a mixture of the functional epoxides in a water/methanol mixture at 60 °C for 2 d. The obtained products were purified by dialysis against water. Table 8 shows the expected and obtained degrees of functionalization for different EA12 and EQ ratios to the primary amine groups of PVAm. The products were soluble in methanol and in some cases (with a lower degree of functionalization with hydrophobic groups) soluble in water. The expected and obtained degrees of functionalization fit satisfactorily.

Table 8. Results for the reaction of PVAm with a mixture of EA12 and EQ.

Name	n [%]*	Degree of functionalization x (EQ) and y (EA12) [%]			
	PVAm	EA12 exp.	EQ exp.	EA12 obt.**	EQ obt.**
PVAm-EQ$_{18}$-EA12$_5$	100	5	19	5	18
PVAm-EQ$_{14}$-EA12$_{11}$	100	10	16	11	14
PVAm-EQ$_{10}$-EA12$_{17}$	100	15	12	17	10
PVAm-EQ$_7$-EA12$_{22}$	100	20	8	22	7
PVAm-EQ$_5$-EA12$_{10}$	100	10	4	10	5
PVAm-EQ$_7$-EA12$_{10}$	100	10	8	10	7
PVAm-EQ$_{19}$-EA12$_{11}$	100	10	19	11	19

exp. = expected, obt. = obtained, * amount of repeating units in %, ** calculated from ^{1}H NMR spectroscopy.

The complete conversion has been proven by Raman spectroscopy (cf. Figure 11 and Figure 12) and the products were characterized by NMR spectroscopy. Each spectrum (^{1}H and ^{13}C NMR) of PVAm-EQ$_x$-EA12$_y$ after purification via dialysis is shown in Figure 10. The degree of functionalization can be calculated from the spectrum as described above. The spectra of the polymer combining both functionalities, the alkyl chain and the quaternary ammonium group, show as expected an overlay of the signals described for the single modification with only one of the functionalities.

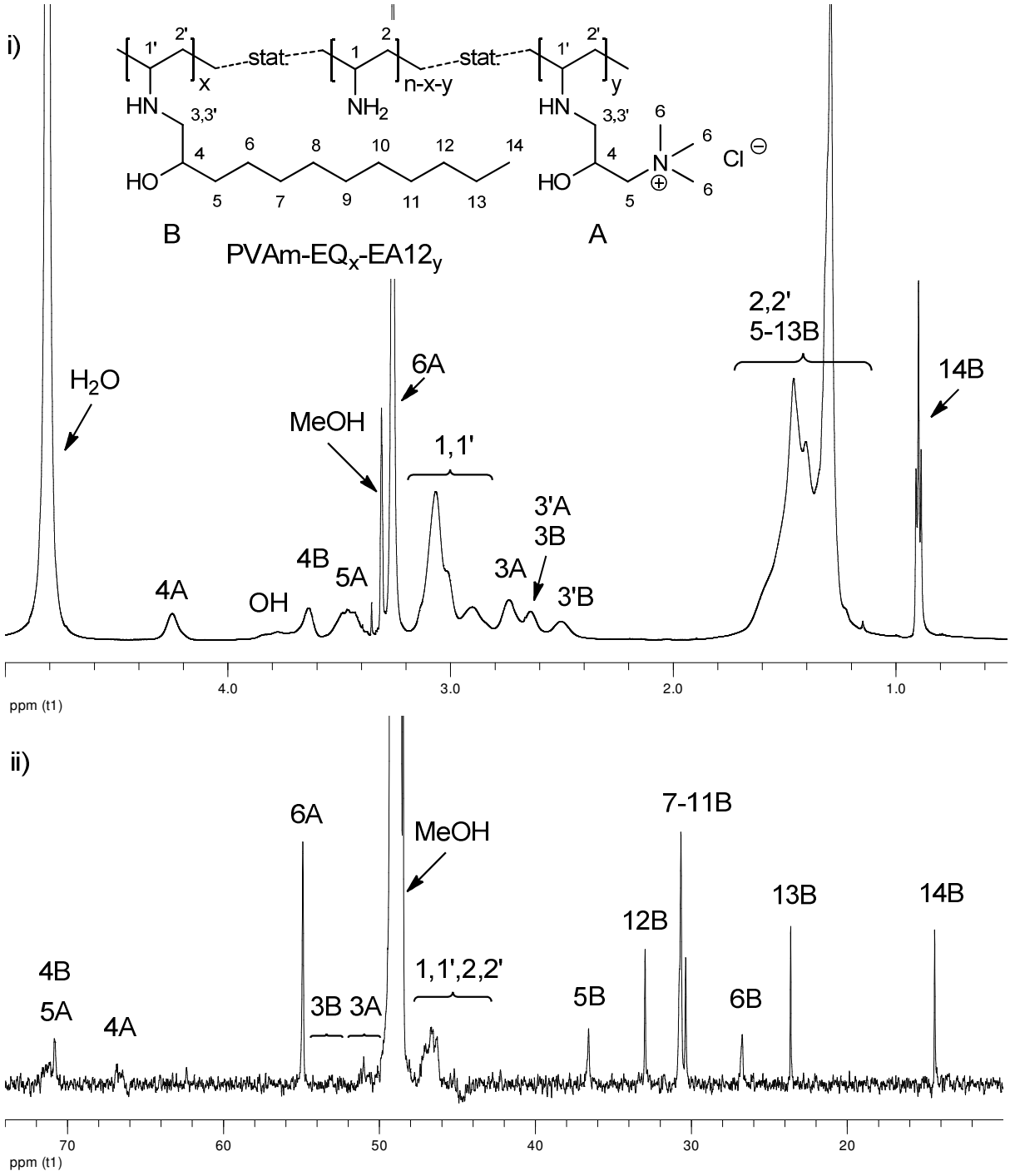

Figure 10. i) ^{1}H and ii) ^{13}C NMR spectrum of PVAm-EQ_x-$EA12_y$ in MeOD.

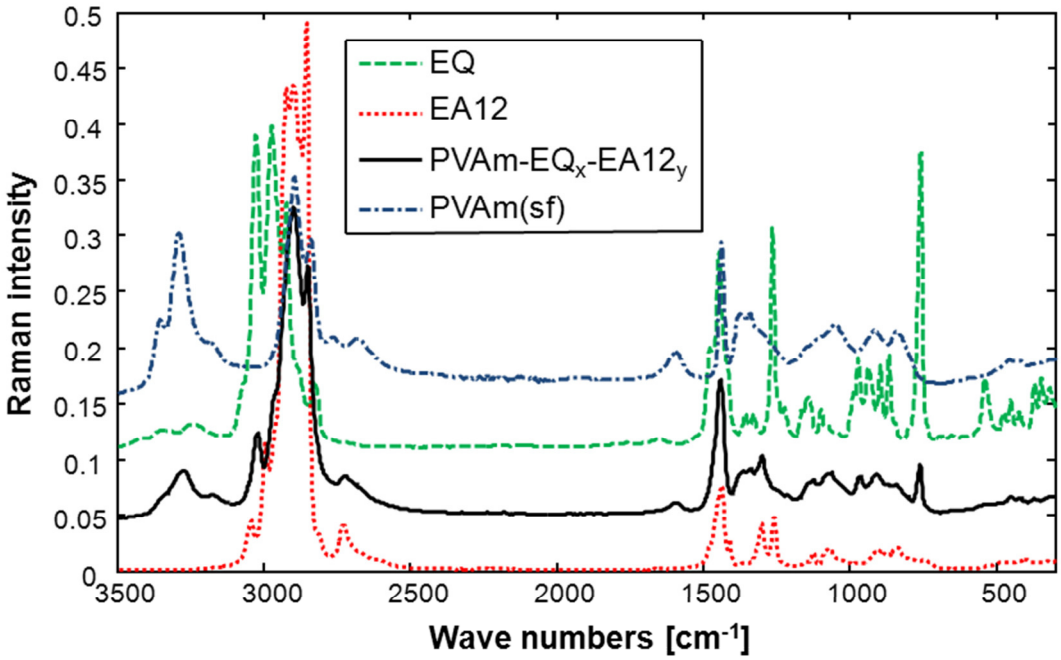

Figure 11. Raman intensities of EA12, EQ, PVAm (sf = salt free) and PVAm-EQ_x-$EA12_y$.

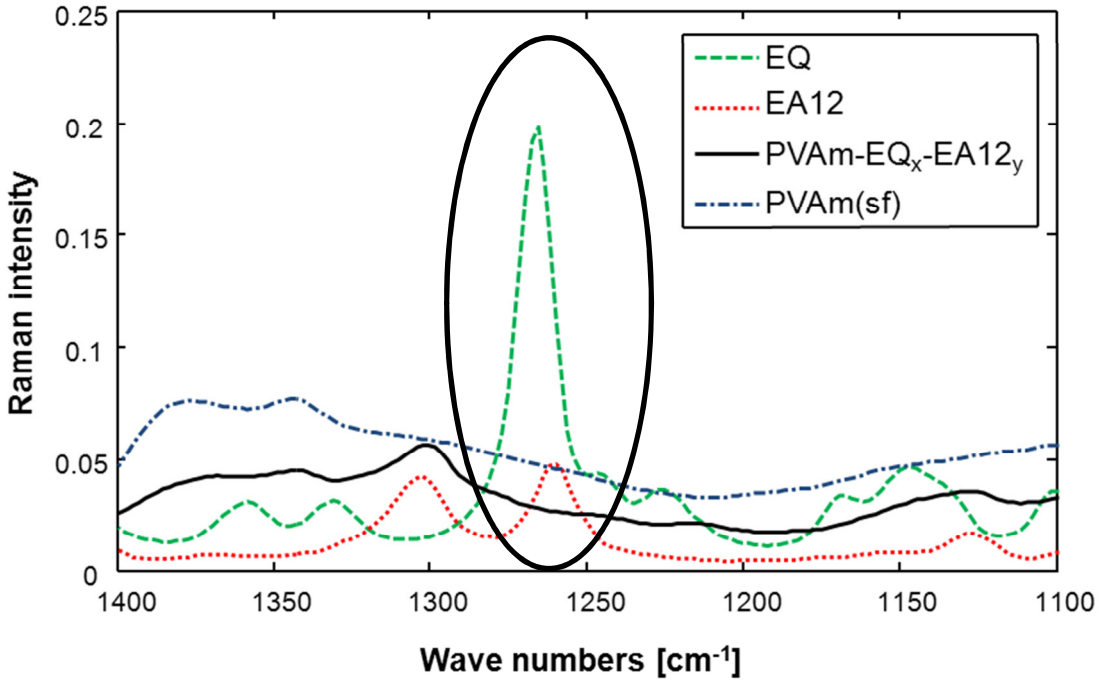

Figure 12. Detail of the Raman intensities of EA12, EQ, PVAm (sf = salt free) and PVAm-EQ_x-$EA12_y$.

The Raman spectra (Figure 11 and Figure 12) show that the typical signals for the epoxide ring at 1260 cm^{-1} for EA12 and 1266 cm^{-1} for EQ are missing in the product spectrum of PVAm-EQ_x-$EA12_y$. In addition to the NMR spectra, the Raman spectra thus prove that no unreacted epoxides are left after the reaction and a full conversion is achieved. For storage, the synthesized functional PVAms were either directly stored as aqueous solution obtained after dialysis or were dissolved in methanol to give 1 wt% (10 mg/g) solutions.

2.3.2 Reaction Kinetics

In the reaction of PVAm (salt free) with an epoxide, only two reactants are involved: the amine group and the epoxide. One amine group reacts with one epoxide. This means that both reactants are first-order reactants and since the reaction depends on the concentration of both reactants, it is a second-order reaction and can be written by

$$A + B \longrightarrow P . \qquad (1)$$

Since 1 eq of the primary amine groups of PVAm is reacted with only 0.27 eq of the epoxide, the concentration of both reactants is different and there is an excess of amine groups. The concentration of one reactant at a given time is therefore $[A] := [A]_0 - x$ or $[B] := [B]_0 - x$, respectively, with $[A]_0$ and $[B]_0$ denoting the concentration of the two reactants at $t = 0$ and x equals the consumption of the reactants. This consumption x is identical for both reactants.

For a second order reaction, the reaction rate is given by:

$$v = \frac{d[A]}{dt} = -k[A][B] \qquad (2)$$

where k equals the reaction rate constant, $[A]$ the concentration of A at time t, and $[B]$ the concentration of B at time t.

Using $[A] := [A]_0 - x$ and $[B] := [B]_0 - x$ for the integration of (2) gives after some manipulation,

$$\ln\left(\frac{[B]/[B]_0}{[A]/[A]_0}\right) = ([B]_0 - [A]_0)kt\,. \qquad (3)$$

Plotting $\ln(([B]/[B]_0)/([A]/[A]_0))$ against t gives a straight line of slope $([B]_0 - [A]_0)k$ and thereby the possibility to determine k.

To follow the reaction kinetics, it is necessary to observe the change in concentration of at least one of the two reactants. In this study, the concentration change was observed via NMR spectroscopy. $[A]$ denotes in what follows the amount of the epoxide in [mol] and $[B]$ the amount of the amine groups in [mol].

The kinetics of the reaction of PVAm (salt free) with EA12 was determined using ^{13}C NMR spectroscopy. PVAm was dissolved in a mixture of deuterated methanol and deuterium oxide and reacted with EA12 at 60 °C and 80 °C, respectively. At defined time instants t, samples were taken for analysis. Unconverted epoxide gives a signal at $\delta = 33.66$ ppm (C^c) in the ^{13}C NMR spectrum (Figure 13). The reaction can be followed by observing the decrease of this signal whereas the signal at $\delta = 33.21$ ppm ($C^{j/12}$) only shifts a little bit to lower fields and serves as reference. The reaction was carried out in deuterated solvents so that no workup had to be done prior to the measurement. The samples were cooled down and measured directly after sampling.

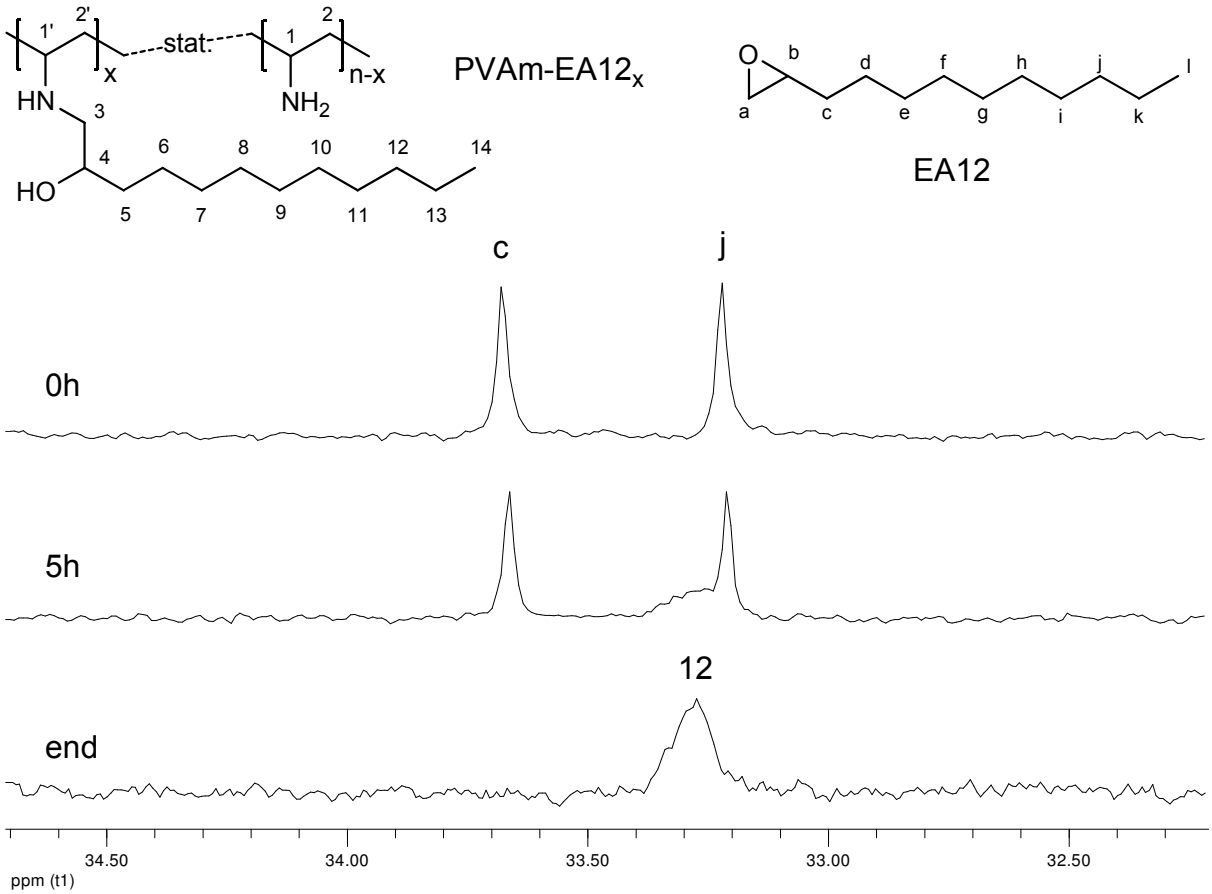

Figure 13. Detail of the ^{13}C NMR spectra of the reaction of PVAm (salt free) with EA12. The shown signals (c, j/12) were used to follow the reaction kinetics.

The epoxide conversion as a function of the reaction time for the two temperatures is plotted in Figure 14. The plot shows a clear temperature dependence of the reaction rate. Increasing the temperature leads to an increased reaction rate. After 7 hours the reaction at 60 °C reaches about 50 % conversion whereas at 80 °C already about 85 % conversion is reached.

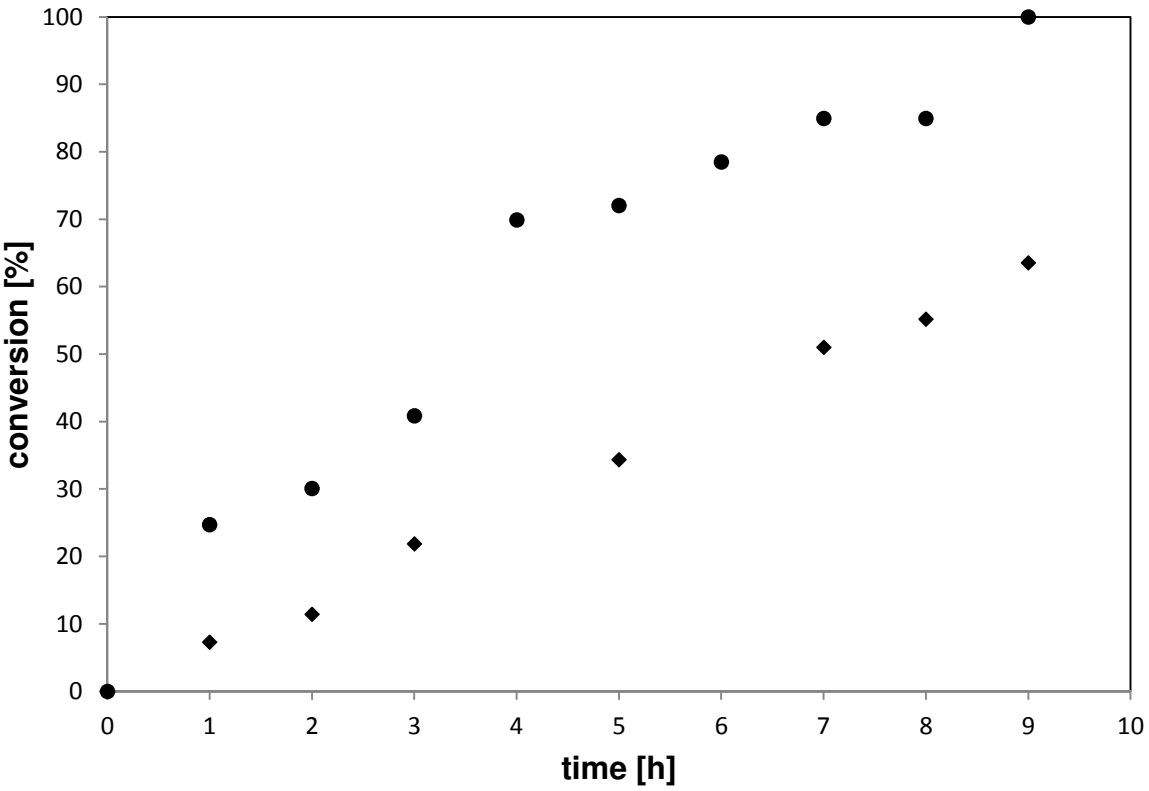

Figure 14. Conversion of PVAm (salt free) with EA12. Conversion versus reaction time (♦ EA12 at 60 °C, ● EA12 at 80 °C). Reaction conditions: PVAm/EA12 = 100/27.

For a more detailed interpretation of the kinetics of the reaction of PVAm with EA12, the data was also plotted as second-order plots (Figure 15). The measured data points were fit by straight lines. The plots clearly show the increase in reaction rate when raising the reaction temperature from 60 °C to 80 °C. The second-order plots were linear for both temperatures indicating the dependence of the reaction rate on both reactants: amino groups of PVAm and EA12. The slope of the lines $([B]_0 - [A]_0)k$ was used to calculate the reaction rate constant *k*. For 60 °C, $k = 32.802\ \text{mol}^{-1} \cdot \text{L} \cdot \text{s}^{-1}$ and for 80 °C, $k = 85.365\ \text{mol}^{-1} \cdot \text{L} \cdot \text{s}^{-1}$ is obtained. The value of *k*(80 °C) is more than twice the value of the reaction rate constant *k*(60 °C).

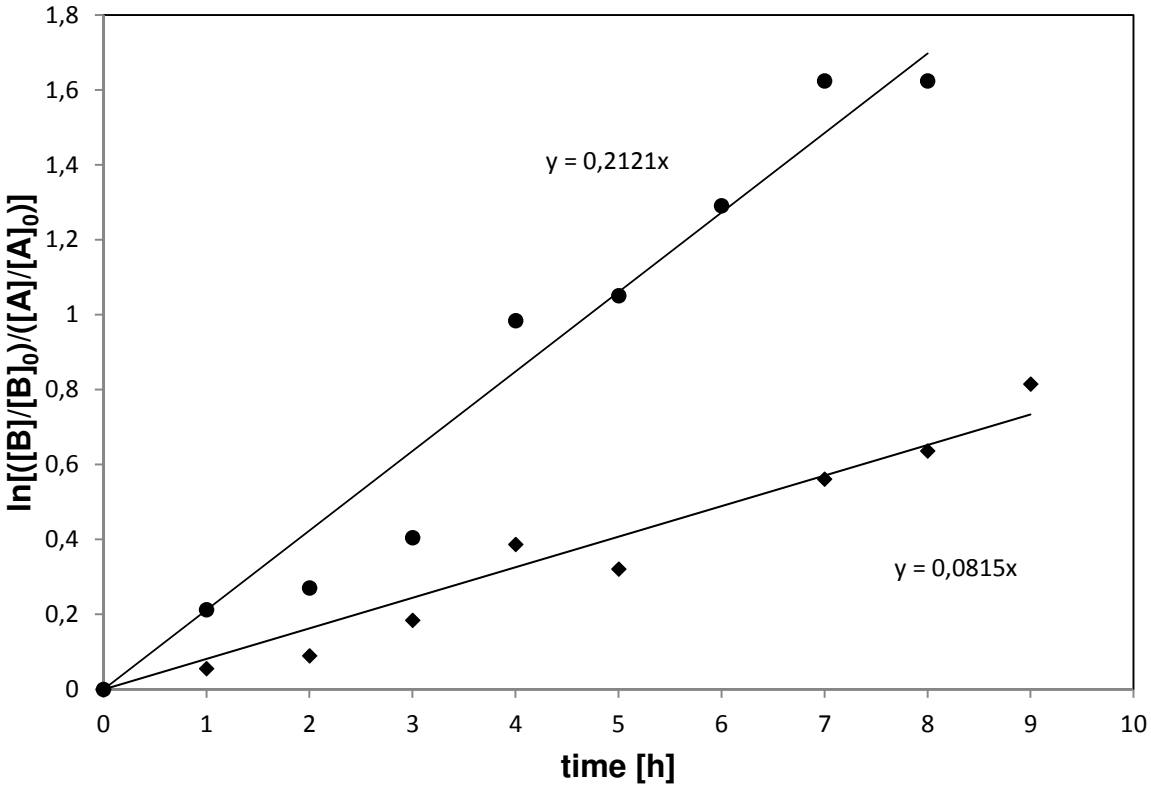

Figure 15. Conversion of PVAm (salt free) with EA12. Second-order plot: (♦ EA12 at 60 °C, ● EA12 at 80 °C), reaction conditions: PVAm/EA12 = 100/27.

The reaction kinetics of the reaction of PVAm (salt free) with EQ was followed with ^{1}H NMR spectroscopy. PVAm was dissolved in a mixture of deuterated methanol and deuterium oxide and converted with EQ at 60 °C. At defined times, samples were taken for analysis. The reaction can be followed by observing the signal of unconverted epoxide at δ = 4.05 ppm (H^{c}, doublet of a doublet) in the ^{1}H NMR spectrum (Figure 16) using the signal of the polymer backbone at δ = 1.17 – 1.88 ppm ($H^{2,2'}$) as reference. The reaction was carried out in deuterated solvents and the samples were cooled down and measured directly after sampling.

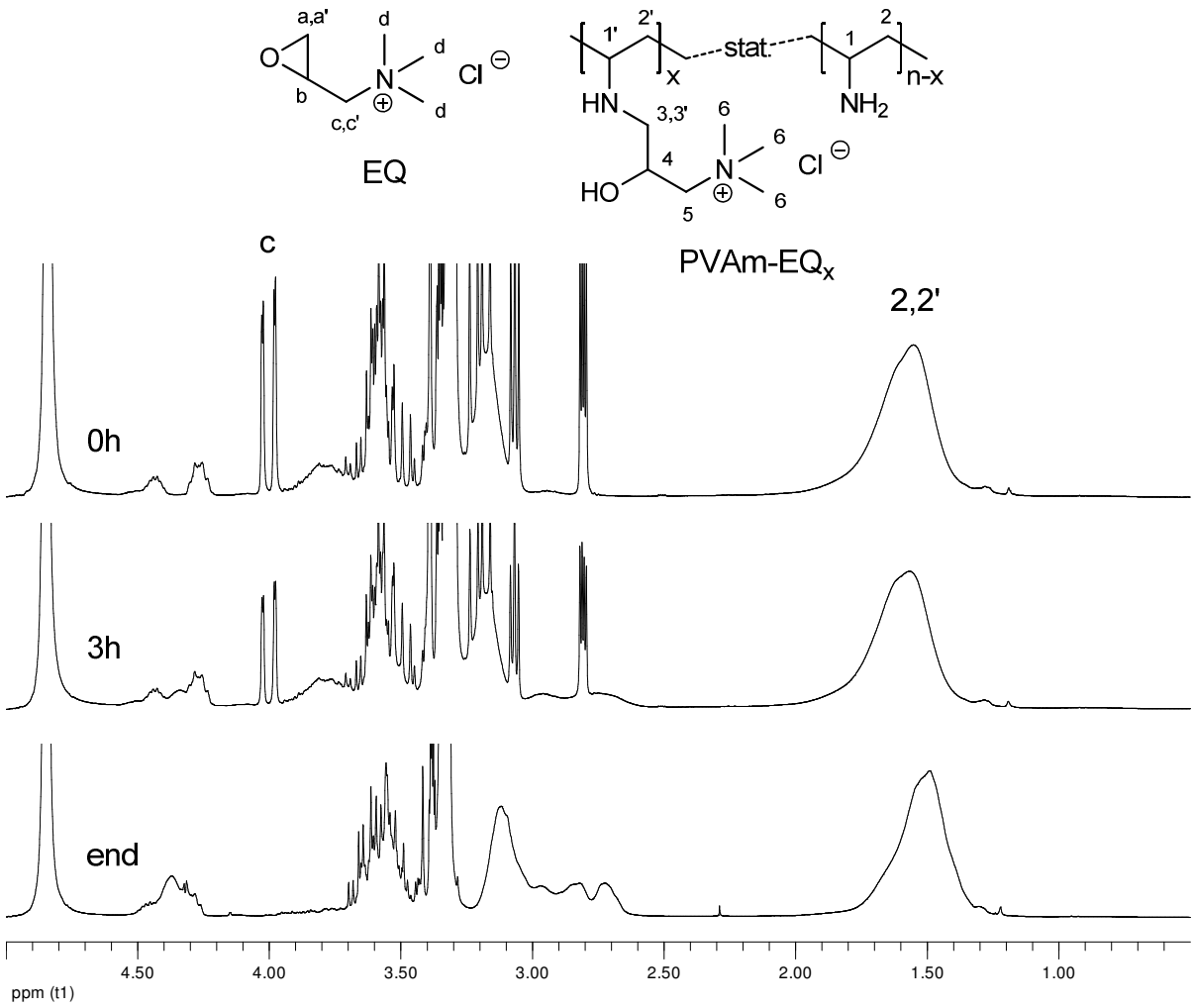

Figure 16. ^{1}H NMR spectra of the reaction of PVAm (salt free) with EQ. Signal c and 2,2' were used to follow the reaction kinetics.

The conversion versus time plot (Figure 17) shows that the reaction proceeds to completeness in about 24 hours. The obtained data for the reaction kinetic was plotted as second-order plot, fitted by a straight line (Figure 18), and is linear up to high conversions, indicating the dependence of the reaction rate on both reactants, amino groups of PVAm and EQ. The reaction rate constant *k* was determined from the slope to be $k = 22.749\ \mathrm{mol^{-1} \cdot L \cdot s^{-1}}$.

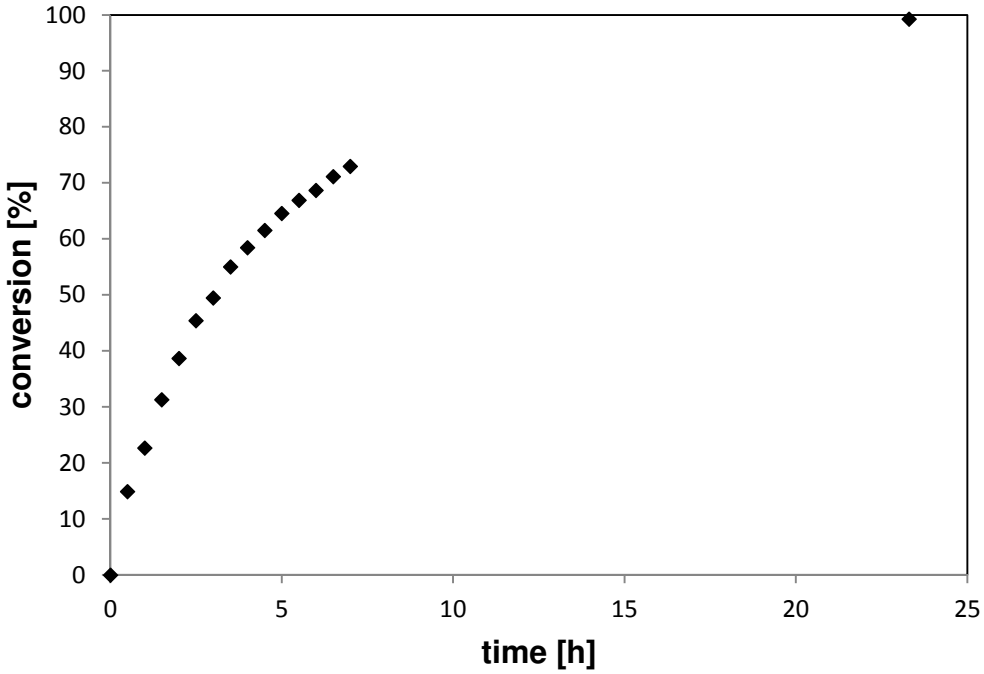

Figure 17. Conversion of PVAm (salt free) with EQ. Conversion versus reaction time (♦ EQ at 60 °C). Reaction conditions: PVAm/EQ = 100/27.

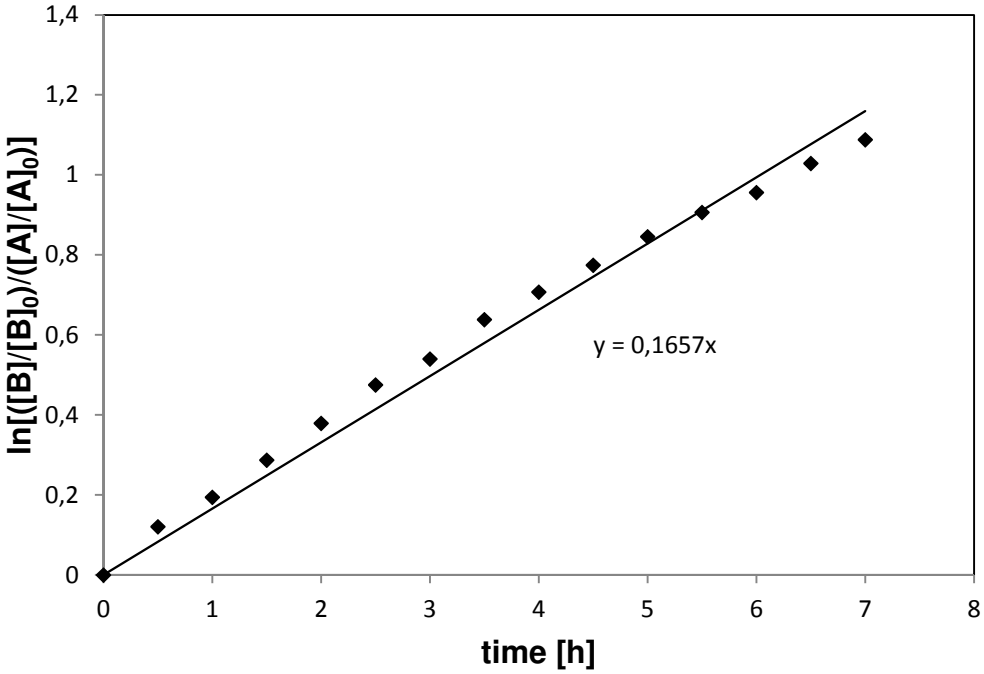

Figure 18. Conversion of PVAm (salt free) with EQ. Second-order plot: (♦ EQ at 60 °C), reaction conditions: PVAm/EQ = 100/27.

2.3.3 Reaction of Lupamins

The aim of this section was to transfer the reaction of PVAm (salt free) with functional epoxides to the salt containing charges Lupamin 9095 and Lupamin 1595. It was observed that the pH-value of the solution plays an important role for the reaction. Freeze-dried PVAm (salt free) dissolved in dist. water has a pH of about 12. Freeze-dried Lupamin 9095 and 1595 dissolved in dist. water have a pH of about 8. This lower pH-value seems to hinder the reaction. At the lower pH of 8, there is no reaction between the Lupamin and the functional epoxide. The pH-value needs to be raised to about 13 before the reaction of the Lupamins with EQ and EA12 can take place. This can be attributed to the lower nucleophilicity of the amine groups at lower pH-values compared to the nucleophilicity at higher pH-values. At low pH-values, the amine groups are partly protonated and not able to nucleophilicly attack the epoxy ring. Both NaOH and KOH were tested to adjust the pH. Unfortunately, due to the added base to raise the pH, some side reactions occurred. The functional epoxide EQ is partly hydrolyzed during the reaction. This needs to be incorporated in the calculation of the amount of educt to use, because the obtained degrees of functionalization for EQ are lower than the adjusted ones. In addition the reaction time is longer for the reaction of Lupamins than for the reaction of salt free PVAm with functional epoxides, using the same reaction conditions. It takes 5 days instead of 2 days. As bases NaOH and KOH were tested whereof KOH leads to slightly better results concerning the degree of functionalization and the reproducibility than NaOH. NH_3 is not suitable as base, because it reacts with the epoxides itself and leads to crosslinking. A careful adjusting of the pH with KOH leads to reproducible results. The hydrolysis of EQ can be determined and disregarded and the reaction with the Lupamins as educts is a good possibility for scale up. Table 9 shows the expected and obtained degrees of functionalization for the reaction of Lupamins with functional epoxides EA12 and EQ.

Table 9. Results for the reaction of Lupamins with epoxides EA12 and EQ.

Name	n [%]*	Degree of functionalization [%]			
	PVAm	EA12 exp.	EQ exp.	EA12 obt.**	EQ obt.**
L9095-EQ$_{11}$-EA12$_{12}$	100	12	12	12	11
L9095-EA12$_{35}$	100	38	-	35	-
L9095-EA12$_{24}$	100	22	-	24	-
L1595-EQ$_{6}$-EA12$_{12}$	100	12	12	12	6
L1595-EA12$_{42}$	100	46	-	42	-
L1595-EA12$_{20}$	100	22	-	20	-

exp. = expected, obt. = obtained, * Amount of repeating units in %, ** calculated from ^{1}H NMR spectroscopy.

2.3.4 Polymer Fractionation

Dealing with polymers one should always be aware of distributions. First, there is a distribution in the molecular weight. And second after a polymer analogous reaction there is a distribution in the functionality. Not every polymer molecule might be functionalized in the same way. It is known from cellulose that the functionalization of cellulose with acet anhydride does not lead to a statistically functionalized polymer but leads to fully functionalized chains and chains that are not functionalized.[13] One approach to determine the distribution in functionalization can be GPC (gel permeation chromatography) experiments. From the obtained molecular weight distributions one can get first hints on the homogeneity of the polymer functionalization. If the distribution is broader than before the post polymerization modification, the functionalization is not statistically distributed. GPC experiments are only possible for water, tetrahydrofuran (THF) or chloroform soluble

polymers due to technical reasons. The polymers prepared in this work are insoluble in THF and chloroform and in some cases also insoluble in water. The polymers which were soluble in water could not be measured with GPC because they were adhering to the GPC columns and could therefore not be detected. Therefore NMR measurements were chosen as approach to determine differences between the different fractions of the polymers. To determine if the reaction of PVAm with functional epoxides gives statistically functionalized polymers, polymer samples were prepared by fractional precipitation.

Fractionation of PVAm-EQ$_{40}$

PVAm-EQ$_{40}$ was fractionated by dissolution in methanol (p.a.) and addition of diethyl ether (p.a.) until an opalescent solution was obtained followed by centrifugation to isolate the precipitate and repeating these steps several times. The resulting six different fractions are listed in Table 10. Fraction 6 is the evaporated rest of the solution. The residual solvent was removed from the fractions by vacuum distillation (15 mbar). Acetone was not suitable for fractionation.

It was observed that the solubility decreases with increasing fraction number. The three later fractions number 4, 5 and 6 could not be brought back into solution properly for NMR measurements. They were swelling and forming a gel. A possible reason for this is that the polymer was fractionated by molecular weight and the later fractions contain polymers of higher molecular weight which causes the reduced solubility once they are isolated. The fractions were analyzed by ^{1}H NMR spectroscopy (Figure 19). Although Fraction 6 formed only a gel it was measured.

Table 10. Composition of the fractions from PVAm-EQ_{40}.

Fraction	Et_2O [mL] [a]	EQ [%] [b]	Solid [mg] ([%]) [c]
1	15	39	44 (18)
2	2	39	73 (29)
3	1	40	34 (14)
4	1.5	- [d]	37 (15)
5	10	- [d]	12 (5)
6	-	38	52 (21)
			Σ252 (101)

[a] mL of diethyl ether used for precipitation, [b] amount of EQ in the polymer fraction determined by ^{1}H NMR spectroscopy, [c] some samples contain small amounts of solvent, [d] precipitate formed only a gel with MeOD and was not measured by NMR spectroscopy.

The degree of functionalization of the different fractions with EQ was in all cases with only small deviations the same. This shows that the polymers are functionalized homogeneously and there are no fractions with lower or higher degree of functionalization. The ^{1}H NMR spectra of fraction 1, 2, 3 and 6 and of the original polymer are shown in Figure 19. It can be seen that they all look the same. The spectrum of fraction 6 shows a lot of solvent peaks and the polymer peaks are broadened. However the spectrum could be analyzed.

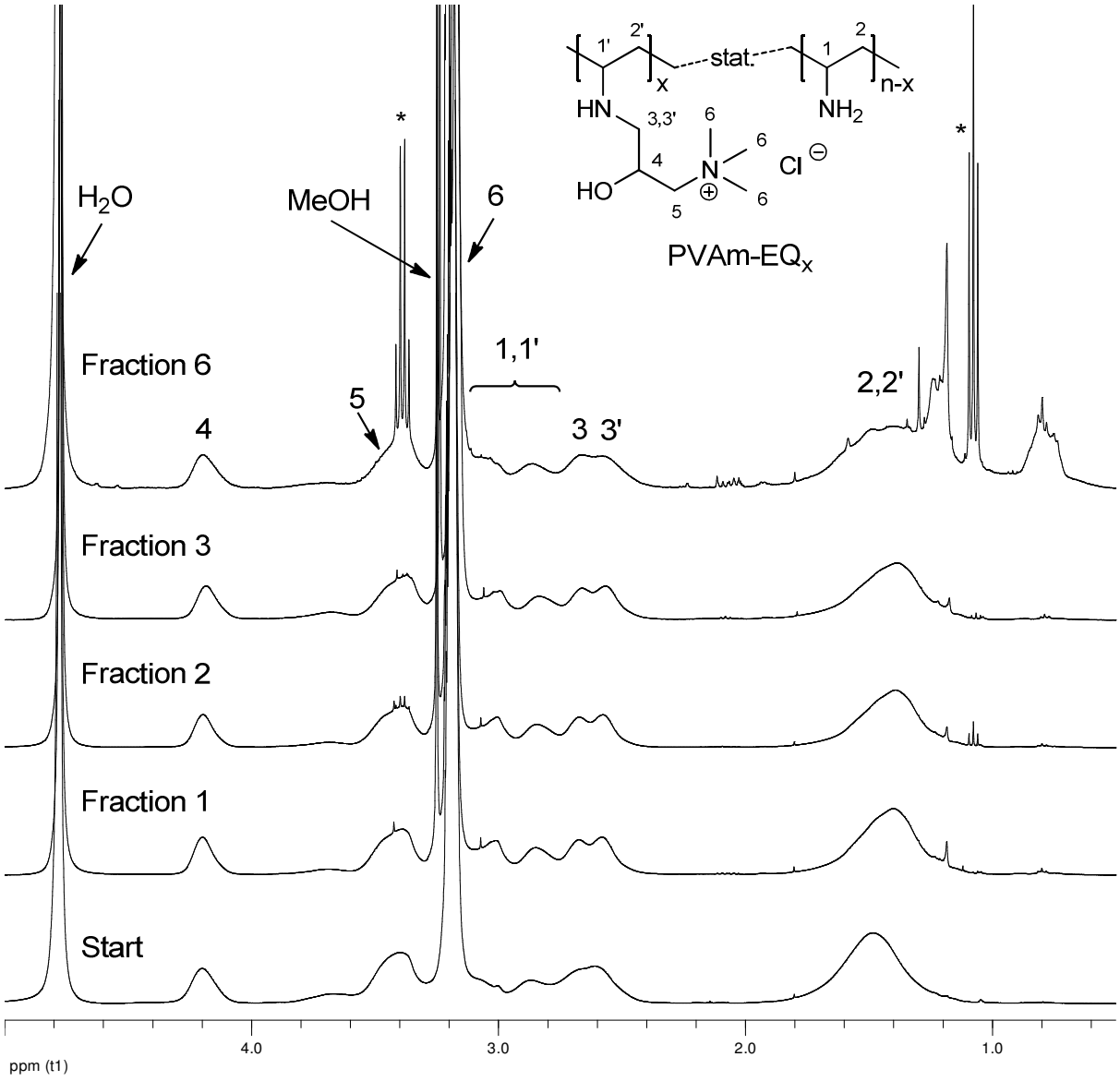

Figure 19. ^{1}H NMR spectra of fraction 1, 2, 3 and 6 of the fractionation of PVAm-EQ_{40} and of the original polymer, solvent MeOD. * residual Et_2O from the precipitation.

Fractionation of PVAm-EA12$_{41}$

The polymer obtained by functionalization of PVAm (salt free) with 41 % EA12 can not be precipitated. None of the tested solvents (Et_2O, acetone, dichloromethane, water) caused a precipitate or an opalescent solution when it was added to the methanolic polymer solution. In

each case a clear solution was obtained. This is a hint towards a statistical functionalization of PVAm with EA12.

Fractionation of PVAm-EA12$_{10}$

PVAm-EA12$_{10}$ was fractionated by dissolution in methanol (p.a., 2 wt%) and then adding diethyl ether (p.a.) until an opalescent solution was obtained followed by centrifugation to isolate the precipitate and repeating these steps several times. The resulting three different fractions are listed in Table 11. Fraction 3 is the evaporated rest of the solution. The residual solvent was removed from the fractions by vacuum distillation (15 mbar). Different solvents were tested for precipitation. Addition of dichloromethane, water or acetone to a methanolic solution of PVAm-EA12$_{10}$ leads only to a clear solution. Only addition of diethyl ether gives a stable opalescent solution.

Table 11. Composition of the fractions from PVAm-EA12$_{10}$.

Fraction	Et_2O [mL] [a]	EA12 [%] [b]	Solid [mg] ([%]) [c]
1	7	10	13 (29)
2	5	12	20 (44)
3	-	10	8 (18)
			Σ41 (91)

[a] mL of diethyl ether used for precipitation, [b] amount of EA12 in the polymer fraction determined by ^{1}H NMR spectroscopy, [c] some samples contain small amounts of solvent.

The fractions were analyzed by ^{1}H NMR spectroscopy. The degree of functionalization of the different fractions with EA12 was in all cases with only small deviations the same. This shows that the polymers are functionalized homogeneously and there are no fractions with

lower or higher degree of functionalization. The ^{1}H NMR spectra of fraction 1, 2 and 3 and of the original polymer are shown in Figure 20. It can be seen that they all look the same.

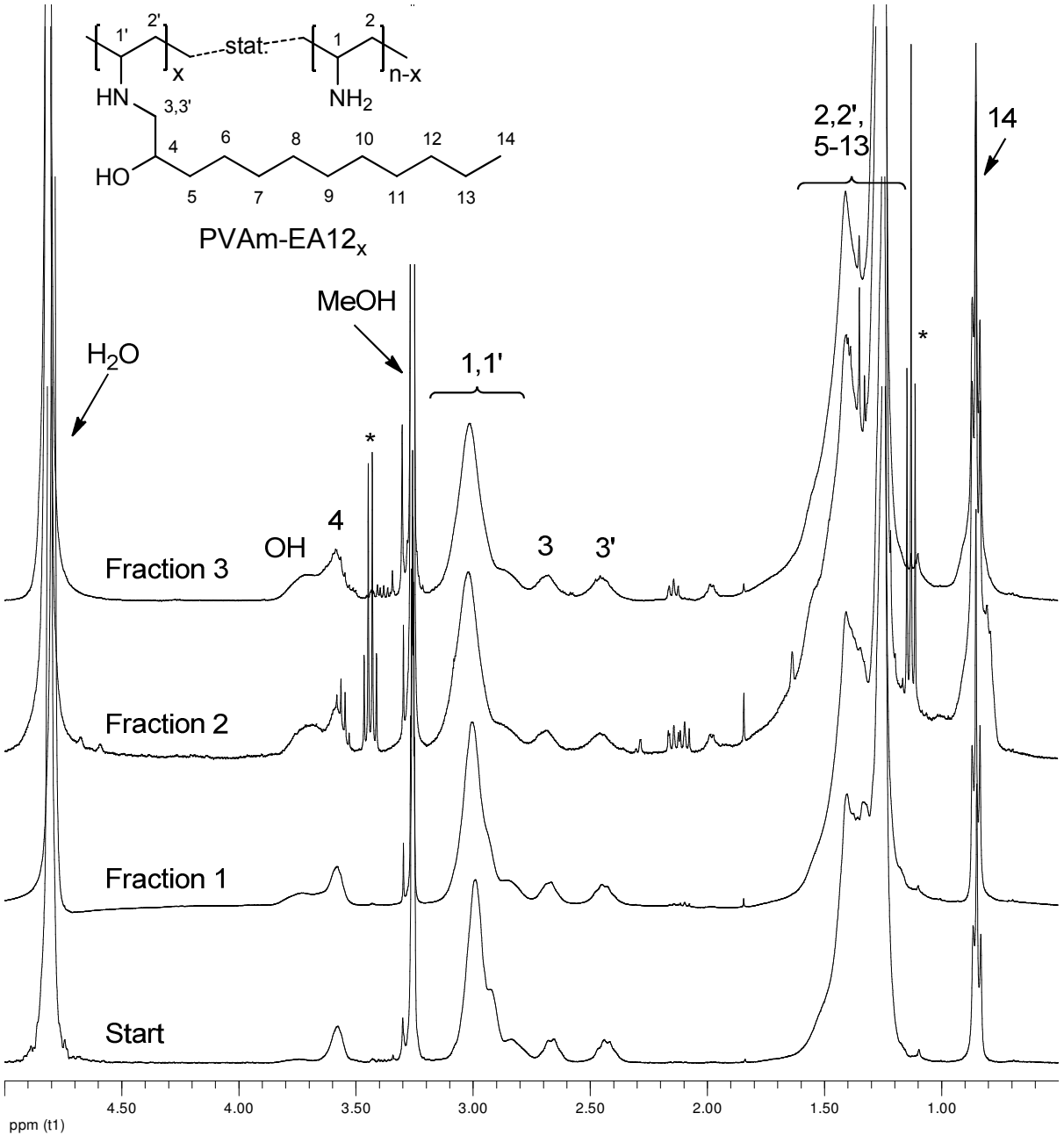

Figure 20. ^{1}H NMR spectra of fraction 1, 2 and 3 of the fractionation of PVAm-EA12$_{10}$ and of the original polymer, solvent MeOD. * residual Et_2O from the precipitation.

Fractionation of PVAm-EQ_{14}-$EA12_{11}$

PVAm-EQ_{14}-$EA12_{11}$ was fractionated by dissolution in methanol (p.a., 2 wt%) and addition of diethyl ether (p.a.) until an opalescent solution was obtained followed by centrifugation to isolate the precipitate and repeating these steps several times. The resulting six different fractions are listed in Table 12. Fraction 6 is the evaporated rest of the solution. The residual solvent was removed from the fractions by vacuum distillation (15 mbar). Different solvents were tested for precipitation. Addition of chloroform, dichloromethane or acetone to a methanolic solution of PVAm-EQ_{14}-$EA12_{11}$ leads only to a clear solution. Only addition of diethyl ether gives a stable opalescent solution.

Table 12. Composition of the fractions from PVAm-EQ_{14}-$EA12_{11}$.

Fraction	Et_2O [mL] [a]	EQ [%] [b]	EA12 [%] [b]	Solid [mg] ([%]) [c]
1	25	14	12	29 (15)
2	4	14	11	59 (30)
3	4	15	12	52 (27)
4	4	14	10	24 (12)
5	4	14	11	12 (6)
6	-	15	12	38 (20)
				Σ214 (110)

[a] mL of diethyl ether used for precipitation, [b] amount of EQ and EA12 in the polymer fraction determined by ^{1}H NMR spectroscopy, [c] some samples contain small amounts of solvent.

The fractions were analyzed with ^{1}H NMR spectroscopy. The degree of functionalization of the different fractions with EQ and EA12 was in all cases with only small deviations the

same. This shows that the polymers are functionalized homogeneously along the polymer chain and there are no fractions with lower or higher degree of functionalization. The ^{1}H NMR spectra of fraction 1, 2, 3, 4, 5 and 6 and of the original polymer are shown in Figure 21. It can be seen that they all look the same.

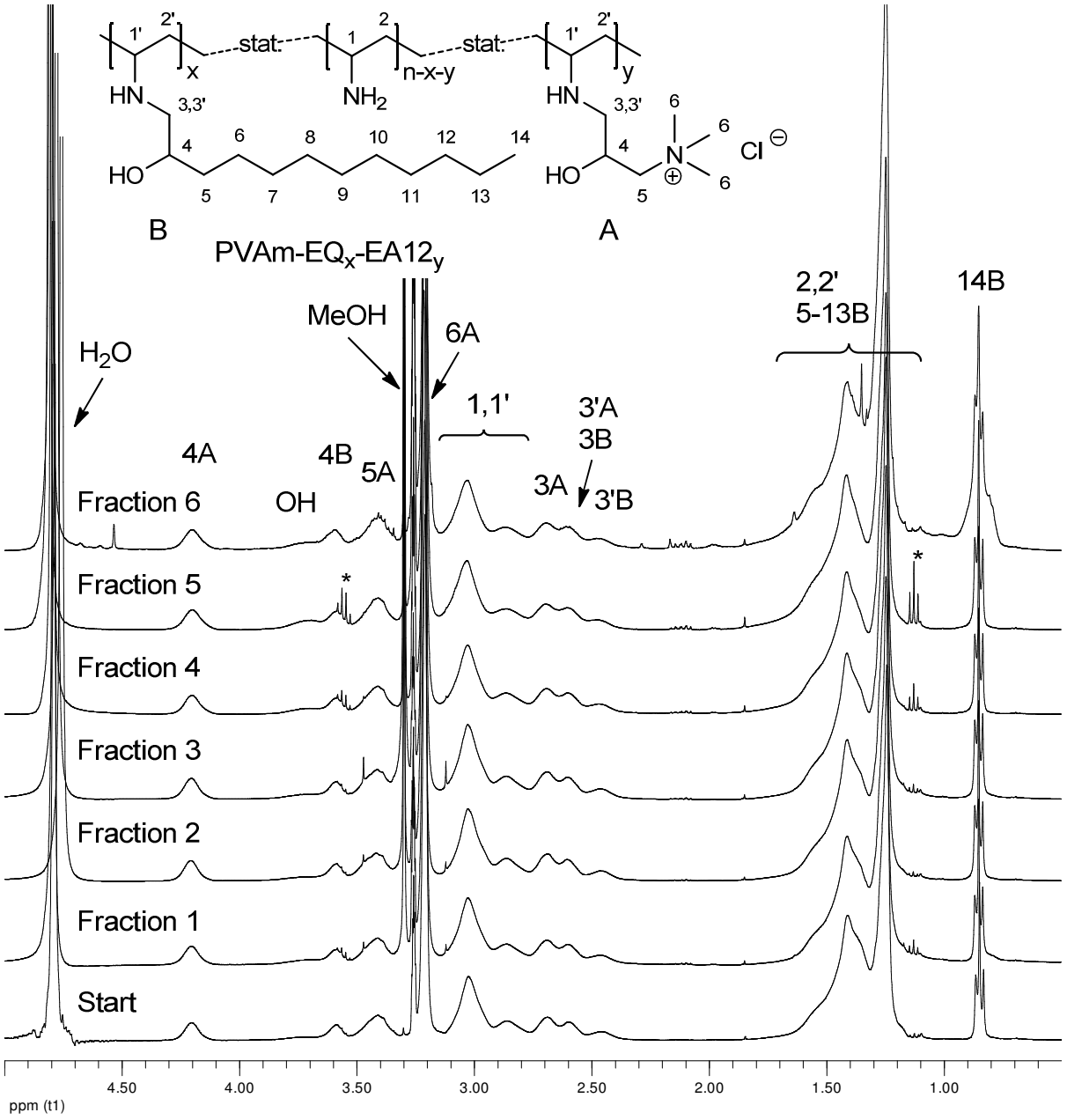

Figure 21. ^{1}H NMR spectra of fraction 1, 2, 3, 4, 5 and 6 of the fractionation of PVAm-EQ$_{14}$-EA12$_{11}$ and of the original polymer, solvent MeOD. * residual Et_2O from the precipitation.

The performed fractionation experiments show that the functionalization of PVAm with different functional epoxides leads to statistically functionalized polymers. Via NMR analysis no differences in functionalization could be determined. Due to differences in solubility and viscosity of the fractions (especially for PVAm-EQ_{40}) it can be assumed that the polymers were fractionated by molecular weight and the later fractions contain polymers of higher molecular weight which causes the reduced solubility once they are isolated.

2.4 Conclusions

Amphiphilic multifunctional poly(vinyl amine)s with long alkyl chains, quaternary ammonium groups or both together were successfully prepared by polymer analogous reaction of PVAm with functional epoxides. The reaction was studied in detail. Equimolar and reproducible conversions were obtained. There is a limit to the degree of functionalization at around 70 % for the functionalization with cationic groups. This limit stems from the electrostatic repulsion of the groups. For the functionalization with epoxyalkanes there seems to be a limit at about 50 %. This can be due to sterical hindrance. A complete conversion of oxiranes has been proven by Raman spectroscopy and the polymers were characterized by NMR spectroscopy. The degree of functionalization can easily be adjusted by the ratio of functional epoxides to amine groups so that a high variety of polymers is accessible. The reaction kinetics were analysed. Both reactions, with the cationic epoxide and with the epoxyalkane, follow a second-order kinetic and are dependent on the concentration of both, amine groups and epoxide. Raising the temperature leads to an increased reaction rate. The reaction rate constants k were calculated from the fitted data. The reaction was successfully transferred to technically available PVAm (Lupamin 9095 and Lupamin 1595) so that a scale up of the reaction is possible. Fractionation experiments were performed and demonstrated that the functionalization of PVAm with different functional epoxides leads to statistically

functionalized polymers. The prepared multifunctional polymers can be used for surface coating. The degree of functionalization with cationic groups will affect the strength of adhesion to the surface.

2.5 Literature

[1] M. A. Gauthier, M. I. Gibson, H-A. Klok, *Angew. Chem. Int. Ed.* **2009**, *48*, 48-58.

[2] Badesso, R.J.; Pinschmidt, Jr., R.K.; Sagl, D.J. *Proc. Am. Chem. Soc., Div. Polym. Mat. Sci. Eng.* **1993**, 69, 251.

Badesso, R.J.; Nordquist, A.F.; Pinschmidt, Jr., R.K.; Sagl, D.J. *In Hydrophilic Polymers: Performance with Environmental Acceptance*; Glass, E., Ed.; American Chemical Society: Washington, D.C., **1995**; 489

[3] Technisches Merkblatt *N-Vinylformamid*, Mitsubishi Kasai, Japan, **1997**.

[4] Pinschmidt Jr., R. K.; Sagl, D. J. *Polymeric Materials Encyclopedia*; Ed.: Salamone, J. C.; CRC Press New York **1996**, 7095 ff.

[5] Gu, L.; Zhu, S.; Hrymak, A. N.; Pelton, R. H. *Polymer* **2001**, *42*, 3077–3086.

[6] Gu, L.; Zhu, S.; Hrymak, A. N. *J. Appl. Polym. Sci.* **2002**, *86*, 3412–3419.

[7] Kröner, M.; Dupuis, J., Winter, M. *J. Prakt. Chem.* **2000**, *342*, 115–131.

[8] Produkt-Informationsbroschüre zu Lupaminen®, BASF AG, Ludwigshafen, **2000**.

[9] T. Tashiro *Macromol. Mater. Eng*. **2001**, *286*, 63-87.

[10] Y. He *Dissertation „From Cyclic Cyrbonate Bifunctional Couplers to Amphiphilic Poly(ethylene imine)s"* **2010**, ITMC RWTH Aachen.

[11] N. Pasquier, H. Keul, E. Heine, M. Moeller *Biomacromolecules* **2007**, *8* (9), 2874-2882.

[12] N. Pasquier, H. Keul, E. Heine, M. Moeller, B. Angelov, S. Linser, R. Willumeit *Macromolecular Bioscience* **2008**, *8* (10), 903-915.

[13] Th. Eicher, W. Fischer *Ullmanns Encyklopädie der technischen Chemie*, 4. Edition, Volume 9, (Celluloseester), 227-246.

CHAPTER 3

SYNTHESIS OF AMPHIPHILIC POLYMERS AND THEIR CHARACTERIZATION IN SOLUTION

3.1 Introduction

The post polymerization modification of poly(vinyl amine) (PVAm) with functional epoxides provides a straightforward route to the synthesis of multifunctional amphiphilic polyamines. Cationic groups and alkyl chains can easily be incorporated into the polymer backbone. PVAm is a linear, weak, cationic polyelectrolyte with up to 100 % free primary amine groups, one per repeating unit. It is nowadays prepared from poly(N-vinyl formamide) (PNVF) by hydrolysis under moderate conditions both in acidic and in basic media and is commercially available from BASF SE (Lupamin). The degree of hydrolysis and thereby the charge density of the polymer backbone can be adjusted by the choice of the hydrolysis conditions like temperature, reaction time, and concentration of acid or base.[1,2,3,4,5,6]

PVAm has been applied in many fields like catalysis[7], waste water treatment[8], paper making[9,10,11], chelation[12], recovery of oil[13,14,15,16,17,18,19,20], and as superabsorber[21,22,23,24]. Some studies on the modification of PVAm with the goal to obtain polymeric water-soluble dyes have been performed.[25] For instance Spange *et al.* modified PVAm with azo dyes to introduce chromophores in the polymeric structure.[26] Furthermore PVAm was modified to give polymer surfactants[27], and to mimic natural enzymes[7].

The objective of this work is the functionalization of PVAm on the one hand with a combination of cationic and alkyl oxiranes of different chain length and on the other hand with different concentrations of an alkyl oxirane only. The aim is to get insight into the

structure-solution properties relation of the developed polymers, in dependence on the chain length and the concentration of introduced alkyl chains.

3.2 Experimental Part

Poly(vinyl amine) is composed of different repeating units: vinyl amine and residual vinyl formamide, whose ratio can be determined by ^{1}H NMR spectroscopy. In what follows, $\overline{M}$ denotes the averaged molecular weight per repeating unit calculated from the ^{1}H NMR spectrum.

3.2.1 Materials

Starting materials were used as received: 1,2-epoxyoctane (**EA8**) (Alfa Aesar, 96 %), 1,2-epoxydecane (**EA10**) (Alfa Aesar, 97 %), 1,2-epoxydodecane (**EA12**) (Alfa Aesar, 96 %), 1,2-epoxytetradecane (**EA14**) (TCI Europe, 95 %), 1,2-epoxyhexadecane (**EA16**) (Aldrich, 86 %), 1,2-epoxyoctadecane (**EA18**) (Alfa Aesar, 90 %) and glycidyltrimethylammonium chloride (**EQ**) (Aldrich, 75-80 % in water; since the oxirane degrades in time, the active content is determined just before use by NMR spectroscopy), Seral-water (conductivity 0.055 µS/cm). Poly(vinyl amine) (PVAm) has been supplied by BASF (explorative material: salt free PVAm, supplier information: purified by ultra filtration, molecular weight = 340.000 g/mol). PVAm was freeze-dried before use. The dialysis tubings of regenerated cellulose had a molecular weight cut off of 50 kDa (CelluSep). The analytical data of the PVAm (salt free) are summarized in Table 1.

Table 1. Analytical data of salt free poly(vinyl amine).

Polymer	MW [a] [g/mol]	DH [a] [%]	DH [b] [%]	Salt content [b] [%]	$\overline{M}$ (repeating unit) [c] [g/mol]
PVAm (salt free)	340.000	100	99	1	43.60

DH = Degree of hydrolysis, [a] average molecular weight and DH according to supplier information, [b] determined by NMR, [c] $\overline{M}$ = averaged molecular weight per repeating unit calculated from NMR.

3.2.2 Measurements

^{1}H and ^{13}C NMR spectra were recorded on a Bruker AV 400 FT-NMR spectrometer at 400 MHz (^{1}H) and 100 MHz (^{13}C), respectively. Deuterated methanol (MeOD) was used as solvent and the solvents residual peak was used as internal standard.

The Raman spectra were recorded at room temperature on a Bruker RFS 100S spectrometer with a Nd:YAG-Laser (1064 nm, 400 mW) at a spectral resolution of 4 cm^{-1} with 1000 scans.

Fluorescence spectroscopy measurements were performed on a Fluoromax-4P spectrofluorometer (HORIBA Jobin Yvon). Air-saturated solutions (at 20 °C) were measured with 90° geometry and a slit opening of 1 nm. An emission wavelength of λ_{Em} = 390 nm was chosen for fluorescence excitation spectra and an excitation wavelength of λ_{Ex} = 339 nm was chosen for fluorescence emission spectra. Spectra were accumulated with an integration time of 30 nm/min.

To prepare the samples for the fluorescence measurements, first a solution of pyrene in acetone with a concentration of 6×10^{-3} mol/L and polymer solutions of 1 mg/mL and 0.01 mg/mL in Seral-water were prepared. To dissolve the polymers the solutions were stirred over night at 60 °C. Each sample solution was prepared by adding 1 mL of the pyrene solution into an empty vial, evaporating the acetone for 12 h at RT, adding the polymer

solution (10 mL) and shaking the solutions for 12 h at 60 °C in a "Thermoshaker (GFL 3032)". Samples with polymer concentrations ranging from 1 mg/mL to 0.0001 mg/mL were prepared. For the fluorescence measurements, ca. 3 mL solution was placed in a quartz cell with a base area of 1.0 × 1.0 cm² and tempered for 15 minutes at 20 °C prior to measurement.

3.2.3 Name of Prepared Products

Polymers are named using a threefold expression: The first part of this expression denotes the used poly(vinyl amine). The second and the third part denote the used epoxides and the corresponding indices show the degrees of functionalization based on the total amount of amino groups. A number in front of the second and third part assigns in which order the epoxides are added to the reaction solution. If there is no number, the epoxides were added simultaneously. The used abbreviations are given in Table 2.

Table 2. Abbreviations for the denotation of the products.

Unit	Correlation
PVAm	salt free PVAm, MW [a)] = 340.000 g/mol
EQ	glycidyltrimethylammonium chloride
EA8	epoxyoctane
EA10	epoxydecane
EA12	epoxydodecane
EA14	epoxytetradecane
EA16	epoxyhexadecane
EA18	epoxyoctadecane

[a)] supplier information

For example, PVAm-1.EQ$_{11}$-2.EA12$_{11}$ stands for the functionalization of salt free PVAm with 11 % EQ and 11 % EA12. In this case the epoxides were added sequentially and PVAm was first reacted with EQ and afterwards reacted with EA12.

3.2.4 Syntheses

General Procedure for the Synthesis of PVAm-1.EQ$_{11}$-2.EAX$_{11}$ Using the Example of PVAm-1.EQ$_{11}$-2.EA8$_{11}$

Step 1: PVAm-EQ$_{11}$

To a solution of freeze-dried salt free PVAm (2.143 g, $\overline{M}$(repeating unit) = 43.60 g/mol, 0.049151 mol repeating units) in dist. water/methanol (p.a.) (40 mL/80 mL) at room temperature a solution of glycidyltrimethylammonium chloride (EQ, 54 %, 1.932 g, M = 151.63 g/mol, 0.006882 mol) in methanol (p.a., 30 mL) was added. The solution was heated to 60 °C and stirred for 3 d and then dialysed against dist. water. The water was exchanged several times. The product was isolated by freeze-drying as a colourless solid. The freeze-dried product was soluble in methanol and in water. The product was characterized by NMR and Raman spectroscopy to verify a full conversion of the epoxide. The degree of functionalization was determined by ^{1}H NMR spectroscopy.

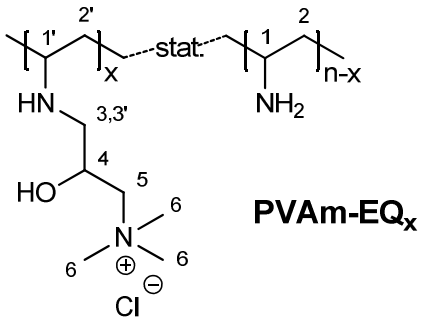

PVAm-EQ$_x$

Yield: 2.917 g, 92 %, degree of functionalization x = 11 %. ^{1}H NMR (MeOD-d_4): δ (ppm) = 1.17 – 1.88 (m, CH(NHR)C**H$_2$**, H$^{2,2'}$), 2.57 – 2.81 (m, R$_2$CHNHC**H$_2$**, H$^{3,3'}$), 2.81 – 3.19 (m,

C**H**(NHR)CH_2, $H^{1,1'}$), 3.19 – 3.32 (s, br, $CH_2N(C\mathbf{H_3})_3$, H^6), 3.36 – 3.58 (m, $CH(OH)C\mathbf{H_2}N(CH_3)_3$, H^5), 3.58 – 3.90 (s, br, CHO**H**), 4.15 – 4.36 (m, $CH_2C\mathbf{H}(OH)CH_2$, H^4). ^{13}C NMR (MeOD-*d*$_4$): δ (ppm) = 41.80 – 48.60 (m, **C**H**C**H_2, $C^{1,1'}$, $C^{2,2'}$, backbone), 50.30 – 51.80 (br, **C**H_2CH(OH)$CH_2N(\mathbf{C}H_3)_3$, C^3), 55.08 (s, br, $CH_2N(\mathbf{C}H_3)_3$, C^6), 66.30 – 67.30 (br, $CH_2\mathbf{C}H(OH)CH_2$, C^4), 70.40 – 71.20 (br, $CH(OH)\mathbf{C}H_2N(CH_3)_3$, C^5), the signals of **C**H**C**H_2 ($C^{1,1'}$, $C^{2,2'}$, backbone) and **C**H_2CH(OH)$CH_2N(\mathbf{C}H_3)_3$ (C^3) are only distinguishable from the baseline noise in quantitative ^{13}C measurements on a 600 MHz spectrometer.

Step 2: PVAm-1.EQ$_{11}$-2.EA8$_{11}$

To a solution of PVAm-EQ$_{11}$ (0.580 g, $\overline{M}$(repeating unit) = 43.60 g/mol, 0.009707 mol repeating units) in methanol (p.a., 30 mL), a solution of epoxyoctane (EA8, 96 %, 0.130 g, M = 128.21 g/mol, 0.000971 mol) in methanol (p.a., 10 mL) was added at room temperature. The solution was heated to 60 °C and stirred for 2.5 d and then dialysed against dist. water. The solvent was exchanged several times. The freeze-dried colourless product was soluble in methanol and in water. The product was characterized by NMR and Raman spectroscopy to verify a full conversion of the epoxide. The degree of functionalization was determined by ^{1}H NMR spectroscopy.

In general, the epoxyalkanes EAX with X = 8, 10, 12, 14 were added to the reaction solution dissolved in methanol (p.a., 10 mL) and the epoxyalkanes EA16 and EA18 were added to the reaction solution dissolved in THF (p.a., 10 mL). The reaction solutions were stirred for different times until the reaction was complete and then dialysed against methanol or THF followed by dialysis against dist. water, depending on the solubility of the educts. Reagents and reaction times are listed in Table 3.

Table 3. Synthesis of PVAm-1.EQ$_{11}$-2.EAX$_{11}$ (**2a – 2f**): reagents and reaction times.

	Name	PVAm-EQ$_{11}$ [g (mol r.u.)][a)]	EAX [g (mol)]	Reaction time [d]
2a	**PVAm-1.EQ$_{11}$-2.EA8$_{11}$**	0.580 (0.009707)	0.130 (0.000971)	2.5
2b	**PVAm-1.EQ$_{11}$-2.EA10$_{11}$**	0.580 (0.009707)	0.158 (0.000971)	2.5
2c	**PVAm-1.EQ$_{11}$-2.EA12$_{11}$**	0.580 (0.009707)	0.186 (0.000971)	5.5
2d	**PVAm-1.EQ$_{11}$-2.EA14$_{11}$**	0.580 (0.009707)	0.217 (0.000971)	5.5
2e	**PVAm-1.EQ$_{11}$-2.EA16$_{11}$**	0.298 (0.004988)	0.125 (0.000499)	11
2f	**PVAm-1.EQ$_{11}$-2.EA18$_{11}$**	0.298 (0.004988)	0.140 (0.000499)	11

[a)] r.u. = repeating unit

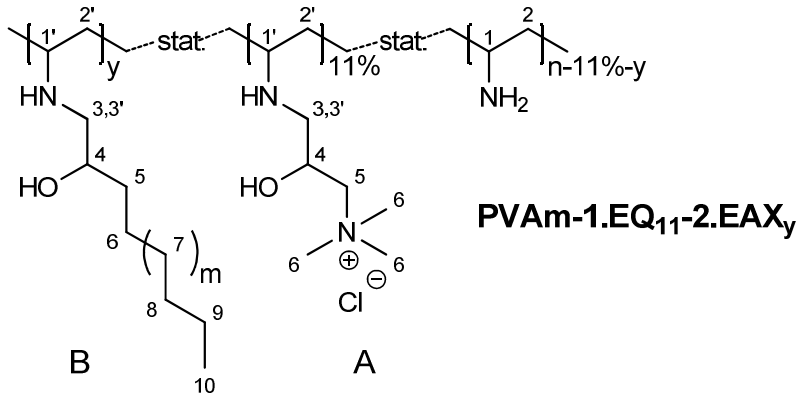

Degree of functionalization y = 11 %. ^{1}H NMR (MeOD-d_4): δ (ppm) = 0.84 – 0.98 (m, CH(OH)(CH$_2$)$_n$C**H$_3$**, H^{10B}), 1.17 – 1.88 (m, CH(OH)(C**H$_2$**)$_n$CH$_3$, H$^{5\text{-}9B}$, CH(NHR)C**H$_2$**, H$^{2,2'}$), 2.35 – 2.57 (m, 1H, R$_2$CHNHC**H$_2$**CH(OH), H$^{3'B}$), 2.57 – 2.81 (m, 3H, R$_2$CHNHC**H$_2$**CH(OH), H$^{3B,3A,3'A}$), 2.81 – 3.19 (m, C**H**(NHR)CH$_2$, H$^{1,1'}$), 3.19 – 3.32 (s, br, CH$_2$N(C**H$_3$**)$_3$, H^{6A}), 3.36 – 3.58 (m, CH(OH)C**H$_2$**N(CH$_3$)$_3$, H^{5A}), 3.58 – 3.73 (m, CH$_2$C**H**(OH)(CH$_2$)$_n$, H^{4B}), 3.73 – 3.90 (s, br, CHO**H**), 4.15 – 4.36 (m, CH$_2$C**H**(OH)CH$_2$, H^{4A}) (m = 1 for EA8, 3 for EA10, 5 for EA12, 7 for EA14, 9 for EA16 and 11 for EA18).

^{13}C NMR (MeOD-d_4): δ (ppm) = 14.80 (br, -$CH_2CH(OH)(CH_2)_n$**C**H_3, C^{10B}), 23.82 (br, -$CH_2CH(OH)(CH_2)_{n-1}$**C**H_2CH3, C^{9B}), 27.01 (br, -$CH_2CH(OH)CH_2$**C**$H_2(CH_2)_{n-2}CH_3$, C^{6B}), 30.22 – 31.61 (m, -$CH_2CH(OH)(CH_2)_2$(**C**$H_2)_{n-4}(CH_2)_2CH_3$, $C^{m(7B)}$), 33.21 (br, -$CH_2CH(OH)(CH_2)_{n-2}$**C**$H_2CH_2CH_3$, C^{8B}), 36.79 (br, -$CH_2CH(OH)$**C**$H_2(CH_2)_{n-1}CH_3$, C^{5B}), 41.80 – 48.60 (m, **C**H**C**H_2, $C^{1,1'}$, $C^{2,2'}$, backbone), 50.30 – 51.80 (br, **C**$H_2CH(OH)CH_2N($**C**$H_3)_3$, C^{3A}), 51.80 – 54.50 (br, **C**$H_2CH(OH)(CH_2)_9CH_3$, C^{3B}), 55.08 (s, br, -$CH_2CH(OH)CH_2N($**C**$H_3)_3$, C^{6A}), 66.30 – 67.30 (br, -CH_2**C**$H(OH)CH_2N(CH_3)_3$, C^{4A}), 70.40 – 71.20 (br, -$CH_2CH(OH)$**C**$H_2N(CH_3)_3$, C^{5A}), 70.40 – 71.20 (m, $CH_2CH(OH)$**C**$H_2N(CH_3)_3$, C^{5A} and CH_2**C**$H(OH)(CH_2)_9CH_3$, C^{4B}), the signals of **C**H**C**H_2 ($C^{1,1'}$, $C^{2,2'}$, backbone), **C**$H_2CH(OH)CH_2N($**C**$H_3)_3$ (C^{3A}) and **C**H_2**C**$H(OH)(CH_2)_9CH_3$ (C^{3B} and C^{4B}) are only distinguishable from the baseline noise in quantitative ^{13}C measurements on a 600 MHz spectrometer (m = 1 for EA8, 3 for EA10, 5 for EA12, 7 for EA14, 9 for EA16 and 11 for EA18).

General Procedure for the Synthesis of PVAm-EA12$_y$ Using the Example of PVAm-EA12$_{40}$

To a solution of freeze-dried salt free PVAm (0.200 g, $\overline{M}$(repeating unit) = 43.60 g/mol, 0.004588 mol repeating units) in dist. water/methanol (p.a.) (4 mL/8 mL) at 60 °C, a solution of 1,2-epoxydodecane (EA12, 96 %, 0.349 g, M = 184.32 g/mol, 0.001817 mol) in methanol (p.a.) (10 mL) was added. The solution was stirred at 60 °C for 2 d. Reagents and reaction times are listed in Table 4.

Table 4. Synthesis of PVAm-EA12$_y$ (**3a – 3d**): reagents and reaction times.

	Name	PVAm [g (mol r.u.)][a)]	EAX [g (mol)]	Reaction time [d]
3a	**PVAm-EA12$_{10}$**	0.200 (0.004588)	0.087 (0.000454)	3
3b	**PVAm-EA12$_{20}$**	0.200 (0.004588)	0.174 (0.000908)	3
3c	**PVAm-EA12$_{30}$**	0.200 (0.004588)	0.262 (0.001363)	3
3d	**PVAm-EA12$_{40}$**	0.200 (0.004588)	0.349 (0.001817)	3

[a)] r.u. = repeating unit

The resulting solution was dialysed first against methanol and second against dist. water. The methanol and the water were exchanged several times. The product was isolated as a colourless solid by freeze-drying. The freeze-dried product was soluble in methanol. The product was characterized by NMR and Raman spectroscopy to verify a full conversion of the epoxides. The degree of functionalization was determined by ^{1}H NMR spectroscopy.

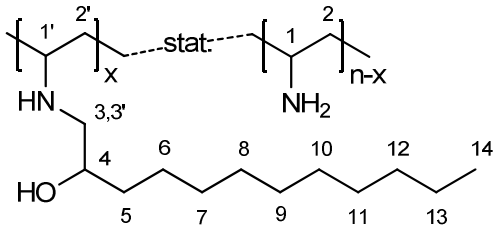

PVAm-EA12$_y$

Yield: 0.449 g, 82 %, degree of functionalization for PVAm-EA12$_{40}$ x = 40 %. ^{1}H NMR (MeOD-d_4): δ (ppm) = 0.84 – 0.98 (m, CH(OH)(CH$_2$)$_9$C**H$_3$**, H^{14}), 1.17 – 1.88 (m, CH(OH)(C**H$_2$**)$_9$CH$_3$, H$^{5\text{-}13}$, CH(NHR)C**H$_2$**, H$^{2,2'}$), 2.35 – 2.57 (m, 1H, R$_2$CHNHC**H$_2$**CH(OH), H$^{3'}$), 2.60 – 2.80 (m, 1H, R$_2$CHNHC**H$_2$**CH(OH), H^3), 2.80 – 3.19 (m, C**H**(NHR)CH$_2$, H$^{1,1'}$), 3.58 – 3.73 (m, CH$_2$C**H**(OH)(CH$_2$)$_9$, H^4), 3.73 – 3.90 (s, br, CHO**H**).

^{13}C NMR (MeOD-d_4): δ (ppm) = 14.80 (br, $(CH_2)_9\mathbf{C}H_3$, C^{14}), 23.82 (br, $(CH_2)_8\mathbf{C}H_2CH_3$, C^{13}), 27.01 (br, $CH_2CH(OH)CH_2\mathbf{C}H_2(CH_2)_7CH_3$, C^6), 30.22 – 31.61 (m, $(CH_2)_2(\mathbf{C}H_2)_5(CH_2)_2CH_3$, $C^{7\text{-}11}$), 33.21 (br, $(CH_2)_7\mathbf{C}H_2CH_2CH_3$, C^{12}), 36.79 (br, $CH_2CH(OH)\mathbf{C}H_2(CH_2)_8CH_3$, C^5), 41.80 – 48.60 (m, $\mathbf{C}H\mathbf{C}H_2$, $C^{1,1'}$, $C^{2,2'}$, backbone), 51.80 – 54.50 (br, $\mathbf{C}H_2CH(OH)(CH_2)_9CH_3$, C^3), 70.40 – 71.20 (br, $CH_2\mathbf{C}H(OH)(CH_2)_9CH_3$, C^4), the signals of $\mathbf{C}H\mathbf{C}H_2$ ($C^{1,1'}$, $C^{2,2'}$, backbone) and $\mathbf{C}H_2\mathbf{C}H(OH)(CH_2)_9CH_3$ (C^3 and C^4) are only distinguishable from the baseline noise in quantitative ^{13}C measurements on a 600 MHz spectrometer.

3.3 Results and Discussion

3.3.1 PVAm Based Amphiphilic Polymers

Based on the grafting-to strategy described in Chapter 2, a series of poly(vinyl amine)s, functionalized with the same concentration of cationic groups and hydrophobic groups with different alkyl chain lengths, was prepared. The aim was to get insight into the structure-solution properties relation of the developed polymers, depending on the length of the introduced alkyl chains. The synthetic route includes two steps:

1) In the first step, PVAm (salt free) is functionalized with EQ yielding a polymer functionalized with 11 mol% of cationic groups (PVAm-EQ_{11}).

2) Afterwards PVAm-EQ_{11} is converted with epoxyalkanes of different chain lengths. The epoxy groups react with the primary amine groups of the polymer to yield a series of polymers functionalized with 11 mol% of EQ and the same molar concentration of alkyl chains of different lengths. An overview of the used epoxyalkanes is given in Scheme 1.

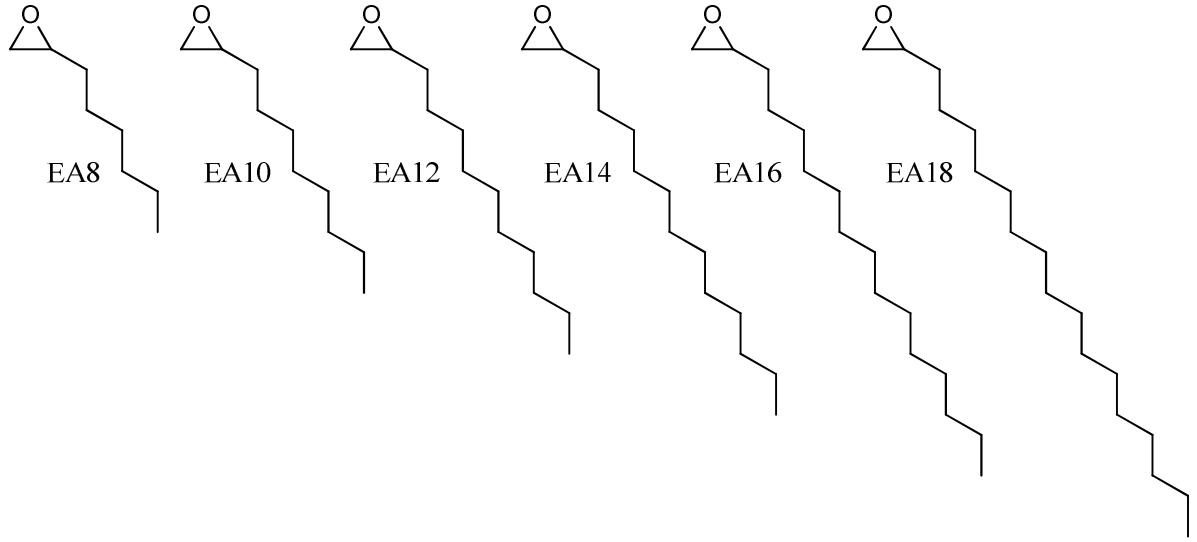

Scheme 1. Structure of epoxyalkanes used for the functionalization of PVAm-EQ_{11}.

The linear PVAm (salt free) used for this study has a molecular weight of 340.000 g/mol according to the supplier information and a degree of hydrolysis of 99 % (found by ^{1}H NMR spectroscopy). This means that 99 % of the repeating units had primary amine groups. This study focused on the functionalization of PVAm with 11 % cationic and 11 % hydrophobic groups, because this combination showed excellent antimicrobial activity as will be described in Chapters 4 and 5. The stepwise reaction of PVAm with the functional epoxides EQ and EAX is shown in Scheme 2. For the first reaction step, PVAm was reacted with EQ at 60 °C in a methanol/water mixture and afterwards purified by dialysis against dist. water. A degree of functionalization of 14 % EQ was aimed at. The degree of functionalization was determined by ^{1}H NMR spectroscopy. According to this analysis, 11 % of the primary amine groups were reacted with the cationic epoxide which satisfactorily fits the targeted degree of functionalization.

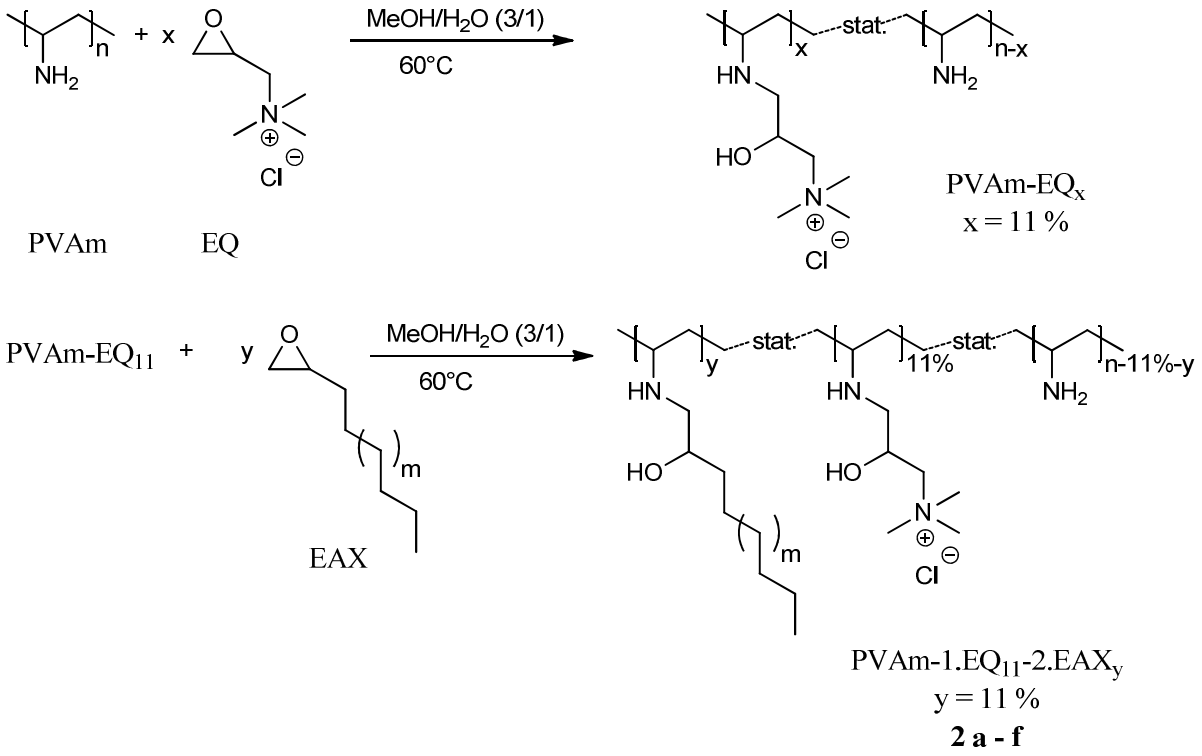

Scheme 2. Stepwise synthesis of PVAm-1.EQ_{11}-2.EAX_y, m = 1 for EA8, 3 for EA10, 5 for EA12, 7 for EA14, 9 for EA16, and 11 for EA18.

In the second reaction step, this product served as educt for the functionalization with the epoxyalkanes. This assures the same degree of functionalization with cationic groups within the series of different alkyl chain lengths. PVAm-EQ_{11} was reacted with different epoxyalkanes at 60 °C. A degree of functionalization of 11 % of hydrophobic groups was targeted. For the epoxyalkanes with shorter alkyl chains up to C14, a methanol/water mixture was used as solvent. The epoxyalkanes with longer alkyl chains were not soluble in methanol but in THF, whereas PVAm-EQ_{11} was not soluble in THF but in methanol or water. Therefore, a THF/methanol mixture was used as solvent for the reaction. The obtained products were purified by dialysis. For the epoxyalkanes with alkyl chain lengths of 14, 16, and 18, depending on the solubility of the educts, first a dialysis against methanol or THF was performed followed by dialysis against water. In low concentrations, the shorter epoxyalkanes

were soluble in water so that a dialysis against dist. water was sufficient to yield a pure product. Table 5 shows the obtained degrees of functionalization (determined by NMR spectroscopy) for the different reactions before and after the dialysis of the final products. The degree of functionalization can be calculated from the ^{1}H NMR spectra as described in Chapter 2. The difference between the degrees of functionalization with the hydrophobic groups EAX before and after the dialysis is very low and within the error of the NMR measurements. The obtained degrees of functionalization nicely fit the expected degrees. This means that the epoxides are completely reacted with the amine groups and that the products are not fractionated during the work up by dialysis. It was found by NMR spectroscopy that dialysis yields a very pure product.

Table 5. Composition of synthesized polymers determined by NMR spectroscopy.

Number	Name	EAX	EQ [%]*	EAX [%]	
	a.D.			b. D.	a. D.
2a	**PVAm-1.EQ$_{11}$-2.EA8$_{11}$**	EA8	11.0	8.4	9.6
2b	**PVAm-1.EQ$_{11}$-2.EA10$_{11}$**	EA10	11.0	9.9	10.1
2c	**PVAm-1.EQ$_{11}$-2.EA12$_{11}$**	EA12	11.0	9.5	10.6
2d	**PVAm-1.EQ$_{11}$-2.EA14$_{11}$**	EA14	11.0	10.3	11.6
2e	**PVAm-1.EQ$_{11}$-2.EA16$_{11}$**	EA16	11.0	12.9	10.6
2f	**PVAm-1.EQ$_{11}$-2.EA18$_{11}$**	EA18	11.0	10.8	10.1

b. D. = before dialysis, a. D. = after dialysis, * the degree of functionalization with EQ was known from step 1 and therefore set to 11 %.

A complete conversion of the epoxide has been verified by Raman spectroscopy, wherein no signals of the unreacted epoxide were found. The products are soluble in methanol. With increasing alkyl chain length, the solubility in methanol decreased so that the signals of the polymers within the NMR spectra broadened. However, this broadening was not disturbing the spectra interpretation and it was possible to calculate the degree of functionalization.

Based on the grafting-to strategy described in Chapter 2, a second series of poly(vinyl amine)s, functionalized with different concentrations of hydrophobic groups only, was prepared. The aim of this experimental study was to get new insight into the structure-solution properties relation of the developed polymers in dependence on the degree of functionalization with alkyl chains. The synthetic route includes only a single step:

1) PVAm (salt free) is reacted with the epoxyalkane EA12 to yield a series of polymers functionalized with different concentrations of alkyl chains.

This one-step reaction of PVAm with the functional epoxide EA12 is shown in Scheme 3.

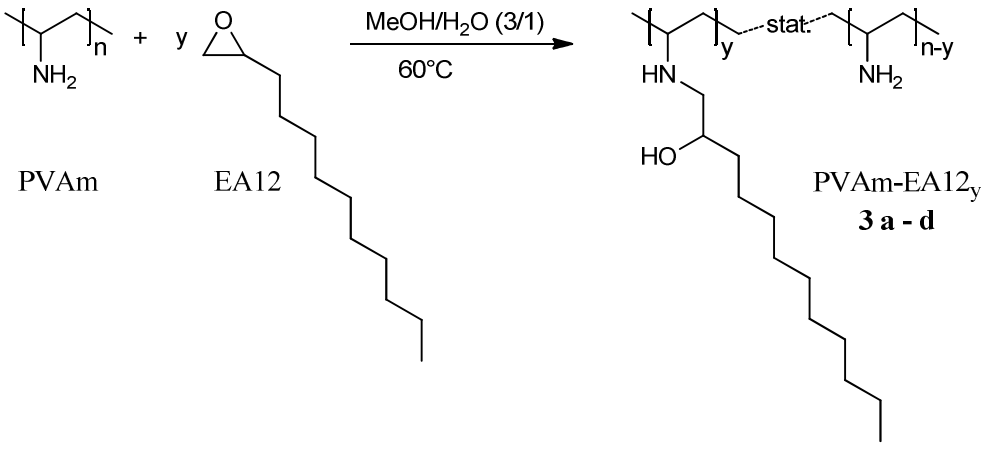

Scheme 3. One-step synthesis of PVAm-EA12$_y$.

PVAm was reacted with EA12 at 60 °C in a methanol/water mixture and afterwards purified by dialysis. Table 6 shows the obtained degrees of functionalization for the different reactions determined by NMR spectroscopy. The degree of functionalization can be calculated from the spectra as described in Chapter 2.

Table 6. Composition of synthesized polymers determined by NMR spectroscopy.

		Degree of functionalization [%]	
	Name	**Expected**	**Obtained***
3a	**PVAm-EA12$_{10}$**	10	10
3b	**PVAm-EA12$_{20}$**	20	21
3c	**PVAm-EA12$_{30}$**	30	32
3d	**PVAm-EA12$_{40}$**	40	41

*calculated from ^{1}H NMR spectroscopy.

The expected and obtained degrees of functionalization fit well. This means that the epoxides are completely reacted with the amine groups and that the products are not fractionated during work up by dialysis. It was verified by NMR spectroscopy that dialysis yields a very pure product. A complete conversion has been proven by Raman spectroscopy where no signals of the unreacted epoxide were found. The products are soluble in methanol and can be brought into an aqueous solution by solvent exchange to water using dialysis.

3.3.2 Fluorescence Measurements of Functional PVAm

The synthesized first series of polymers with cationic and hydrophobic groups of different chain lengths **2a-f** was characterized in solution by determining their critical concentration where aggregates start to form (critical aggregation concentration, CAC). The CAC was

determined by fluorescence measurements using pyrene as fluorescent dye (Scheme 4).[28,29,30,31] The influence of the alkyl chain length on the CAC was determined.

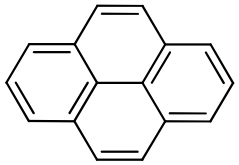

Scheme 4. Chemical structure of pyrene.

Fluorescence spectroscopy is a widely used, reliable technique to study the association behaviour of amphiphilic polymers. Depending on its chemical environment, the used fluorescent dye pyrene shows different fluorescence spectra. Pyrene itself is hydrophobic, i.e., if micelles are built by the polymer in an aqueous environment, pyrene transfers into the hydrophobic region inside of the micelles and the fluorescence spectrum changes. Due to this performance, it is possible to investigate the association behaviour and to determine the CAC of the different polymers. Going from a hydrophilic to a hydrophobic environment a red shift of the absorption band can be observed in the excitation spectrum of pyrene alongside an enhanced excitation intensity. In the emission spectrum, a red shift of the absorption band is also observed. The absorption band at 371 nm is shifted to 373 nm. In addition, a new absorption band at 383 nm appears. Figure 1 shows the emission spectrum of pyrene in an aqueous solution in comparison to a spectrum of pyrene in an aqueous solution containing polymer **2c** (PVAm-1.EQ$_{11}$-2.EA12$_{11}$) above the CAC. The red shift of the absorption band from 371 nm to 373 nm and the appearance of the new absorption band at 383 nm can clearly be seen.

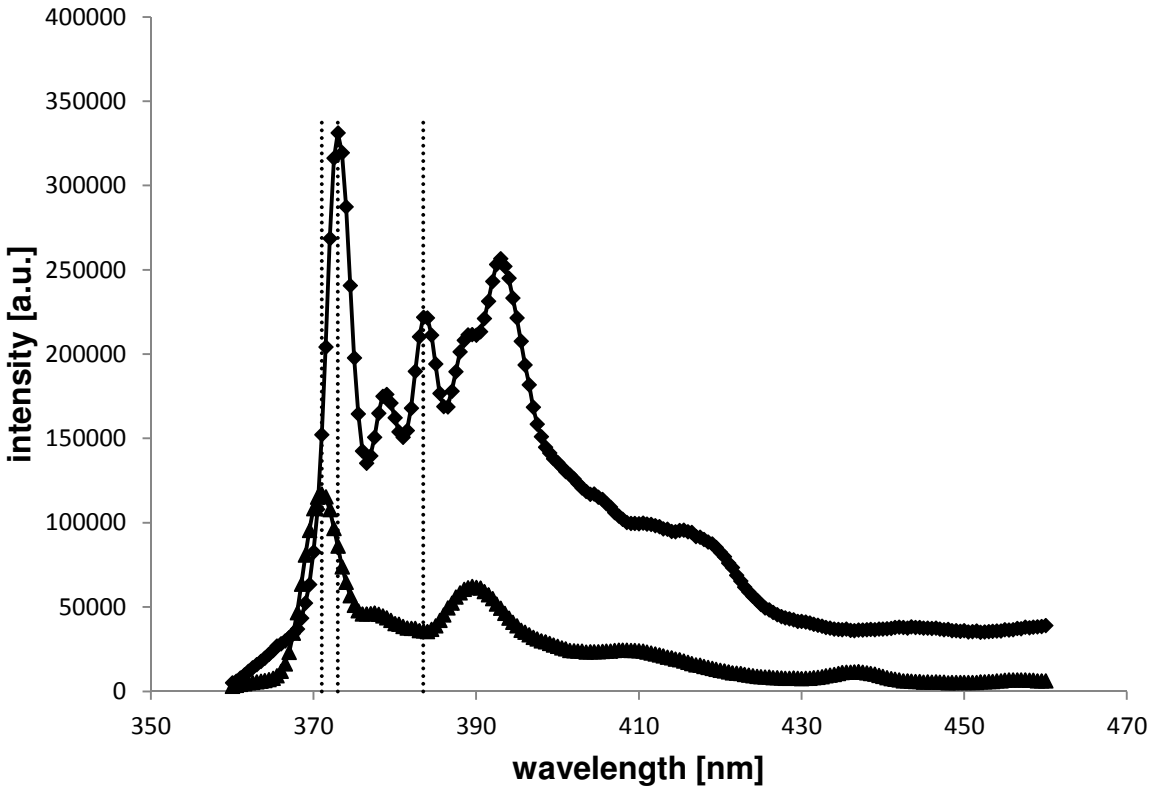

Figure 1. Emission spectra of pyrene in water (▲) and in a 0.5 mg/mL aqueous polymer solution of **2c** (PVAm-1.EQ$_{11}$-2.EA12$_{11}$) (♦). Dashed lines mark the absorption bands at wavelengths of 371 nm, 373 nm, and 383 nm.

In Figure 2, the emission spectra of pyrene in a series of aqueous polymer solutions of polymer **2c** (PVAm-1.EQ$_{11}$-2.EA12$_{11}$) with different concentrations ranging from 0 mg/mL to 1 mg/mL is shown. It can be observed that for low polymer concentrations up to about 0.025 mg/mL, the measured spectra do not differ from the spectrum of pyrene in pure water. With rising concentrations above 0.025 mg/mL, the increase of the new absorption band at 383 nm and the red shift of the absorption band from 371 nm to 373 nm are observed.

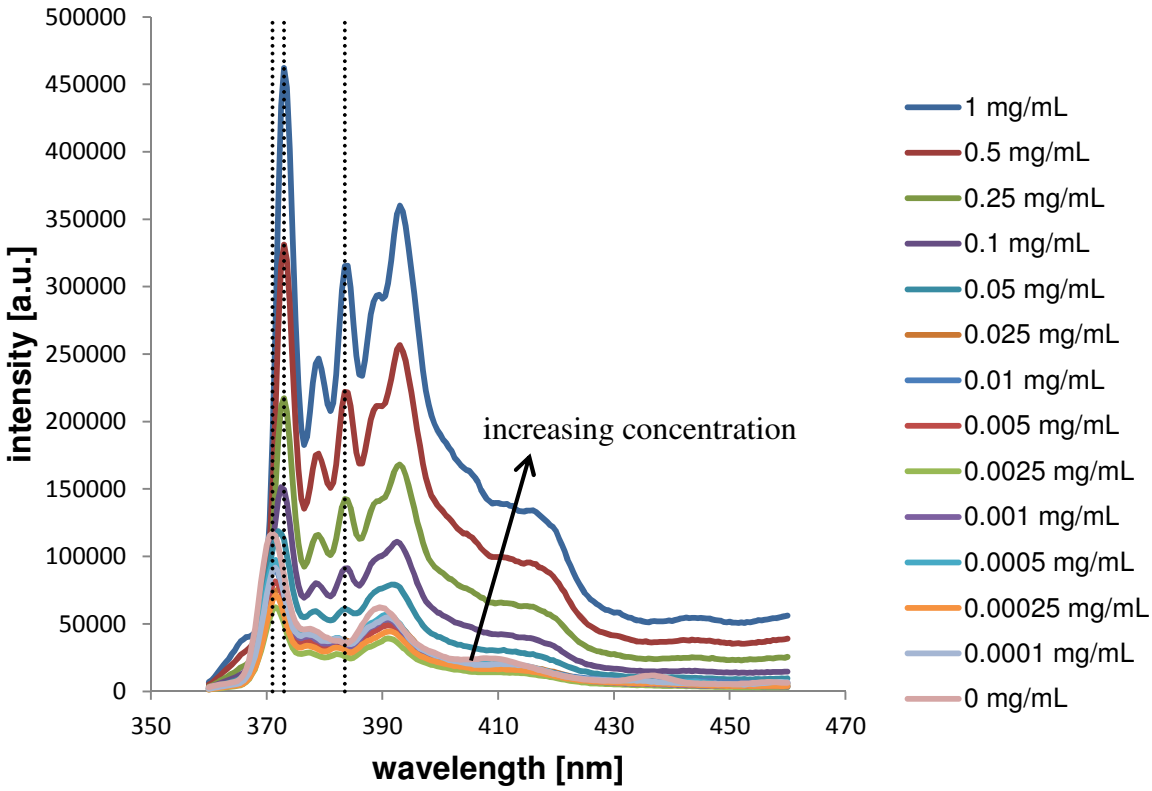

Figure 2. Emission spectra of pyrene in aqueous polymer solutions of polymer **2c** (PVAm-1.EQ$_{11}$-2.EA12$_{11}$) with different concentrations ranging from 0 mg/mL to 1 mg/mL. Dashed lines mark the absorption bands at wavelengths of 371 nm, 373 nm, and 383 nm.

The CAC can be determined by plotting the intensity ratio I_{373}/I_{371}, or the intensity ratio I_{373}/I_{383}, from the emission spectra against the logarithmic concentration of the polymer solutions. In this work mainly the first ratio was used to calculate the CAC (see Figure 3). Low intensity ratios indicate a hydrophilic surrounding of the pyrene, whereas high intensity ratios indicate a hydrophobic surrounding of the pyrene, which is caused by the formation of micellar aggregates. The experimental data were fitted by sigmoidal curves[32] and the intersection point of the tangent of the intensity ratio curve at the deflection point and the tangent of that curve at low polymer concentrations is defined as the CAC.

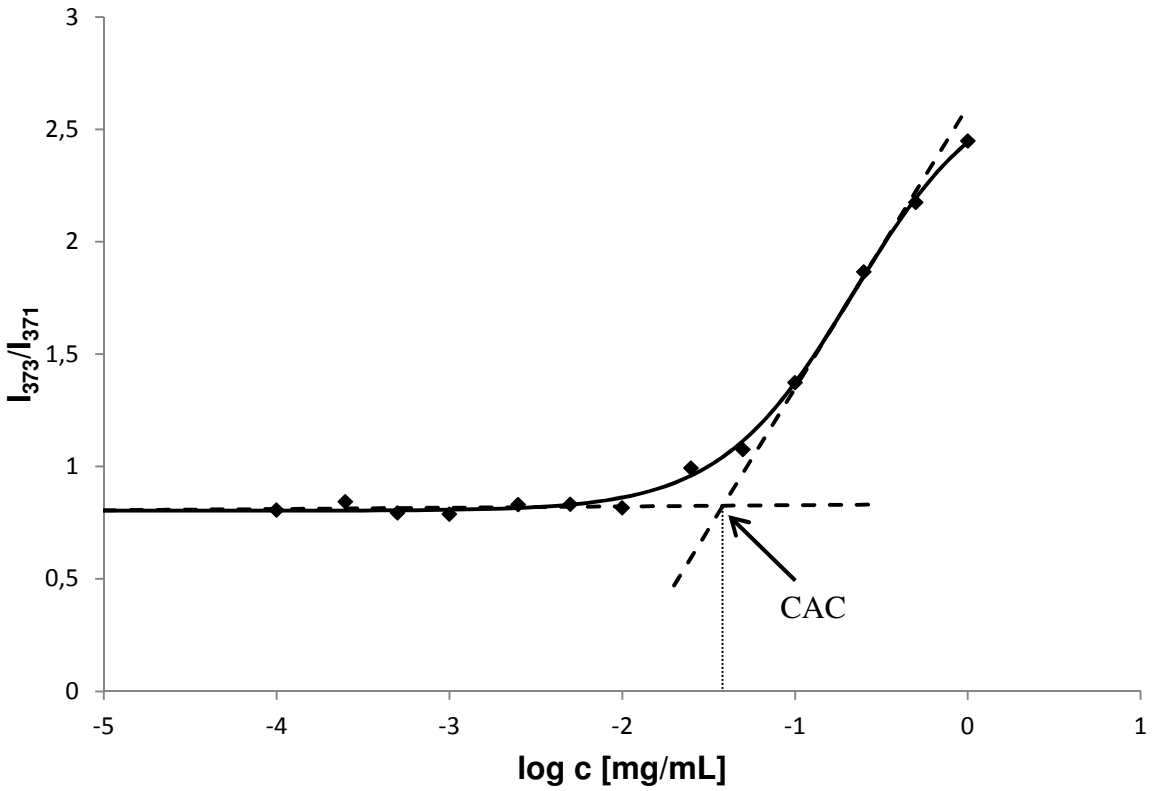

Figure 3. Intensity ratio I_{373}/I_{371} of the emission spectra of pyrene in aqueous polymer solutions of **2c** (PVAm-1.EQ_{11}-2.$EA12_{11}$) against the logarithmic concentration of the polymer solutions. The solid line shows the sigmoidal fit to the experimental data and the dashed lines show the tangent of the intensity ratio curve at the deflection point and the tangent of that curve at low polymer concentrations (the intersection point of the two tangents is defined as the CAC).

The influence of the alkyl chain length on the CAC was studied. The determined CAC values and the composition of the polymers are given in Table 7. The corresponding sigmoidally shaped data curves are shown in Figure 4.

Table 7. Critical aggregation concentration (CAC) values of the polymers with different alkyl chain lengths.

Number	Name a.D.	EAX	CAC[a)] [mg/mL]
2a	**PVAm-1.EQ$_{11}$-2.EA8$_{11}$**	EA8	0.2176
2b	**PVAm-1.EQ$_{11}$-2.EA10$_{11}$**	EA10	0.1557
2c	**PVAm-1.EQ$_{11}$-2.EA12$_{11}$**	EA12	0.0292
2d	**PVAm-1.EQ$_{11}$-2.EA14$_{11}$**	EA14	0.0096
2e	**PVAm-1.EQ$_{11}$-2.EA16$_{11}$**	EA16	-*
2f	**PVAm-1.EQ$_{11}$-2.EA18$_{11}$**	EA18	-*

a. D. = after dialysis, * not soluble in water, therefore not determined. [a)] CAC value from intensity ratio I_{373}/I_{371} from the emission spectra (intersection point of the tangent of the intensity ratio curve at the deflection point and the tangent of that curve at low polymer concentrations).

It was expected that the CAC decreases with increasing alkyl chain lengths due to a better aggregation behaviour of the longer alkyl chains. The experimental data confirmed this expectation. With increasing alkyl chain length, a decrease in the CAC was observed (see Table 7 and Figure 4). The polymers **2e** and **2f** could not be measured due to a lack of solubility in water. It is expected that their CAC values are lower than the CACs of the measured polymers because of the increased chain lengths of the introduced alkyl chains.

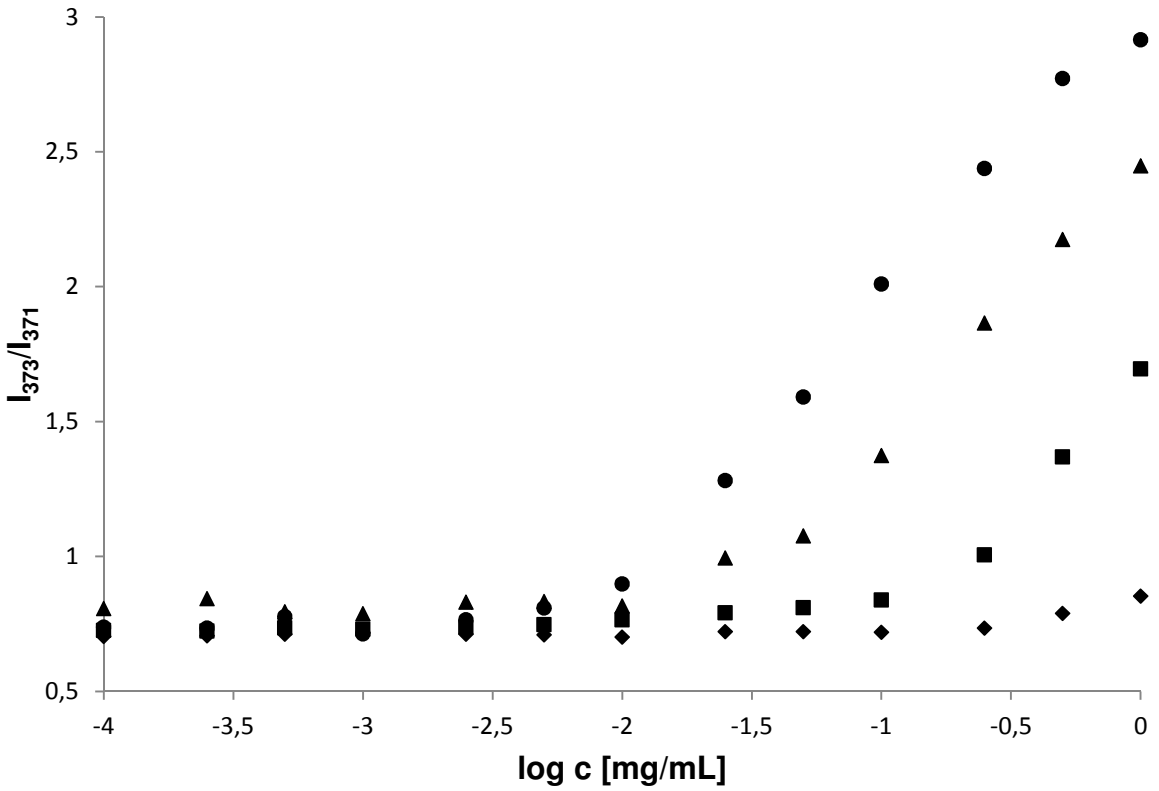

Figure 4. Intensity ratio I_{373}/I_{371} of the emission spectra of pyrene in aqueous polymer solutions of **2a** (PVAm-1.EQ$_{11}$-2.EA8$_{10}$) (♦), **2b** (PVAm-1.EQ$_{11}$-2.EA10$_{10}$) (■), **2c** (PVAm-1.EQ$_{11}$-2.EA12$_{11}$) (▲) and **2d** (PVAm-1.EQ$_{11}$-2.EA14$_{12}$) (●) against the logarithmic concentration of the polymer solutions.

The plot of the intensity ratio I_{373}/I_{383} (instead of I_{373}/I_{371}) from the emission spectra against the logarithmic concentration of the polymer solutions leads to more scattered values (see Figure 5). Thus, this plot was not used for calculating the CAC. For the polymer with the highest alkyl chain length for which the CAC was determined (**2d**, PVAm-1.EQ$_{11}$-2.EA14$_{12}$), the values already scatter too much to allow a useful interpretation. Nevertheless, an interesting behaviour can be observed: For the concentration range below the critical aggregation concentration, the molecular environment (namely the polarity of the environment) of pyrene is different for the examined polymers.

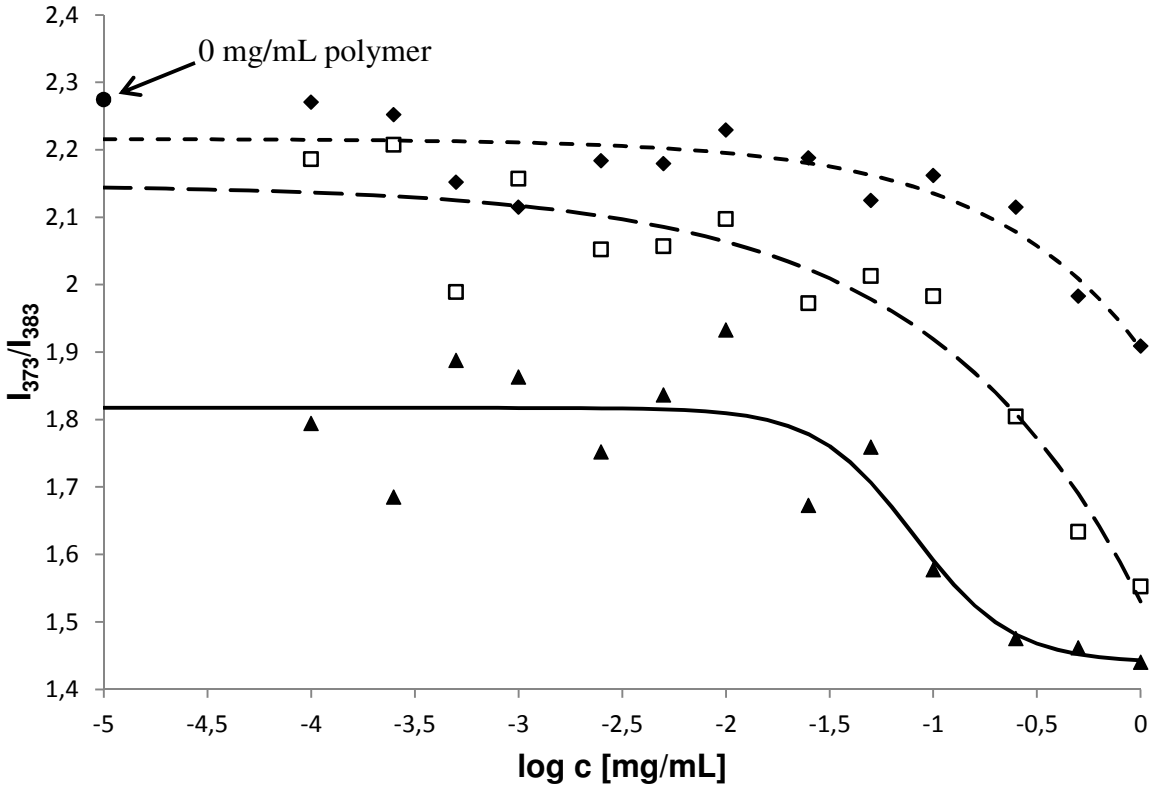

Figure 5. Intensity ratio I_{373}/I_{383} of the emission spectra of pyrene in aqueous polymer solutions of **2a** (PVAm-1.EQ$_{11}$-2.EA8$_{10}$) (♦, - - - -), **2b** (PVAm-1.EQ$_{11}$-2.EA10$_{10}$) (□,– – – –), and **2c** (PVAm-1.EQ$_{11}$-2.EA12$_{11}$) (▲, ——) against the logarithmic concentration of the polymer solutions. (Lines are guides for the eye).

The intensity ratios I_{373}/I_{383} are lower than the value of pure water (2.27) and with increasing alkyl chain lengths, this difference is increasing. This behavior gives evidence to a decrease in polarity with increasing alkyl chain lengths, due to the formation of hydrophobic microdomains within the polymers which can be regarded as unimolecular micelles. These hydrophobic regions do not depend on the concentration, which gives evidence to the assumption that hydrophobic domains are built within the polymer during the reaction. During the reaction, the alkyl chains form segregated domains and lead to a micro structuring of the polymer. A similar behavior was recently observed by Kiss *et al.* for branched poly(ethylene

imine)s ($\overline{M}_w$ = 25.000 g/mol) modified with alkyl chains of different lengths.[33] The formation of unimolecular micelles was also reported for block copolymers[34,35,36] and hydrophobically modified cationic polyelectrolytes.[37]

For the second synthesized series of polymers with different concentrations of hydrophobic groups (**3a-d**), the CAC was determined in the same way, using fluorescence measurements with pyrene as fluorescent dye (Table 8). The CAC was determined by plotting the intensity ratio I_{373}/I_{371}, from the emission spectra against the logarithmic concentration of the polymer solutions (see Figure 6). Again low intensity ratios indicate a hydrophilic surrounding of the pyrene, whereas high intensity ratios indicate a hydrophobic surrounding of the pyrene, and thereby the formation of micellar aggregates.

Table 8. Critical aggregation concentration (CAC) values of the polymers with different concentrations of alkyl chains.

Number	Name a.D.	EA12 [%]	CAC[a)] [mg/mL]
3a	**PVAm-EA12$_{10}$**	10	0.0179
3b	**PVAm-EA12$_{20}$**	21	0.0123
3c	**PVAm-EA12$_{30}$**	32	0.0011
3d	**PVAm-EA12$_{40}$**	41	0.0010

a. D. = after dialysis. [a)] CAC value from intensity ratio I_{373}/I_{371} from the emission spectra (intersection point of the tangent at the deflection point and the tangent at low polymer concentrations).

The experimental data were fitted by sigmoidal curves[32] and the intersection point of the tangent of the intensity ratio curve at the deflection point and the tangent of that curve at low polymer concentrations is defined as the CAC. With this second series of polymers the influence of the concentration of hydrophobic groups within the polymer on the CAC was investigated. The data curves (Figure 6), which are shifting to lower polymer concentrations for higher alkyl chain concentrations, and the resulting CAC values show the decrease of the CAC with increasing alkyl chain concentration. It is interesting to see in Figure 6 that polymer **3a** with 10 % alkyl chains and **3b** with 21 % alkyl chains, respectively, possess almost the same CAC values. The CAC of polymers **3c**, which contains 32 % alkyl chains is more than 10 times lower than the CAC values of polymer **3a** and **3b** and shares the same CAC value with polymer **3d** (41 % of alkyl chains). This means that the increase of the concentration of alkyl chains from 10 % to 21 %, or from 32 % to 41 %, respectively, has no influence on the ability of the polymer to form micelles. In contrast, the increase from 21 % to 32 % alkyl chains seems to be a crucial step for increasing the ability of the polymer to form micelles.

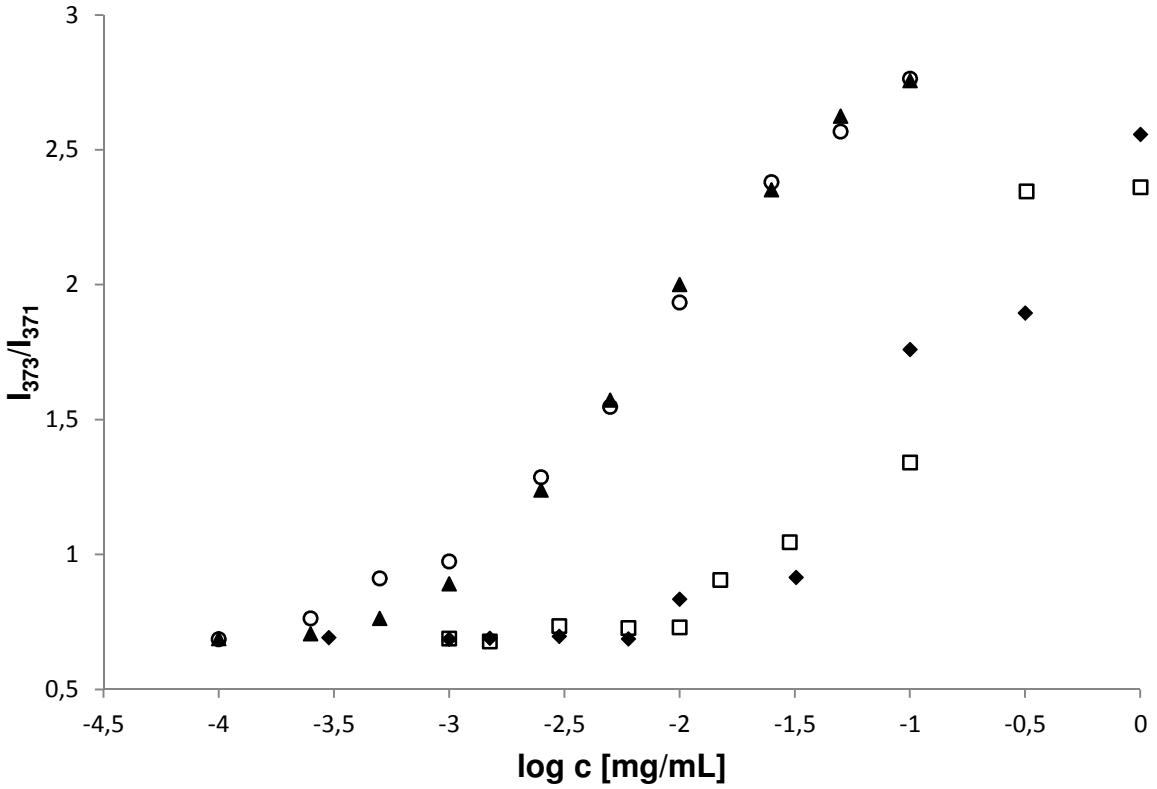

Figure 6. Intensity ratio I_{373}/I_{371} of the emission spectra of pyrene in aqueous polymer solutions of **3a** (PVAm-EA12$_{10}$) (♦), **3b** (PVAm-EA12$_{21}$) (□), **3c** (PVAm-EA12$_{32}$) (○) and **3d** (PVAm-EA12$_{41}$) (▲) against the logarithmic concentration of the polymer solutions.

3.4 Conclusions

Two different series of polymers were prepared and characterized. The amphiphilic poly(vinyl amine)s of the first series were obtained in a stepwise reaction of PVAm with 11 % cationic and 11 % hydrophobic groups with different alkyl chain lengths via a post polymerization reaction. The second series of amphiphilic polymers was prepared from PVAm and contained different concentrations of alkyl chains of the same lengths. The polymers were analyzed by NMR spectroscopy and their association behaviors in aqueous solutions, more precisely their CAC values, were determined. The increasing chain length in the first series leads to a decrease in CAC values. This means that the longer alkyl chains

build more rapidly and more easily bigger hydrophobic domains within the polymer than the shorter alkyl chains. It was additionally found that at concentrations below the CAC, unimolecular micelles are built and an increasing alkyl chain length leads to larger (and thus eventually more stable) unimolecular micelles. In the second series of polymers, no linear but a stepwise decrease of the CAC value with increasing concentration of alkyl chains was found. Raising the concentration of alkyl chains from 21 % to 32 % decreases the CAC value by a factor larger than 10. The other changes in alkyl chain concentration only have a marginal influence on the CAC. This indicates that the increase from 21 % to 32 % alkyl chains seems to be a crucial step to increase the ability of the polymer to form micelles. This is expected to be different for varying chain lengths.

3.5 Literature

[1] Technisches Merkblatt *N-Vinylformamid*, Mitsubishi Kasai, Japan, **1997**.

[2] R. K. Pinschmidt Jr., D. J. Sagl, *Polymeric Materials Encyclopedia*; Ed.: Salamone, J. C.; CRC Press New York **1996**, 7095 ff.

[3] L. Gu, S. Zhu, A. N. Hrymak, R. H. Pelton, *Polymer* **2001**, *42*, 3077–3086.

[4] L. Gu, S. Zhu, A. N. Hrymak, *J. Appl. Polym. Sci.* **2002**, *86*, 3412–3419.

[5] M. Kröner, J. Dupuis, M. Winter, *J. Prakt. Chem.* **2000**, *342*, 115–131.

[6] Produkt-Informationsbroschüre zu Lupaminen®, BASF AG, Ludwigshafen, **2000**.

[7] B. Martel, A. Pollet, M. Morcellet, *Macromolecules* **1994**, *27*, 5258–5262.

[8] F. Brunnmueller, R. Schneider, M. Kroener, H. Mueller, F. Linhart, H. Burkert, K.-H. Beyer, *Patent* **1982**, EP 071050.

[9] F. Linhart and W. Auhorn, *Das Papier* **1992**, *10A*, V38–V45.

[10] U. Riebeling, A. De Clercq, A. Stange, N. Sendhoff, C. Nilz, M. Kröner, *Patent* **1990**, *EP* 553135.

[11] F. Wang, H. Tanaka, *J. Appl. Polym. Sci.* **2000**, *78*, 1805–1810.

[12] S. Kobayashi, K. D. Suh and Y. Shirokura, *Macromolecules* **1989**, *22*, 2363–2366.

[13] R. K Pinschmidt Jr, B. R. Vijayendran, Ta.-W. Lai, *Patent* **1992**, US 5085787.

[14] R. K. Pinschmidt, *Patent* **1990**, US 4931194.

[15] P. Shu, *Patent* **1992**, US 5134176.

[16] S. Stinson, *Chem. Eng. News* **1993**, 71 (36), 32.

[17] D. Monech, H. Hartmann, E. Freudenberg, A. Stange, *Patent* **1993**, US 5262008; W. Auhorn, F. Linhart, P. Lorencak, M. Kroener, N. Sendhoff, W. Deninger, H. Hartmann, *Patent* **1992**, US 5145559; S. Pfohl, M. Kroener, H. Hartmann, W. Denzinger, *Patents* **1989**, US 4978427, US 4880497 and **1988**, US 4774285.

[18] H. Burkert, F. Brunnmueller, K. Beyer, M. Kroener, H. Mueller, *Patent* **1984**, US 4444667.

[19] D. Monech, H. Hartmann, K. Buechner, *Patent* **1993**, US 5225088.

[20] R.K. Pinschmidt Jr., T. Lai, *Patent* **1990**, US 4931194.

[21] T. Beihoffer, M. Mitchell, L. T. Truzpek, J. W. Darlington, M. Anderson, *Patent* **2001**, US 6194631.

[22] T. Beihoffer, M. Mitchell, J. W. Darlington, M. Anderson, *Patent* **1997**, WO 99/25745.

[23] T. Beihoffer, M. Mitchell, *Patent* **2000**, US 6159591.

[24] T. Beihoffer, M. Mitchell, *Patent* **2001**, US 6235965.

[25] D. Dawson, R. D. Gless, R. E. Wingard Jr., *J. Am. Chem. Soc*. **1976**, *98*, 5996–6000.

[26] K. Hofmann, S. Brumm, C. Mende, K. Nagel, A. Seifert, I. Roth, D. Schaarschmidt, H. Lang, S. Spange, *New J. Chem.* **2012**, *36*, 1655–1664

[27] Y. Qui, T. Zang, M. Ruegsegger, R. E. Marchant, *Macromolecules* **1998**, *31*, 165–171.

[28] M. Wilhelm, C-L. Zhao, Y. Wang, R. Xu, M. A. Winnik, *Macromolecules* **1991**, *24*, 1033-1040

[29] K. Kalyanasundaram, *Langmuir* **1988**, *4*, 942.

[30] K. Kalyanasundaram, J. K. Thomas, *J. Am. Chem. Soc.* **1977**, *99*, 2039-2044.

[31] J. Z. Du, D. P. Chen, Y. C. Wang, C. S. Xiao, Y. L. Lu, J. Wang, G. Z. Zhang, *Biomacromolecules* **2006**, *7*, 1898-1904.

[32] J. Aguiar, P. Carpena, J.A. Molina-Bolívar, C. Carnero Ruiz, *Journal of Colloid and Interface Science* **2003**, *258*, 116–122.

[33] É. Kiss, E. T. Heine, K. Hill, Y.-C. He, N. Keusgen, C. B. Pénzes, D. Schnöller, G. Gyulai, A. Mendrek, H. Keul, M. Moeller, *Macromol. Biosci*. **2012**, *12* (*9*), 1181–1189.

[34] F. M. Winnik, S. T. A. Regismond, *Colloids Surf. A* **1996**, *118*, 1.

[35] K. Nakashima, P. Bahadur, *Adv. Colloid Interface Sci.* **2006**, *123-126*, 75.

[36] M. Burkhardt, N. Martinez-Castro, S. Tea, M. Drechsler, I. Babin, I. Grishagin, R. Schweins, D. V. Pergushov, M. Gradzielski, A. B. Zezin, A. H. E. Müller, *Langmuir* **2007**, *23*, 12864.

[37] P. Deo, N. Deo, P. Somasundaran, S. Jockusch, N. J. Turro, *J. Phys. Chem. B* **2005**, *109*, 20714.

CHAPTER 4

AMPHIPHILIC POLYMERS WITH ANTIMICROBIAL ACTIVITY

4.1 Introduction

Multi-resistant bacteria and increasing antibiotic resistances are nowadays a growing problem especially in the medical sector.[1,2,3,4,5,6,7,8] The demand for new antimicrobial systems is rising.[9,10] Polymers with antimicrobial activity which can be used for molecular surface engineering are therefore of enlarging interest. They can be used as high molecular weight substances for functional coatings on surfaces and thereby help to overcome the problem of excessive bacterial growth and spreading which would result in increased health risks. Besides the modification of the surface, modifying the whole bulk material to obtain an antimicrobial effect is possible, but such an approach shows several disadvantages. By such a modification, the bulk properties like hardness, density, strength of the material, elasticity, stiffness, and resistance to corrosion to name only some, can be changed significantly. In addition, an antimicrobial effect inside the material is not needed and noticeably rises the price of the material. Functional coatings have the advantage that valuable bulk properties are maintained while an antimicrobial barrier to the environment is built at the same time. Antimicrobial coatings can be very important to avoid bacterial contaminations.[11] Such contaminations can cause severe risks for the human health, especially in the fields of fostering and sick care, for example for textiles for hospitals and nursing homes, bandages and ortheses or for non-regularly accessible textile materials like stationary mounted felts, filters, insulations or door linings, or for poorly reachable surfaces in the household.

A drawback of common antimicrobial coatings is that these coatings often release their active component (like triclosan or Ag^+ ions) into the environment.[12] This causes two (negative) effects: 1. the antimicrobial effect is lost over time and 2. the long term effect on the environment – like, e.g., accumulation of the active component and its effect on the flora and fauna, as well as the development of microbial resistances due to too low concentrations of the active agent – is often not known. In comparison to release systems, non-release systems have the advantage that they are not consumed over time and therefore don't need to be renewed. Furthermore, if the active compound is not released, it can only be active in the desired region and not accumulate in the environment. Thus it is desirable to develop non-leaching coatings. In this context, antimicrobial polymers play an important role because they can be immobilized on surfaces without the risk to release low molecular weight compounds. According to Klibanov, another advantage of antimicrobial polymers, in contrast to antibiotics, is that polymers render the development of resistances unlikely due to their mode of action.[13] Furthermore, antimicrobial polymers possess, concerning to Tashiro, a higher efficiency against bacteria in comparison to their monomeric equivalents.[14]

Poly(vinyl amine) (PVAm) has a linear structure with up to 100 % primary amine groups, one per repeating unit. It is a weak cationic polyelectrolyte and possesses the highest actually known charge density for a technical polymer. The high number of primary amine groups in PVAm opens the door to various possibilities of functionalization by post polymerization modification. The unmodified polymer is already antimicrobial active to some extent. To improve the antimicrobial effect, long alkyl chains and quaternary ammonium groups were introduced into the polymer. For this modification, the reaction of PVAm with functional epoxides was used. More details on the synthesis of multifunctional PVAm are given in Chapter 2.

4.2 Experimental Part

Poly(vinyl amine) is composed of different repeating units: vinyl amine and residual vinyl formamide. The ratio of these repeating units was determined by ^{1}H NMR spectroscopy. In what follows, $\overline{M}$ denotes the averaged molecular weight per repeating unit calculated from the ^{1}H NMR spectrum.

4.2.1 Materials

Starting materials were used as received: 1,2-epoxydodecane (**EA12**) (Alfa Aesar, 96 %) and glycidyltrimethylammonium chloride (**EQ**) (Aldrich, 75-80 % in water; since the oxirane degrades in time, the active content is determined just before use by NMR spectroscopy). Poly(vinyl amine) (PVAm) has been supplied by BASF (explorative material: salt free PVAm, supplier information: purified by ultra filtration, molecular weight = 340.000 g/mol). PVAm was freeze-dried before use. The dialysis tubings of regenerated cellulose had a molecular weight cut off of 50 kDa (CelluSep). The analytical data of the PVAm (salt free) are summarized in Table 1.

Table 1. Analytical data of salt free poly(vinyl amine).

Polymer	**MW** [a] **[g/mol]**	**DH** [a] **[%]**	**DH** [b] **[%]**	**Salt content** [b] **[%]**	$\overline{M}$ **(repeating unit)** [c] **[g/mol]**
PVAm (salt free)	340.000	100	99	1	43.60

DH = Degree of hydrolysis, [a] supplier information, [b] determined by NMR, [c] $\overline{M}$ = averaged molecular weight per repeating unit calculated from NMR.

4.2.2 Measurements

^{1}H and ^{13}C NMR spectra were recorded on a Bruker AV 400 FT-NMR spectrometer at 400 MHz (^{1}H) and 100 MHz (^{13}C), respectively. Deuterated methanol (MeOD) or deuterium oxide (D_2O) were used as solvents and the solvents residual peaks were used as internal standards.

Raman spectra were recorded at room temperature on a Bruker RFS 100S spectrometer with a Nd: YAG-Laser (1064 nm, 400 mW) at a spectral resolution of 4 cm^{-1} with 1000 scans.

A thermal shaker (Heidolph), a Microplate Incubator/Reader Genios Pro (Tecan), a Photometer Cary 100 (Varian), a drying oven, a climate chamber (Voetsch) and a Clean Bench (Kendro) were used for the antimicrobial assay.

4.2.3 Name of Prepared Products

Polymers are named using a threefold expression: The first part of this expression denotes the used poly(vinyl amine). The second and the third part denote the used epoxides and the corresponding indices show the degrees of functionalization based on the total amount of amino groups. The used abbreviations are given in Table 2.

Table 2. Abbreviations for the denotation of the products.

Unit	Correlation
PVAm	salt free PVAm, MW[a)] = 340.000 g/mol
EQ	glycidyltrimethylammonium chloride
EA12	epoxydodecane

[a)] supplier information

For example, PVAm-EQ_{15}-$EA12_{10}$ stands for the functionalization of salt free PVAm with 15 % EQ and 10 % EA12.

4.2.4 Microorganisms

The antimicrobial activity of the polymers was tested against the Gram-negative bacterium *Escherichia coli* (DSMZ 498).

4.2.5 Bacterial Culture

The nutrient solution (NL1, pH 7) contained 5 g peptone and 3 g meat extract per liter bidistilled water. The phosphate-buffered saline (PBS) contained 9.0 g NaCl per liter of 0.1 M disodium hydrogenophosphate/sodium dihydrogenophosphate buffer solution adjusted to pH 6.5. Soft agar was prepared from 10.0 g peptone, 3.0 g meat extract, 6.0 g NaCl, and 7.0 g agar-agar per liter of bidistilled water. All solutions were autoclaved for 15 min at 120 °C prior to use. The bacteria were suspended in nutrient solution and in PBS, respectively. The final suspension in nutrient solution or PBS contained DOW (superwetting agent Q2-5211 from DOW Chemicals) in a concentration of 0.01 % and 2×10^6 colony forming units per mL (cfu/mL). All solutions were autoclaved for 15 min at 120 °C prior to inoculation.

4.2.6 Surface Coating

Glass substrates (Marienfeld, 18 mm × 18 mm) or silicon wafer cut into pieces (15 mm × 15 mm) were used as model surfaces. The substrates were ultrasonically cleaned in acetone (p.a.), dist. water, and isopropanol (p.a.) for 5 minutes each and afterwards dried under nitrogen-flush. After cleaning, the substrates were directly used for coating.

Drop Casting

150 µL of a methanolic polymer solution (1 wt% (w/w), 0.1 wt% (w/w), 0.05 wt% (w/w)) were uniformly casted onto a glass substrate and the solvent was allowed to evaporate overnight.

Spin Coating

100 µL of a methanolic polymer solution (1 wt% (w/w)) were applied onto the silicon wafer and rotated with 2000 rpm for 30 seconds.

Annealing in Methanol Atmosphere

The bottom of an exsiccator was filled with methanol up to a level of about 1 cm. The exsiccator was closed and stored for two days at RT so that a methanol atmosphere had built. The coated substrates were placed into the exsiccator, annealed in methanol atmosphere and removed after defined times.

4.2.7 Antimicrobial Assessment of the Functional Polymers

Antimicrobial Test of Coated Surfaces

The antimicrobial effect was tested both under growth (bacteria suspension in nutrient solution) and under non-growth (bacteria suspension in PBS) conditions. All tests were carried out at least twice. To ensure a complete wetting of the surface, enabling the bacteria to interact with the coated polymer the wetting agents DOW (Q2-5211; 3-(polyoxy-ethylene)propylheptamethyltrisiloxane) or Triton X-100 (octylphenolpoly(ethylene-glycolether)$_x$) were added to the test solutions and their effect was compared. Substrates coated with functionalized PVAm (non sterilized) were placed into Petri dishes (Ø = 3 cm) and 20 µL bacteria suspension of *E. coli* (2×10^6 colony forming units per mL (cfu/mL)) were

inoculated onto each surface (parallel samples a and b). As reference an uncoated substrate was exposed to 20 µL bacteria suspension of *E. coli* (2×10^6 cfu/mL). As sterility control, a coated substrate was exposed to 20 µL of nutrient solution or PBS (in the absence of bacteria), for the testing under growth and under non-growth conditions, respectively (sample c). The exposure was performed in a climate chamber at 25 °C and 97 % rH (relative humidity) for 2.5 h or 22 h. Thereafter, 1 mL of the nutrient solution was pipetted (dilution 1 : 50) in every Petri dish (a – c) and the samples were shaken at RT for 30 min with 150 revolutions per minute (rpm). Then, from each Petri dish 200 µL solution were transferred to a well plate to monitor the residual growth.

Leaching test: 180 µL of the shake solution of the sterility control (sample c) were transferred to a well plate, inoculated with 20 µL bacteria suspension of *E. coli* (2×10^6 cfu/mL), and the bacterial growth was monitored. This leaching test served as a proof that during the growth test no inhibition is caused due to an amount of polymer transferred from the coated surface to the well plate of the growth test, i.e., as a proof that the growth test is valid and the growth inhibition is only due to the influence of the polymer on *E. coli* during the exposure on the surface.

Real leaching: Real leaching from the surface was tested with three methods.

(i) The antimicrobial effect of higher concentrated extracts of the coatings was measured. Six coated substrates were each exposed for 2.5 h (25 °C) to 30 µL nutrient solution, containing DOW in a concentration of 0.01 %. After the exposure the nutrient solution was collected from each substrate and the substrates were washed with a total amount of 60 µL nutrient solution. From the combined exposure and washing solution (in total 240 µL), 120 µL were transferred to a well plate, inoculated with 20 µL bacteria suspension of *E. coli* (2×10^6 cfu/mL) and the residual growth was monitored.

(ii) The leaching was tested by measuring the residual antimicrobial effect of the coated surfaces before and after washing. For washing, the samples were shaken three times with 1 mL of sterile bidistilled water for 30 min at 170 rpm. Afterwards the samples were dried overnight lying on filter papers in open petri dishes in the clean bench.

(iii) The leaching was tested via patching the coated surfaces onto nutrient agar inoculated with *E. coli*, followed by incubation. For the patching of the coated surfaces onto agar plates the coated glass substrates were placed into Petri dishes (Ø = 3 cm) and exposed to 25 µL nutrient solution (containing DOW in a concentration of 0.05 %). The exposure was performed in a climate chamber at 25 °C and 95 % relative humidity (rH) for 2.5 h. 200 µL bacteria suspension of *E. coli* (5×10^5 colony forming units per mL (cfu/mL)) were pipetted and plated onto agar plates. The inoculated agar plates were incubated for 30 min at 37 °C. The exposed coated surfaces were patched with their upside onto the inoculated agar plates and afterwards incubated at 37 °C overnight, or the coated surfaces were removed after 60 seconds followed by an incubation of the inoculated agar plates (37 °C, overnight). The colony growth was documented and the plates were checked for the appearance of a zone of inhibition.

Growth test: The growth of the bacteria was followed by measuring the optical density (OD) of the solutions (transferred to the well plates) at 612 nm overnight at 37 °C in the micro well plate incubator/reader. To insert oxygen into the solution (for the bacterial metabolism) and to assure the homogeneity of the OD measurement, the solutions were shaken for 1000 seconds once per measuring cycle of 30 min. This test does not discriminate whether the substance is bactericidal or bacteriostatic.

Antimicrobial Test in Solution

Suspensions of strains with defined colony forming units (*E. coli*, 6×10^7 cfu/mL) were incubated at 37 °C in nutrient solutions with different concentrations of the test substances (functional polymers). The wetting agent DOW (Q2-5211; 3-(polyoxyethylene)-propylhepta-methyltrisiloxane) was added to the test solutions in a concentration of 0.01 %. The bacterial growth was followed during the incubation overnight, by using a micro well plate reader/incubator and the measurement procedure (growth test) described. Experiments were triplicated. With this test, the minimum inhibitory concentrations (MIC) of the tested polymers were determined. Based on standard specifications[15], the MIC is defined in this thesis as the lowest concentration of an antimicrobial that inhibits the bacterial growth by 99.99 % (log-4 reduction[16] of the colony forming units) compared to the reference. Table 3 shows the reduction of the bacterial growth in log-x and in %, compared to an exemplarily number of bacteria in the test solution.

Table 3. Reduction of bacterial growth in log-x and in %, compared to an exemplarily number of bacteria in the test solution.

Log reduction of growth	% inhibition of growth	Example number of bacteria
log-0	0	1.000.000.000
log-1	90	100.000.000
log-2	99	10.000.000
log-3	99.9	1.000.000
log-4	99.99	100.000
log-5	99.999	10.000
log-6	99.9999	1.000

4.2.8 Langmuir Film Experiments

The preparation of the lipid layers and the penetration experiments were carried out using a Langmuir trough (KSV MiniMicro, $5 \times 20 \times 0.6\ cm^3$) with two barriers to provide a symmetric film compression. The surface pressure was recorded with an accuracy of ± 0.05 mN/m with the aid of a Wilhelmy plate made of chromatography paper (Whatman Chr1) which was connected to a force transducer. The trough was made of teflon while the barriers were made of polyoxymethylene (POM), which is suggested for lipid layers.[17] Dichloromethane (purity ≥ 99.9 %, Spectrum-3D Kft. Hungary) and methanol (purity ≥ 99.9 %, Sigma-Aldrich Kft. Hungary) were used for cleaning the Langmuir trough and the POM barriers, respectively. Afterwards, the trough and the barriers were rinsed with water. The trough was placed on a thermo-regulated plate and into a box of plexiglass in order to minimize air turbulence and possible contaminations. All measurements were performed at 23 ± 0.5 °C. As subphase, double distilled water, which was checked by its conductivity (< 5 mS) and surface tension (> 72.0 mN/m at 23 ± 0.5 °C) values, was used.

DPPC (Dipalmitoylphosphatidylcholine) was used as lipid for the Langmuir layers. For the preparation of the lipid layers, 13 µL of the lipid solution (1.0 g/L in chloroform (purity > 99.8 %, Fisher Chemicals)) were spread onto the aqueous subphase and the solvent was allowed to evaporate for 10 min before the compression to form the molecular lipid layer on the surface. Before the penetration experiment surface pressure-area isotherms were determined at a barrier speed of 10 cm^2/min. The reason for this preliminary process is to bring the lipid layer into a reproducible state (compactness, ordering of chains). For the penetration experiments the lipid monolayer was compressed to a given surface pressure of 20 mN/m. At a fixed barrier position, the aqueous solution of the polymer was injected below the lipid layer to reach a final polymer concentration of 0.025 mg/mL or 0.075 mg/mL in the subphase (concentration of the polymer solution = 1 and 3 mg/mL, injected volume: 2.4 mL).

The change in surface pressure ($\Delta\pi$) as indicator of the lipid/polymer interaction was recorded as a function of time for 1 h. The result of the penetration of the polymer into the lipid monolayer (the saturation value after 1 h of the increase of the surface pressure, $\Delta\pi$) was given as the average of two independent measurements with an estimated error of ± 0.5 mN/m.

4.2.9 Syntheses

The reaction of PVAm with functional epoxides was optimized to the following procedure. More details on the synthesis of multifunctional PVAm are given in Chapter 2.

General Procedure for the Functionalization of PVAm with Functional Epoxides

To a solution of freeze-dried salt free PVAm (200 mg) in dist. water/methanol (p.a.) (2 mL/4 mL) at 60 °C, a solution of the desired functional epoxides in methanol (p.a., 8 mL) was added. The solution was stirred at 60 °C for 2 d. The reaction solution was then dialyzed against dist. water to remove impurities originating from the educts (especially from EQ). The water was exchanged several times. The product was then isolated by freeze-drying. The freeze-dried products were all soluble in methanol, in some cases swellable in water and in some cases soluble in water. Along this route, long alkyl chains and quaternary ammonium groups were introduced into the polymer in different ratios. For more details on the synthesis see Chapter 2.

4.3 Results and Discussion

Based on the grafting-to strategy described in Chapter 2, five series of multifunctional amphiphilic poly(vinyl amine)s were prepared. Different concentrations of cationic and hydrophobic groups were introduced into the polymer. The goal of this study was to get new

insights into the influence of the hydrophilic/hydrophobic balance on the antimicrobial effect and on the ability to penetrate into lipid monolayers. The synthesis was performed in a single step, introducing both the cationic and the hydrophobic groups at the same time into the polymer. The linear PVAm (salt free) used for this study had a molecular weight of 340.000 g/mol according to the supplier, and a degree of hydrolysis of 99 % found by ^{1}H-NMR spectroscopy. This means that 99 % of the repeating units bore primary amine groups and were available for modification reactions. The remaining 1 % of non-hydrolyzed repeating units contained residual formamide groups. The reaction-scheme of the one-step reaction of PVAm with the functional epoxides EQ and EA12 is shown in Scheme 1. PVAm was reacted with both epoxides in a methanol/water mixture at 60 °C for two days. Afterwards, the functionalized PVAm was purified by dialysis and analyzed by NMR and Raman spectroscopy. Table 4 gives an overview of the prepared functional polymers. For a better comparison the polymers were arranged in five different series. Note that one polymer can belong to more than one series. This allows for a better comparison and investigation of structure properties relations. The degrees of functionalization of the polymers were calculated from the ^{1}H-NMR spectra as described in Chapter 2. The polymers were soluble in methanol and in water.

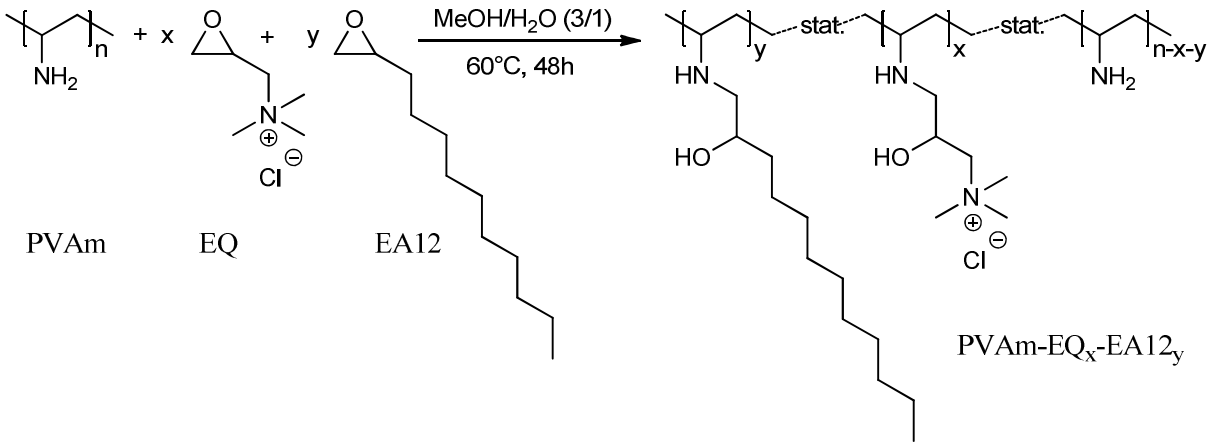

Scheme 1. One-step synthesis of PVAm-EQ$_x$-EA12$_y$.

Table 4. Composition and assignment to different series of the prepared polymers.

Series[a)]	Name	degree of functionalization [%][b)]	
		EQ	EA12
1	**PVAm-EQ$_7$-EA12$_{22}$**	7	22
1	**PVAm-EQ$_7$-EA12$_{10}$**	7	10
2a	**PVAm-EQ$_{14}$-EA12$_{11}$**	14	11
2a	**PVAm-EQ$_7$-EA12$_{10}$**	7	10
2a	**PVAm-EQ$_5$-EA12$_{10}$**	5	10
2a	**PVAm-EA12$_{10}$**	-	10
2b	**PVAm-EQ$_{28}$-EA12$_{11}$**	28	11
2b	**PVAm-EQ$_{21}$-EA12$_{11}$**	21	11
2b	**PVAm-EQ$_{17}$-EA12$_{11}$**	17	11
2b	**PVAm-EQ$_{13}$-EA12$_{11}$**	13	11
3	**PVAm-EA12$_{10}$**	-	10
3	**PVAm-EA12$_{21}$**	-	21
3	**PVAm-EA12$_{32}$**	-	32
3	**PVAm-EA12$_{41}$**	-	41
4	**PVAm-EQ$_{23}$**	23	-
4	**PVAm-EQ$_{30}$**	30	-
4	**PVAm-EQ$_{73}$**	73	-

[a)] Note that one polymer can belong to more than one series. This allows for a better comparison and investigation of structure properties relations. [b)] Degree of functionalization in [%] calculated from ^{1}H-NMR spectroscopy.

4.3.1 Surface Coating of the Functional Polymers

As already mentioned in Chapter 1, PVAm is a weak cationic polyelectrolyte and possesses the highest currently known charge density of all technical polymers. Due to the high charge density, it shows very good adsorption behavior to glass[18], metal, and negatively charged surfaces (e.g., cellulose)[19,20]. As for every weak cationic polyelectrolyte, the concentration of positive charges within the polymer depends on the pH-value of the surrounding medium. At a low pH, all amine groups are protonated and therefore positively charged. At a high pH, the amine groups are not protonated and therefore not charged. By reaction of PVAm with the quaternary ammonium group bearing epoxide EQ, additional permanent cationic groups are introduced into the polymer. These permanent cationic groups are not only important to improve the antimicrobial effect, but also to get a permanent ionic interaction and therefore permanent adhesion to negatively charged surfaces. It is assumed that the alkyl chains self-assemble during the reaction and build up domains in the polymer. The reaction is carried out in an aqueous medium. The alkyl chains are hydrophobic and therefore reject this environment. After the first epoxyalkanes have reacted with the polymer, the next ones react in the same regions oriented to the inside of the polymer coil. The alkyl chains align and build up microstructures. The cationic groups are hydrophilic and are therefore oriented towards the outside of the polymer coil. As a result of this self-assembling, the polymer coil has got an unimolecular micelle-like structure.

When the polymer comes into contact with a negatively charged surface, the polymer adsorbs to it via a part of the cationic groups. A schematic illustration of the microstructured, functionalized PVAm and its adsorption onto a negatively charged surface is shown in Figure 1.

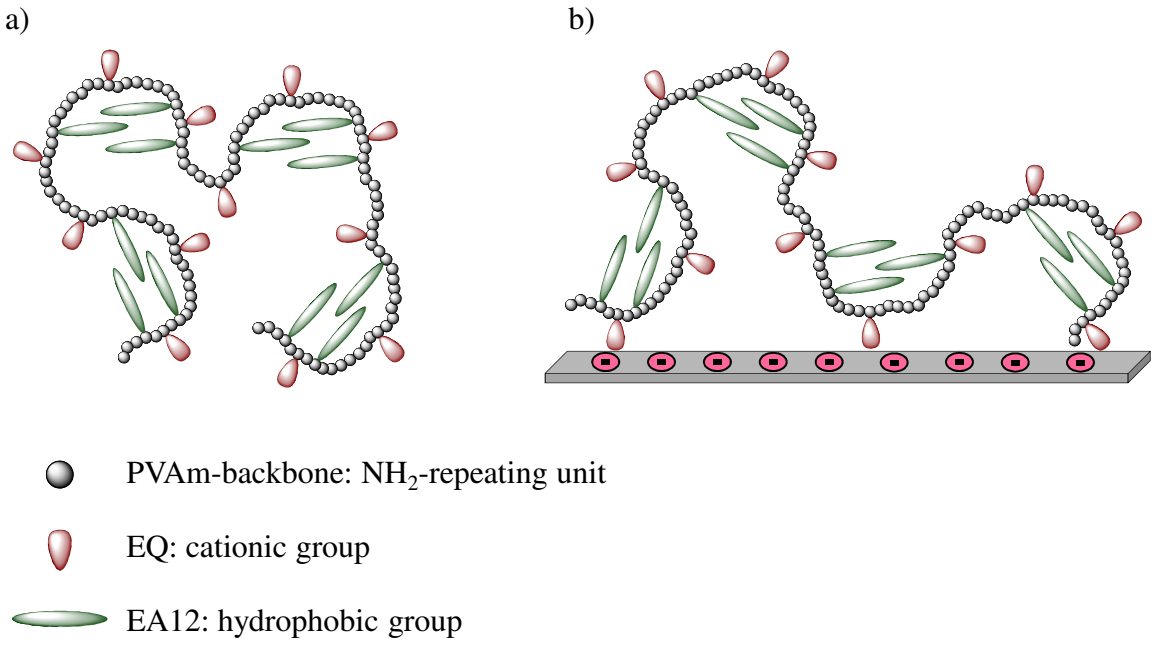

Figure 1. Schematic illustration of a) the microstructured, functionalized PVAm and b) its adsorption onto a negatively charged surface.

4.3.2 Antimicrobial Action of the Functional Polymers Coated on Surfaces

In a first step the negative charges on the outside of the bacterial cell are attracted by the positive charges of the developed polymers. When the bacteria come into contact to the antimicrobial polymer on the coated surface, in a second step, the alkyl chains of the functional polymer rearrange and interact with the outer membrane of the bacteria, or even penetrate that membrane. Parts of the polymer chains can diffuse through the cell wall and some minor parts of the polymer might even be consumed completely (restricted release). This causes a severe damage of the cell-membrane. The membrane is either broken such that the inside of the bacteria is leaking out, or the metabolism of the cell-membrane of the bacteria is disturbed essentially. Both interactions between the polymer and the cell-

membrane cause the death of the bacteria. A schematic illustration of the interaction of self-organized functionalized PVAm with a bacteria cell-membrane is shown in Figure 2.

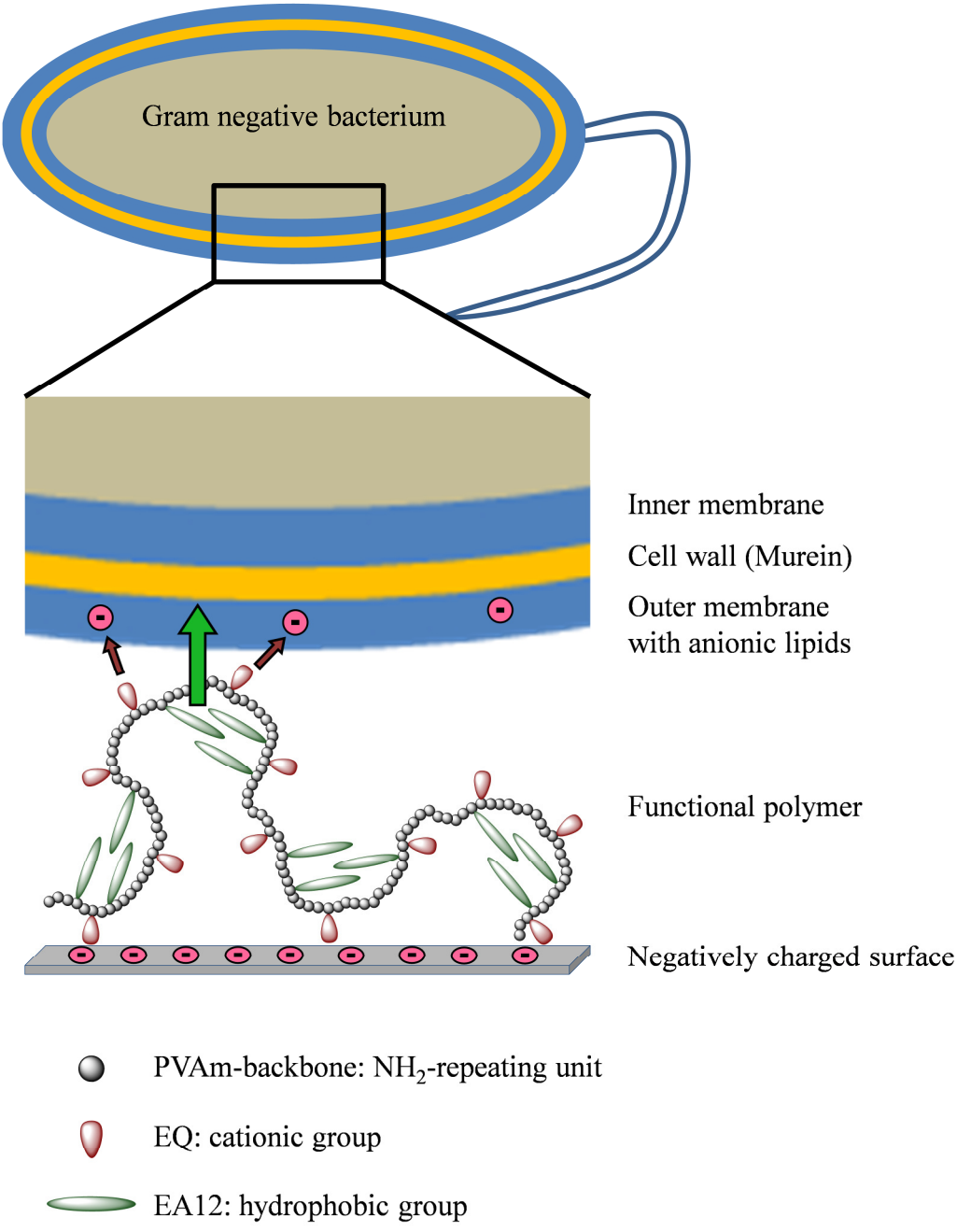

Figure 2. Schematic illustration of the interaction of self-organized, functionalized PVAm (adsorbed on a negatively charged surface) with a Gram-negative bacterium. First step: attraction of the cell-membrane by the cationic groups of the coated polymer (red arrows). Second step: penetration of the cell-membrane by the alkyl chains (green arrow).

4.3.3 Antimicrobial Effect of the Synthesized Polymers

The antimicrobial effect of the synthesized polymers was tested on coated surfaces. A direct testing in solution was for most of the polymers too imprecise due to the appearance of turbidities by adding PBS or nutrient solution to the aqueous polymer solutions. As the testing method used here measures the change in the optical density of the polymer solution caused by the bacterial growth, this turbidity is unwanted and disturbs the test. With increasing concentration of cationic groups (EQ) and decreasing concentration of hydrophobic groups (EA12) in the polymer the solubility of the polymers in water increases and the turbidity of the polymer solution (in PBS or nutrient solution) decreases. Only polymers with high concentrations of cationic groups (EQ) and no hydrophobic groups (EA12) in the polymer showed no turbidity and could be tested for their antimicrobial effect in solution (see later).

To test the antimicrobial effect of the polymers, 1 wt% methanolic polymer solutions (w/w) were diluted with methanol (p.a.) to the desired concentrations. The solutions were then coated onto glass substrates serving as model surfaces for negatively charged surfaces, e.g., textile surfaces. Glass is negatively charged at the surface so that the functional polymers can bind to it via ionic interaction. The glass substrates were cleaned prior to the coating. They have been ultrasonic-cleaned in acetone (p.a.), dist. water, and isopropanol (p.a.) each for 5 minutes and dried under nitrogen-flush. To coat the substrates, 150 µL of the methanolic polymer solution were applied onto the substrate and the solvent was allowed to evaporate overnight. Concentrations of 1 wt% (w/w), 0.1 wt% (w/w) and 0.05 wt% (w/w) were applied.

The antimicrobial effect was tested under growth (bacteria suspension in nutrient solution) and under non-growth (bacteria suspension in PBS) conditions. All tests were carried out at least twice. The antimicrobial testing system is depicted in Figure 3. The coated glass substrates were placed into Petri dishes (Ø = 3 cm) and inoculated with 20 µL bacteria suspension of *E. coli* (2×10^6 colony forming units per mL (cfu/mL)). As reference, an

uncoated glass substrate was exposed to 20 µL bacteria suspension of *E. coli* (2×10^6 cfu/mL) and as sterility control, a coated glass substrate was exposed to 20 µL nutrient solution or PBS, for the testing under growth and under non-growth conditions, respectively. The exposure was performed in a climate chamber at 25 °C and 97 % relative humidity (rH) for 2.5 h or 22 h. Thereafter, 1 mL nutrient solution was pipetted into every Petri dish and the samples were shaken at RT with 150 revolutions per minute (rpm) for 30 min. From each Petri dish, 200 µL of the solution were transferred to a well plate and a growth test was performed. The proliferation curves were obtained by measuring the increase in optical density at 612 nm. The increase in optical density is plotted as a function of the number of cycles (1 cycle = 30 minutes). By comparison of the proliferation curves of the bacteria which have been in contact to the antimicrobial surfaces and the proliferation curves of the bacteria without contact to the antimicrobial surfaces, the reduction of the bacterial growth and thereby the antimicrobial effect of the coatings can be determined. For the performed test, the internal benchmark for a good antimicrobial activity is a log-4 reduction of the colony forming units, respectively a 99.99 % inhibition of bacterial growth.[21]

The antimicrobial testing was done under both growth (in nutrient solution) and non-growth (in PBS only) conditions to determine whether the antimicrobial effect takes place during the cell division or not. The wetting agents DOW and Triton X-100 were used and compared to ensure a complete wetting of the surface, enabling the bacteria to interact with the coated polymer. The wetting agents themselves are not antimicrobially active. Different amounts of functionalized PVAm were coated onto the surfaces and were tested for their antimicrobial activity.

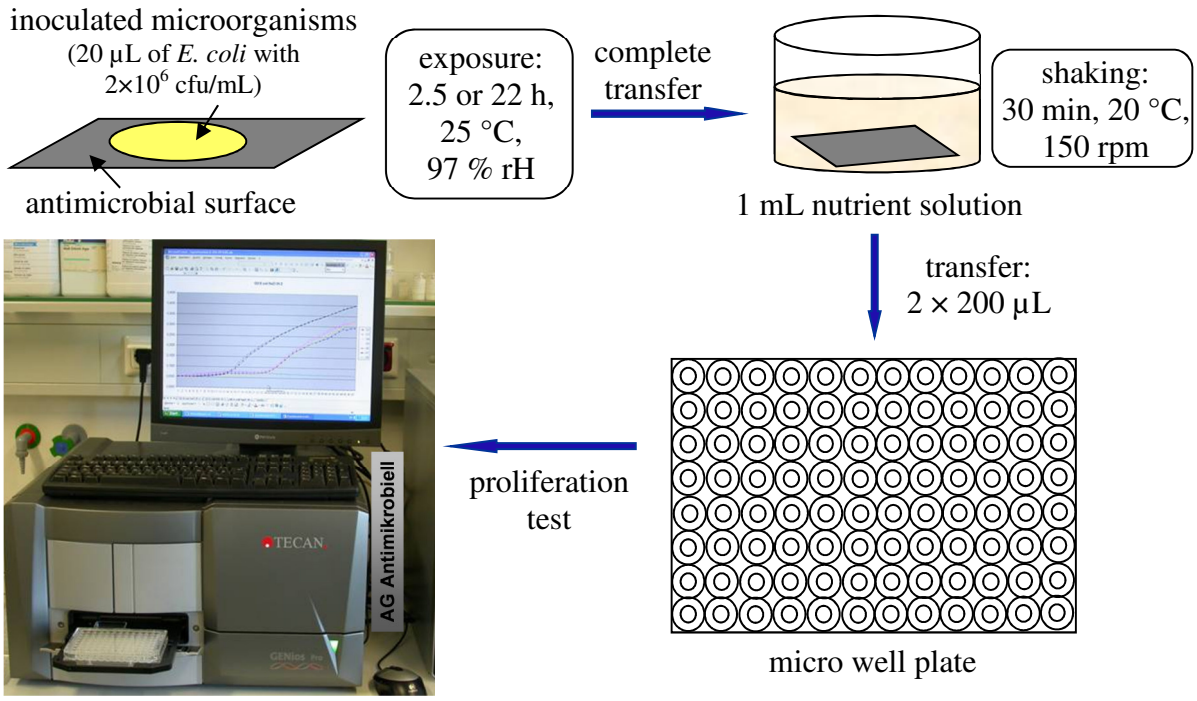

Figure 3. Antimicrobial testing system.

Substrates Coated with 1 wt% Polymer Solutions

The methanolic polymer solutions (1 wt% (w/w)) were casted onto each glass substrate and the solvent was allowed to evaporate overnight. The polymer concentration has been calculated to be 460 µg/cm². The antimicrobial effect of the polymers against *E. coli* was tested following the method described above. The two mentioned wetting agents were tested to assure the wetting of the surface and the contact of the bacteria to the substrate. The test was performed under growth and under non-growth conditions. It was repeated after two and after four weeks, to determine changes in activity over time. Therefore, all samples were prepared at the same time and the ones that were not directly used were stored at room temperature in air. The composition of the functional polymers and the antimicrobial results are shown in Table 5 (freshly prepared), Table 6 (after two weeks) and Table 7 (after four weeks). The proliferation curves of *E. coli* after exposure on the surfaces coated with the tested polymers are shown in Appendix A.

All samples functionalized with both EQ and EA12 (Series 1 and 2a) showed very good efficacies against *E. coli*. Under growth conditions, all polymers show between 99.99 % up to complete inhibitions of growth, satisfying completely the above mentioned criterion for a good antimicrobial effect (≥ 99.99 % inhibition of growth). Within the storage time of two and four weeks no change in antimicrobial activity was observed. Thus it can be concluded that the samples were stable over time.

The polymers functionalized with EA12 only (Series 3), showed different antimicrobial activities depending on the degree of functionalization. Pasquier et al. showed for branched poly(ethylene imine)s (PEI) an increase of the antimicrobial activity with increasing concentration of alkyl chains.[22] Poly(ethylene imine) can be regarded as the branched version of poly(vinyl amine). In contrast to the amine groups in PVAm, only 25 % of the amine groups in PEI are primary amine groups and can be modified. The primary amine groups are oriented to the outside of the branched polymer structure. Pasquier et al. modified the primary amine groups by post polymerization modification with functional carbonate couplers. Due to the branched structure and the peripherally distribution of the primary amines, the alkyl chains are located on the surface of the branched PEI structure. The alkyl chains can hardly self-assemble to domains within the polymer structure of PEI, as they can in the case of PVAm. The influence of the amount of alkyl chains on the antimicrobial activity of PVAm was determined. It was investigated, weather the trend in antimicrobial activity observed for PEI was also observed for PVAm.

It was observed that with an increasing degree of functionalization with alkyl chains, the antimicrobial effect decreases from 99.99-100 % inhibition of growth for the polymer PVAm-EA12$_{10}$, to 90 % inhibition of growth for the polymer PVAm-EA12$_{41}$. This means that for the coating thickness tested in this experiment, the polymers with only 10 % and 20 % of alkyl chains satisfy the criterion for a good antimicrobial effect (≥ 99.99 % inhibition of

growth), whereas the polymers with higher concentrations of alkyl chains do not satisfy this criterion anymore. The antimicrobial effect was again stable over time.

The results show that the linear structure of PVAm leads, compared to the branched structure of PEI, to a completely different behavior in the antimicrobial activity. In case of the functionalized PEI all introduced alkyl chains are located at the surface of the polymer and available for an antimicrobial interaction with the bacterial membrane. In contrast, due to the linear structure, the polymer chains of PVAm are very flexible and the alkyl chains can self-assemble to domains within the polymer structure. The alkyl chains inside of the rigid domains are not available for the antimicrobial activity. In addition, the formation of hydrophobic domains leads to a reduced solubility of the polymers in aqueous media and thereby to a reduction of the total availability of the polymers for antimicrobial interactions.

The antimicrobial effect was independent of the wetting agents (DOW or Triton) used. There was also no difference in the antimicrobial effect if 0.01 % or 0.05 % DOW was used. Therefore, it can be concluded, that the wetting of the surface was assured. All further experiments were performed with a concentration of 0.01 % DOW as wetting agent. For all samples, the measured antimicrobial activity was better under growth than under non-growth conditions. This observation is a hint that the antimicrobial effect of the tested polymers takes place more pronouncedly during the bacterial growth, i.e., during cell division and active metabolism.

Table 5. Composition of the functional polymers and inhibition[a)] of bacterial growth (*E. coli*) after exposure (2.5 h) on the freshly coated glass substrates (460 µg/cm² polymer).

				Inhibition of growth [%][a)]		
				growth	**growth**	**non-growth**
Series[b)]	**Name**	**EQ [%]**	**EA12 [%]**	**0.01 % DOW**	**0.01 % Triton**	**0.01 % DOW**
1	**PVAm-EQ$_7$-EA12$_{22}$**	7	22	99.9	> 99.99	< 90
1	**PVAm-EQ$_7$-EA12$_{10}$**	7	10	100	100	90
2a	**PVAm-EQ$_{14}$-EA12$_{11}$**	14	11	100	100	~ 100
2a	**PVAm-EQ$_7$-EA12$_{10}$**	7	10	100	100	90
2a	**PVAm-EQ$_5$-EA12$_{10}$**	5	10	100	100	90
2a	**PVAm-EA12$_{10}$**	-	10	> 99.99	100	99
3	**PVAm-EA12$_{10}$**	-	10	> 99.99	100	99
3	**PVAm-EA12$_{21}$**	-	21	> 99.99	> 99.99	< 90
3	**PVAm-EA12$_{32}$**	-	32	~ 99.9	~ 99.9	90
3	**PVAm-EA12$_{41}$**	-	41	> 90	> 90	< 90

[a)] The given values are the mean values obtained by averaging the outcomes of two measurements of the freshly prepared substrates. [b)] Note that one polymer can belong to more than one series. This allows for a better comparison and investigation of structure properties relations.

Table 6. Composition of the functional polymers and inhibition[a)] of bacterial growth (*E. coli*) after exposure (2.5 h) on the coated glass substrates after two weeks (460 µg/cm² polymer).

				Inhibition of growth [%][a)]	
				growth	**non-growth**
Series[b)]	**Name**	**EQ [%]**	**EA12 [%]**	**0.01 % DOW**	**0.01 % DOW**
1	**PVAm-EQ$_7$-EA12$_{22}$**	7	22	~ 100	> 90
1	**PVAm-EQ$_7$-EA12$_{10}$**	7	10	100	> 90
2a	**PVAm-EQ$_{14}$-EA12$_{11}$**	14	11	100	100
2a	**PVAm-EQ$_7$-EA12$_{10}$**	7	10	100	> 90
2a	**PVAm-EQ$_5$-EA12$_{10}$**	5	10	100	~ 90
2a	**PVAm-EA12$_{10}$**	-	10	100	99
3	**PVAm-EA12$_{10}$**	-	10	100	99
3	**PVAm-EA12$_{21}$**	-	21	> 99.99	< 90
3	**PVAm-EA12$_{32}$**	-	32	~ 99	< 90
3	**PVAm-EA12$_{41}$**	-	41	< 90	< 90

[a)] The given values are the mean values obtained by averaging the outcomes of two measurements of the substrates stored for two weeks. [b)] Note that one polymer can belong to more than one series. This allows for a better comparison and investigation of structure properties relations.

Table 7. Composition of the functional polymers and inhibition[a)] of bacterial growth (*E. coli*) after exposure (2.5 h) on the coated glass substrates after four weeks (460 µg/cm² polymer).

				Inhibition of growth[a)]		
				growth	**non-growth**	
Series[b)]	**Name**	**EQ [%]**	**EA12 [%]**	**0.05 % DOW**	**0.01 % DOW**	**0.05 % DOW**
1	**PVAm-EQ$_7$-EA12$_{22}$**	7	22	~ 99.99	> 90	< 90
1	**PVAm-EQ$_7$-EA12$_{10}$**	7	10	100	> 90	> 90
2a	**PVAm-EQ$_{14}$-EA12$_{11}$**	14	11	100	90-99.99	> 90
2a	**PVAm-EQ$_7$-EA12$_{10}$**	7	10	100	> 90	> 90
2a	**PVAm-EQ$_5$-EA12$_{10}$**	5	10	100	> 90	99
2a	**PVAm-EA12$_{10}$**	-	10	100	nd	> 99
3	**PVAm-EA12$_{10}$**	-	10	100	nd	> 99
3	**PVAm-EA12$_{21}$**	-	21	> 99.99	nd	> 90
3	**PVAm-EA12$_{32}$**	-	32	> 90	nd	> 90
3	**PVAm-EA12$_{41}$**	-	41	< 90	nd	< 90

nd = not determined, [a)] The given values are the mean values obtained by averaging the outcomes of two measurements of the substrates stored for four weeks.. [b)] Note that one polymer can belong to more than one series. This allows for a better comparison and investigation of structure properties relations.

The intention of the antimicrobial testing of the different polymer compositions was to study the influence of the hydrophilic/hydrophobic balance on the antimicrobial effect of the polymers and thereby to determine the most active polymer composition. All of the tested polymers, beside the polymers PVAm-EA12$_{32}$ and PVAm-EA12$_{41}$, showed very good

antimicrobial results for the tested amount of polymer per cm². The inhibition of growth was so high that no tendencies with regard to antimicrobial efficiency and degree of functionalization could be detected. It seems that the amount of the polymer per cm² and therefore the thickness of the coating has been too high to detect differences. Therefore, the coating solutions were diluted with methanol (p.a.), coated onto glass substrates and tested again. With a lower coating thickness, it should be possible to detect differences in the antimicrobial activity of the tested polymers. Furthermore, in a thinner coating the entire polymer is in close contact to the surface and is therefore stronger bound to it by ionic interaction than in a thicker coating. Such a thinner coating thereby makes a leaching of the material more unlikely.

Substrates Coated with 0.1 wt% and 0.05 wt% Polymer Solutions

To study the influence of the amount of polymer per cm², glass substrates coated with 46 µg/cm² polymer (0.1 wt% polymer solutions) and 23 µg/cm² polymer (0.05 wt% polymer solutions) were prepared. The antimicrobial effect of the polymers against *E. coli* was then tested following the above described method. A concentration of 0.01 % of the wetting agent DOW was used for all the tests. The test was performed under growth and under non-growth conditions.

To study the influence of the degree of functionalization with EA12 on the antimicrobial effect in more detail, Series 3 with different concentrations of EA12 ranging from 10 % to 40 % was tested again. In the test of the coating thickness of 460 µg/cm² polymer, a trend in the antimicrobial effect had already been observed, but it was not possible to distinguish between the two polymers with 10 % and 20 % of alkyl chains. Both polymers showed almost the same antimicrobial effect and had a growth inhibition of > 99.99 % up to a complete inhibition of growth. To obtain a more distinct trend, these two polymers were tested again

with a lower amount of polymer per cm². The composition of the functional polymers and the antimicrobial results are shown in Table 8. The results confirm the previously observed trend that with an increasing degree of functionalization with alkyl chains, the antimicrobial effect decreases.

Table 8. Composition of the functional polymers of Series 3 and inhibition[a)] of bacterial growth (*E. coli*) after exposure (2.5 h) on the coated glass substrates (46 µg/cm² and 23 µg/cm² polymer).

Series	Name	EQ [%]	EA12 [%]	Inhibition of growth[a)] [%]	
				46 µg/cm²	23 µg/cm²
3	**PVAm-EA12$_{10}$**	-	10	99.9	< 90
3	**PVAm-EA12$_{21}$**	-	21	< 90	< 90
3	**PVAm-EA12$_{32}$**	-	32	-	-
3	**PVAm-EA12$_{41}$**	-	41	-	-

[a)] The test was performed under growth conditions and a concentration of 0.01 % DOW was used. The given values are the mean values obtained by averaging the outcomes of two measurements.

The previous study showed that a functionalization with 10 % alkyl chains (EA12) gave the highest antimicrobial activity. To study the influence of different degrees of functionalization with EQ (cationic) at a constant degree of functionalization with EA12, the concentration of EA12 was set to a fixed value of 10 % within Series 2a and the concentration of EQ was varied. The results on the inhibition of growth of *E. coli* under growth conditions for 46 µg/cm² and 23 µg/cm² are shown in Table 9. It was observed that with an increasing concentration of cationic groups (EQ), the antimicrobial effect increases. The polymer

PVAm-EQ_{14}-$EA12_{11}$ with 14 % EQ and 11 % EA12 led to the best result within this series (>> log-4 reduction of cfu). The proliferation curves of *E. coli* after exposure on the surfaces coated with the polymers of Series 2a are exemplarily shown in Figure 4.

Table 9. Composition of the functional polymers of Series 2 and inhibition[a)] of bacterial growth (*E. coli*) after exposure (2.5 h) on the coated glass substrates (46 µg/cm² and 23 µg/cm² polymer).

Series	Name	EQ [%]	EA12 [%]	Inhibition of growth[a)] [%]	
				46 µg/cm²	23 µg/cm²
2a	**PVAm-EQ_{14}-$EA12_{11}$**	14	11	100	>> 99.99
2a	**PVAm-EQ_{7}-$EA12_{10}$**	7	10	100	99.99
2a	**PVAm-EQ_{5}-$EA12_{10}$**	5	10	100	99
2a	**PVAm-$EA12_{10}$**		10	99.9	< 90

[a)] The test was performed under growth conditions and a concentration of 0.01 % DOW was used. The given values are the mean values obtained by averaging the outcomes of two measurements.

To study the influence of the concentration of alkyl chains at a constant degree of functionalization with EQ, the concentration of EQ was kept constant at 7 % and the degree of functionalization with EA12 was set to 22 % and 10 % in Series 1. The results on the inhibition of growth of *E. coli* under growth conditions for 46 µg/cm² and 23 µg/cm² are shown in Table 10. It can again be observed that with an increasing concentration of EA12, the antimicrobial effect decreases.

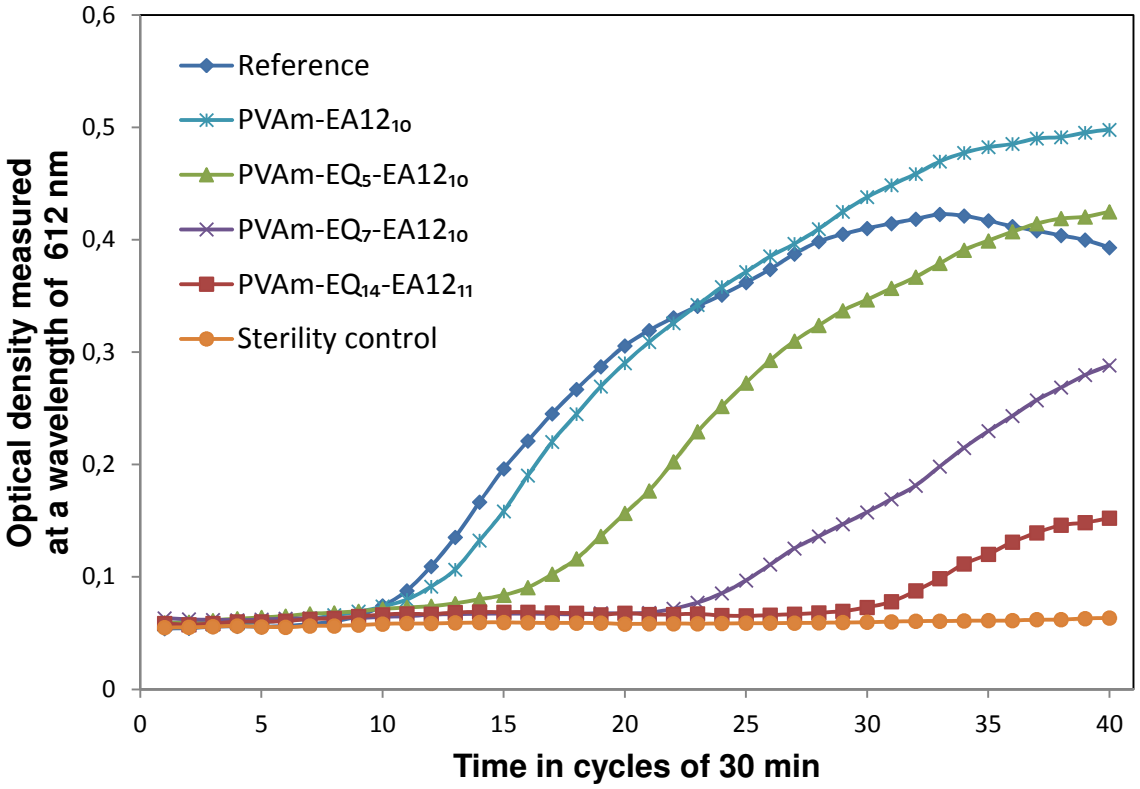

Figure 4. Proliferation curves of *E. coli* after exposure in nutrient solution (containing the wetting agent DOW in a concentration of 0.01 %) on the differently coated glass surfaces (Series 2a, with 23 µg/cm^2). Influence of the concentration of EQ at constant concentration of ~10 % EA12. Sterility control = coated glass sample inoculated with 20 µL nutrient solution + 0.01 % DOW; Reference = growth control, i.e., growth of *E. coli* after exposure on a non-coated glass surface. All measuring points are the mean values obtained by averaging the outcomes of two measurements.

Similarly to the earlier results with 460 µg/cm² polymer (1 wt% polymer solutions), the antimicrobial activity is for all samples higher under growth than under non-growth conditions. This affirms the assumption that the antimicrobial effect of the tested polymers takes place more pronouncedly during bacterial growth, i.e., during cell division and active metabolism.

Table 10. Composition of the functional polymers of Series 1 and inhibition[a)] of bacterial growth (*E. coli*) after exposure (2.5 h) on the coated glass substrates (46 µg/cm² and 23 µg/cm² polymer).

Series	Name	EQ [%]	EA12 [%]	Inhibition of growth[a)] [%]	
				46 µg/cm²	23 µg/cm²
1	**PVAm-EQ$_7$-EA12$_{22}$**	7	22	99	< 90
1	**PVAm-EQ$_7$-EA12$_{10}$**	7	10	100	99.99

[a)] The test was performed under growth conditions and a concentration of 0.01 % DOW was used. The given values are the mean values obtained by averaging the outcomes of two measurements.

Leaching

A leaching test was performed in parallel to the growth test. The leaching test served as a proof that during the growth test no inhibition is caused due to an amount of polymer transferred from the coated surface to the well plate of the test. It thereby proves that the growth test is valid and the growth inhibition is only due to the influence of the polymer on *E. coli* during the exposure on the surface. The shake solutions of the sterility control were transferred to a well plate, inoculated with a bacteria suspension of *E. coli*, and the proliferation curves were obtained by measuring the increase in optical density. If no material has leached from the surface into the solution, the bacteria can grow unhinderedly and the proliferation curves resemble the ones of the reference. If material has leached from the surface into the solution, the bacterial growth is influenced and the proliferation curves show differences compared to the reference. Within the performed tests, no leaching of the polymer coatings that would falsify the growth test was observed.

To investigate the leaching in more detail, three additional leaching tests were performed. Real leaching from the surface was tested (i) by measuring the antimicrobial effect of higher concentrated extracts of the coatings, (ii) by measuring the antimicrobial effect of the coated surfaces before and after washing, and (iii) via patching of the coated surfaces onto nutrient agar inoculated with *E. coli*, followed by incubation of the agar plates.

(i) Antimicrobial Effect of Higher Concentrated Extracts of the Coatings (460 µg/cm²)

Six substrates coated with the highest amount of polymer per cm² investigated in this chapter, were each exposed to nutrient solution. Parts of the combined exposure and washing solutions were inoculated with bacteria suspension of *E. coli* and the residual growth was monitored. All samples showed turbidities of the solutions. The turbidities already indicated the release of material from the surfaces. Because of these turbidities, the measured values for the antimicrobial activity of the extracts (Table 11) scattered strongly and are only guiding values. For all of the samples, besides the sample of polymer PVAm-EA12$_{21}$, the extracts of the coatings showed some antimicrobial activity, what proves the release of material from the surface. The antimicrobial activities of the extracts show the same trend as observed before. The activity of the extracts is increasing with increasing concentration of cationic groups and increasing with decreasing concentration of hydrophobic groups. From this test it is not possible to determine if for the higher active polymers more material is released, yielding in a higher activity of the extracts, or if this higher activity of the extracts comes from the higher activity of the polymer itself. Thus this leaching test does not quantify the polymer released from the surfaces.

Table 11. Leaching: Composition of the functional polymers and inhibition[a)] of bacterial growth (*E. coli*) of extracts of the coated glass substrates (460 µg/cm² polymer).

Name	EQ [%]	EA12 [%]	Inhibition of growth[a)] [%]
PVAm-EQ$_7$-EA12$_{22}$	7	22	~ 90[b)]
PVAm-EQ$_{14}$-EA12$_{11}$	14	11	100[b)]
PVAm-EQ$_7$-EA12$_{10}$	7	10	100[b)]
PVAm-EQ$_5$-EA12$_{10}$	5	10	> 99.9[b)]
PVAm-EA12$_{10}$	-	10	> 99[b)]
PVAm-EA12$_{21}$	-	21	0
PVAm-EA12$_{32}$	-	32	n.d.
PVAm-EA12$_{41}$	-	41	n.d.

n.d. = not determined; [a)] The given values are the mean values obtained by averaging the outcomes of minimum two measurements. [b)] The turbidity of the solution was very high and disturbing the OD measurement.

(ii) Antimicrobial Effect of Coated Surfaces (460 µg/cm²) Before and After Washing

The samples already used in the normal growth tests, described in the previous paragraphs (four weeks of storage, Table 7), were washed and used for a second growth test under growth conditions. For washing, the samples were shaken three times with sterile, bidistilled water. The samples were dried overnight lying on filter papers in open petri dishes in the clean bench. Then they were tested for their antimicrobial activity.

Table 12. Composition of the functional polymers and inhibition[a)] of bacterial growth (*E. coli*, 0.05 % DOW) after exposure under growth conditions (2.5 h) on the coated glass substrates after washing with sterile bidistilled water (460 µg/cm² polymer, four weeks of storage).

Name	EQ [%]	EA12 [%]	Inhibition of growth[a)] [%]	
			before washing	after washing
PVAm-EQ$_7$-EA12$_{22}$	7	22	~99.99	99
PVAm-EQ$_{14}$-EA12$_{11}$	14	11	100	100
PVAm-EQ$_7$-EA12$_{10}$	7	10	100	100
PVAm-EQ$_5$-EA12$_{10}$	5	10	100	100
PVAm-EA12$_{10}$	-	10	100	99.999999
PVAm-EA12$_{21}$	-	21	>99.99	90
PVAm-EA12$_{32}$	-	32	>90	90
PVAm-EA12$_{41}$	-	41	<90	0

[a)] The test was performed under growth conditions and a concentration of 0.05 % DOW was used. The given values are the mean values obtained by averaging the outcomes of two measurements.

The antimicrobial activities of the tested polymer coatings before and after washing are summarized in Table 12. The samples coated with the polymers PVAm-EQ$_{14}$-EA12$_{11}$, PVAm-EQ$_5$-EA12$_{10}$, and PVAm-EQ$_7$-EA12$_{10}$ swell strongly during the washing. The swollen layers were partly detached through physical abrasion. However, although some material was released, the growth of *E. coli* was completely inhibited. The coatings of the other polymers (PVAm-EQ$_7$-EA12$_{22}$, PVAm-EA12$_{10}$, PVAm-EA12$_{21}$, PVAm-EA12$_{32}$, and PVAm-EA12$_{41}$)

did not swell. For these polymers a lower inhibition of growth was observed after the washing, showing the release of polymer from the surface.

(iii) Patching of the Coated Surfaces (460 µg/cm²) onto Nutrient Agar Inoculated with *E. coli*, Followed by Incubation

The coated glass substrates were placed into Petri dishes and exposed to nutrient solution (containing DOW in a concentration of 0.05%) in a climate chamber at 25 °C and 95 % relative humidity (rH) for 2.5 h. Parts of the bacteria suspension of *E. coli* were pipetted and plated onto agar plates and afterwards incubated at 37 °C.

In the first test, the coated surfaces were patched with their upside onto the inoculated agar plates and afterwards incubated. A picture of the samples after incubation is shown in Figure 5. None of the samples show an inhibition zone. The absence of inhibition zones proves that during this test no material diffuses into the surrounding agar. For a better comparison an agar diffusion test of the antimicrobial agent triclosan is shown in Figure 6. The picture clearly shows the formation of inhibition zones around the filter pad patches containing triclosan, which cannot be observed for the samples coated with functionalized PVAm.

In a second test, the coated surfaces were patched with their upside onto the inoculated agar plates and were removed after a short time. The agar plates were incubated overnight at 37 °C and the colony growth was documented. A picture of the samples after incubation is shown in Figure 7.

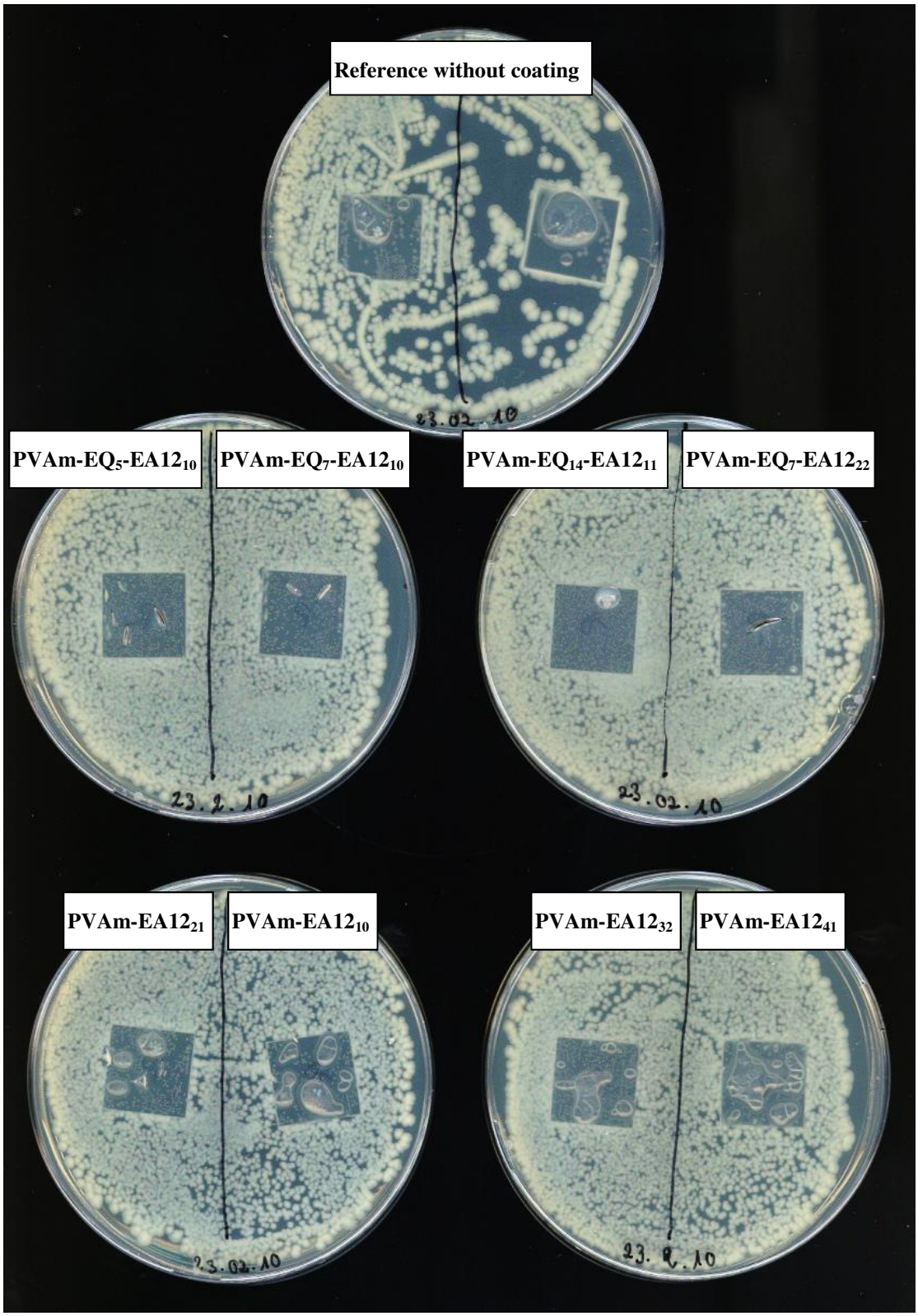

Figure 5. Glass patches of the tested polymer coatings on inoculated agar plates after incubation (37 °C, overnight) (with resting glass substrates). None of the samples shows an inhibition zone.

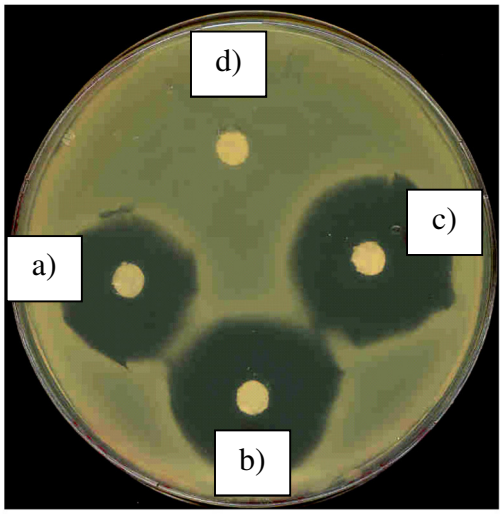

Figure 6. Agar diffusion test with *E. coli*: inhibition zones around the filter pads containing (a) 0.5 µg, (b) 5 µg, and (c) 10 µg of triclosan in comparison to (d) the reference.[23]

For the samples of the polymers PVAm-EQ_{14}-$EA12_{11}$ and PVAm-EQ_5-$EA12_{10}$, a growth inhibition of the bacteria was observed below the glass patches (Figure 7), which indicates a leaching of the coating. Below the samples of the polymers PVAm-EQ_7-$EA12_{22}$ and PVAm-EQ_7-$EA12_{10}$, a minor growth inhibition was observed which shows a modified growth. The sample of polymer PVAm-$EA12_{10}$ shows a slight leaching and for the samples of the polymers PVAm-$EA12_{21}$, PVAm-$EA12_{32}$, and PVAm-$EA12_{41}$, the leaching is not significant or not to be monitored. None of the samples show a clear inhibition zone, i.e., the samples only exhibit restricted leaching directly below the patches due to swelling and physical abrasion of the coatings. Restricted leaching was also monitored for the samples coated with 46 µg/cm² and 23 µg/cm² of polymer PVAm-EQ_{14}-$EA12_{11}$. With a restricted leaching, the polymer does not get into the environment. Instead, the polymer is better available for the bacteria and for that reason the antimicrobial activity of the polymer is higher. Hence, a restricted leaching is not only tolerable but also beneficial to get a higher antimicrobial activity.

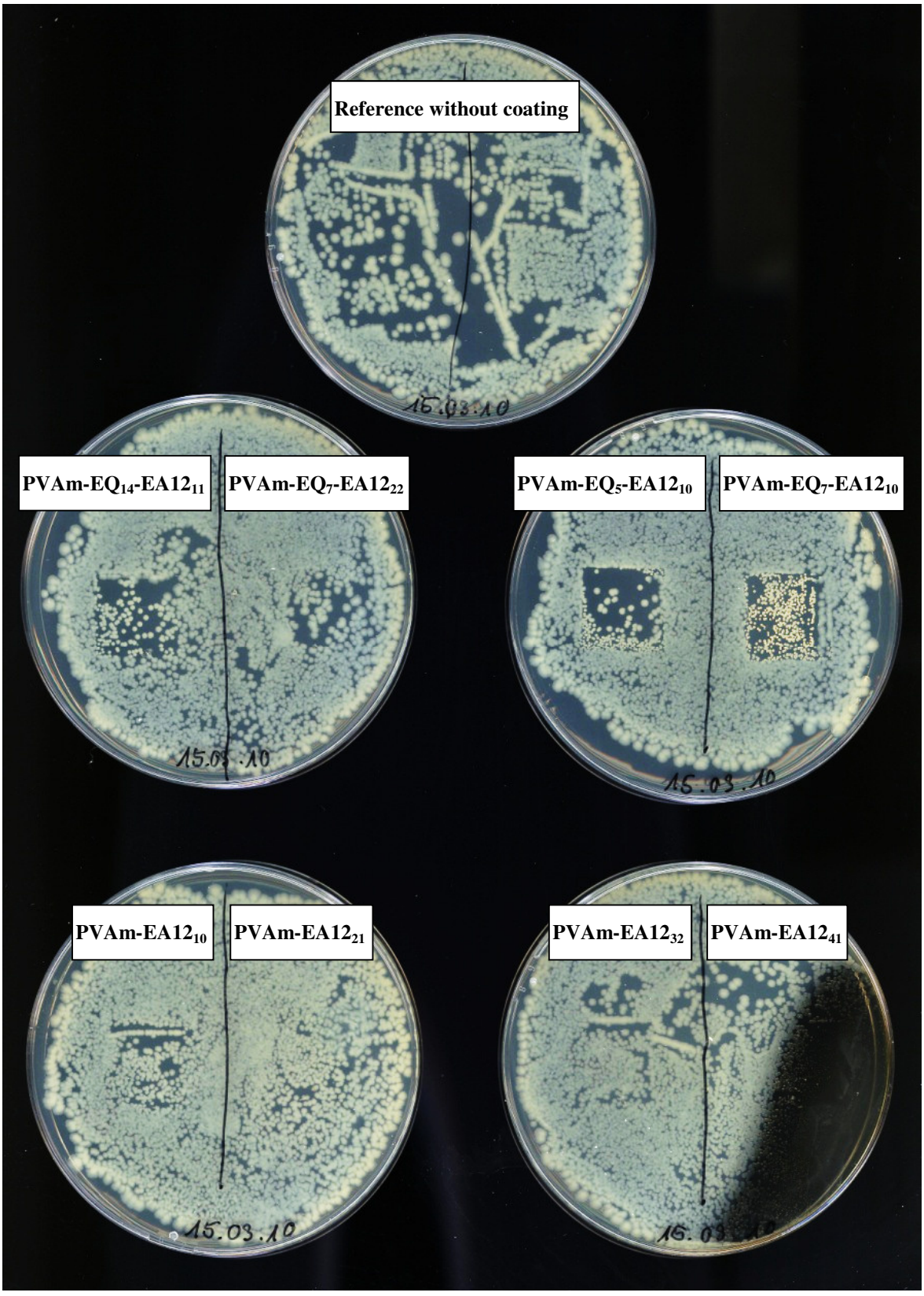

Figure 7. Glass patches of the tested polymer coatings on inoculated agar plates after incubation over night at 37 °C (removed glass substrates).

Spin Coated and Annealed Substrates

As observed and described in the previous paragraphs, the antimicrobial effect increases with an increasing concentration of cationic groups (EQ) which are introduced into the polymer. For 23 µg/cm² polymer (0.05 wt% solutions), the polymer PVAm-EQ_{14}-$EA12_{11}$ (Series 2a) showed almost a complete inhibition of growth. With the previously described coating technique of evaporating the solvent overnight, a thinner, homogeneous coating cannot be obtained. To analyze tendencies within the antimicrobial effect of the polymers with more than 14 % of cationic groups, a different coating technique was performed. To obtain thinner, homogeneous coatings, the polymer solution was applied onto the substrates by spin coating. Silicon wafers have been used as substrate. The silicon substrates were cleaned prior to their use. The methanolic polymer solutions (1 wt% in MeOH) have been spin coated on the substrates. To obtain a homogeneous surface and to give the polymer chains time to arrange in a thermodynamically stable conformation, the coatings were annealed in a methanol atmosphere for 5 h. The color of the coatings on the silicon wafer during the annealing changed from a deep blue to green. After removal of the substrates from the methanol atmosphere the blue color was recovered immediately. For more details on the influence of the annealing time on the antimicrobial effect and on the reproducibility of the measurements see Chapter 5. It was found that an annealing time of 5 h leads to homogeneous, thermodynamically stable coatings and to very good reproducible antimicrobial results.

To perform ellipsometry measurements a reflective surface is needed. The surface of the silicon wafers is reflective and almost similar to the glass substrates used in previous experiments. The results are therefore comparable. A coating thickness of about 90 nm was determined, which corresponds to an amount of 9 µg/cm² polymer. For details on the ellipsometry measurements and the calculations please see Chapter 5.

In the described way, the polymers of Series 2b and Series 4 were coated onto silicon wafers and annealed in methanol atmosphere. The antimicrobial activity of the coatings was investigated under growth conditions against *E. coli*. The composition and the antimicrobial activities of the tested polymers are summarized in Table 13.

Table 13. Composition of the functional polymers of Series 2b and Series 4, inhibition[a)] of bacterial growth (*E. coli*) after exposure (22 h) on the spin coated and annealed silicon substrates (9 µg/cm² polymer), and antimicrobial effect in the leaching test.

Series	Name	EQ [%]	EA12 [%]	Inhibition of growth[a)] [%]	
				growth	leaching
2b	**PVAm-EQ$_{28}$-EA12$_{11}$**	28	11	99.9 – 100	0
2b	**PVAm-EQ$_{21}$-EA12$_{11}$**	21	11	99 – 100	0
2b	**PVAm-EQ$_{17}$-EA12$_{11}$**	17	11	< 90	0
2b	**PVAm-EQ$_{13}$-EA12$_{11}$**	13	11	< 90	0
4	**PVAm-EQ$_{23}$**	23	-	100	100
4	**PVAm-EQ$_{30}$**	30	-	100	> 99.99
4	**PVAm-EQ$_{73}$**	73	-	100	> 99.99

[a)] The test was performed under growth conditions and a concentration of 0.01 % DOW was used. The given values are the mean values obtained by averaging the outcomes of two measurements in % of inhibition of growth.

The polymers of Series 2b, containing both cationic and hydrophobic groups, follow the expected trend in antimicrobial activity: with increasing concentration of cationic groups within the polymers the antimicrobial effect increases. The highest antimicrobial effect (99.9 – 100 %) within this series was, as expected, observed for the polymer

PVAm-EQ_{28}-$EA12_{11}$ with the highest concentration of 28 % cationic groups. For Series 2b no leaching was observed that would falsify the growth test. In contrast, the polymers of Series 4, containing only cationic groups, show a complete inhibition of growth and a significant leaching that falsifies the test. The measured antimicrobial effect of the coatings does not come from the coatings alone. It is also caused by material, which was released from the coatings and was transferred into the test solution. This different leaching behavior clearly shows the influence of the introduced hydrophobic groups on the solubility of the polymers and thereby on the stability of the coatings. Depending on the field of application, the introduction of alkyl chains into the polymer is beneficial for a stable non leaching coating, although it decreases the antimicrobial activity.

Antimicrobial Test in Solution

For most of the polymers a direct testing in solution was too imprecise due to the appearance of turbidity by adding PBS or nutrient solution to the aqueous polymer solutions. With an increasing concentration of cationic groups (EQ) in the polymer, the solubility in water increases and the turbidity of the polymer solution (in PBS or nutrient solution) decreases. A test in solution is therefore possible if the concentration of introduced cationic groups within the polymer is high enough. The polymers of Series 2b (increasing concentration of cationic groups at a constant concentration of 11 % alkyl chains) and Series 4 (only cationic groups with increasing concentration) were tested in solution for their antimicrobial activity against *E. coli*.

To determine the minimum inhibitory concentration (MIC) of the polymers, suspensions of *E. coli* with defined colony forming units were incubated in nutrient solutions with different concentrations of the functional polymers. The bacterial growth was followed during the incubation overnight, by measuring the optical density (OD) of the solutions. Table 14 shows

the composition and the measured MIC values of the tested polymers. Based on standard specifications[15], the MIC is defined in this thesis as the lowest concentration of an antimicrobial that inhibits the bacterial growth by 99.99 % (log-4 reduction[16] of the colony forming units) compared to the reference.

Table 14. Composition[a)] and MIC[b)] against *E. coli* of the functional polymers of Series 2b and Series 4.

Series	Name	EQ [%]	EA12 [%]	MIC[b)] [mg/mL]
2b	**PVAm-EQ$_{28}$-EA12$_{11}$**	28	11	0.05[c)]
2b	**PVAm-EQ$_{21}$-EA12$_{11}$**	21	11	0.1[c)]
2b	**PVAm-EQ$_{17}$-EA12$_{11}$**	17	11	0.2[c)]
2b	**PVAm-EQ$_{13}$-EA12$_{11}$**	13	11	0.2[c)]
4	**PVAm-EQ$_{23}$**	23	-	0.02
4	**PVAm-EQ$_{30}$**	30	-	0.01

[a)] Values given in % of the polymer repeating units. [b)] The MIC is defined as the lowest concentration of an antimicrobial that gives a log-4 reduction of the colony forming units. The shown values are mean values obtained by averaging the outcomes of three measurements. The test was performed under growth conditions and a concentration of 0.01 % DOW was used. [c)] The test solutions of Series 2b showed turbidities and the real MIC might be lower.

Even though the solubility of the polymers increased with increasing concentration of cationic groups, the solutions of the polymers of Series 2b were still turbid in the concentration range of the MIC. Due to this turbidity, the error of the resulting MIC values is quite high. In addition, the appearance of turbidity means that the polymer is not completely dissolved and

that not all of the polymer might be available for an antimicrobial interaction. The real MIC values can therefore be lower. The solubility of the polymers of Series 4 was very high and for these polymers no turbidity in the concentration range of the MIC was observed. These values can therefore be assumed to be reliable.

With Series 2b, the influence of a rising concentration of cationic groups (EQ) (at a constant concentration of ~11 % alkyl chains (EA12)) on the MIC was studied. As for the previous studies on substrates, it was observed that with an increasing concentration of cationic groups (EQ), the antimicrobial effect increases and the MIC values decrease from 0.2 mg/mL (10 % EQ) to 0.05 mg/mL (28 % EQ). This trend was also observed in Series 4 (only cationic groups and no alkyl chains) where the MIC decreases from 0.02 mg/mL (23 % EQ) to 0.01 mg/mL (30 % EQ).

The comparison of the polymers PVAm-EQ_{21}-$EA12_{11}$ and PVAm-EQ_{28}-$EA12_{11}$ of Series 2b with the polymers PVAm-EQ_{23} and PVAm-EQ_{30} of Series 4 shows that the introduction of only 11 % alkyl chains into the polymer significantly decreases the solubility. Due to the appearance of turbidities, the values of the two series are not directly comparable and can give only trends. However, the measured MIC values of the polymers of Series 4 are much lower than the MIC values of the respective polymers of Series 2b. This different activity confirms the finding from the antimicrobial test on substrates, where it was found that the antimicrobial activity is decreased by the introduction of alkyl chains.

The described structure solution properties show that for an application of the polymers in solution, it might be better to introduce cationic groups only. For an application as coating, a decreased solubility in aqueous solutions can, however, be appreciated and the introduction of alkyl chains into the polymer can be beneficial to obtain a permanent coating.

4.3.4 Membrane Penetration in Langmuir Film Experiments

The molecular interaction with lipid films or rather the ability of the developed polymers to penetrate into membranes was tested for the polymers of Series 2b, Series 3, and Series 4 (for the compositions of the polymers see Table 4). Therefore, the degree of penetration of the polymers into Langmuir monolayers of neutral lipids was measured.

An ordered monomolecular lipid layer of DPPC (dipalmitoylphosphatidylcholine) on the surface of bidistilled water (subphase) in a Langmuir trough was used as model membrane system. The density of the lipid molecules in the surface monolayer was adjusted by compression and indicated by the surface pressure of the film. Within this test, an initial surface pressure of 20 mN/m was used. The layer was compressed with the Langmuir balance to reach the initial surface pressure. Thereafter, the polymer solution was injected into the subphase and the increase of surface pressure (mN/m) was recorded for 60 min (Figure 8). After the 60 min a new equilibrium was established and the surface pressure was stable. An increased surface pressure shows the adsorption of the polymer to the lipid layer and a penetration into it. The increase of the surface pressure $\Delta\pi$ is the most widely used parameter to characterize the membrane affinity/penetration ability of a molecule in Langmuir layer studies.[24,25,26,27,28]

Series 2b and Series 4 were tested with two different polymer concentrations (0.025 mg/mL and 0.075 mg/mL) in the subphase. Series 2b contains polymers with different concentrations of EQ (cationic groups) and a constant concentration of 11 % EA12 (alkyl chains), whereas the polymers in Series 4 only contain cationic groups (EQ) in different concentrations and no alkyl chains. The increase of the surface pressure of the lipid film ($\Delta\pi$) as a result of the penetration of the polymers into the monolayers of DPPC is shown together with the concentration of cationic groups in the polymers in Figure 9.

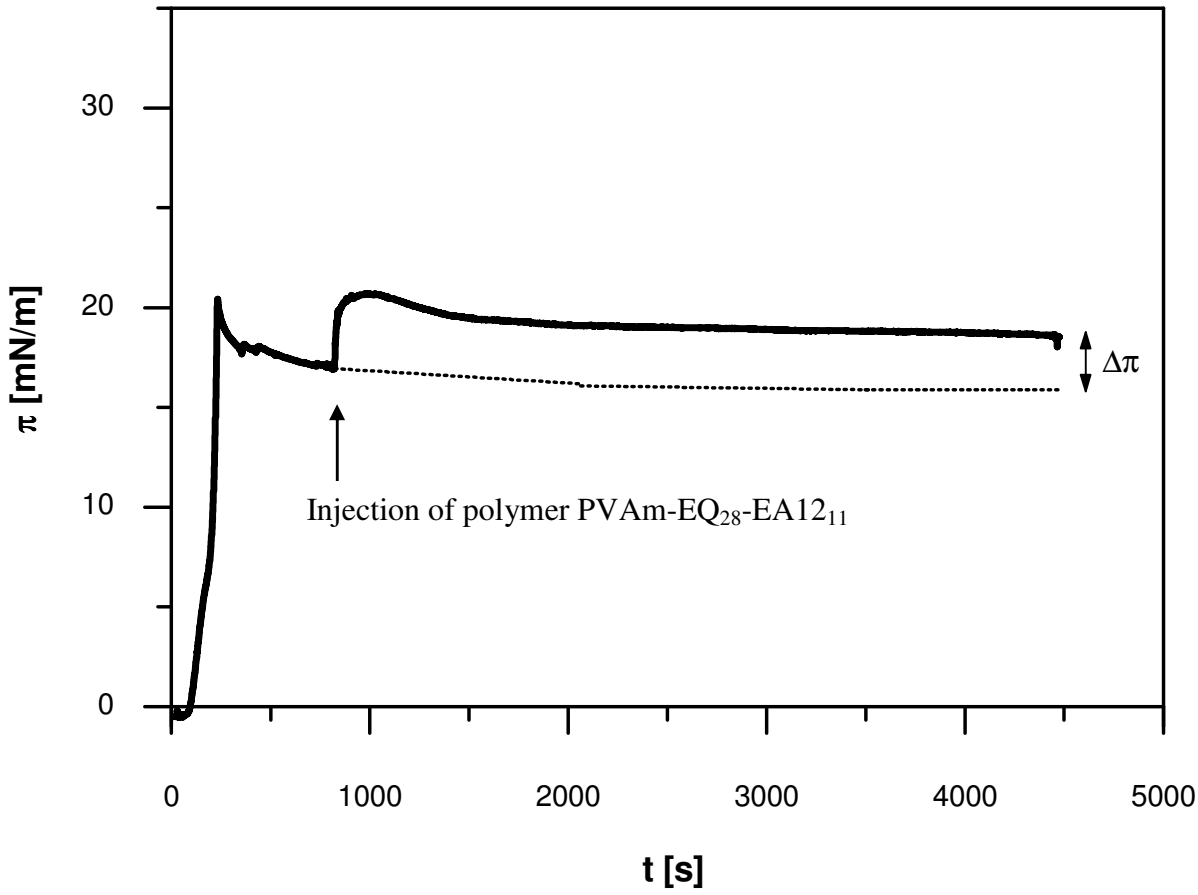

Figure 8. Surface pressure π (mN/m) of the DPPC lipid film on water (at 23.7 °C), following the injection of the polymer PVAm-EQ_{28}-$EA12_{11}$ (0.025 g/L) as a function of time t (s).

For a polymer concentration of 0.025 mg/mL in the subphase (black bars), all polymers of Series 2b show almost the same low penetration into the DPPC layer of around 3 mN/m. The polymers of Series 4 with no alkyl chains show a lower or no penetration at all into the DPPC layer. The aqueous solubility of the polymers is highly increased by the introduction of charged groups (EQ), which decrease their surface activity and their membrane affinity.

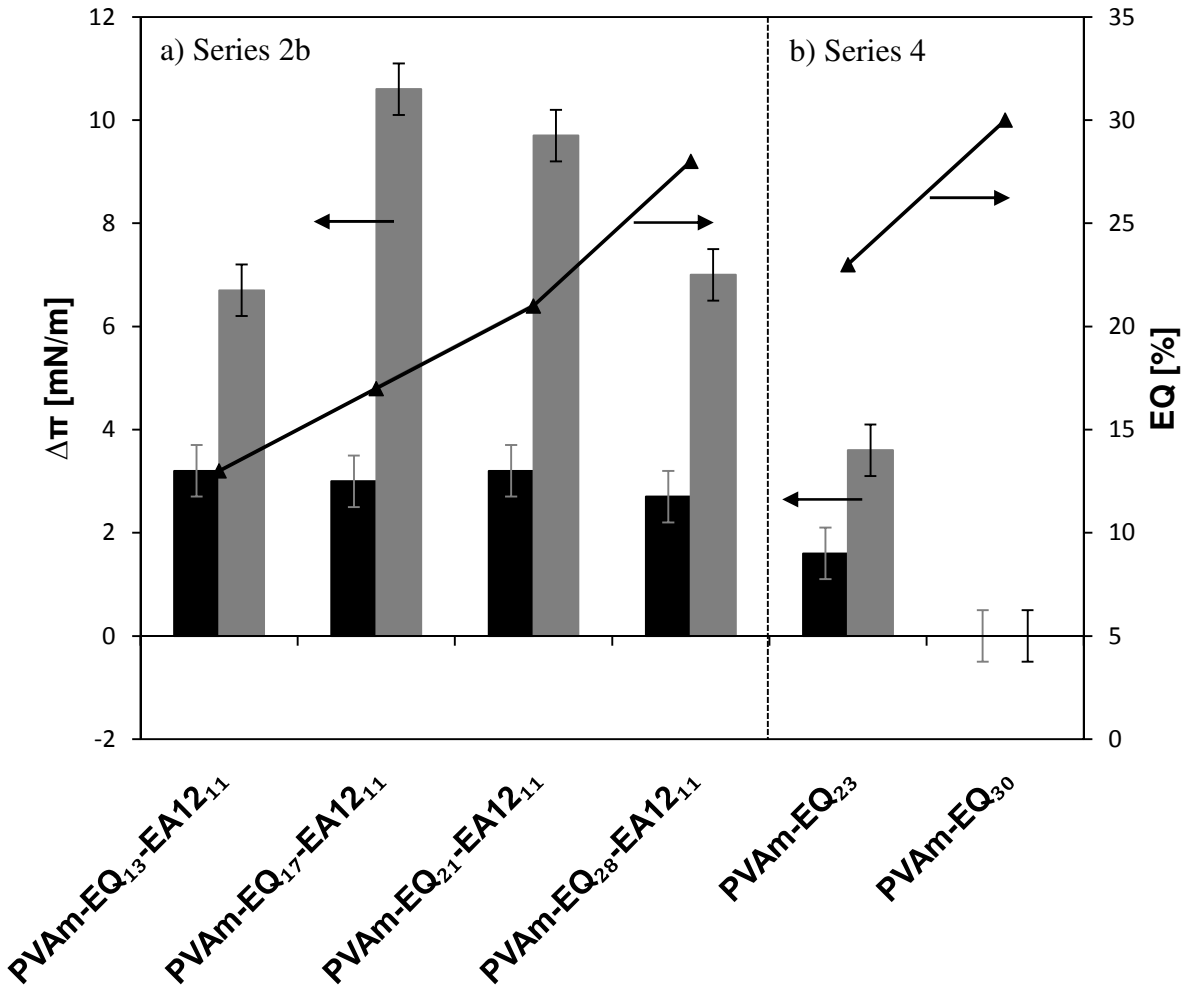

Figure 9. Increase of the surface pressure of the lipid film (Δπ) as a result of the penetration of (a) **PVAm-EQ$_x$-EA12$_{11}$** (Series 2b), polymers with different concentrations of EQ (cationic groups) and constant concentration of 11 % EA12 (alkyl chains) and of (b) **PVAm-EQ$_x$** (Series 4), polymers with different concentrations of EQ (cationic groups), into monolayers of DPPC with an initial surface pressure of 20 mN/m. Two different polymer concentrations in the subphase are displayed: 0.025 mg/mL (black), 0.075 mg/mL (grey). The estimated error of the measured values amounts to ± 0.5 mN/m.

The measurements were repeated with a polymer concentration of 0.075 mg/mL in the subphase (grey bars). For this higher concentration, a relation between the polymer composition and the ability of the polymer to penetrate into a lipid membrane can be observed. The increase in surface pressure ($\Delta\pi$) and therefore the membrane affinity of the polymers of Series 2b rises in the beginning (with an increasing concentration of cationic groups) to 10.6 mN/m for the polymer PVAm-EQ_{17}-$EA12_{11}$ with 17 % EQ. With a further increasing concentration of cationic groups, the penetration ability decreases. This behavior shows that the penetration ability reaches a maximum at a concentration of 17 % cationic groups in the polymer. The membrane affinity is in general higher for the polymers of Series 2b containing 11 % alkyl chains compared to the polymers of Series 4 without alkyl chains.

The polymers of Series 3 with different concentrations of EA12 (alkyl chains) were tested with a polymer concentration of 0.025 mg/mL in the subphase. The increase of the surface pressure of the lipid film ($\Delta\pi$) as a result of the penetration of the polymers into the monolayers of DPPC is shown together with the concentration of alkyl chains in the polymers in Figure 10. A clear trend in the degree of penetration is observable. The penetration ability of the polymers is a function of the concentration of alkyl chains in the polymer. The penetration ability increases with an increasing concentration of alkyl chains in the polymer. It is expected that this trend continues for higher concentrations of alkyl chains and that for higher concentrations of the polymer in the subphase, higher penetration values can be reached. A direct test of higher polymer concentrations and higher degrees of functionalization with alkyl chains was not possible, as the solubility of the polymers in water decreases with increasing concentration of alkyl chains.

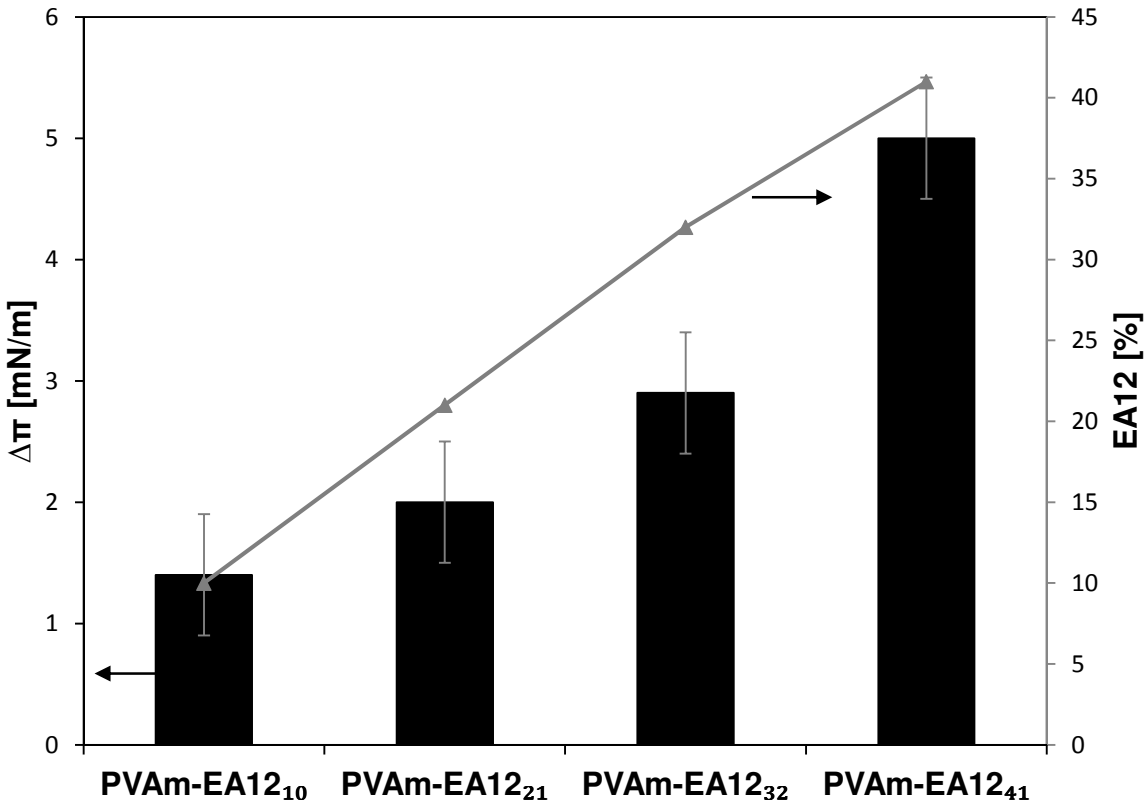

Figure 10. Increase of the surface pressure of the lipid film ($\Delta\pi$) as a result of the penetration of **PVAm-EA12$_x$** (Series 3), polymers with different concentrations of EA12 (alkyl chains) into monolayers of DPPC with an initial surface pressure of 20 mN/m. A polymer concentration in the subphase of 0.025 mg/mL was tested. The estimated error of the measured values amounts to ± 0.5 mN/m.

The comparison between the different series indicates the importance of alkyl chains within the polymer to achieve a penetration of the polymers into a lipid layer. This observation seems to be contradictory to the observations for the antimicrobial effect. On the one hand, the antimicrobial effect clearly increases with increasing concentration of cationic groups and with decreasing concentration of alkyl chains. On the other hand, the membrane affinity increases with increasing concentration of alkyl chains and reaches a maximum at a concentration of 17 % cationic groups within the polymer. This different behavior can be due

to different membrane polarities. The DPPC monolayer used for the penetration experiment is neutral in charge, whereas the bacterial membrane has negative charges on its surface. Thus, in the case of the DPPC layer, the hydrophobic interaction plays the major role in the interaction between the polymer and the model membrane system. In contrast, in the case of the real bacterial membrane, the hydrophilic interaction is essential for the antimicrobial effect. In the polymer system presented here, the concentration of cationic groups (EQ) (and thereby the ionic interactions of the polymer with the bacteria) has a greater impact on the antimicrobial effect than the concentration of alkyl chains in the polymer. The antimicrobial effect is not caused by the penetration of the alkyl chains into the lipid layer alone. As described in Chapter 1 there are several ways of antimicrobial action and the penetration into the lipid layer is only one of them. The antimicrobial effect of the here developed polymers is caused by a combination of effects and their activity is determined by their hydrophilic-hydrophobic balance.

4.4 Conclusions

The amphiphilic multifunctional poly(vinyl amine)s were tested for their antimicrobial activities and the influence of the hydrophilic/hydrophobic balance on the antimicrobial activity was investigated. It was found that the coating thickness of the polymers has an impact on the antimicrobial activity. The activity increases with increasing coating thickness. First the polymers coated on glass surfaces were tested. It was found that with 460 µg/cm² of functional polymer (on model glass surfaces) for all the polymers (with the exception of the polymers PVAm-EA12$_{32}$ and PVAm-EA12$_{41}$) the inhibition of growth was 99.99 % up to a complete inhibition of growth. For 23 µg/cm² of functional polymer, it was possible to determine the influence of the hydrophilic/hydrophobic balance on the antimicrobial effect. The antimicrobial activity increases with an increasing degree of functionalization with the

quaternary ammonium group bearing epoxide EQ and decreases with an increasing degree of functionalization with the long alkyl chain containing epoxide EA12. The polymer PVAm-EQ_{14}-$EA12_{11}$ of Series 2a, which contains the highest concentration of cationic groups within this series, showed the best antimicrobial activity under the polymers tested on coated substrates prepared by drop casting. Among the substrates which were coated with the lowest amount of polymer (23 µg/cm²), the polymer PVAm-EQ_{14}-$EA12_{11}$ gave the highest antimicrobial activity (>> 99.99 % up to a complete inhibition of growth under growth conditions). As discussed above, a lower thickness of the coating leading to the same antimicrobial effect is valuable, because it means that less polymer is needed to achieve the antimicrobial effect what makes a later application cheaper.

In the second part of the investigation of the antimicrobial effect, the polymers with higher concentrations of cationic groups were tested on coated substrates prepared by spin coating followed by annealing in methanol atmosphere, which yields much lower coating thicknesses than the coating by drop casting. The tests were also carried out in aqueous solution. The trend already discovered for the substrates coated by drop casting was reconfirmed and studied in more detail for higher concentrations of cationic groups. For both, the coated substrates and the aqueous solutions, the antimicrobial effect increases again with an increasing concentration of cationic groups and a decreasing concentration of alkyl chains. This shows that the behavior on coated surfaces and in solution is comparable. With an increasing concentration of cationic groups the solubility of the polymers increased. The polymers without hydrophobic groups leached from the surface during the antimicrobial test, whereas the polymers with about 10 % hydrophobic groups were stable on the surface such that the antimicrobial test was not falsified by a leaching of the material. The polymer PVAm-EQ_{28}-$EA12_{11}$ of Series 2b showed with 99.9 % up to a complete inhibition of growth the highest antimicrobial activity of the polymer coatings which were prepared by spin

coating (9 µg/cm²), containing both cationic and hydrophobic groups. The polymers containing only cationic groups showed higher activities, with complete inhibitions of growth, but also showed a strong leaching of the coated material from the surface that falsified the antimicrobial test. The polymers were tested in aqueous solutions and showed low MIC values down to 0.01 mg/mL for the polymer PVAm-EQ_{30}. It is expected that higher concentrations of cationic groups give even lower MIC values.

The polymers were tested in Langmuir film experiments for their membrane affinity/penetration ability of a molecule into a neutral lipid layer of DPPC. It was found that for this membrane system, the ability of the polymer to penetrate into the lipid layer is maximal for a concentration of 17 % cationic groups within the polymer and increases with an increasing concentration of alkyl chains in the polymer. This tendency is different to the trend in the antimicrobial activity. This difference can be due to distinctions between the membrane polarity of the model system DPPC (neutral) and the natural bacterial membrane (negative). The different membrane polarities lead to differences in the interaction of the polymer and the membrane. In the neutral DPPC lipid layer system, hydrophobic interactions play the major role, whereas in the case of the negative bacterial membrane, ionic interactions play the crucial role in the polymer membrane interaction.

4.5 Literature

[1] Infectious Diseases Society of America (IDSA), *Clin. Infect. Dis.* **2012**, *55* (*8*), 1031-1046.

[2] M. E. Falagas, I. A. Bliziotis, *Int. J. Antimicrob. Agents* **2007**, *29*, 630–636.

[3] M. E. Falagas, P. I. Rafailidis, D. K. Matthaiou, S. Virtzili, D. Nikita, A. Michalopoulos, *Int. J. Antimicrob. Agents* **2008**, *32*, 450–454.

[4] R. Valencia, L. A. Arroyo, M. Conde, *Infect. Control. Hosp. Epidemiol.* **2009**, *30*, 257–263.

[5] M. S. Hoffmann, M. R. Eber, R. Laxminarayan, *Infect. Control Hosp. Epidemiol.* **2010**, *31*, 196–197.

[6] M. D. Adams, G. C. Nickel, S. Bajaksouzian, *Antimicrob. Agents Chemother.* **2009**, *53*, 3628–3634.

[7] E. Lautenbach, M. Synnestvedt, M. G. Weiner, *Infect. Control Hosp. Epidemiol.* **2009**, *30*, 1186–1192.

[8] S. Navon-Venezia, A. Leavitt, Y. Carmeli, *J. Antimicrob. Chemother.* **2007**, *59*, 772–774.

[9] E. F. Palermo, K. Kuroda, *Appl Microbiol Biotechnol* **2010,** *87*, 1605–1615.

[10] H. W. Boucher, G. H. Talbot, J. S. Bradley, J. E. Edwards, D. Gilbert, L. B. Rice, M. Scheld, B. Spellberg, J. Bartlett, *Clin. Infect. Dis.* **2009**, *48*, 1–12.

[11] P. A. Tran, T. J. Webster, *Nanotechnology* **2013**, *24***,** 155101/1-155101/7.

[12] E. M. Hetrick, M. H. Schoenfisch*, Chem. Soc. Rev*. **2006**, *35*, 780-789

[13] A. Klibanov, *J. Mater. Chem*. **2007**, *17*, 2479–2482.

[14] T. Tashiro, *Macromol. Mater. Eng*. **2001**, *286*, 63-87.

[15] DIN EN ISO 14160:2011-10, German Version EN ISO 14160:2011.

[16] Log-Reduction-Fact-Sheet: http://www.garnerdecontaminationsolutions.com/resources/HFI-Log-Reduction-Chart.pdf.

[17] N. J. Hardy, T. H. Richardson, F. Grunfeld, *Colloids Surf. A* **2006**, *202*, 284.

[18] E. Poptoshev, M. W. Rutland, P. M. Claesson, *Langmuir* **2000**, 16, 1987–1992.

[19] A. Shulga, J. Widmaier, E. Pefferkorn, S. Champ, H. Auweter, *Journal of Colloid and Interface Science* **2003**, *258*, 219–227.

[20] A. Shulga, J. Widmaier, E. Pefferkorn, S. Champ, H. Auweter, *Journal of Colloid and Interface Science* **2003**, *258*, 228–234.

[21] Antimicrobial testing method for coated substrates developed by *DWI an der RWTH Aachen e.V.:* EXPOSE. The testing method was developed on the basis of DIN EN ISO 20743 (a).

[22] N. Pasquier, Multi-Functional Polymers from Polyamines and Functional Five-Membered Cyclic Carbonates, In: *Dissertation*, ITMC, RWTH Aachen **2008**.

[23] Result shown with permission from: E. Heine, *AiF* 12865.

[24] W. R. Glomm, S. Volden, O. Halskau, Jr., M.-H. G. Ese, *Anal. Chem.* **2009**, *81*, 3042.

[25] É. Kiss, E. T. Heine, K. Hill, Y-C. He, N. Keusgen, Cs. B. Pénzes, D. Schnöller, G. Gyulai, A. Mendrek, H. Keul, M. Möller, *Macromolecular Bioscience* **2012**, *12 (9)*, 1181–1189.

[26] Cs. B. Pénzes, D. Schnöller, K. Horváti, Sz. Bősze, G. Mező, É. Kiss, *Colloids Surf. A* **2012**, *413*, 142– 148.

[27] K. Hill, Cs. B. Pénzes, D. Schnöller, K. Horváti, Sz. Bősze, F. Hudecz, T. Keszthelyi, É. Kiss, *Phys. Chem. Chem. Phys.* **2010**, *12*, 11498–11506.

[28] K. Hill, Cs. B. Pénzes, B. G. Vértessy, Z. Szabadka, V. Grolmusz, É. Kiss, *Progr. Colloid Polymer Sci.* **2008**, *135*, 87-92.

CHAPTER 5

SYNTHESIS AND CHARACTERIZATION OF POLYMERS WITH THE SAME COMPOSITION BUT DIFFERENT MICROSTRUCTURES

5.1 Introduction

In the last decades an increasing interest arose in the structure – antimicrobial property relation of synthetic polymers. Many of these polymers have been designed to mimic natural host-defense proteins, such as, e.g., magainins and cecropins.[1,2,3,4,5,6,7,8,9,10,11,12,13,14] Such proteins are produced in all higher forms of life to protect against bacterial infections.[15] The human body produces defensins as host-defense proteins. Defensins are amphiphilic peptides with a high number of cationic and hydrophobic amino acid residues.[16,17,18,19] These residues build a hydrophobic face and a spatially opposing hydrophilic face in the peptide. The hydrophilic face can selectively act on bacterial cell membranes which have an overall negative charge. The mechanism of the antimicrobial action is not yet completely understood.[15] In contrast to synthetic polymers, natural proteins exhibit defined secondary and tertiary structures beside the defined primary structures. The association of two or more proteins can result in distinctive quaternary structures. The thereby defined three-dimensional structure is characteristic and crucial for the biological function of each protein. Vast research efforts are focusing on the folding principles of sequence-specific heteropolymers (e.g., peptoids) with the goal to realize defined three-dimensional structures and to mimic the functions of natural proteins.[20,21,22,23,24,25,26,27,28] The rules governing the kinetics and thermodynamics of the folding process of the polymer chains into stable secondary and

tertiary structures are still not fully understood. Synthetic polymers do not exhibit a uniform folding, however polymers containing ionic and hydrophobic groups can self-assemble and form micelle-like structures in selective solvents. This ability can, amongst others, be tailored by the microstructure and/or architecture of the polymers.[29,30]

In Chapter 4 the antimicrobial effect of multifunctional polymers from poly(vinyl amine) (PVAm) was analyzed. These polymers were synthesized in one-step, reacting the free amine groups of PVAm with a mixture of functional epoxides. Here the question arises if by sequential addition and different order of addition of the epoxides, different microstructures can be obtained within the polymer, while the composition stays the same, as depicted in Figure 1. The difference in microstructure should lead to differences in the polymer properties and can thus be determined.

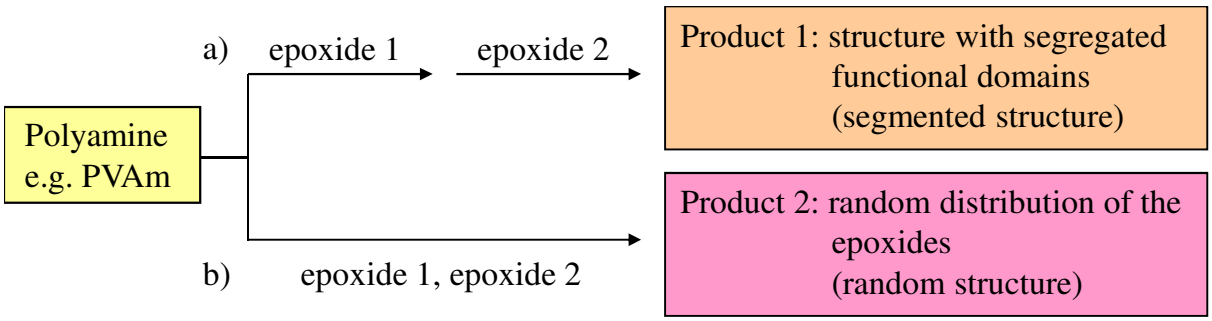

Figure 1. a) Sequential and b) simultaneous addition of functional epoxides to PVAm; consequences on the resulting microstructure.

In this chapter, the micro structuring of functionalized poly(vinyl amine)s (PVAm) via different synthetic routes is presented. The influence of the micro structuring on the antimicrobial effect, the CAC (critical aggregation concentration), the viscosity, the ability to penetrate into a model DPPC membrane, the ability to penetrate into the outer/inner membrane of *E. coli*, and the hemolytic activity of the polymers was determined.

5.2 Experimental Part

Poly(vinyl amine) is composed of different repeating units: vinyl amine and residual vinyl formamide. The ratio of these repeating units can be determined by ^{1}H NMR spectroscopy. In what follows, $\overline{M}$ denotes the averaged molecular weight per repeating unit calculated from the ^{1}H NMR spectrum.

5.2.1 Materials

Starting materials were used as received: 1,2-epoxydodecane (EA12) (Alfa Aesar, 96 %), glycidyltrimethylammonium chloride (EQ) (Aldrich, 75-80 % in water; since the oxirane degrades in time, the active content is determined just before use by NMR spectroscopy), and Seral-water (conductivity 0.055 µS/cm). Poly(vinyl amine) (PVAm) has been supplied by BASF (explorative material: salt free PVAm, supplier information: purified by ultra filtration, molecular weight = 340.000 g/mol). PVAm was freeze-dried before use. The dialysis tubings of regenerated cellulose had a molecular weight cut off of 50 kDa (CelluSep). The analytical data of the PVAm (salt free) are summarized in Table 1.

Table 1. Analytical data of salt free poly(vinyl amine).

Polymer	**MW** [a] **[g/mol]**	**DH** [a] **[%]**	**DH** [b] **[%]**	**Salt content** [b] **[%]**	$\overline{M}$ **(repeating unit)** [c] **[g/mol]**
PVAm (salt free)	340.000	100	99	1	43.60

[a] supplier information, DH = degree of hydrolysis, [b] determined by NMR, [c] $\overline{M}$ = averaged molecular weight per repeating unit calculated from NMR.

5.2.2 Measurements

^{1}H and ^{13}C NMR spectra were recorded on a Bruker AV 400 FT-NMR spectrometer at 400 MHz and 100 MHz, respectively. Deuterated methanol (MeOD) was used as solvent and the solvent's residual peak was used as internal standard.

The Raman spectra were recorded at room temperature on a Bruker RFS 100S spectrometer with a Nd: YAG-Laser (1064 nm, 400 mW) at a spectral resolution of 4 cm^{-1} with 1000 scans.

Fluorescence spectroscopy measurements were performed on a Fluoromax-4P spectrofluorometer (HORIBA Jobin Yvon). Air-saturated solutions (at 20 °C) were measured with 90° geometry and a slit opening of 1 nm. An emission wavelength of λ_{Em} = 390 nm was chosen for fluorescence excitation spectra while an excitation wavelength of λ_{Ex} = 339 nm was chosen for fluorescence emission spectra. Spectra were accumulated with an integration time of 30 nm/min.

To prepare the samples for the fluorescence measurements, first a solution of pyrene in acetone with a concentration of 6×10^{-3} mol/L and polymer solutions of 1 mg/mL and 0.01 mg/mL in Seral-water were prepared. To dissolve the polymers, the solutions were stirred over night at 60 °C. Each sample solution was prepared by adding the pyrene solution (1 mL, 6×10^{-6} mol) into an empty vial, evaporating the acetone for 12 h at room temperature, adding the polymer solution (10 mL) and shaking the solutions for 12 h at 60 °C in a "Thermoshaker (GFL 3032)". Samples with polymer concentrations ranging from 1 mg/mL to 0.0001 mg/mL were prepared. For the fluorescence measurements, the solution (ca. 3 mL) was placed in a quartz cell with a base area of 1.0 × 1.0 cm^2 and tempered for 15 minutes at 20 °C prior to measurement.

The ellipsometry measurements were performed with an OMT instrument, using the VisuEl software version 3.4.1 (Optische Messtechnik GmbH) at an angle of incidence of 70º and a spectral method in the wavelength range from 460 to 870 nm. In order to measure ultrathin

coatings, the azimuthal angle was set to 15º. The resulting thickness is obtained by taking the average of at least 5 measurements from different areas of the silicon substrate.

The contact angle measurements were performed using the sessile drop method with a G40 contact angle measuring instrument (Krüss GmbH), using the DSAII software (drop shape analyzer). A minimum number of 5 droplets of dist. water were applied onto each sample. From each droplet, 10 independent sessile drop measurements were performed and the average contact angles were calculated.

The surface topology of spin coated, thin polymer films was investigated using an atomic force microscope (AFM) (Nanoscope Multimode IIIa, Digital Instruments, Santa Barbara, CA, USA). The tapping mode imaging was performed with standard silicon cantilevers (Nanosensors, Wetzlar, Germany). The force constant and the resonant frequency were reported by the manufacturer as 42 N/m and 320 kHz, respectively.

The viscosity measurements were performed with an Ubbelohde viscometer for different polymer concentrations in Seral-water. The resulting measurement points are the mean values obtained by averaging the outcomes of at least six independent measurements at a constant temperature of 20 °C.

5.2.3 Name of Prepared Products

Polymers are named using a threefold expression: The first part of this expression denotes the used poly(vinyl amine). The second and the third part denote the used epoxides and the corresponding indices show the degrees of functionalization based on the total amount of amino groups. A number in front of the second and third part assigns the order in which the epoxides were added to the reaction solution. If there is no number, the epoxides were added simultaneously. The used abbreviations are given in Table 2.

Table 2. Abbreviations for the denotation of the products.

unit	correlation
PVAm	salt free PVAm, MW [a)] = 340.000 g/mol
EQ	glycidyltrimethylammonium chloride
EA12	epoxydodecane

[a)] supplier information

For example, PVAm-1.EQ_{11}-2.$EA12_{11}$ stands for the functionalization of salt free PVAm with 11 % EQ and 11 % EA12. In this case the epoxides were added sequentially and PVAm was first reacted with EQ and afterwards reacted with EA12.

5.2.4 Microorganisms

The antimicrobial activity of the polymers was tested against the Gram-negative bacterium *Escherichia coli* (DSMZ 498).

5.2.5 Bacterial Culture

The nutrient solution (NL1, pH 7) contained 5 g peptone and 3 g meat extract per liter bidistilled water. The phosphate-buffered saline (PBS) contained 9.0 g NaCl per liter of 0.1 M disodium hydrogenophosphate/sodium dihydrogenophosphate buffer solution adjusted to pH 6.5. Soft agar was prepared from 10.0 g peptone, 3.0 g meat extract, 6.0 g NaCl, and 7.0 g agar-agar per liter of bidistilled water. All solutions were autoclaved for 15 min at 120 °C prior to use. The bacteria were suspended in nutrient solution and in PBS, respectively. The final suspension in nutrient solution or PBS contained DOW (superwetting agent Q2-5211; 3-(Polyoxyethylene)propylhepta-methyltrisiloxane from DOW Chemicals) in a

concentration of 0.01 % and 2×10^6 colony forming units per mL (cfu/mL). All solutions were autoclaved for 15 min at 120 °C prior to inoculation.

5.2.6 Surface Coating

Glass substrates (Marienfeld, 18 mm × 18 mm) or silicon wafer cut into pieces (15 mm × 15 mm) were used as model surfaces. The substrates were ultrasonically cleaned in acetone (p.a.), dist. water, and isopropanol (p.a.) for 5 minutes each and afterwards dried under nitrogen-flush. After cleaning, the substrates were directly used for coating.

Drop Casting

150 µL of a methanolic polymer solution (0.05 wt% (w/w), and 0.025wt% (w/w)) were uniformly casted onto a glass substrate and the solvent was allowed to evaporate overnight. The polymer concentration can be calculated to be 23 µg/cm² (for the 0.05 wt% polymer solution) and 11.5 µg/cm² (for the 0.025 wt% polymer solution).

Spin Coating

100 µL of a methanolic polymer solution (1 wt% (w/w)) were applied onto the silicon wafer and rotated with 2000 revolutions per minute (rpm) for 30 sec.

Annealing in Methanol Atmosphere

The bottom of an exsiccator was filled with methanol up to a level of about 1 cm. The exsiccator was closed and stored for two days at RT so that a methanol atmosphere had built. The coated substrates were placed into the exsiccator, annealed in methanol atmosphere, and removed after defined times.

5.2.7 Antimicrobial Assessment of Polymer Coatings

Antimicrobial Test of Coated Surfaces

The antimicrobial effect was tested under growth (bacteria suspension in nutrient solution) conditions. All tests were carried out at least twice (in order to reduce statistical artifacts). To ensure a complete wetting of the surface enabling the bacteria to interact with the coated polymer, the wetting agent DOW (Q2-5211; 3-(polyoxyethylene)propylheptamethyltri-siloxane) was added to the test solutions in a concentration of 0.01 %. The antimicrobial testing system for coated surfaces is depicted in Figure 2. Substrates coated with functionalized PVAm (non sterilized) were placed into Petri dishes (Ø = 3 cm) and 20 µL bacteria suspension of *E. coli* (2×10^6 colony forming units per mL (cfu/mL)) were inoculated onto each surface (parallel samples a and b) and covered with a coverslip. As reference, an uncoated substrate was exposed to 20 µL bacteria suspension of *E. coli* (2×10^6 cfu/mL). As sterility control, a coated substrate was exposed to 20 µL of nutrient solution or PBS, for the testing under growth and under non-growth conditions, respectively (sample c). The exposure was performed in a climate chamber at 25 °C and 97 % rH (relative humidity) for 22 h. Thereafter, 1 mL of the nutrient solution was pipetted (dilution 1 : 50) in every Petri dish (a – c) and the samples were shaken at RT for 30 min with 150 rpm. Then 200 µL solution were transferred from each Petri dish to a well plate in order to monitor the residual growth (growth test).

Leaching test: 180 µL of the shake solution of sample c (sterility control) were transferred to a well plate and inoculated with 20 µL bacteria suspension of *E. coli* (2×10^6 cfu/mL). This leaching test served as a proof that during the growth test, no inhibition is caused due to an amount of polymer transferred from the coated surface to the well plate of the growth test, i.e., as a proof that the growth test is valid and the growth inhibition is only due to the influence of the polymer on *E. coli* during the exposure on the surface.

Growth test: The growth of the bacteria was followed by measuring the optical density (OD) of the solutions (transferred to the well plates) at 612 nm overnight at 37 °C in the micro well plate incubator/reader. To insert oxygen into the solution (for the bacterial metabolism) and to assure the homogeneity of the OD measurement, the solutions were shaken for 1000 seconds once per measuring cycle of 30 min. This test does not discriminate whether the substance is bactericidal or bacteriostatic.

The increase in optical density is plotted as a function of the number of cycles (1 cycle = 30 minutes). By comparison of the proliferation curves of the bacteria which have been in contact to the antimicrobial surfaces and the proliferation curves of the bacteria without contact to the antimicrobial surfaces (reference), the reduction of the bacterial growth and thereby the antimicrobial effect of the coatings can be determined. For the performed test, the internal benchmark for a good antimicrobial activity is a log-4 reduction of the colony forming units, respectively a 99.99 % inhibition of the bacterial growth.[31]

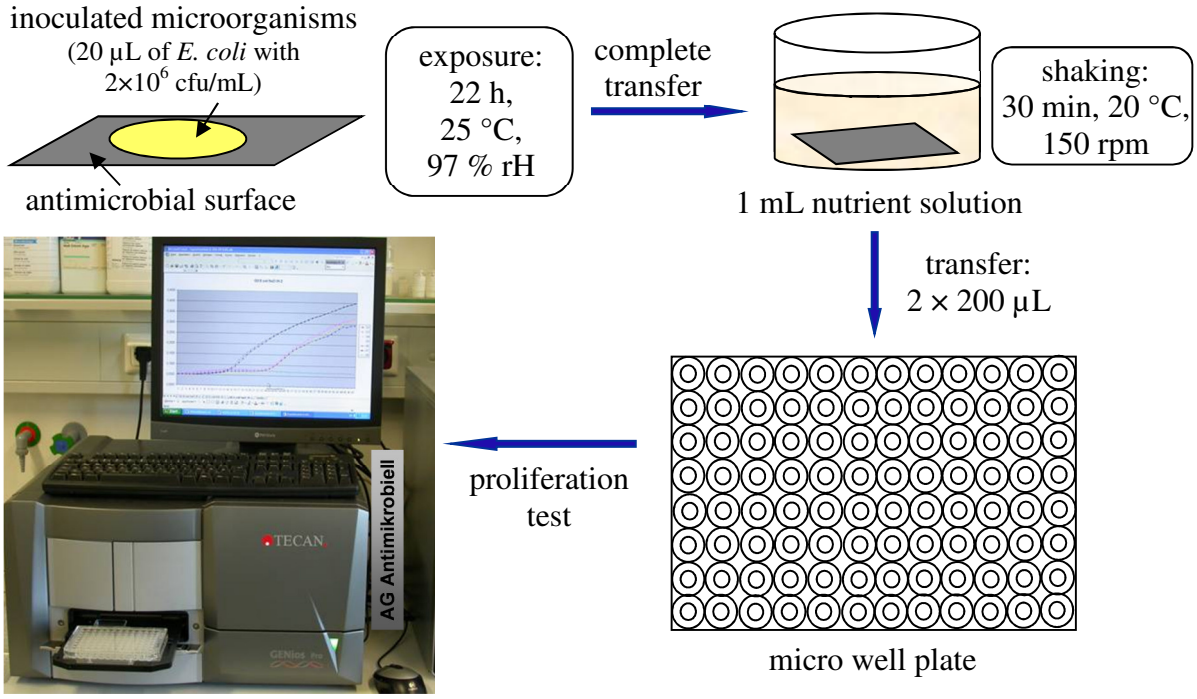

Figure 2. Antimicrobial testing system.

Antimicrobial Test in Solution

Suspensions of strains with defined colony forming units (*E. coli*, 6×10^7 cfu/mL) were incubated at 37 °C in nutrient solutions with different concentrations of the test substances (functional polymers). The wetting agent DOW (Q2-5211; 3-(Polyoxyethylene)-propylhepta-methyltrisiloxane) was added to the test solutions in a concentration of 0.01 %. The bacterial growth was followed during the incubation overnight, by using a micro well plate reader/incubator and the measurement procedure (growth test) described above. The experiments were triplicated.

With this test, the minimum inhibitory concentrations (MIC) of the tested polymers were determined. Based on standard specifications[32], the MIC is defined in this thesis as the lowest concentration of an antimicrobial that inhibits the bacterial growth by 99.99 % (log-4 reduction[33] of the colony forming units) compared to the reference.

5.2.8 Hemolytic Activity

The assessment of the hemolytic activity of the polymers coated onto substrates was performed by a hemoglobin release assay according to the literature.[34] Human erythrocytes (red blood cells (RBC), blood type 0, Rh positive) were obtained by the centrifugation of whole blood (3000 rpm, 10 min) to remove the plasma. The RBC were washed three times in PBS and finally diluted into PBS to obtain a stock suspension containing 3.5×10^8 RBC/mL. The hemolytic activity of the coated substrates was tested directly on the surface and in extracts of the substrates. The final amount of RBC in the suspension was 1.2×10^8 RBC/mL. The RBC were exposed to the surfaces for 3 h at 37 °C, thereafter centrifuged (4000 rpm, 10 min) and the absorption of the supernatant was determined at a wavelength of 414 nm. As reference solutions, (i) PBS for spontaneous hemolysis and (ii) 1 % Triton X100 for 100 % hemolysis (positive control) were used.

The hemolysis was plotted as a function of the polymer concentration and the hemolytic activity was defined as the polymer concentration that causes 50 % hemolysis of the human RBC relative to the positive control (EC50). All experiments were triplicated.

Test Directly on the Surface[35]

For the test of the hemolytic activity directly on the coated surfaces, the coated samples with a size of 2.25 cm² were covered with 1.14 mL RBC in PBS (1.2×10^8 RBC/mL) at 37 °C. Every 30 min, the samples were gently shaken to assure a complete wetting. After 3 h of incubation, the liquor was separated from the surfaces and was centrifuged for 10 min at 4000 rpm. The supernatant was removed and measured at a wavelength of 414 nm in the photometer. As positive control (100 % lysis), glass substrates were covered with Triton X100, dried and incubated with RBC in the same way as the coated samples. Uncoated silicon wafers, uncoated glass substrates, and PBS buffer were used as further controls.

Test of Surface Extracts[36]

To test the hemolytic activity of the substrate extracts, the coated substrates were incubated overnight at 37 °C in 2.28 mL of a 0.01 M PBS solution. Every hour, the vessels were shaken for 30 min at 120 rpm to assure a full wetting of the surfaces. After 24 h, the extracts were removed and their hemolysis was tested. Therefore, the extracts were pipetted into 500 µL of the RBC stock suspension and incubated at 37 °C. The final amount of RBC in the suspension was 1.2×10^8 RBC/mL. Every 30 min, the samples were gently shaken to assure a complete wetting. After 3 h of incubation, the RBC suspension was centrifuged (4000 rpm, 10 min) and the absorption of the supernatant was determined at a wavelength of 414 nm.

5.2.9 Langmuir Film Experiments

The preparation of the lipid layers and the penetration experiments were carried out[37] using a Langmuir trough (KSV MiniMicro, $5 \times 20 \times 0.6\ cm^3$) with two barriers to provide a symmetric film compression. The surface pressure was recorded with an accuracy of ± 0.05 mN/m with the aid of a Wilhelmy plate made of chromatography paper (Whatman Chr1) which was connected to a force transducer. The trough was made of teflon while the barriers were made of polyoxymethylene (POM), which has been suggested for lipid layers.[38] Dichloromethane (purity ≥ 99.9 %, Spectrum-3D Kft., Hungary) and methanol (purity ≥ 99.9 %, Sigma-Aldrich Kft., Hungary) were used for cleaning the Langmuir trough and the POM barriers, respectively. Afterwards, the trough and the barriers were rinsed with water. The trough was placed on a thermo-regulated plate and into a box of plexiglass in order to minimize air turbulences and possible contaminations. All measurements were performed at 23 ± 0.5 °C. As subphase, bidistilled water, which was checked by its conductivity (< 5 mS) and surface tension (> 72.0 mN/m at 23 ± 0.5 °C) values, was used.

DPPC (dipalmitoylphosphatidylcholine) was used as lipid for the neutral Langmuir layers and a mixture of 75 mol% DPPC and 25 mol% DPPG (dipalmitoylphosphatidylglycerol) was used as lipids for the charged Langmuir layers. For the preparation of the Langmuir layers, 13 µL of the lipid solution (1.0 g/L in chloroform (purity > 99.8 %, Fisher Chemicals)) were spread onto the aqueous subphase and the solvent was allowed to evaporate for 10 min before the compression forming the molecular lipid layer on the surface. Before the penetration experiment, surface pressure-area isotherms were determined at a barrier speed of $10\ cm^2$/min. The reason for this preliminary process is to bring the lipid layer into a reproducible state (compactness, ordering of chains). For the penetration experiments, the lipid monolayer was compressed to a given surface pressure of 20 mN/m. At a fixed barrier position, the aqueous solution of the polymer was injected below the lipid layer to reach a

final polymer concentration of 0.025 mg/mL or 0.075 mg/mL in the subphase (concentration of the polymer solution = 1 or 3 mg/mL, injected volume: 2.4 mL). The change in surface pressure ($\Delta\pi$) as indicator of the lipid/polymer interaction was recorded as a function of time over a period of 1 h. The result of the penetration of the polymer into the lipid monolayer (the saturation value after 1 h of the increase in surface pressure $\Delta\pi$) was given as the average of two independent measurements with an estimated error of ± 0.5 mN/m.

5.2.10 Membrane Permeabilization of *E. coli*

The permeabilization of the outer/inner membrane was investigated by using the ONPG hydrolysis assay[39] (ONPG = o-Nitrophenyl-β-D-galactopyranosid). The bacterial cells (*E. coli* ML35 strain (ATCC 43827)) were grown at 38 °C to mid-log (middle of the exponential growth phase) in a nutrient solution, containing 5 g/L yeast extract, 10 g/L tryptone and 0.5 g/L sodium chloride. Afterwards, the cells were centrifugated and washed twice with an equal volume of PBS. The cells were then diluted in PBS to 107 cfu/mL (OD_{600} ~ 0.5–0.7) and 15 µL (~105 cfu/mL) of this bacteria suspension were added to 165 µL of PBS which contained 1.5 mM ONPG and between 0.2 mg/mL and 0.5 mg/mL of the respective polymers. The rate of permeabilization was evaluated by following the hydrolysis of ONPG to *o*-nitrophenol (ONP) with a measurement of the absorbance at a wavelength of 405 nm on a microplate reader (Tecan Infinite 200, Tecan Group Ltd., Switzerland). The maximal permeabilization (corresponding to 100 % lysis) was determined by evaluating cells which were pretreated with PopCulture® reagent (1 – 10 dilution of the bacteria suspension), for 10 min. As positive control (normal bacterial growth), one experiment was performed without polymer and with only bacteria suspension added whereas as negative control (no bacterial growth), one experiment was performed with PBS only.

5.2.11 Syntheses

Procedure 1: Simultaneous Addition of EQ and EA12 (One-step Reaction, e.g., PVAm-EQ$_9$-EA12$_{10}$)

To a solution of freeze-dried salt free PVAm (2.0 g, $\overline{M}$ (repeating unit) = 43.60 g/mol, 0.045875 mol repeating units) in dist. water/methanol (p.a.) (40 mL/80 mL) at 60 °C, a solution of glycidyltrimethylammonium chloride (EQ, 36 %, 1.932 g, M = 151.63 g/mol, 0.0045875 mol) and 1,2-epoxydodecane (EA12, 96 %, 0.8808 g, M = 184.32 g/mol, 0,0045875 mol) in methanol (p.a., 160 mL) was added. The solution was stirred at 60 °C for 5 d and stayed clear over the whole reaction time. The reaction solution was then dialysed against dist. water to remove impurities originating from the educts (especially from EQ). The water was exchanged several times. The product was isolated by freeze-drying as a colorless solid. The freeze-dried product was soluble in methanol and in water. The product was characterized by NMR and Raman spectroscopy to verify a full conversion of the epoxide groups. The degree of functionalization was determined by ^{1}H-NMR spectroscopy.

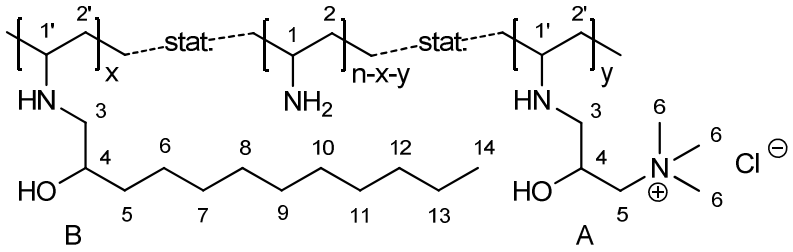

Degree of functionalization x = 10 % and y = 9 %. ^{1}H-NMR (MeOD-d_4): δ (ppm) = 0.84 – 0.98 (m, CH(OH)(CH$_2$)$_9$C**H$_3$**, H^{14B}), 1.17 – 1.88 (m, CH(OH)(C**H$_2$**)$_9$CH$_3$, H$^{5\text{-}13B}$, CH(NHR)C**H$_2$**, H$^{2,2'}$), 2.35 – 2.57 (m, 1H, R$_2$CHNHC**H$_2$**CH(OH), H$^{3''B}$), 2.57 – 2.81 (m, 3H, R$_2$CHNHC**H$_2$**CH(OH), H$^{3'B,3'A,3''A}$), 2.81 – 3.19 (m, C**H**(NHR)CH$_2$, H$^{1,1'}$), 3.19 – 3.32 (s, br, CH$_2$N(C**H$_3$**)$_3$, H^{6A}), 3.36 – 3.58 (m, CH(OH)C**H$_2$**N(CH$_3$)$_3$, H^{5A}), 3.58 – 3.73 (m, CH$_2$C**H**(OH)(CH$_2$)$_9$, H^{4B}), 3.73 – 3.90 (s, br, CHO**H**), 4.15 – 4.36 (m, CH$_2$C**H**(OH)CH$_2$, H^{4A}).

^{13}C-NMR (MeOD-d_4): δ (ppm) = 14.80 (br, $CH_2CH(OH)(CH_2)_9\mathbf{C}H_3$, C^{14B}), 23.82 (br, $CH_2CH(OH)(CH_2)_8\mathbf{C}H_2CH_3$, C^{13B}), 27.01 (br, $CH_2CH(OH)CH_2\mathbf{C}H_2(CH_2)_7CH_3$, C^{6B}), 30.22 – 31.61 (m, $CH_2CH(OH)(CH_2)_2(\mathbf{C}H_2)_5(CH_2)_2CH_3$, $C^{7\text{-}11B}$), 33.21 (br, $(CH_2)_7\mathbf{C}H_2CH_2CH_3$, C^{12B}), 36.79 (br, $CH_2CH(OH)\mathbf{C}H_2(CH_2)_8CH_3$, C^{5B}), 41.80 – 48.60 (m, $\mathbf{C}H\mathbf{C}H_2$, $C^{1,1'}$, $C^{2,2'}$, backbone), 50.30 – 51.80 (br, $\mathbf{C}H_2CH(OH)CH_2N(\mathbf{C}H_3)_3$, C^{3A}), 51.80 – 54.50 (br, $\mathbf{C}H_2CH(OH)(CH_2)_9CH_3$, C^{3B}), 55.08 (s, br, $CH_2CH(OH)CH_2N(\mathbf{C}H_3)_3$, C^{6A}), 66.30 – 67.30 (br, $CH_2\mathbf{C}H(OH)CH_2N(CH_3)_3$, C^{4A}), 70.40 – 71.20 (m, $CH_2CH(OH)\mathbf{C}H_2N(CH_3)_3$, C^{5A} and $CH_2\mathbf{C}H(OH)(CH_2)_9CH_3$, C^{4B}), the signals of $\mathbf{C}H\mathbf{C}H_2$ ($C^{1,1'}$, $C^{2,2'}$, backbone), and $\mathbf{C}H_2\mathbf{C}H(OH)(CH_2)_9CH_3$ (C^{3B} and C^{4B}) are only distinguishable from the noise of the baseline in quantitative ^{13}C measurements on a 600 MHz spectrometer.

Procedure 2: Sequential Addition of EQ and EA12 (Stepwise Reaction, Cationic First, e.g., PVAm-1.EQ$_{10}$-2.EA12$_{10}$)

To a solution of freeze-dried salt free PVAm (2.0 g, $\overline{M}$ (repeating unit) = 43.60 g/mol, 0.045875 mol repeating units) in dist. water/methanol (p.a.) (40 mL/80 mL) at 60 °C, a solution of glycidyltrimethylammonium chloride (EQ, 36 %, 1.932 g, M = 151.63 g/mol, 0.0045875 mol) in methanol (p.a., 80 mL) was added. The solution was stirred at 60°C for 3 d. Then a solution of 1,2-epoxydodecane (EA12, 96 %, 0.8808 g, M = 184.32 g/mol, 0.0045875 mol) in methanol (p.a., 80 mL) was added. The solution was stirred at 60 °C for three more days. Contrary to the reaction where EQ and EA_{12} were added at once (procedure 1), the reaction solution appeared turbid at the end of the reaction time. The reaction solution was dialysed against dist. water to remove impurities that originate from the educts (especially from EQ). The water was exchanged several times. The product was isolated by freeze-drying as a colorless solid. The freeze-dried product was soluble in methanol and in water. The product was characterized by NMR and Raman spectroscopy to

verify a full conversion of the epoxide groups. The degree of functionalization was determined by ^{1}H-NMR spectroscopy.

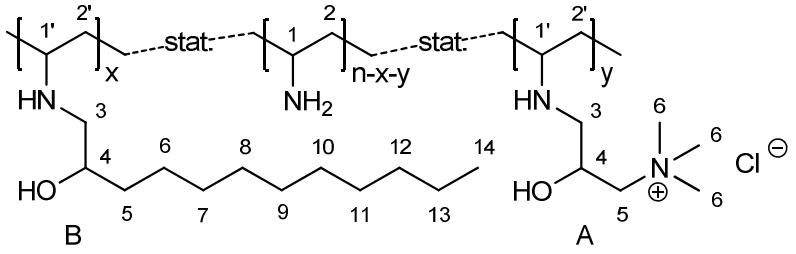

Degree of functionalization x = 10 % and y = 10 %. ^{1}H-NMR (MeOD-d_4): δ (ppm) = 0.84 – 0.98 (m, CH(OH)$(CH_2)_9$C**H$_3$**, H^{14B}), 1.17 – 1.88 (m, CH(OH)(C**H$_2$**)$_9$$CH_3$, $H^{5\text{-}13B}$, CH(NHR)C**H$_2$**, $H^{2,2'}$), 2.35 – 2.57 (m, 1H, R_2CHNHC**H$_2$**CH(OH), $H^{3''B}$), 2.57 – 2.81 (m, 3H, R_2CHNHC**H$_2$**CH(OH), $H^{3'B,3'A,3''A}$), 2.81 – 3.19 (m, C**H**(NHR)CH_2, $H^{1,1'}$), 3.19 – 3.32 (s, br, CH_2N(C**H$_3$**)$_3$, H^{6A}), 3.36 – 3.58 (m, CH(OH)C**H$_2$**$N(CH_3)_3$, H^{5A}), 3.58 – 3.73 (m, CH_2C**H**(OH)$(CH_2)_9$, H^{4B}), 3.73 – 3.90 (s, br, CHO**H**), 4.15 – 4.36 (m, CH_2C**H**(OH)CH_2, H^{4A}).

^{13}C-NMR (MeOD-d_4): δ (ppm) = 14.80 (br, $CH_2CH(OH)(CH_2)_9$**C**H_3, C^{14B}), 23.82 (br, $CH_2CH(OH)(CH_2)_8$**C**H_2CH_3, C^{13B}), 27.01 (br, $CH_2CH(OH)CH_2$**C**$H_2(CH_2)_7CH_3$, C^{6B}), 30.22 – 31.61 (m, $CH_2CH(OH)(CH_2)_2$(**C**$H_2)_5(CH_2)_2CH_3$, $C^{7\text{-}11B}$), 33.21 (br, $(CH_2)_7$**C**$H_2CH_2CH_3$, C^{12B}), 36.79 (br, $CH_2CH(OH)$**C**$H_2(CH_2)_8CH_3$, C^{5B}), 41.80 – 48.60 (m, **C**H**C**H_2, $C^{1,1'}$, $C^{2,2'}$, backbone), 50.30 – 51.80 (br, **C**$H_2CH(OH)CH_2N$(**C**$H_3)_3$, C^{3A}), 51.80 – 54.50 (br, **C**$H_2CH(OH)(CH_2)_9CH_3$, C^{3B}), 55.08 (s, br, $CH_2CH(OH)CH_2N$(**C**$H_3)_3$, C^{6A}), 66.30 – 67.30 (br, CH_2**C**H(OH)$CH_2N(CH_3)_3$, C^{4A}), 70.40 – 71.20 (m, $CH_2CH(OH)$**C**$H_2N(CH_3)_3$, C^{5A} and CH_2**C**H(OH)$(CH_2)_9CH_3$, C^{4B}), the signals of **C**H**C**H_2 ($C^{1,1'}$, $C^{2,2'}$, backbone), and **C**H_2**C**H(OH)$(CH_2)_9CH_3$ (C^{3B} and C^{4B}) are only distinguishable from the noise of the baseline in quantitative ^{13}C measurements on a 600 MHz spectrometer.

Procedure 3: Sequential Addition of EQ and EA12 (Stepwise Reaction, Hydrophobic First, e.g., PVAm-1.EA12$_{10}$-2.EQ$_9$)

To a solution of freeze-dried salt free PVAm (2.0 g, $\overline{M}$ (repeating unit) = 43.60 g/mol, 0.045875 mol repeating units) in dist. water/methanol (p.a.) (40 mL/80 mL) at 60 °C, a solution of 1,2-epoxydodecane (EA12, 96 %, 0.8808 g, M = 184.32 g/mol, 0,0045875 mol) in methanol (p.a., 80 mL) was added. The solution was stirred at 60 °C for 3 d. Then a solution of glycidyltrimethylammonium chloride (EQ, 36 %, 1.932 g, M = 151.63 g/mol, 0.0045875 mol) in methanol (p.a., 80 mL) was added. The solution was stirred at 60 °C for three more days. Contrary to the reaction where EQ and EA$_{12}$ were added at once (procedure 1), the reaction solution appeared turbid at the end of the reaction time. The reaction solution was dialysed against dist. water to remove impurities that originate from the educts (especially from EQ). The water was exchanged several times. The product was isolated by freeze-drying as a colorless solid. The freeze-dried product was soluble in methanol and in water. The product was characterized by NMR and Raman spectroscopy to verify a full conversion of the epoxide groups. The degree of functionalization was determined by ^{1}H-NMR spectroscopy.

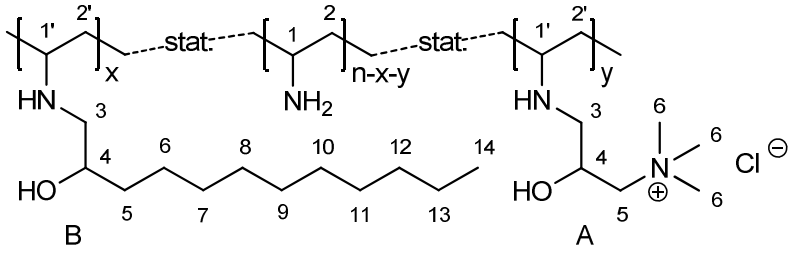

Degree of functionalization x = 10 % and y = 9 %. ^{1}H-NMR (MeOD-d_4): δ (ppm) = 0.84 – 0.98 (m, CH(OH)(CH$_2$)$_9$C**H$_3$**, H^{14B}), 1.17 – 1.88 (m, CH(OH)(C**H$_2$**)$_9$CH$_3$, H$^{5\text{-}13B}$, CH(NHR)C**H$_2$**, H$^{2,2'}$), 2.35 – 2.57 (m, 1H, R$_2$CHNHC**H$_2$**CH(OH), H$^{3''B}$), 2.57 – 2.81 (m, 3H, R$_2$CHNHC**H$_2$**CH(OH), H$^{3'B,3'A,3''A}$), 2.81 – 3.19 (m, C**H**(NHR)CH$_2$, H$^{1,1'}$), 3.19 – 3.32 (s, br, CH$_2$N(C**H$_3$**)$_3$, H^{6A}), 3.36 – 3.58 (m, CH(OH)C**H$_2$**N(CH$_3$)$_3$, H^{5A}), 3.58 – 3.73 (m,

$CH_2C\mathbf{H}(OH)(CH_2)_9$, H^{4B}), 3.73 – 3.90 (s, br, CHO**H**), 4.15 – 4.36 (m, $CH_2C\mathbf{H}(OH)CH_2$, H^{4A}).

^{13}C-NMR (MeOD-*d*$_4$): δ (ppm) = 14.80 (br, $CH_2CH(OH)(CH_2)_9\mathbf{C}H_3$, C^{14B}), 23.82 (br, $CH_2CH(OH)(CH_2)_8\mathbf{C}H_2CH_3$, C^{13B}), 27.01 (br, $CH_2CH(OH)CH_2\mathbf{C}H_2(CH_2)_7CH_3$, C^{6B}), 30.22 – 31.61 (m, $CH_2CH(OH)(CH_2)_2(\mathbf{C}H_2)_5(CH_2)_2CH_3$, $C^{7\text{-}11B}$), 33.21 (br, $(CH_2)_7\mathbf{C}H_2CH_2CH_3$, C^{12B}), 36.79 (br, $CH_2CH(OH)\mathbf{C}H_2(CH_2)_8CH_3$, C^{5B}), 41.80 – 48.60 (m, $\mathbf{C}H\mathbf{C}H_2$, $C^{1,1'}$, $C^{2,2'}$, backbone), 50.30 – 51.80 (br, $\mathbf{C}H_2CH(OH)CH_2N(\mathbf{C}H_3)_3$, C^{3A}), 51.80 – 54.50 (br, $\mathbf{C}H_2CH(OH)(CH_2)_9CH_3$, C^{3B}), 55.08 (s, br, $CH_2CH(OH)CH_2N(\mathbf{C}H_3)_3$, C^{6A}), 66.30 – 67.30 (br, $CH_2\mathbf{C}H(OH)CH_2N(CH_3)_3$, C^{4A}), 70.40 – 71.20 (m, $CH_2CH(OH)\mathbf{C}H_2N(CH_3)_3$, C^{5A} and $CH_2\mathbf{C}H(OH)(CH_2)_9CH_3$, C^{4B}), the signals of $\mathbf{C}H\mathbf{C}H_2$ ($C^{1,1'}$, $C^{2,2'}$, backbone), and $\mathbf{C}H_2\mathbf{C}H(OH)(CH_2)_9CH_3$ (C^{3B} and C^{4B}) are only distinguishable from the noise of the baseline in quantitative ^{13}C measurements on a 600 MHz spectrometer.

5.3 Results and Discussion

In the previous chapters the synthesis of multifunctional poly(vinyl amine)s was optimized and discussed in detail. In this chapter, the goal is to introduce different microstructures into the polymers having the same chemical composition. The sequential and simultaneous addition of the monomers (EQ and EA12) was chosen as approach. The effect of the microstructure on the antimicrobial effect, the CAC (critical aggregation concentration), the viscosity, the ability to penetrate into a model DPPC membrane, the ability to penetrate into the outer/inner membrane of *E. coli*, and the hemolytic activity of the polymers were determined.

5.3.1 Syntheses

Functional poly(vinyl amine)s with different microstructures were prepared by simultaneous and sequential addition of functional epoxides. Following this approach three different types of polymers were prepared (Scheme 1) and named following the threefold expression explained in section 5.2.3:

1) PVAm was reacted simultaneously with the epoxides EQ (cationic) and EA12 (hydrophobic): PVAm-EQ_x-$EA12_y$.
2) In the first step PVAm was reacted with the cationic epoxide EQ and in the next step with the hydrophobic epoxide EA12: PVAm-1.EQ_x-2.$EA12_y$.
3) In the first step PVAm was reacted with the hydrophobic epoxide EA12 and in the second step with the cationic epoxide EQ: PVAm-1.$EA12_x$-2.EQ_y.

PVAm was reacted with the two epoxides and afterwards purified by dialysis. NMR and Raman spectra showed only the expected signals and the degree of functionalization was determined by ^{1}H-NMR spectroscopy as already described in Chapter 2. In order to obtain polymers with the same chemical composition but different microstructures, a series of polymers was prepared in different ways, starting with the same amounts of educts. The series aimed at degrees of functionalization of 10 % EQ and 10 % EA12. In Table 3, the obtained degrees of functionalization are listed. During the reaction some differences between the sequential and the simultaneous addition of the epoxides have already been observed. After the sequential addition of the epoxides the reaction solution appeared turbid, whereas after the simultaneous addition of the epoxides, a clear solution was obtained. This observation already indicated that differences in the resulting products of the simultaneous and the sequential addition of the epoxides could be expected.

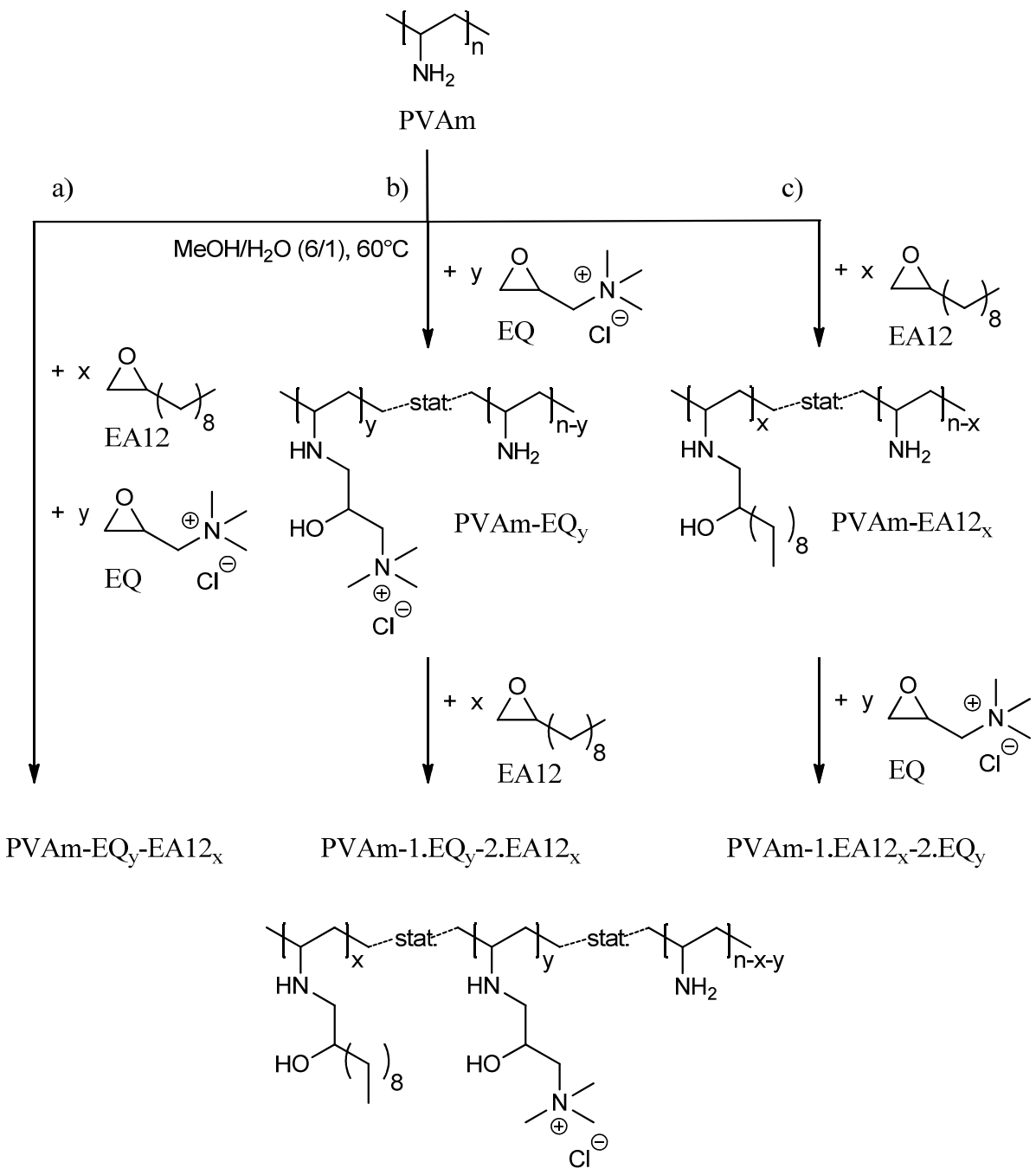

Scheme 1. Synthesis of functional polymers. a) simultaneous addition of epoxides, b) sequential addition of epoxides, cationic groups (EQ) first, and c) sequential addition of epoxides, hydrophobic groups (EA12) first.

Table 3. Composition* of the synthesized polymers determined by NMR spectroscopy.

Name	1. EQ	2. EA12	2. EQ	1. EA12	EQ	EA12
PVAm-EQ$_9$-EA12$_{10}$					9	10
PVAm-1.EQ$_{10}$-2.EA12$_{10}$	10	10				
PVAm-1.EA12$_{10}$-2.EQ$_9$			9	10		

* values given in % of the polymer repeating units

The obtained degrees of functionalization fitted the adjusted degrees of functionalization (cf. Table 3). To prove the formation of different microstructures, the polymer properties like CAC, antimicrobial effect, and hemolytic activity, etc., have been investigated.

5.3.2 Fluorescence Measurements of Functional PVAm

The polymers were characterized in solution by determining their critical concentration above which aggregates are formed (critical aggregation concentration, CAC). The influence of the synthetic route and thereby the influence of the microstructure on the CAC was investigated. The CAC was determined by fluorescence measurements using pyrene as fluorescent dye.[29,40,41,42]

Fluorescence spectroscopy has proved to be a reliable, widely used technique to study the association behavior of amphiphilic polymers. Depending on its chemical environment, the used fluorescent dye pyrene shows different fluorescence spectra. Due to this behavior, it is possible to investigate the association behavior and to determine the CAC of the different polymers. Going from a hydrophilic to a hydrophobic environment, the excitation spectrum of pyrene undergoes a red shift of the absorption band and an enhanced excitation intensity is observed. In the emission spectrum, a red shift of the absorption band is observed as well. The absorption band at a wavelength of 371 nm is shifted to 373 nm. In addition, a new absorption

band at a wavelength of 383 nm appears. Figure 3 shows the fluorescence spectrum of pyrene in aqueous solution compared with a spectrum of pyrene in aqueous solution containing the polymer PVAm-1.EQ_{10}-2.$EA12_{10}$ above the CAC. The red shift of the absorption band from 371 nm to 373 nm and the appearance of the new absorption band at 383 nm can clearly be observed.

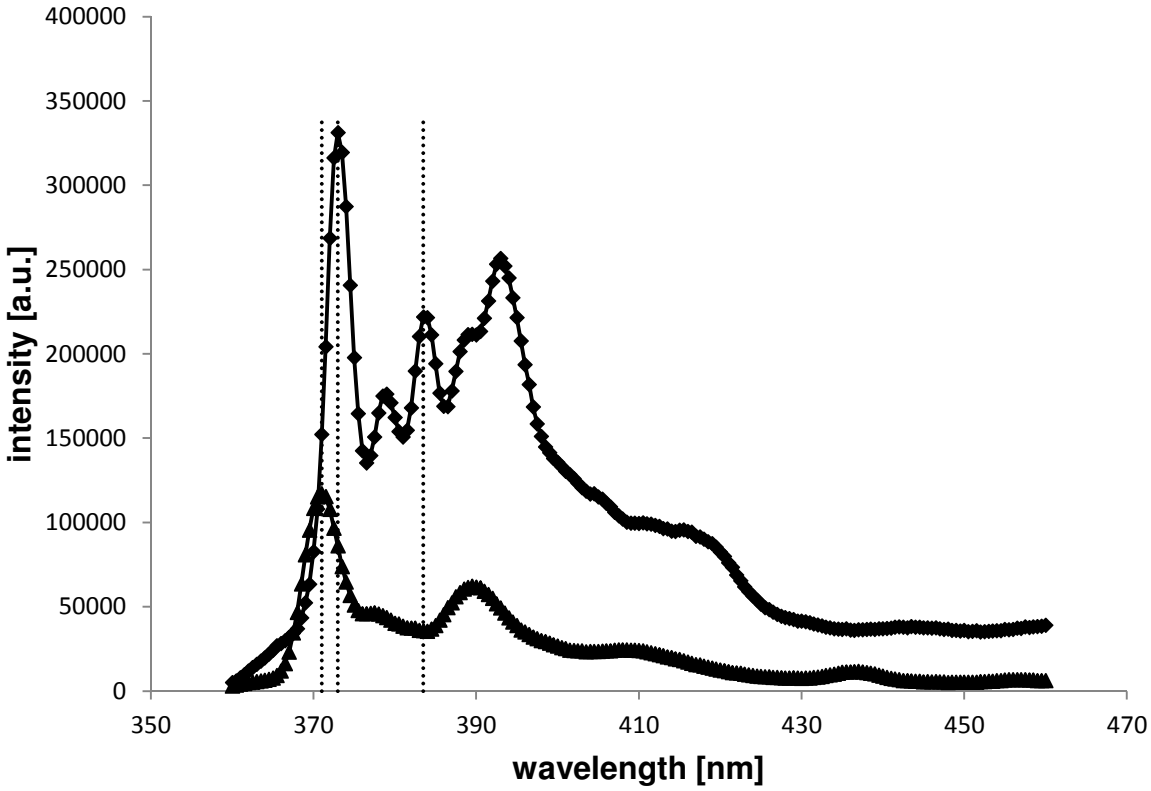

Figure 3. Emission spectra of pyrene in water (▲) and in a 0.5 mg/mL aqueous polymer solution of PVAm-1.EQ_{10}-2.$EA12_{10}$ (♦). Dashed lines mark the absorption bands at wavelengths of 371 nm, 373 nm, and 383 nm.

In Figure 4, the emission spectra of pyrene in a series of aqueous polymer solutions of PVAm-1.EQ_{10}-2.$EA12_{10}$ with different concentrations ranging from 0 mg/mL to 1 mg/mL is shown. The CAC can be determined by plotting the intensity ratio I_{373}/I_{371} or the intensity

ratio I_{373}/I_{383} obtained from the emission spectra against the logarithmic concentration of the polymer solutions (see also Chapter 3). In this chapter, both ratios were used to calculate the CAC and compared with each other. Low intensity ratios indicate a hydrophilic surrounding of the pyrene whereas high intensity ratios indicate a hydrophobic surrounding of the pyrene caused by the formation of micellar aggregates.

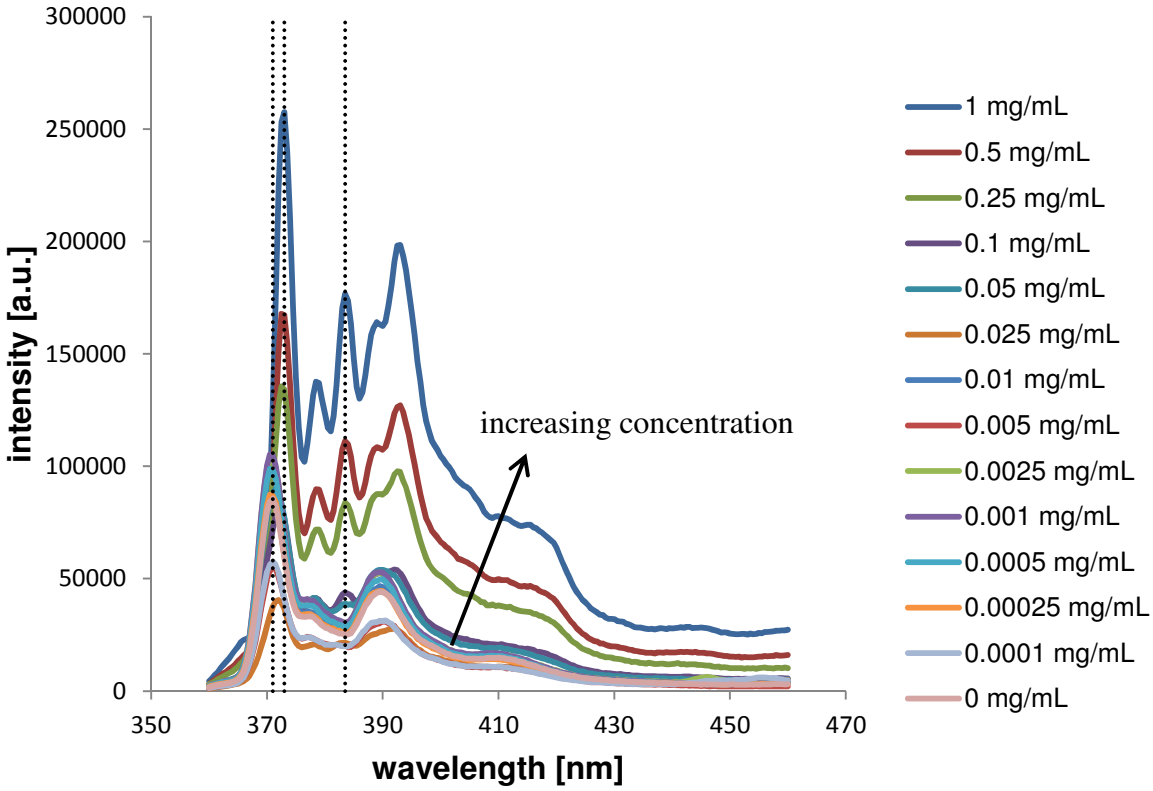

Figure 4. Emission spectra of pyrene in aqueous polymer solutions of PVAm-1.EQ_{10}-2.$EA12_{10}$ with different concentrations ranging from 0 mg/mL to 1 mg/mL. Dashed lines mark the absorption bands at wavelengths of 371 nm, 373 nm, and 383 nm.

The experimental data were fitted by sigmoidal curves.[43] Analogous to Chapter 3, the intersection point of the tangent at the deflection point and the tangent at low polymer concentrations is defined as the CAC. Satisfactory sigmoidal curves were obtained for the

intensity ratios I_{373}/I_{383}. The obtained experimental data points and the fitted sigmoidal curve of PVAm-1.EQ_{10}-2.$EA12_{10}$ are shown exemplarily in Figure 5. For the intensity ratios I_{373}/I_{371} however, only a part of the sigmoidal curve could be obtained with the measured concentration range. The obtained experimental data points and the two tangents used for the CAC calculation of PVAm-1.EQ_{10}-2.$EA12_{10}$ are shown exemplarily in Figure 6.

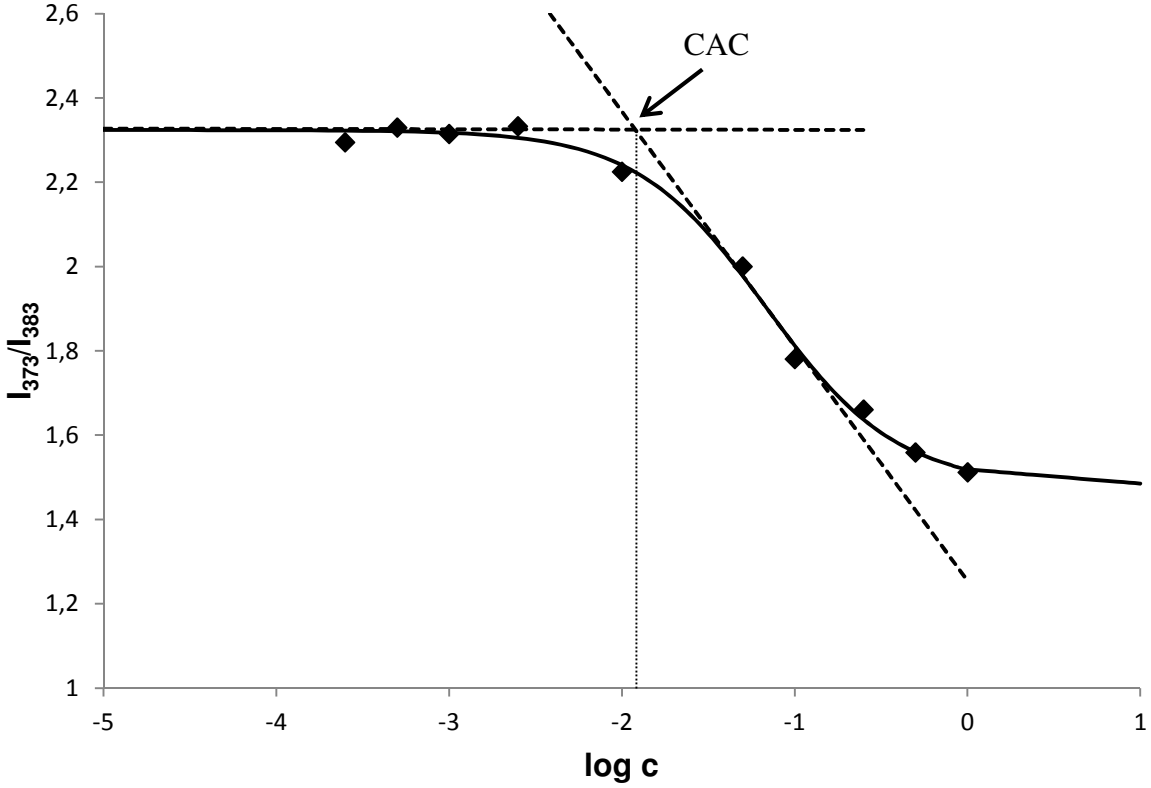

Figure 5. Intensity ratio I_{373}/I_{383} of the emission spectra of pyrene in aqueous polymer solutions of (♦) PVAm-1.EQ_{10}-2.$EA12_{10}$ against the logarithmic concentration of the polymer solutions. The solid line shows the sigmoidal fit to the experimental data, the dashed lines show the tangents used for the CAC calculation.

Table 4. CAC values of the polymers prepared via different synthetic routes.

Name	CAC (I_{373}/I_{383}) [mg/mL]	CAC (I_{373}/I_{371}) [mg/mL]
PVAm-1.EQ$_{10}$-2.EA12$_{10}$	0.012	0.044
PVAm-1.EA12$_{10}$-2.EQ$_9$	0.004	0.037
PVAm-EQ$_9$-EA12$_{10}$	0.001	0.018

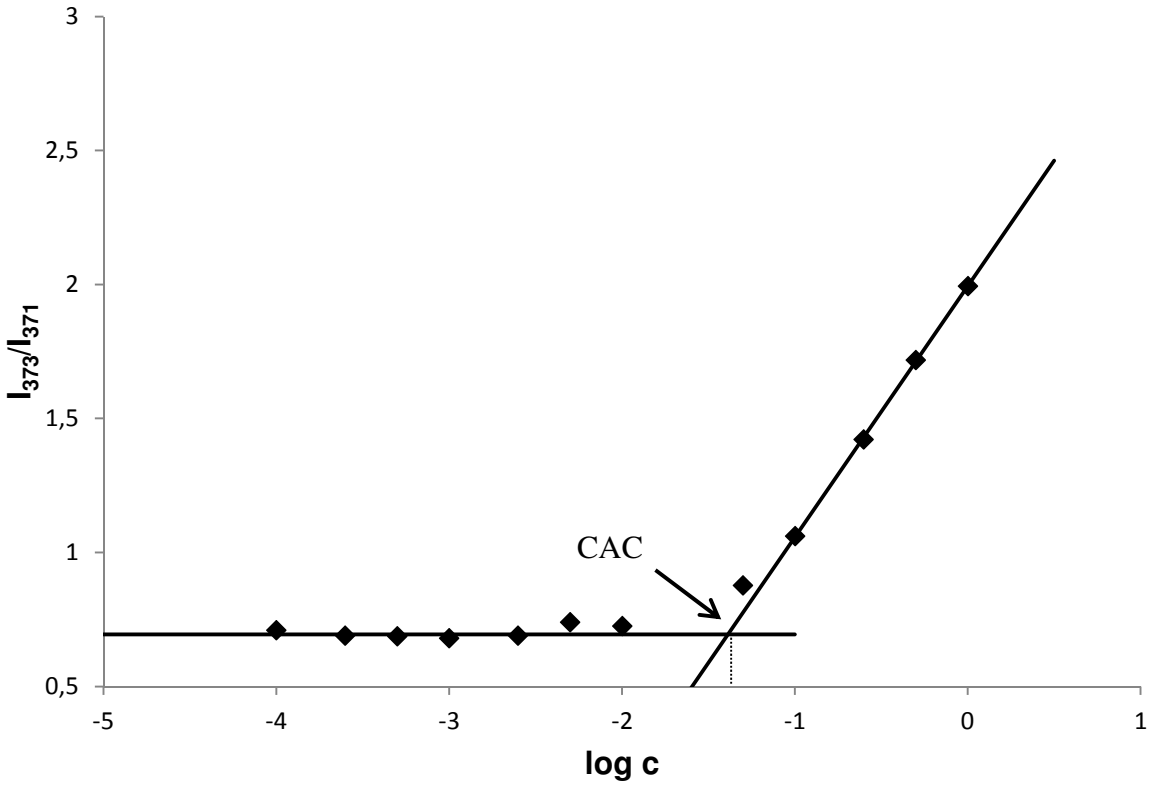

Figure 6. Intensity ratio I_{373}/I_{371} of the emission spectra of pyrene in aqueous polymer solutions of (♦) PVAm-1.EQ$_{10}$-2.EA12$_{10}$ against the logarithmic concentration of the polymer solutions. The solid lines show the tangents used for the CAC calculation.

The influence of the microstructure on the CAC was studied. The determined CAC values for both methods and the composition of the polymers can be found in Table 4. For a better

comparison, Figure 7 visualizes the CAC values as a bar chart. The CAC values are different for each of the three polymers. This is an indication for different chain mobilities within the three polymers and therefore an evidence for different microstructures.

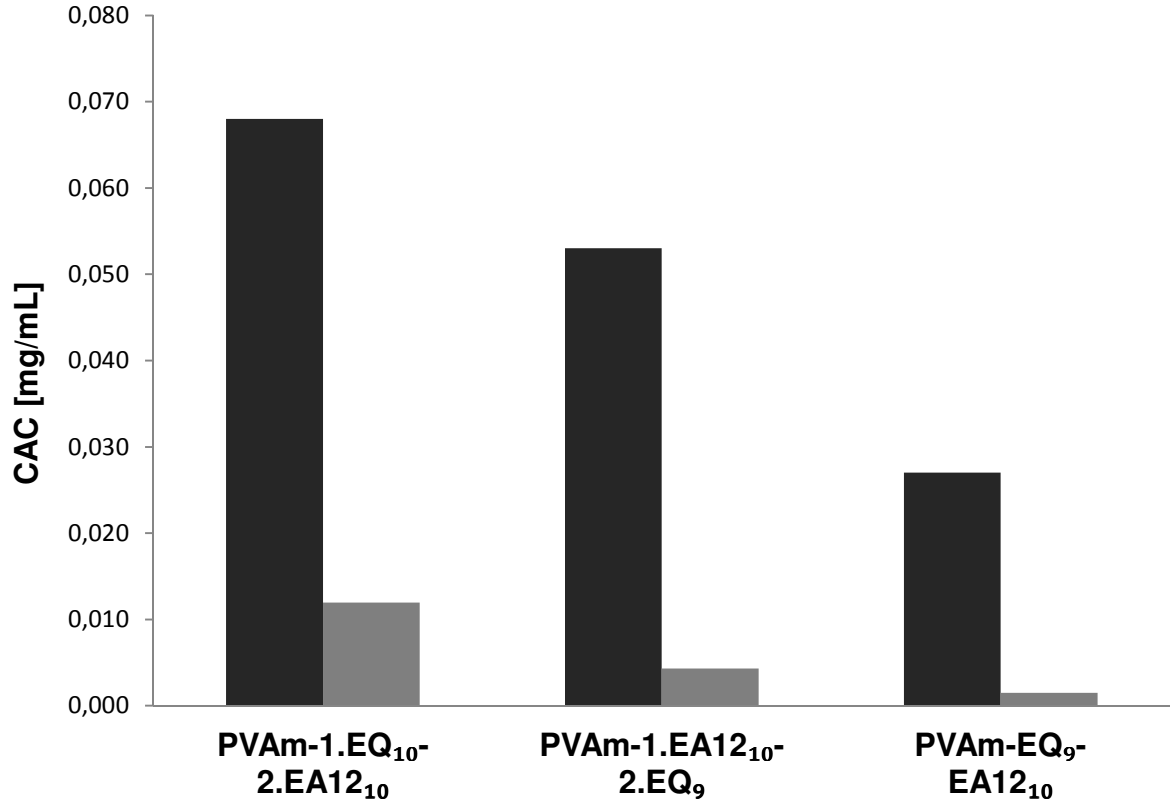

Figure 7. CAC values in mg/mL calculated from the intensity ratio I_{373}/I_{383} (black) and from the intensity ratio I_{373}/I_{371} (grey) for the polymers: PVAm-1.EQ_{10}-2.$EA12_{10}$, PVAm-1.$EA12_{10}$-2.EQ_9 and PVAm-EQ_9-$EA12_{10}$.

The CAC values obtained by both methods follow the same trend. The polymer obtained by simultaneous addition of the functional epoxides possesses the lowest CAC value, the polymer obtained by sequential addition of the functional epoxides, by adding the cationic epoxide EQ first, exhibits the highest CAC value and the CAC value for the polymer obtained by first adding the hydrophobic epoxide EA12 lies in between both other CAC values. This

shows that the polymer obtained by simultaneous addition of the epoxides possesses the highest chain mobility and can build micelles more easily than the polymers obtained by sequential addition of the epoxides. This is due to the formation of segregated domains within the polymers during the sequential reaction. These segregated domains are relatively rigid and the polymers cannot easily rearrange to form micelles.

5.3.3 Antimicrobial Effect of the Synthesized Polymers

Test in Solution

The antimicrobial effect of the synthesized polymers was tested in aqueous solution. To investigate the influence of the pH on the antimicrobial effect, the pH of the clear aqueous polymer solutions (pH ~ 10) was adjusted with acetic acid to pH = 5.5 and pH = 8.0. The clear polymer solutions were diluted to the testing concentrations by adding nutrient solution. During this addition, some turbidities appeared. To determine the minimum inhibitory concentration (MIC) of the polymers, suspensions of *E. coli* with defined colony forming units were incubated at 37 °C in nutrient solutions with different concentrations of the test substances (functional polymers). The bacterial growth was monitored overnight during the incubation by measuring the optical density (OD) of the solutions. Table 5 shows the composition and the measured MIC values of the tested polymers. Based on standard specifications[32], the MIC is defined in this thesis as the lowest concentration of an antimicrobial agent that inhibits the bacterial growth by 99.99 % (log-4 reduction[33] of the colony forming units) compared to the reference. All test solutions showed turbidities above a polymer concentration of 0.05 – 0.1 mg/mL. Since with values of about 0.2 mg/mL, the measured MIC values lie in a concentration range above 0.1 mg/mL, these turbidities disturb the measurement of the antimicrobial activity in solution, which relies on the optical density to detect the bacterial growth. In addition, the polymers might not be completely available for

the antimicrobial interaction and the real MIC values can thus be lower than the measured values. The obtained MIC values are therefore imprecise and the slight differences in the antimicrobial activity between the polymer solutions with pH = 5.5 and pH = 8.0 are not significant. The MIC values show no differences between the activities of the three polymers.

Table 5. MIC against *E. coli* (under growth conditions) of the synthesized polymers.

	MIC [mg/mL][a)]	
Name	**pH = 5.5**	**pH = 8.0**
PVAm-EQ$_9$-EA12$_{10}$	> 0.2	0.2
PVAm-1.EQ$_{10}$-2.EA12$_{10}$	> 0.2	0.2
PVAm-1.EA12$_{10}$-2.EQ$_9$	> 0.2	0.2

[a)] The MIC is defined as the lowest concentration of an antimicrobial that gives a log-4 reduction of the colony forming units. The shown values are the mean values obtained by averaging the outcomes of three independent measurements. The test was performed under growth conditions and a concentration of 0.01 % DOW was used. The test solutions showed turbidities and the real MIC might thus be lower.

Test on Substrate

Since the antimicrobial test in solution measures only relative and no absolute values due to the turbidity of the test solutions, the antimicrobial effect was also tested on surfaces. The developed polymers can be coated and adhered to negatively charged surfaces via ionic interaction. A test on surfaces is also interesting for later applications of the polymers, e.g., as textile coatings. The different coating strategies (drop casting, spin coating, and spin coating followed by annealing in methanol atmosphere) used for the antimicrobial testing are depicted in Figure 8 and described in the following paragraphs.

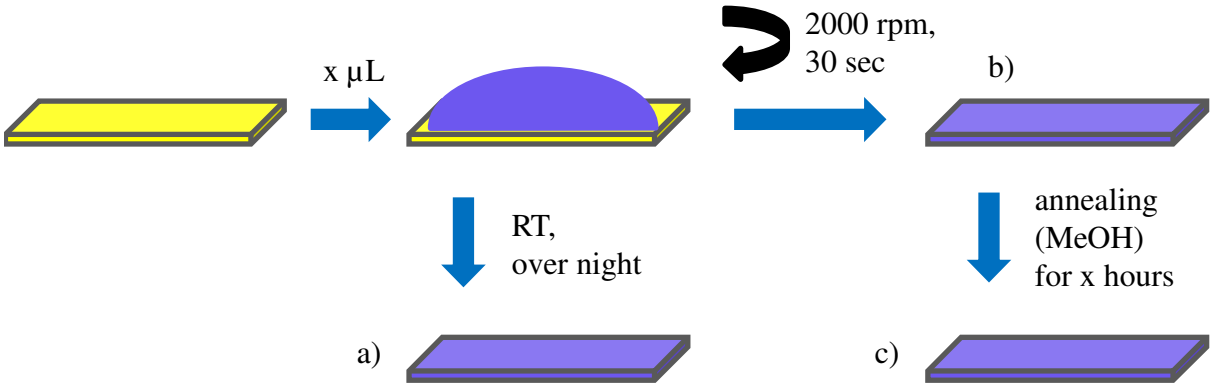

Figure 8. Surface coating of the functional polymers. a) Drop casting: 150 µL of a methanolic polymer solution were casted onto the glass substrate and the solvent was allowed to evaporate overnight at RT. b) Spin coating of 100 µL methanolic polymer solution on the silicon substrate with 2000 rpm for 30 sec. c) The same as b) followed by annealing in methanol atmosphere for defined times.

Drop Casting

In Chapter 4, the antimicrobial testing of five different series of polymers with different amounts of polymer on the substrates has been described. It was found that a coating thickness of 23 µg/cm² polymer or less is needed to detect differences in the antimicrobial activities of the polymers. For higher coating thicknesses, the polymers functionalized with more than 5 % cationic groups EQ and less than 20 % hydrophobic groups EA12 show a complete inhibition of bacterial growth (under growth conditions). As a starting point for the antimicrobial testing, amounts of 23 µg/cm² polymer and 11.5 µg/cm² polymer were chosen.

The three functional polymers PVAm-EQ_9-$EA12_{10}$, PVAm-1.EQ_{10}-2.$EA12_{10}$, and PVAm-1.$EA12_{10}$-2.EQ_9 were coated onto glass substrates serving as model surfaces for negatively charged surfaces, e.g., textile surfaces (cf. Figure 8 a)). The glass substrates were cleaned prior to use. The antimicrobial effect was tested under growth conditions (bacteria suspension in nutrient solution). To ensure the complete wetting of the surface, enabling the

bacteria to interact with the coated polymer, the wetting agent DOW was used with a concentration of 0.01 %. All tests were carried out at least twice (in order to reduce statistical artifacts). The composition and the antimicrobial activities of the tested polymers are summarized in Table 6.

Table 6. Inhibition of bacterial growth (*E. coli*) after exposure on the coated glass substrates (drop casting from 0.05 wt% and 0.025 wt% methanolic polymer solutions; 23 µg/cm² and 11.5 µg/cm² polymer, respectively).

	Inhibition of growth[a] [%]	
Name	**23 µg/cm²**	**11.5 µg/cm²**
PVAm-EQ$_9$-EA12$_{10}$	99.9999-100	-
PVAm-1.EQ$_{10}$-2.EA12$_{10}$	100	99.99 – 99.9999
PVAm-1.EA12$_{10}$-2.EQ$_9$	100	~95 – 99.999

[a] The given values are the mean values obtained by averaging the outcomes of two independent measurements. Within the performed tests, no leaching of the polymer coatings that would falsify the growth test was observed. The test was performed under growth conditions and a concentration of 0.01 % DOW was used.

All polymers coated on substrates obtained by drop casting from 0.05 wt% solutions (23 µg/cm² polymer) showed 99.9999 % up to a complete inhibition of growth *(E. coli*) within the antimicrobial test. Both polymers obtained by sequential addition of the monomers EQ and EA12 (PVAm-1.EQ$_{10}$-2.EA12$_{10}$ and PVAm-1.EA12$_{10}$-2.EQ$_9$) seemed to have a slightly higher antimicrobial activity than the polymer obtained by simultaneous addition of the functionalities (PVAm-EQ$_9$-EA12$_{10}$), but it was not possible to detect significant differences between the polymers.

The substrates coated with 0.025 wt% polymer solutions (11.5 µg/cm² polymer) showed very high standard deviations for the measured inhibitions of growth. Thus the difference between the polymers cannot be regarded as significant. An explanation for the high standard deviations can be found in the coating method. During the evaporation of the solvent, drying effects occurred. For this low polymer concentration, these drying effects led to defects in the coating. The coating was not sufficiently homogeneous to obtain reproducible results in the antimicrobial tests.

Spin Coating

To obtain reproducible antimicrobial results, a homogeneous surface coating is required. Therefore, another coating method (spin coating) was performed to obtain homogeneous coatings for polymer concentrations lower than 23 µg/cm².

Silicon wafers have been used as substrates for the spin coating (cf. Figure 8 b)). The silicon substrates were cleaned prior to use. Silicon wafers have been chosen as substrate because their surface is almost similar to the surface of the glass substrates. Therefore the antimicrobial results on glass and on silicon surfaces are comparable. The advantage of the silicon wafers, compared to glass substrates, is their reflective surface. This reflective surface enables the analysis of the coated substrates with ellipsometry in order to determine the thickness of the coatings (cf. Table 7). The coating thickness of the substrates obtained by spin coating from 1 wt% solutions lies around 90 nm for all of the polymers. Other lower polymer concentrations lead to lower coating thicknesses. For each concentration, the thickness values are similar for all of the tested polymers. This is important for the antimicrobial testing because the obtained results are only comparable if the test is carried out under the same testing conditions for each polymer.

Table 7. Coating thickness of the spin coated silicon substrates from different methanolic polymer solutions determined by ellipsometry.

Name	coating thickness [nm]			
	1 wt%	**0.75 wt%**	**0.5 wt%**	**0.25 wt%**
PVAm-EQ$_9$-EA12$_{10}$	93.9	61.7	38.7	18.4
PVAm-1.EQ$_{10}$-2.EA12$_{10}$	89.9	60.2	39.2	18.2
PVAm-1.EA12$_{10}$-2.EQ$_9$	93.4	60.7	38.9	18.2

Amount of Polymer per Surface-Area and Antimicrobial Activity

Spin coated substrates from 1 wt% solution have been prepared for the antimicrobial testing. Assuming a density of 1 g/cm³ for the polymers, the amount of polymer on the surface can be calculated from the coating thickness of 90 nm and the surface of the substrate of 1.5 cm × 1.5 cm.

Let V denote the coating volume. We have $V = 1.5\ \text{cm} \cdot 1.5\ \text{cm} \cdot 9 \cdot 10^{-6}\ \text{cm} = 2.025 \cdot 10^{-5}\ \text{cm}^3$. Furthermore, let A denote the substrate surface area with $A = 1.5\ \text{cm} \cdot 1.5\ \text{cm} = 2.25\ \text{cm}^2$. With a density of $\delta = 1\ \text{g/cm}^3$, this coating volume V leads to a mass of $m = 20.25\ \mu\text{g}$ on the area A. Thus, the amount of polymer on the surface can be determined to be $m/A = 9\ \mu\text{g/cm}^2$. This amount is considerably lower than the amount of polymer on the surface obtained by drop casting from a 0.05 wt% polymer solution (23 µg/cm², 230 nm), but only slightly lower than the amount of polymer on the surface obtained by drop casting from a 0.025 wt% polymer solution (11.5 µg/cm², 115 nm). The antimicrobial testing of the polymers on coated substrates obtained by drop casting with 23 µg/cm² polymer showed 99.9999 % up to a complete inhibition of growth for all polymers. The measured values for the inhibition of growth on the substrates with 11.5 µg/cm² polymer were distributed with a high standard deviation due to inhomogeneities of the coating. It was investigated whether the homogeneity

of the coatings, obtained by spin coating (with 9 µg/cm² polymer), was sufficient for the antimicrobial testing. The antimicrobial testing was done under growth conditions (in nutrient solution). To ensure the complete wetting of the surface, enabling the bacteria to interact with the coated polymer, the wetting agent DOW was used. The composition and the antimicrobial activities of the tested polymers are summarized in Table 8.

Table 8. Inhibition of bacterial growth (*E. coli*) after exposure on the coated silicon substrates (spin coating from 1 wt% methanolic polymer solutions; 9 µg/cm² polymer).

Name	Inhibition of growth[a)] [%]
PVAm-EQ_9-$EA12_{10}$	99.9
PVAm-1.EQ_{10}-2.$EA12_{10}$	99.9
PVAm-1.$EA12_{10}$-2.EQ_9	90[b)]

[a)] The given values are the mean values obtained by averaging the outcomes of two independent measurements. Within the performed tests, no leaching of the polymer coatings that would falsify the growth test was observed. The test was performed under growth conditions and a concentration of 0.01 % DOW was used. [b)] 0.85 wt% solution instead of 1 wt% solution.

For an amount of 9 µg/cm² polymer, all polymers showed about 99.9 % inhibition of growth *(E. coli*) within the antimicrobial test (cf. Table 8). It was not possible to detect significant differences between the polymers. The antimicrobial effect of the coatings obtained by spin coating was lower than it was for the coatings obtained by drop casting with 11.5 µg/cm² polymer (up to 99.9999 % inhibition of bacterial growth). The standard deviation of the obtained values was lower for the spin coated substrates than it was for the drop casted substrates, but it was still relatively high. A possible reason for the still relatively high

standard deviation of the values could have been the different orientation of the polymer chains at the surface, although the surface obtained by spin coating was very homogeneous compared to a surface coated by drop casting. During the drop casting, the polymer chains had much more time (evaporation overnight) to orient in a thermodynamically stable conformation than during the spin coating process where they had only 30 seconds to orient. This short orientation time led to a mixture of conformations on the spin coated surface. Some of these conformations were more active against bacteria than others. Thereby the mixture of conformations caused the variance of the measured values. To overcome this problem, an annealing in methanol atmosphere was performed after the spin coating (cf. Figure 8 c)). This annealing gave the polymer chains the opportunity to orient in a thermodynamically more stable conformation. During the annealing, the color of the coatings on the silicon wafers changed from a deep blue to green. After the removal of the substrates from the methanol atmosphere, the blue color was recovered immediately.

Influence of the Annealing Time

The antimicrobial activity of the coatings was exemplarily investigated for the polymer PVAm-EQ_9-$EA12_{10}$ after 0 h, 1 h, 2 h, 3 h, and 4 h of annealing in methanol atmosphere. The antimicrobial test was performed under growth conditions (in nutrient solution). To ensure the complete wetting of the surface, enabling the bacteria to interact with the coated polymer, the wetting agent DOW was used. The proliferation curves are shown together with the standard deviations of the growth tests after the different annealing times in Figure 9. The results on the inhibition of growth of *E. coli* for the different annealing times are shown in Table 9.

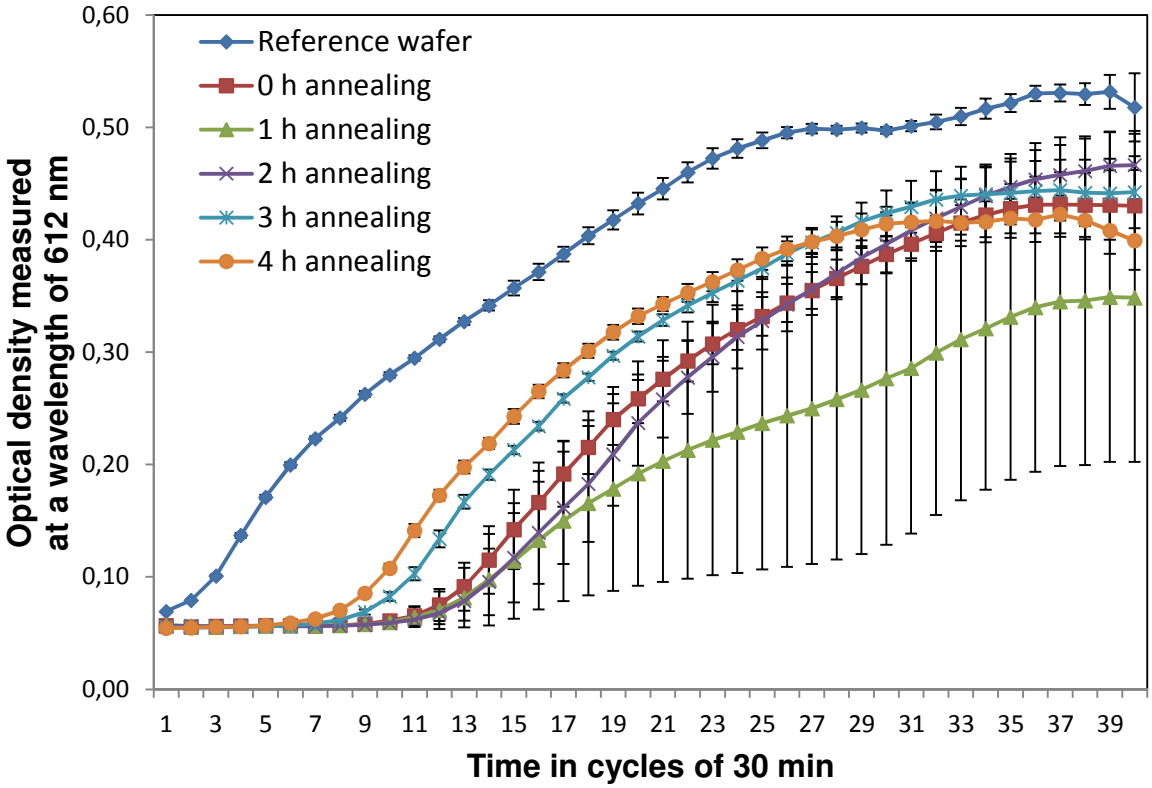

Figure 9. Proliferation curves of *E. coli* after exposure in nutrient solution (a concentration of 0.01 % of the wetting agent DOW was used) on the spin coated silicon surfaces (PVAm-EQ_9-$EA12_{10}$, with 9 µg/cm^2). Influence of the different times of annealing in methanol atmosphere. Reference wafer = growth control, i.e., growth of *E. coli* after exposure on a non-coated silicon surface. All measuring points are the mean values obtained by averaging the outcomes of six independent measurements.

It can be observed in Figure 9 that with an increasing annealing time the standard deviation of the values decreases. This decrease implies that the chains are now oriented on the surface in a thermodynamically more stable conformation, yielding a coating which is homogeneous concerning the antimicrobial activity of the polymers at the surface. Additionally it can be observed that the antimicrobial effect decreases with the annealing time (cf. Figure 9 and Table 9). This decrease shows that the thermodynamically stable conformation, which is obtained after the annealing, exhibits a lower antimicrobial activity than the mixture of

conformations which has been on the surface before. Before the annealing, some species in the mixture of conformations were antimicrobially more active than the species after annealing. This mixture of antimicrobial activities resulted in a higher activity of the coating before the annealing, but at the same time led to a higher deviation of the measured values. After 4 h of annealing, the reproducibility of the results was good, resulting in a low standard deviation. This good reproducibility of the results is a crucial and important point for comparing the antimicrobial effect of the different polymers.

Table 9. Inhibition[a)] of bacterial growth (*E. coli*) after exposure on the coated silicon substrates. Sample preparation: Spin coating from 1 wt% methanolic polymer solutions of PVAm-EQ_9-$EA12_{10}$, followed by annealing in methanol atmosphere for different times; 9 µg/cm² polymer.

time	**Inhibition of growth[a)]**
[h]	**[%]**
0	> 99 - 99.9
1	> 99 - 99.99999
2	> 99 - > 99.9
3	> 99
4	> 99

[a)] The given values are the mean values obtained by averaging the outcomes of six independent measurements. Within the performed tests, no leaching of the polymer coatings that would falsify the growth test was observed. The test was performed under growth conditions and a concentration of 0.01 % DOW was used.

Coating Thickness and Contact Angle

The impact of the annealing of the coatings in methanol atmosphere on the coating thickness and on the contact angle was investigated in a further step. For this investigation, the coating thickness and the contact angle of the substrates which were spin coated with PVAm-EQ_9-$EA12_{10}$ were measured after the different annealing times (cf. Table 10).

Table 10. Coating thicknesses and contact angles of the coated silicon substrates prepared by spin coating from a 1 wt% methanolic polymer solution of PVAm-EQ_9-$EA12_{10}$ (9 µg/cm^2) followed by annealing in methanol atmosphere for different times.

time [h]	coating thickness [nm]	contact angle [°]
0	90.1	131.9
1	89.4	112.8
2	89.0	115.9
3	94.1	115.7
4	89.7	107.7

The coating thickness, determined by ellipsometry, constantly lies at about 90 nm and is not influenced by the annealing. The contact angle changes significantly with the annealing time from 131.9° (not annealed coating) to 107.7° (coating after 4 h of annealing), showing the formation of more hydrophilic surfaces. The change in the contact angle indicates the rearrangement of the polymer chains and thereby confirms the observation that the annealing leads to a reorientation of the polymer chains at the surface. The hydrophobic alkyl chains reorganize and orient to the inside of the coating, whereas the hydrophilic cationic groups rearrange and realign to the surface of the coating.

The change of the contact angle to lower values, showing the rearrangement of the alkyl chains to the inside of the coating, together with the decreased antimicrobial activity after the annealing, can give a hint on the antimicrobial interaction of the polymer with the bacteria. The changes show that the alkyl chains lying at the surface or even pointing away from the surface towards the bacteria are important for the antimicrobial interaction. After the annealing, the alkyl chains are oriented more to the inside of the coating so that both the contact angle and the antimicrobial activity decrease. Since surfaces with contact angles above 90° are defined as hydrophobic, the surface with a contact angle of 107.7° is still hydrophobic after the annealing. The hydrophobic surface indicates that there are still alkyl chains at the surface which are available for an antimicrobial interaction. On the other hand, this observation is contradictory to an observation made in Chapter 4, where it was found that the antimicrobial activity increases with decreasing concentration of alkyl chains. The orientation of the alkyl chains to the inside of the coating decreases the concentration of the alkyl chains at the surface and should therefore lead to an increased antimicrobial activity. The opposite was observed: the antimicrobial activity decreased. Thus, all the observations show that not only the composition of the material is important, but also the orientation of the polymer chains on the surface is important for the antimicrobial activity. It is not easily possible to give overall conclusions about what composition a polymer should have to obtain a good antimicrobial effect in a coating. Besides the hydrophilic/hydrophobic balance, several other factors exist, including the orientation of the polymer chains at the surface and the chain mobility. These other factors play a role for the antimicrobial activity of a polymer in a surface coating.

Antimicrobial Activity of the Spin Coated Surfaces After 5 h of Annealing

The antimicrobial activity of spin coated substrates after annealing with methanol for 5 h was measured for all three polymers: PVAm-EQ_9-$EA12_{10}$, PVAm-1.EQ_{10}-2.$EA12_{10}$ and PVAm-1.$EA12_{10}$-2.EQ_9. The antimicrobial test was done under growth conditions (in nutrient solution). To ensure the complete wetting of the surface, enabling the bacteria to interact with the coated polymer, the wetting agent DOW was used. The results on the inhibition of growth of *E. coli* of the spin coated substrates after annealing in methanol atmosphere for 5 h are shown in Table 11. With 90 – 99 % inhibition of growth, the same antimicrobial effect was observed for all three polymers. These results show that the different microstructures of the polymers are only present in solution. When being coated on surfaces, the three-dimensional structure is lost and all considered polymers exhibit the same properties.

Table 11. Inhibition of bacterial growth (*E. coli*) after exposure on the spin coated and annealed silicon substrates (9 µg/cm² polymer).

Name	Inhibition of growth[a)] [%]
PVAm-EQ_9-$EA12_{10}$	90 - 99
PVAm-1.EQ_{10}-2.$EA12_{10}$	90 - 99
PVAm-1.$EA12_{10}$-2.EQ_9	90 - 99

[a)] The test was performed under growth conditions and a concentration of 0.01 % DOW was used. The given values are the mean values obtained by averaging the outcomes of two independent measurements. Within the performed tests, no leaching of the polymer coatings that would falsify the growth test was observed.

5.3.4 Atomic Force Microscopy Measurements

The surface of the polymer films obtained by spin coating of the polymer PVAm-EQ_9-$EA12_{10}$ from 1 wt% methanolic solutions (9 µg/cm² polymer) after different annealing times with methanol was analyzed by atomic force microscopy (AFM) measurements. The surface roughness was analyzed with the NanoScope analysis program. The resulting surface roughnesses R_q (root mean squared) and R_a (arithmetic average of absolute values) are listed in Table 12. Figure 10 shows a bar chart of the surface roughness R_q after the different annealing times.

Table 12. Surface roughnesses R_q and R_a of substrates spin coated with PVAm-EQ_9-$EA12_{10}$ from 1 wt% methanolic solutions (9 µg/cm² polymer) after different annealing times for different scan sizes (AFM).

time[a)] [h]	R_q 10 µm[b)]	R_q 2 µm[b)]	R_q 500 nm[b)]	R_a 10 µm[b)]	R_a 2 µm[b)]	R_a 500 nm[b)]
0	0.329	0.265	0.192	0.220	0.210	0.153
1	0.294	0.284	0.202	0.234	0.225	0.160
2	0.354	0.294	0.210	0.268	0.232	0.163
3	0.319	0.291	0.255	0.255	0.231	0.200
4	0.341	0.301	0.263	0.273	0.240	0.208

[a)] annealing time in [h], [b)] scan size

The measurements show very flat surfaces with surface roughnesses of, e.g., about 0.29 nm (R_q) for scan sizes of 2 µm. The roughness does not significantly change during the annealing time. If it changes at all, the surfaces might become only minimally rougher.

The results of the surface analysis with AFM fit well to the results of the antimicrobial investigation. They confirm that there are no differences in the two-dimensional surface structure of the polymers. The different microstructures, which were verified by the CAC measurements, are only present in solution (three dimensional). A projection into two dimensions destroys the microstructures.

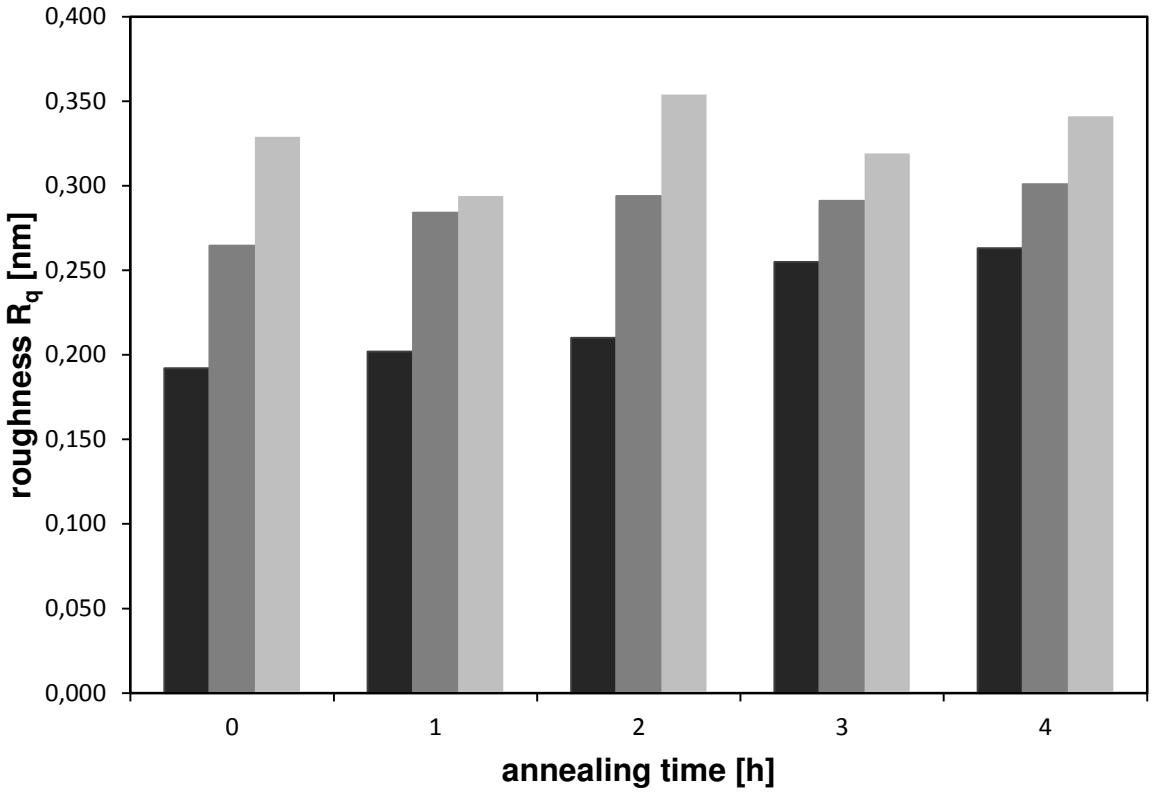

Figure 10. Surface roughness R_q of substrates spin coated with PVAm-EQ_9-$EA12_{10}$ from 1 wt% methanolic solutions (9 µg/cm² polymer) after different annealing times. Black bars: scan size 500 nm, dark grey bars: scan size 2 µm, light grey bars: scan size 10 µm.

5.3.5 Hemolytic Activity

The antimicrobial activity is not the only important characteristic for polymers used in antimicrobial applications in contact with human tissue. Besides the antimicrobial activity, the

polymers have to be selectively active against bacteria and should not be active against human cells. To evaluate the selectivity of the polymers, their hemolytic activity was determined. The hemolysis is the destruction or dissolution of red blood cells (erythrocytes, RBCs) with a subsequent release of their contents (hemoglobin) into the surrounding fluid. The hemolytic activity of the polymers was investigated directly on coated substrates and in extracts of the coated substrates. Therefore a hemoglobin release assay for polymer solutions as described in the literature[34] was adapted to test the polymer coatings. The hemolytic activity is usually defined as the polymer concentration that causes 50 % hemolysis of the human RBCs relative to the positive control (EC50).[13,34] Since the polymer is coated on surfaces in the tests carried out in the scope of this thesis, it is not possible to analyze a dilution series and thereby to give a polymer concentration that causes 50 % hemolysis of the RBC. It is however possible to determine to what extend the tested coatings are hemolytically active, and if the hemolytic activity is above or below the 50 % benchmark.

The hemolytic activity of the three polymers PVAm-EQ_9-$EA12_{10}$, PVAm-1.EQ_{10}-2.$EA12_{10}$ and PVAm-1.$EA12_{10}$-2.EQ_9 was examined for spin coated substrates (1 wt% polymer solutions, 9 µg/cm² polymer) before and after annealing for 5 h in methanol atmosphere. For comparison, the hemolytic activities of an uncoated glass surface, an uncoated silicon surface, and of the PBS solution were tested as negative control and the hemolytic activities of a 1 % Triton X100 solution alone and coated on a glass surface were tested as positive control. The hemolytic activity of the positive control (Triton X100 coated on a glass surface) was defined as 100 %. The hemolytic activity was tested directly on the surface and in extracts of the surface. Within this test, the hemolytic activity of all polymers was not significantly higher than the negative controls and the polymer coatings can therefore be evaluated as hemolytically inactive. The annealing in methanol atmosphere had almost no influence on the hemolytic activity. Only for the polymer PVAm-1.EQ_{10}-2.$EA12_{10}$, the hemolytic activity

before the annealing was slightly higher than it was after annealing. In addition, the hemolytic activity of the polymer PVAm-1.EQ_{10}-2.$EA12_{10}$ was slightly higher before the annealing than it was for the other polymers. Besides these observations, it was not possible to distinguish between the three polymers. The results on the test of the hemolytic activity are shown in Figure 11, they again show that a projection into two dimensions destroys the microstructures.

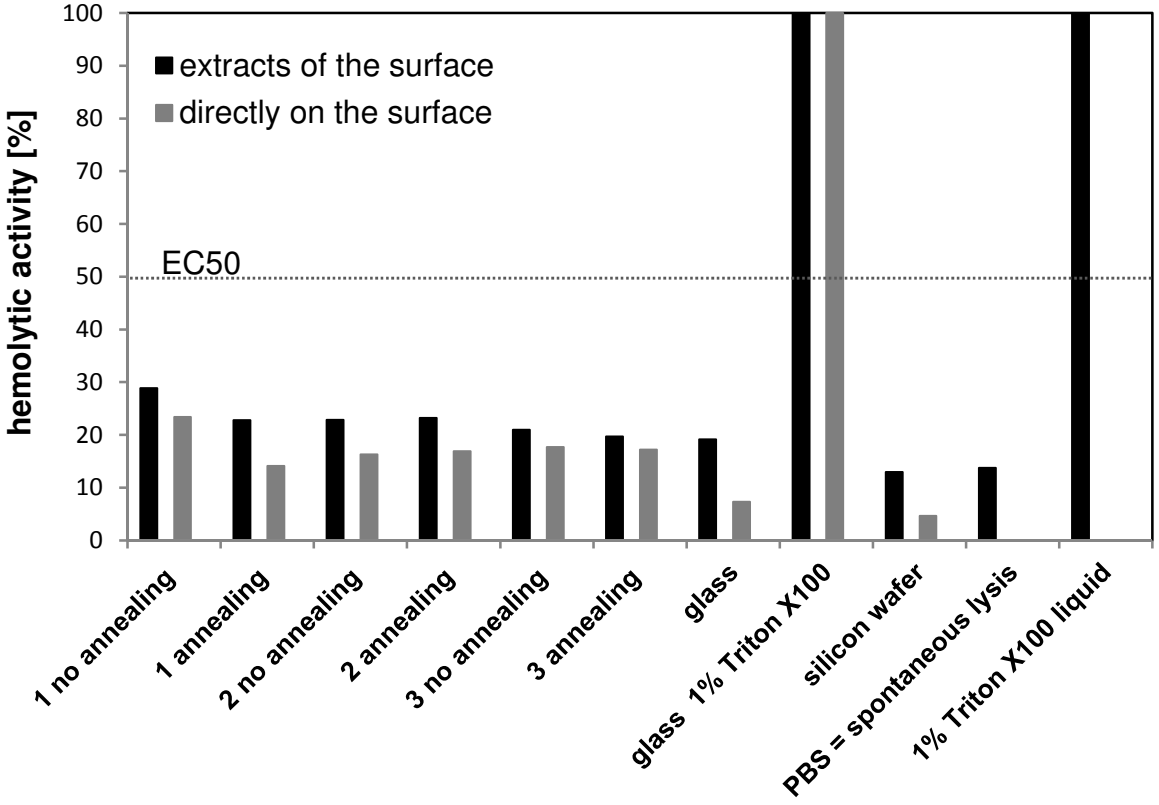

Figure 11. Hemolytic activity of the polymers **1** (PVAm-1.EQ_{10}-2.$EA12_{10}$), **2** (PVAm-1.$EA12_{10}$-2.EQ_9), and **3** (PVAm-EQ_9-$EA12_{10}$), of the negative controls (glass surface, silicon surface, PBS solution) and of the positive controls (1 % Triton X100 solution alone and on glass surface). Blue (left bars): extracts of the surface, green (right bars): directly on the surface, dotted line: EC50 = 50 % benchmark of the hemolytic activity.

5.3.6 Membrane Penetration in Langmuir Film Experiments

The molecular interaction with lipid films or rather the ability of the developed polymers to penetrate into membranes was tested for the three polymers PVAm-1.EQ_{10}-2.$EA12_{10}$, PVAm-1.$EA12_{10}$-2.EQ_9 and PVAm-EQ_9-$EA12_{10}$. Therefore, the degree of penetration of the polymers into Langmuir monolayers of neutral and of charged lipids was measured. The goal was to determine differences in the penetration behavior of the three polymers and thereby to get evidence for the existence of different microstructures within the polymers.

An ordered monomolecular lipid layer of DPPC (dipalmitoylphosphatidylcholine) on the surface of bidistilled water (subphase) in a Langmuir trough with an initial surface pressure of 20 mN/m was used as neutral model membrane system. For the charged model membrane system, an ordered monomolecular lipid layer consisting of 75 mol% DPPC and of 25 mol% DPPG (dipalmitoylphosphatidylglycerol) was used. After the injection of the polymer solution into the subphase, the increase of the surface pressure (mN/m) was recorded for 60 min until a new equilibrium was established. The increase of the surface pressure $\Delta\pi$ is the most widely used parameter to characterize the membrane affinity/penetration ability of a molecule in Langmuir layer studies.[13,44,45,46,47]

The polymers were tested with two different polymer concentrations (0.025 mg/mL and 0.075 mg/mL) in the subphase. All three polymers exhibit the same composition of 10 % hydrophobic groups EA12 and about 9 % cationic groups EQ. The increase of the surface pressure of the lipid film ($\Delta\pi$) as a result of the penetration of the polymers into the monolayers of DPPC and of DPPC/DPPG, is shown for two different polymer concentrations in Table 13 and as a bar chart in Figure 12. An increase of the surface pressure indicates the adsorption of the polymers to the lipid monolayer and a substantial penetration into the monolayer.

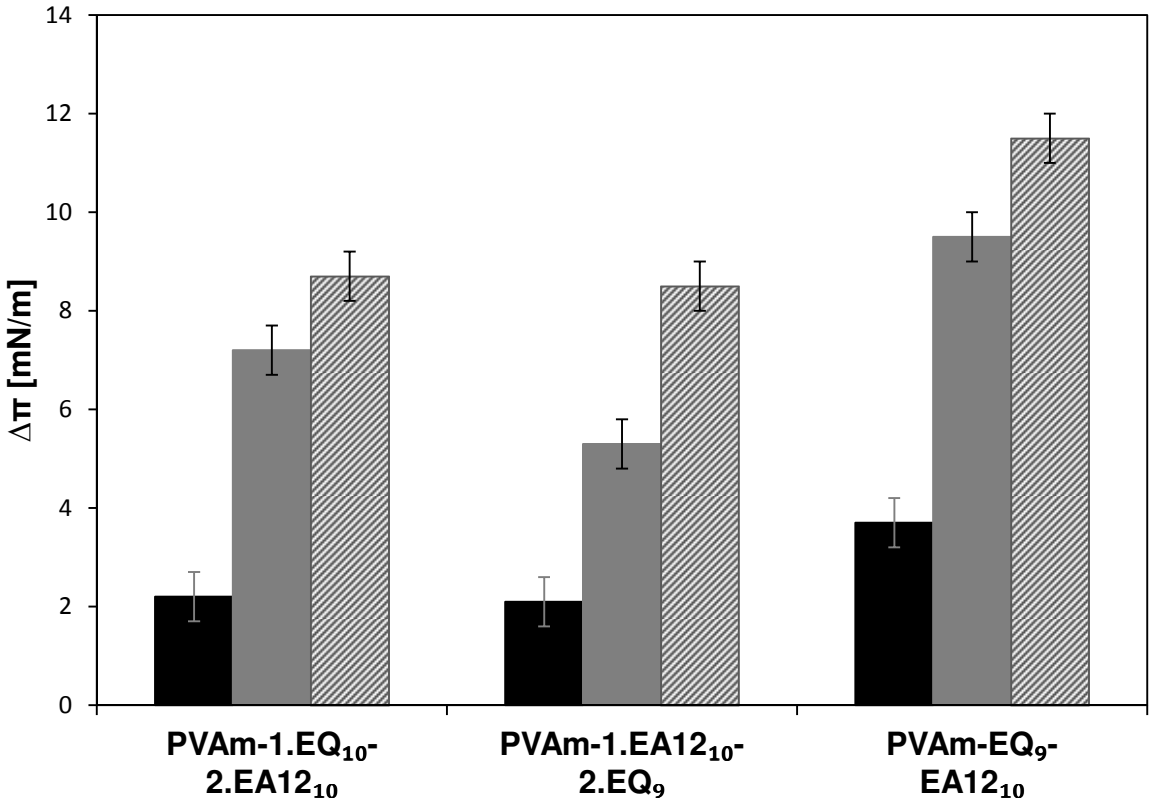

Figure 12. Increase of the surface pressure of the lipid film ($\Delta\pi$) as a result of the penetration of polymers (PVAm-1.EQ_{10}-2.$EA12_{10}$, PVAm-1.$EA12_{10}$-2.EQ_9 and PVAm-EQ_9-$EA12_{10}$) with different microstructures but the same composition into lipid monolayers with an initial surface pressure of 20 mN/m. Two different compositions of the lipid monolayer were tested: DPPC monolayer and 75 mol% DPPC + 25 mol% DPPG monolayer. Two different polymer concentrations in the subphase are displayed for the DPPC monolayer: 0.025 mg/mL (black), 0.075 mg/mL (grey). The penetration into the DPPC/DPPG monolayer was investigated for a polymer concentration of 0.075 mg/mL (striped). The estimated error of the measured values amounts to ± 0.5 mN/m.

Table 13. Increase of the surface pressure of the lipid film ($\Delta\pi$) as a result of the penetration of the polymers with different microstructures but the same composition into lipid monolayers with an initial surface pressure of 20 mN/m.

Name	membrane composition[a)]	c[b)] [mg/mL]	$\Delta\pi$[c)] [mN/m]
PVAm-1.EQ$_{10}$-2.EA12$_{10}$	**DPPC**	0.025	2.2
	DPPC	0.075	7.2
	DPPC/DPPG	0.075	8.7
PVAm-1.EA12$_{10}$-2.EQ$_9$	**DPPC**	0.025	2.1
	DPPC	0.075	5.3
	DPPC/DPPG	0.075	8.5
PVAm-EQ$_9$-EA12$_{10}$	**DPPC**	0.025	3.7
	DPPC	0.075	9.5
	DPPC/DPPG	0.075	11.5

[a)] Two different compositions of the lipid monolayers were tested: DPPC monolayer and 75 mol% DPPC + 25 mol% DPPG monolayer. [b)] Two different polymer concentrations in the subphase were tested for the DPPC monolayer: 0.025 mg/mL and 0.075 mg/mL. The penetration into the DPPC/DPPG monolayer was investigated for a polymer concentration of 0.075 mg/mL. [c)] The estimated error of the measured values amounts to ± 0.5 mN/m.

The obtained data show significant differences in the penetration ability between the three polymers. The differences in the penetration ability into neutral monolayers of DPPC between the three polymers is most explicit for a polymer concentration of 0.075 mg/mL. The polymer obtained by simultaneous addition of the functionalities (PVAm-EQ$_9$-EA12$_{10}$) exhibits the highest penetration ability with $\Delta\pi$ = 9.5 mN/m, whereas the polymer obtained by first adding

the hydrophobic groups (PVAm-1.EA12$_{10}$-2.EQ$_9$) possesses the lowest penetration ability with $\Delta\pi = 5.3$ mN/m. For the lower polymer concentration in the subphase, the degrees of penetration were lower, but relative to each other, the three polymers show the same trend in penetration ability.

The penetration ability of the polymers into charged monolayers of DPPC/DPPG is higher than the penetration ability into neutral monolayers. Comparing the penetration ability of the polymers into charged monolayers among each other, the same trend in the penetration ability as for the neutral monolayers is observed. However, the difference between the two polymers obtained by sequential addition of the functionalities is much smaller.

The results of the membrane penetration experiments support the assumption of the existence of different microstructures within the polymers. The different microstructures lead to differences in the penetration ability of the polymers. In all experiments, the polymer obtained by simultaneous addition exhibited the highest penetration ability. This observation fits well to the result of the CAC measurement where this polymer showed the lowest CAC value and thereby the highest chain mobility. To penetrate the membrane, the polymer structure needs to be flexible to be able to rearrange.

5.3.7 Membrane Permeabilization of *E. coli*

The permeabilization of the outer/inner membrane of *E. coli* was investigated by using the ONPG hydrolysis assay[39] (ONPG = o-Nitrophenyl-β-D-galactopyranosid). In the ONPG hydrolysis method, a suspension of bacteria is added to a buffer containing ONPG and the test substance. The cytoplasm of *E. coli* contains β-galactosidase. This hydrolase is used by the bacterium to catalyze the hydrolysis of β-galactosides into monosaccharides. ONPG is a β-galactoside which does not penetrate the inner membranes of intact *E. coli* ML35 bacteria and remains extracellular because the mutant *E. coli* ML35 has no lactose permease. If the

inner membrane of the bacterium is disrupted by the antimicrobial agent, the ONPG can diffuse into the cytoplasm of the bacterium, where it is hydrolyzed by the β-galactosidase to *o*-nitrophenol (ONP) as shown in Figure 13. The permeabilization of the outer/inner membrane of the bacteria can be followed by measuring the absorbance of ONP at a wavelength of 405 nm over time. The maximal permeabilization (100 % lysis) was determined by evaluating cells which were pretreated with PopCulture® reagent. As positive control, one experiment was performed without addition of the polymer, with only bacteria suspension added. As negative control, one experiment was performed with PBS only.

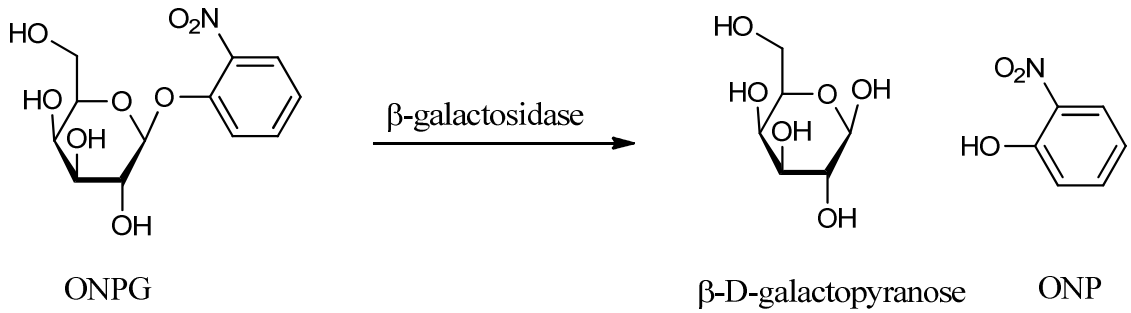

Figure 13. Hydrolysis of ONPG by β-galactosidase to ONP.

The polymers (PVAm-1.EQ$_{10}$-2.EA12$_{10}$, PVAm-1.EA12$_{10}$-2.EQ$_9$ and PVAm-EQ$_9$-EA12$_{10}$) were tested for their ability to penetrate the outer/inner membrane of *E. coli* by using the ONPG hydrolysis assay (Figure 14). ONPG is only hydrolyzed to ONP if not only the outer, but also the inner membrane of the bacterium is disrupted. The bulk concentration of polymer in the medium is significantly higher than that which reaches the inner membrane because a certain amount of the polymer is excluded by the cell wall and/or bound to lipopolysaccharides.

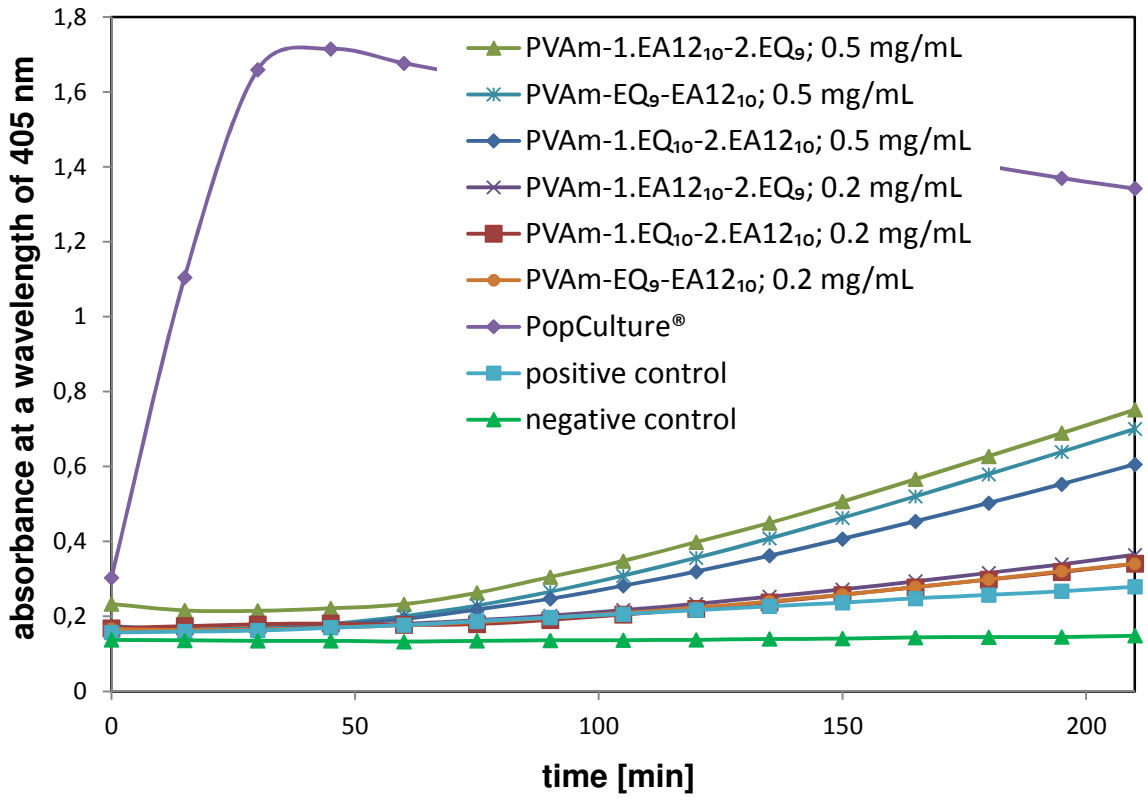

Figure 14. Inner membrane permeabilization of *E. coli* ML35, caused by the three polymers PVAm-1.EQ$_{10}$-2.EA12$_{10}$, PVAm-1.EA12$_{10}$-2.EQ$_9$ and PVAm-EQ$_9$-EA12$_{10}$, as a function of time at different concentrations (0 – 0.5 mg/mL), at a temperature of 38 °C. The reaction of ONPG with β-galactosidase was measured every 15 min by measuring the absorbance at a wavelength of 405 nm. PopCulture® reagent: maximal permeabilization (100 % lysis) was determined by evaluating cells which were pretreated with PopCulture® reagent; Positive control: experiment without polymer, with only bacteria suspension added; Negative control: experiment with only PBS. Each data point represents an average of the outcomes of four independent trials.

The inner membrane permeabilization was much slower for the tested polymers than with the PopCulture® reagent (100 % lysis), as it took approximately 60 min until the polymer began to permeabilize the inner membrane. This is in contrast to a direct start of the

permeabilization if the PopCulture® reagent was used. Although there was only a small amount of ONPG influx through the inner membrane into the cytoplasm, the increasing absorbance, showing the formation of ONP, demonstrates that the polymers are capable of damaging the inner membrane. Furthermore, the effectiveness of the polymers increases with increasing polymer concentration.

For a concentration of 0.2 mg/mL, which is equal to the measured MIC value, the three polymers only showed a slightly higher membrane permeabilization than the positive control. The positive control was an experiment without polymer, with only bacteria suspension added to the test solution. After an experiment duration of 60 min, a small increase in the absorbance of the positive control that could be caused by some dying bacteria was observed as well. The permeability of the inner membrane of dying bacteria increases over time and allows some diffusion of molecules through the inner membrane. In addition, the absorbance of the solution can be increased due to an increased turbidity, caused by the normal proliferation of the bacteria.

For a concentration of 0.5 mg/mL, the polymers showed a clear membrane permeabilization after 60 min. Only small differences in the membrane permeabilization were observed for the three polymers. The polymer PVAm-1.EA12$_{10}$-2.EQ$_9$ has got a slightly higher activity, followed by the polymer PVAm-EQ$_9$-EA12$_{10}$ which has a slightly lower activity, and the polymer PVAm-1.EQ$_{10}$-2.EA12$_{10}$ which shows a slightly lower activity than both other polymers.

5.3.8 Proposed Microstructures of the Synthesized Polymers

Based on the different polymer properties three different microstructures are proposed. The microstructures of the polymers prepared via different routes with a ratio of EQ to EA12 of 1 : 1 will be explained and described in what follows:

1) Addition of cationic groups first (e.g., PVAm-1.EQ_{10}-2.$EA12_{10}$)

During the reaction of the polymer with the cationic groups in the first reaction step, the cationic charges repel each other so that the polymers conformation is expanded. The cationic charges are homogeneously distributed along the polymer chain and they force the polymer chain to a linear conformation with the highest possible distance between the charges. In the second step of the reaction, the alkyl chains are introduced into the polymer. After the first chains are attached to the polymer, the next ones will react in their neighborhood because of the more hydrophobic surrounding. In this way, segregated domains of hydrophobic groups will arise along the backbone of the polymer. The elongated conformation generated in the first reaction step will be conserved as shown in Figure 15 a).

2) Addition of hydrophobic groups first (e.g., PVAm-1.$EA12_{10}$-2.EQ_9)

If in the first reaction step the alkyl chains are added to the polymer backbone, they will build segregated micelle-like domains within the polymer and force the polymer into a strongly accumulated conformation. The interaction within these domains is so strong that the repulsion of the cationic groups added in the next step is not high enough to expand the conformation (Figure 15 b)).

3) Addition of cationic and hydrophobic groups together (e.g., PVAm-EQ_9-$EA12_{10}$)

If both functional groups are added simultaneously, two opponent forces, the repulsive expanding force of the cationic groups and the accumulating force of the hydrophobic groups, are active at the same time. The emerging microstructure will be somewhere in between the structure of the two sequential additions. The polymer chain will stay more flexible (Figure 15 c)).

The described microstructures fit quite well to what is expected by considering the measured CAC values of the three different polymers. The polymer obtained by the reaction where the cationic groups are added first (Figure 15 a)) yielded the highest CAC value. The chains of this polymer are least flexible and form micelles at higher concentrations than the polymer chains of the other polymers. The lowest CAC value has been obtained for the polymer prepared via simultaneous addition of both functionalities (Figure 15 c)), giving evidence that this conformation has got the most flexible polymer chain and therefore builds up micelles more easily. The CAC value as well as the chain mobility of the third polymer prepared by the reaction where the hydrophobic groups were added in the first reaction step lies in between the two other polymers.

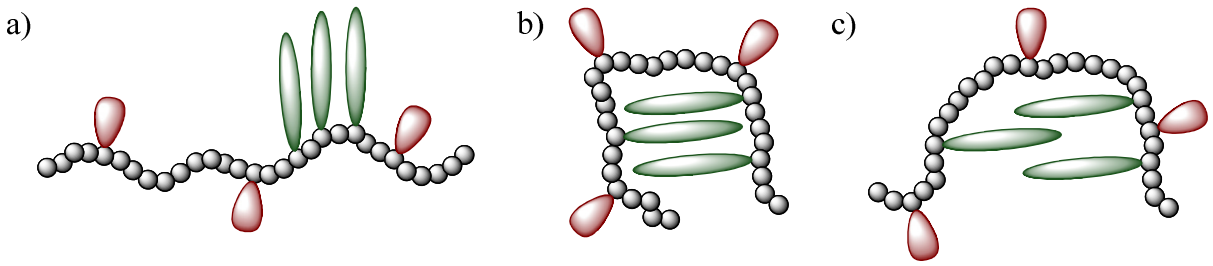

Figure 15. Microstructures within the polymer obtained by a) addition of cationic groups first, b) addition of hydrophobic groups first and c) simultaneous addition of both groups.

5.3.9 Viscosity of the Synthesized Polymers

The viscosity of the three polymers was measured with an Ubbelohde viscometer for different polymer concentrations in Seral-water. The plot of the reduced viscosity (η_{sp}/c) over the polymer concentration is shown in Figure 16. The typical viscosity behavior for polyelectrolytes is observed.[48] Usually, for other substances, the viscosity decreases with a decreasing concentration of the measured substance. For polyelectrolytes this behavior is different. With a decreasing polymer concentration, the viscosity increases. As discussed in

Chapter 1, polyelectrolytes are polymers with charges along the backbone. Electrostatic interactions between the polyions and their counterions represent a dominant factor influencing the polyion conformation. Besides this, the conformation also depends on the chemical structure of the polyelectrolyte, its size and charge density, and the environmental properties like ionic strength and solvent polarity. With a decreasing polyelectrolyte concentration, the counter ions do not shield the charges along the backbone any more. The charges repel each other and force a conformation change of the polymer towards an elongated conformation. By this, the viscosity increases with decreasing polymer concentration and it is quite complex to calculate an intrinsic viscosity.

The experimental data show differences in the viscosity behavior of the three polymers, giving again evidence for the existence of different microstructures in the polymers. A lower viscosity for the same polymer concentration shows a more condensed conformation of the polymer, which on the one hand can be due to a better shielding of the charges. On the other hand, it can be due to different microstructures within the polymer. The observed differences between the three polymers can be explained as a result of the different microstructures described above. Polymer PVAm-1.$EA12_{10}$-2.EQ_9 (hydrophobic first) shows the lowest viscosity and thereby the most condensed conformation. The more condensed conformation is due to the strong interaction in the hydrophobic domains, which were built during the synthesis and prevent the expansion of the polymer chains. In contrast, the polymer PVAm-1.EQ_{10}-2.$EA12_{10}$ (cationic first) exhibits the highest viscosity. This high viscosity is due to the highly elongated conformation, which is caused by the expansion of the structure through the initial introduction of the cationic groups into the polymer. The viscosity of the polymer PVAm-EQ_9-$EA12_{10}$ (simultaneous addition) lies in between the viscosities of the two other polymers, just like the conformation, which is in between the conformation of the two other polymers.

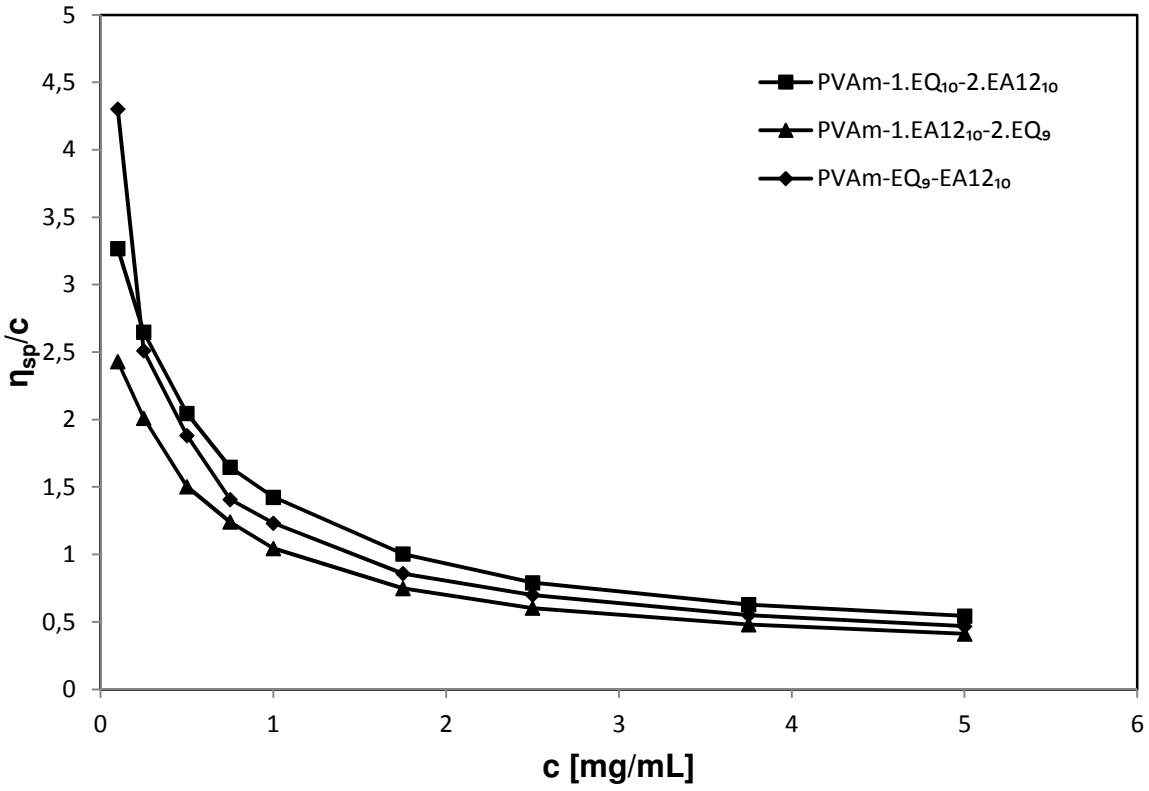

Figure 16. Reduced viscosity η_{sp}/c over polymer concentration [mg/mL] for the polymers PVAm-1.EQ_{10}-2.$EA12_{10}$ (■), PVAm-1.$EA12_{10}$-2.EQ_9 (▲), and PVAm-EQ_9-$EA12_{10}$ (♦). All measurement points are the mean values obtained by averaging the outcomes of at least six independent measurements at a constant temperature of 20 °C.

Fuoss and Strauss[49,50] developed an empirical equation to calculate the intrinsic viscosity for polyelectrolytes:

$$c/\eta_{sp} = [\eta]^{-1} + (B/[\eta])\sqrt{c} \qquad (1)$$

with $[\eta]$ = intrinsic viscosity, and B = constant. However, this equation is not always valid.[48,51] For example, Pavlov *et al.* studied the viscosity behavior of poly(styrenesulfonate)s of various molecular weights[48], and Dragan *et al.* studied the viscosity behavior of

poly(sodium 2-acrylamido-2-methylpropanesulfonate)s with different molar masses[51]. In both cases, it was not possible to linearize the viscometric data over the whole polyion concentration range using the Fuoss and Strauss procedure.

According to the procedure by Fuoss and Strauss, c/η_{sp} is plotted over $\sqrt{c}$ and the data values are approximated by a linear regression (Figure 17 and Figure 18). The value $[\eta]^{-1}$ (and thus $[\eta]$) is obtained by setting $\sqrt{c} = 0$ in the linear fit, which corresponds to the intersection of the linear fit with the ordinate.

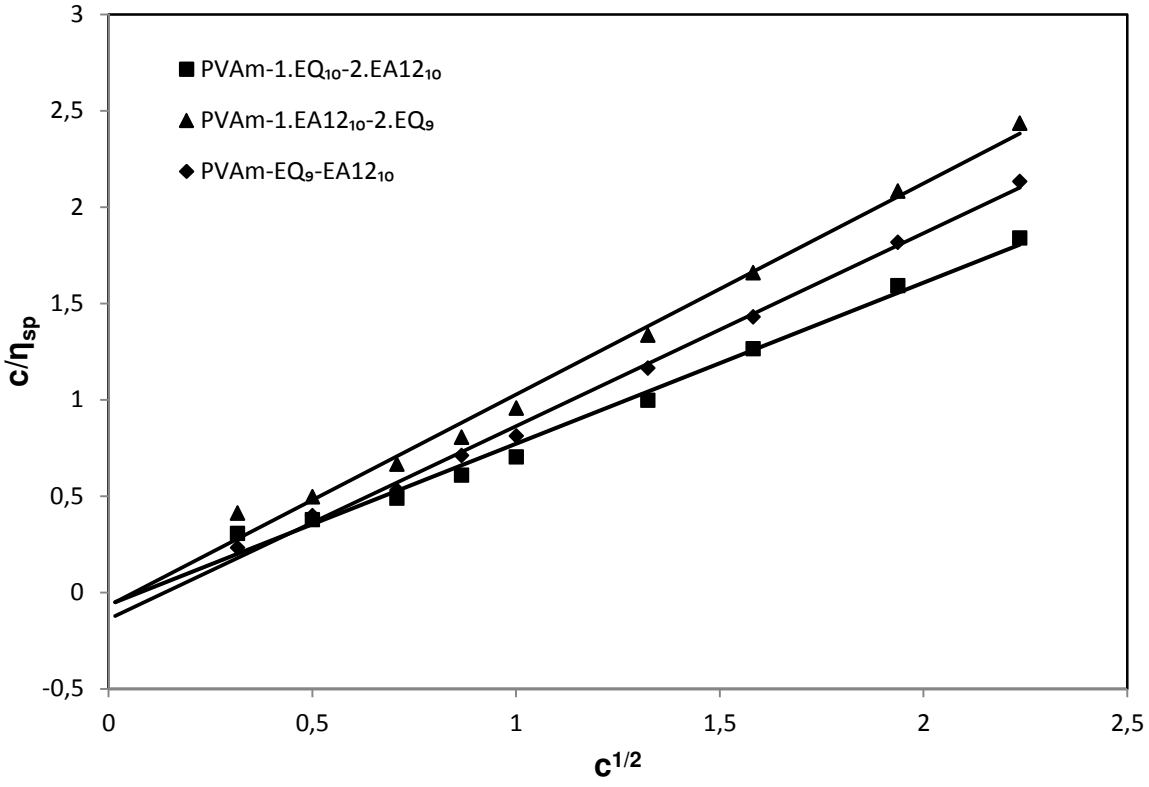

Figure 17. Fitting of the Fuoss and Strauss equation on the viscometric data of the polymers PVAm-1.EQ_{10}-2.$EA12_{10}$ (■), PVAm-1.$EA12_{10}$-2.EQ_9 (▲), and PVAm-EQ_9-$EA12_{10}$ (♦), in the concentration range of 0.1 – 5.0 mg/mL.

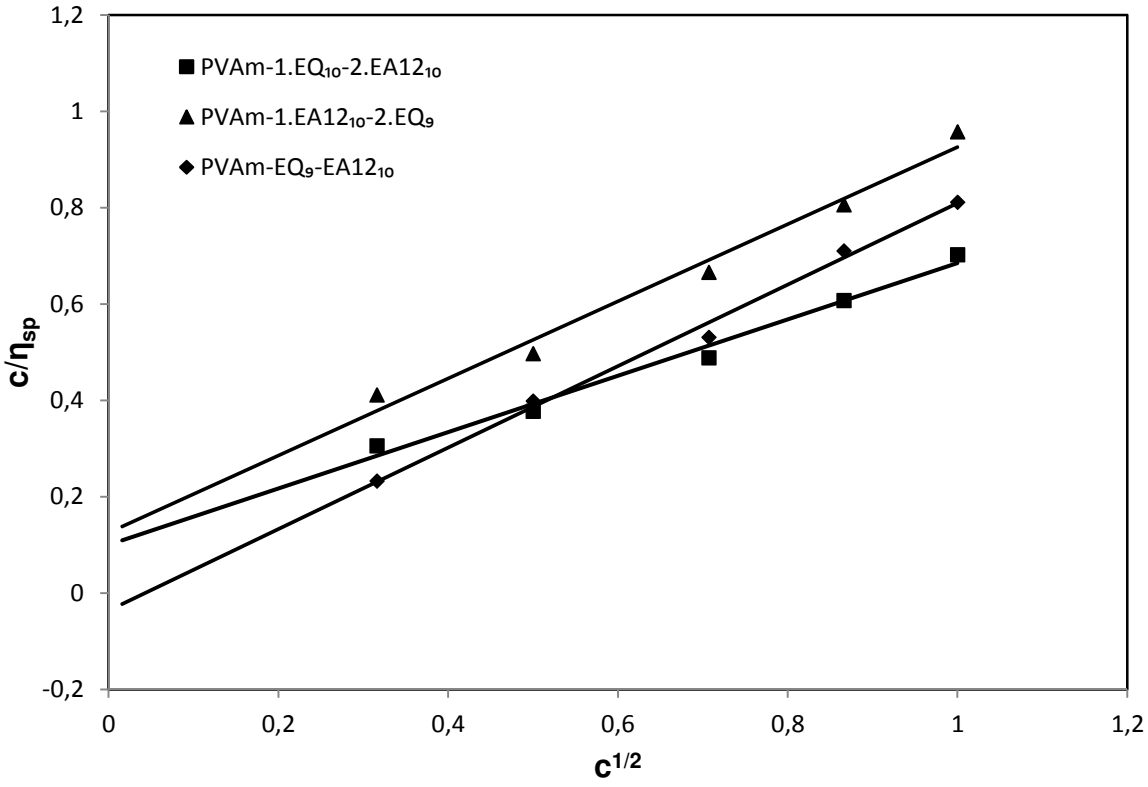

Figure 18. Fitting of the Fuoss equation on the viscometric data of the polymers PVAm-1.EQ_{10}-2.$EA12_{10}$ (■), PVAm-1.$EA12_{10}$-2.EQ_9 (▲), and PVAm-EQ_9-$EA12_{10}$ (♦), in the concentration range of 0.1 – 1.0 mg/mL.

As Figure 17 shows, the measured data for the polymers PVAm-1.$EA12_{10}$-2.EQ_9, PVAm-1.EQ_{10}-2.$EA12_{10}$, and PVAm-EQ_9-$EA12_{10}$ cannot be fitted over the whole concentration range and the calculation of the intrinsic viscosity from the axis intersection leads to impossible negative values. A fitting of the data over a concentration range of 0.1 – 1.0 mg/mL (Figure 18) leads to a better fit. Positive intrinsic viscosity values can be calculated for the polymer PVAm-1.$EA12_{10}$-2.EQ_9 ($[\eta]$ = 8.02 mL/mg) and for the polymer PVAm-1.EQ_{10}-2.$EA12_{10}$ ($[\eta]$ = 10.01 mL/mg). For the polymer PVAm-EQ_9-$EA12_{10}$ still a negative value for the intrinsic viscosity is obtained. In addition, the fit is however still not satisfactory

and the Fuoss and Strauss equation does not seem to be valid for the polymers investigated in this section.

5.4 Conclusions

For a better overview, Table 14 and Table 15 give a short summary of the results of some of the different analyses which have been performed on the synthesized polymers.

Table 14. Overview on the results of some of the different analyses of the synthesized polymers.

Name	CAC (I_{373}/I_{383}) [mg/mL]	CAC (I_{373}/I_{371}) [mg/mL]	$\Delta\pi$[a)] [mN/m]	Viscosity [-[b)]]	MP [-[c)]]
PVAm-EQ$_9$-EA12$_{10}$	0.001	0.018	9.5	2	2
PVAm-1.EQ$_{10}$-2.EA12$_{10}$	0.012	0.044	7.2	3	1
PVAm-1.EA12$_{10}$-2.EQ$_9$	0.004	0.037	5.3	1	3

[a)] Increase of the surface pressure of the lipid film ($\Delta\pi$) as a result of the penetration of the polymers (0.075 mg/mL) into lipid monolayers of DPPC. Higher value ($\Delta\pi$) = higher penetration ability. [b)] Qualitative result: 1 = lowest viscosity, 2 = middle viscosity, and 3 = highest viscosity. [c)] MP = membrane permeabilization of *E. coli*. ONPG hydrolysis assay: qualitative result: 1 = lowest activity, 2 = middle activity, and 3 = highest activity.

Table 15. Overview on the results of some of the different analyses of the synthesized polymers.

Name	MIC[a)] [mg/mL] pH = 8.0	Growth inhibition[b)] [%] 9 µg/cm²	Hemolytic activity
PVAm-EQ$_9$-EA12$_{10}$	0.2	90 - 99	Not active
PVAm-1.EQ$_{10}$-2.EA12$_{10}$	0.2	90 - 99	Not active
PVAm-1.EA12$_{10}$-2.EQ$_9$	0.2	90 - 99	Not active

[a)] MIC = lowest concentration of an antimicrobial that gives a log-4 reduction of the cfu. The test solutions showed turbidities and the real MIC might be lower. [b)] Inhibition of bacterial growth (*E. coli*) after exposure on spin coated and annealed (5 h MeOH) silicon substrates.

In this chapter the synthesis of polymers with the same composition but different microstructures is described. Different microstructures were obtained by sequential and simultaneous addition of functional epoxides to poly(vinyl amine). The polymers showed different CAC values. The polymer obtained by sequential addition of cationic groups first possesses the highest CAC value, the polymer obtained by simultaneous addition possesses the lowest CAC value and the CAC of the polymer obtained by sequential addition of hydrophobic groups first lies in between. This fits well to the discussed microstructures of the polymers where the addition of cationic groups first leads to an extended non-flexible conformation. The addition of hydrophobic groups first leads to micelle-like segregated hydrophobic domains within the polymer which builds more easily larger micelles but is still relatively inflexible, whereas the simultaneous addition of both functionalities gives the most flexible conformation due to the contrary forces during the reaction and builds micelles easier than the other two polymers.

The polymers show differences in their viscosity behavior, which confirm the discussed different microstructures. Polymer PVAm-1.$EA12_{10}$-2.EQ_9 shows the lowest viscosity and thereby the most condensed conformation. Polymer PVAm-1.EQ_{10}-2.$EA12_{10}$ exhibits the highest viscosity and thereby the most elongated conformation. The viscosity and the conformation of polymer PVAm-EQ_9-$EA12_{10}$ lies in between the two other polymers.

The antimicrobial effect of the polymers was investigated in solution and on surface. Due to the appearance of turbidity by adding PBS or nutrient solution to the aqueous polymer solution the antimicrobial effect in solution could not be determined properly. All three polymers showed MIC values of about 0.2 mg/mL. The real MIC values might be lower. The antimicrobial effect of the polymers immobilized on surfaces was tested. Different ways of film preparation were developed. Drop casting of 0.05 wt% solutions led to very good results up to 100 % inhibition of growth, however, no differences between the polymers could be detected. Lowering the amount of polymer in the casting solution to 0.025 wt% led to inhomogeneities in the surface coating and a high variance in the measured values (up to 99.9999 % inhibition of growth) was obtained. Due to this high variance of the measured values, no differences in antimicrobial activity between the three polymers could be detected at this point. In the next step the surface coating was optimized and the properties of polymer coatings obtained by spin coating and annealing in methanol atmosphere for different times were determined. The coating thickness was determined by ellipsometry to be about 90 nm and is not influenced by the annealing. Annealing with methanol for 4 h leads to homogeneous surfaces. The antimicrobial effect decreases through the annealing from 99.9 % to 99 % inhibition of growth, due to the formation of thermodynamically stable conformations of the polymer chains, which have got a lower antimicrobial activity than the mixture of conformations which has been on the surface before the annealing. However, the antimicrobial results are very good reproducible and this is the most important point to

compare the properties of the developed polymers. Again it is not possible to distinguish between the three polymers. Contact angle measurements showed that the surfaces are more hydrophilic after annealing. This proves the rearrangement of the chains. The hydrophobic parts go to the inside and the hydrophilic parts go to the outside of the coating.

The hemolytic activity of the polymers on spin coated surfaces before and after annealing was studied directly on the surface and as an extract of the surface. Under all testing conditions the polymers exhibit no significant hemolytic activity. The different microstructures do not lead to differences in hemolytic activity.

The penetration ability of the polymers into membranes was tested (i) for Langmuir monolayers of neutral and of charged lipids and (ii) by using the ONPG hydrolysis assay the permeabilization of the outer/inner membrane of *E. coli* was investigated:

(i) It was found that the penetration ability of the polymers into charged monolayers of DPPC/DPPG is higher than the penetration ability into neutral monolayers (DPPC). The different microstructures lead to differences in the penetration ability of the polymers. The polymer obtained by simultaneous addition of the functionalities (PVAm-EQ_9-$EA12_{10}$) exhibits the highest penetration ability, whereas the polymer obtained by adding the hydrophobic groups first (PVAm-1.$EA12_{10}$-2.EQ_9) possesses the lowest penetration ability.

(ii) The ONPG hydrolysis assay showed that it takes ~ 60 min for the polymer to begin to permeabilize the inner membrane. The formation of ONP demonstrates that the polymer is capable of damaging the inner membrane. The different microstructures lead to only small differences in permeabilization ability.

The differences in the polymer properties like CAC, penetration ability into membranes, viscosity, and so on, prove the successful introduction of different microstructures into the polymers.

5.5 Literature

[1] E. F. Palermo, K. Kuroda, *Appl Microbiol Biotechnol* **2010,** *87*, 1605–1615.

[2] G. N. Tew, R. W. Scott, M. L. Klein, W. F. Degrado, *Acc. Chem. Res.* **2010** *43*, 30–39.

[3] C. Z. S. Chen, S. L. Cooper, *Adv Mater* **2000**, *12*, 843–846.

[4] M. F. Ilker, K. Nusslein, G. N. Tew, E. B. Coughlin, *J. Am. Chem. Soc.* **2004**, *126*, 15870–15875.

[5] K. Kuroda, G. A. Caputo, W. F. DeGrado, *Chem. Eur. J.* **2009**, *15*, 1123–1133.

[6] B. P. Mowery, S. E. Lee, D. A. Kissounko, R. F. Epand, R. M. Epand, B. Weisblum, S. S. Stahl, S. H. Gellman, *J. Am. Chem. Soc.* **2007**, *129*, 15474.

[7] B. P. Mowery, A. H. Lindner, B. Weisblum, S. S. Stahl, S. H. Gellman, *J. Am. Chem. Soc.* **2009**, *131*, 9735–9745.

[8] E. F. Palermo, K. Kuroda, *Biomacromolecules* **2009**, *10*, 1416–1428.

[9] E. F. Palermo, I. Sovadinova, K. Kuroda, *Biomacromolecules* **2009**, *10*, 3098–3107.

[10] P. H. Sellenet, B. Allison, B. M. Applegate, J. P. Youngblood, *Biomacromolecules* **2007**, *8*, 19–23.

[11] T. R. Stratton, J. L. Rickus, J. P. Youngblood, *Biomacromolecules* **2009**, *10*, 2550–2555.

[12] N. Pasquier, H. Keul, E. Heine, M. Moeller, B. Angelov, S. Linser, R. Willumeit, *Macromol. Biosci.* **2008**, *8*, 903–915.

[13] É. Kiss, E. T. Heine, K. Hill, Y-C. He, N. Keusgen, Cs. B. Pénzes, D. Schnöller, G. Gyulai, A. Mendrek, H. Keul, M. Möller, *Macromolecular Bioscience* **2012**, *12 (9)*, 1181–1189.

[14] Y. He, E. Heine, N. Keusgen, H. Keul*, M. Möller, *Biomacromolecules* **2012**, *13* (*3*), 612–623.

[15] B. Michaels, *MPMN* **2010**, 26 (*7*), Synthetic Polymer Mimics Antimicrobial Properties of Host-Defense Proteins.

[16] D. M. Hoover, K. R. Rajashankar, R. Blumenthal, A. Puri, J. J. Oppenheim, O. Chertov, J. Lubkowski, *J. Biol. Chem.* **2000**, *275* (*42*), 32911–32918.

[17] M. V. Sawai, H. P. Jia, L. Liu, V. Aseyev, J. M. Wiencek, P. B. McCray, Jr., T. Ganz, W. R. Kearney, B. F. Tack, *Biochemistry* **2001**, *40*, 3810–3816.

[18] F. Bauer, K. Schweimer, E. Klüver, J.-R. Conejo-Garcia, W.-G. Forssmann, P. Rösch, K. Adermann, H. Sticht, *Protein Sci.* **2001**, *10*, 2470–2479.

[19] D. Yang, A. Biragyn, L. W. Kwak, J. J. Oppenheim, *Trends Immunol.* **2002**, *23* (*6*), 291–296.

[20] G. L. Butterfoss, B. Yoo, I. Chorny, J. N. Jaworski, K. A. Dill, K. Kirshenbaum, R. Bonneau, R. N. Zuckermann, V. A. Voelz, *PNAS* **2012**, *109* (*36*), 14320-14325.

[21] B.-C. Lee, T. K. Chu, K. A. Dill, R. N. Zuckermann, *J. Am. Chem. Soc*. **2008**, *130*, 8847-8855.

[22] C. M. Goodman, S. Choi, S. Shandler, W. F. DeGrado, *Nat. Chem. Biol*. **2007**, *3*, 252-262.

[23] K. Kirshenbaum, R. N. Zuckermann, K. A. Dill, *Curr. Opin. Struct. Biol*. **1999**, *9*, 530-535.

[24] A. E. Barron, R. N. Zuckermann, *Curr. Opin. Struct. Biol.* **1999**, *9*, 681-687.

[25] D. J. Hill, M. J. Mio, R. B. Prince, T. S. Hughes, J. S. Moore, *Chem. Rev*. **2001**, *101*, 3893-4012.

[26] T. L. Raguse, J. R. Lai, P. R. LePlae, S. H. Gellman, *Org. Lett*. **2001**, *3*, 3963–3966.

[27] B.-C. Lee, R. N. Zuckermann, K. A. Dill, *J. Am. Chem. Soc*. **2005**, *127*, 10999–11009.

[28] J. L. Goodman, E. J. Petersson, D. S. Daniels, J. X. Qiu, A. Schepartz, *J. Am. Chem. Soc*. **2007**, *129*, 14746-14751.

[29] M. Wilhelm, C. L. Zhao, Y. Wang, R. Xu, M. A. Winnik, J. L. Mura, G. Riess, M. D. Croucher, *Macromolecules* **1991**, *24*, 1033-1040.

[30] A. Ramzi, M. Prager, D. Richter, V. Efstratiadis, N. Hadjichristidis, R. N. Young, J. B. Allgaier, *Macromolecules* **1997**, *30*, 7171-7177.

[31] Antimicrobial testing method for coated substrates developed by *DWI an der RWTH Aachen e.V.:* EXPOSE. The testing method was developed on the basis of DIN EN ISO 20743 (a).

[32] DIN EN ISO 14160:2011-10, German Version EN ISO 14160:2011.

[33] Log-Reduction-Fact-Sheet: http://www.garnerdecontaminationsolutions.com/resources/HFI-Log-Reduction-Chart.pdf.

[34] Y. Wang, J. Xu, Y. Zhang, H. Yan, K. Liu, *Macromol. Biosci.* **2011**, *11*, 1499.

[35] Test based on the *Standard Practice for Assessment of Hemolytic Properties of Materials* ASTM F756-08.

[36] Test based on the *Standard Practice for Extraction of Medical Plastics* ASTM F619-03.

[37] The Langmuir Film Experiments were carried out in cooperation with Kiss *et al.* at the Laboratory of Interfaces and Nanostructures, Institute of Chemistry, Eötvös Loránd University, Budapest, Hungary.

[38] N. J. Hardy, T. H. Richardson, F. Grunfeld, *Colloids Surf. A* **2006**, *202*, 284.

[39] L. Silvestro, J. N. Weiser, P. H. Axelsen, *Antimicrobial Agents and Chemotherapy* **2000**, *44* (*3*), 602-607.

[40] K. Kalyanasundaram, *Langmuir* **1988**, *4*, 942.

[41] K. Kalyanasundaram, J. K. Thomas, *J. Am. Chem. Soc.* **1977**, *99*, 2039-2044.

[42] J. Z. Du, D. P. Chen, Y. C. Wang, C. S. Xiao, Y. L. Lu, J. Wang, G. Z. Zhang, *Biomacromolecules* **2006**, *7*, 1898-1904.

[43] J. Aguiar, P. Carpena, J.A. Molina-Bolívar, C. Carnero Ruiz, *Journal of Colloid and Interface Science* **2003**, *258*, 116–122.

[44] W. R. Glomm, S. Volden, O. Halskau, Jr., M.-H. G. Ese, *Anal. Chem.* **2009**, *81*, 3042.

[45] Cs. B. Pénzes, D. Schnöller, K. Horváti, Sz. Bősze, G. Mező, É. Kiss, *Colloids Surf. A* **2012**, *413*, 142– 148.

[46] K. Hill, Cs. B. Pénzes, D. Schnöller, K. Horváti, Sz. Bősze, F. Hudecz, T. Keszthelyi, É. Kiss, *Phys. Chem. Chem. Phys.* **2010**, *12*, 11498–11506.

[47] K. Hill, Cs. B. Pénzes, B. G. Vértessy, Z. Szabadka, V. Grolmusz, É. Kiss, *Progr. Colloid Polymer Sci.* **2008**, *135*, 87-92.

[48] G. M. Pavlov, A. S. Gubarev, I. I. Zaitseva, M. A. Sibileva, *Russ. J. App. Chem*. **2006**, *79* (*9*), 1407 – 1412.

[49] R. M. Fuoss, *J. Polym. Sci*. **1948**, *3*, 603.

[50] R. M. Fuoss, U. P. Strauss, *Ann. N. Y. Acad Sci*, **1949**, *51*, 836.

[51] S. Dragan, M. Mihai, L. Ghimici, *Europ. Polym. J*. **2003**, *39*, 1847-1854.

CHAPTER 6

SUMMARY

This thesis deals with the preparation and characterization of novel multifunctional poly(vinyl amine)s. Poly(vinyl amine) was functionalized with quaternary ammonium groups and alkyl groups with the goal to mimic natural antimicrobial peptides. The resulting materials can be used as antimicrobial agents for surface coatings or textile finishings.

All polymer structures within this thesis are based on poly(vinyl amine) (PVAm), a linear cationic polyelectrolyte bearing one primary amine group in each repeating unit. The post polymerization modification with functional epoxides in a one-step reaction is a versatile approach to introduce hydrophobic and hydrophilic functionalities into the polymer.

At first, Chapter 1 gives an overview on the used polymer poly(vinyl amine), the post polymerization modification technique, as well as the constitution of bacteria and modes of action of antimicrobial agents.

To study the post polymerization modification, PVAm was reacted with different epoxyalkanes (-dodecane (EA12), -decane, and -octane) and the quaternary ammonium group bearing epoxide glycidyltrimethylammonium chloride (EQ) in Chapter 2. These epoxides were successfully introduced into the polymer with different degrees of functionalization. The limit of the degree of functionalization with epoxyalkanes was found to be around 50 %, probably due to sterical hindrance. Due to the repulsion of the cationic groups of EQ, the degree of functionalization with quaternary ammonium groups is limited to around 70 %. For degrees of functionalization below these limits, it is possible to obtain equimolar and reproducible conversions of the educts. The degree of functionalization can easily be adjusted

by the ratio of functional epoxides to amine groups giving access to a high variety of polymers. Fractionation experiments with NMR analysis proved a homogenous modification of the polymers. Finally, the reaction was successfully transferred from the poly(vinyl amine) of high purity to technically available poly(vinyl amine) (Lupamins) rendering a scale up of the reaction for later applications possible.

In Chapter 3, the new functional poly(vinyl amine)s containing hydrophobic moieties were studied with regard to their ability to form micelle-like aggregates in aqueous solution. Critical aggregation concentrations (CAC) were determined as a function of the chain length. In comparison to Chapter 2, the reaction was extended to include even longer alkyl chains (chain lengths from 8 to 18, in steps of two carbon atoms). It turned out that an increasing chain length induces a decrease of the CAC values (from 0.2176 mg/mL to 0.0096 mg/mL). This shows that the longer alkyl chains form hydrophobic domains within the polymer more rapidly and more easily than the shorter alkyl chains. It was found that at concentrations below the CAC, unimolecular micelles are built and an increasing alkyl chain length leads to larger (and thus eventually more stable) unimolecular micelles. These hydrophobic regions do not depend on the concentration, giving evidence to the assumption that hydrophobic domains are built within the polymer during the reaction. For the epoxides EA12, the CAC of the resulting polymers was additionally determined as a function of the concentration (10 % to 40 %, in steps of 10 %) of the introduced alkyl chains. It was found that an increasing concentration of alkyl chains leads to a stepwise decrease of the CAC. The increase of the alkyl chain concentration from 20 % to 30 % seems to be a crucial step to increase the ability of the polymers to form micelles. This is expected to be different for varying chain lengths.

Due to increasing resistances of bacteria towards common antimicrobial agents, there is a significant need for new antimicrobial compounds. To illustrate the effectiveness of the newly developed polymers as antimicrobial agents, their antimicrobial activity against *E. coli* was

examined in solution and coated on substrates in Chapter 4. Different ways of film preparation were developed for coating the polymers on surfaces and the antimicrobial activity of each of these coatings was investigated. It was found that for very thin coatings, the best results in terms of surface homogeneity and thereby reproducibility of the antimicrobial results were obtained by spin coating and annealing in methanol atmosphere.

The influence of the hydrophilic/hydrophobic balance on the antimicrobial activity and on the ability to penetrate into lipid monolayers was studied. This required the preparation and testing of different series of polymers. In a first series of experiments, the antimicrobial effect of the functional poly(vinyl amine)s was investigated as a function of different concentrations of cationic groups (23 %, 30 %, (and 73 %)). In a second series, the antimicrobial effect was studied as a function of varying concentrations of alkyl chains (EA12, 10 %, 21 %, 32 %, and 41 %). Afterwards, the antimicrobial activity of polymers containing both hydrophilic and hydrophobic functionalities was examined. First, the concentration of alkyl chains was varied (EA12, 10 %, 22 %) while keeping the concentration of cationic groups constant (7 %). Second, the concentration of cationic groups was varied (0 %, 5 %, 7 %, 14 %, 17 %, 21 %, and 28 %) at a constant concentration of alkyl chains (EA12, 11 %). The antimicrobial testing of the polymer coatings revealed that the antimicrobial activity increases with an increasing concentration of the cationic epoxide EQ and decreases with an increasing concentration of the epoxyalkane EA12. It was observed that the coating thickness of the polymers has an impact on the antimicrobial activity, which increases with increasing coating thickness. It turned out that the solubility of the polymers in water increased with an increasing concentration of cationic groups and that the polymers without introduced alkyl chains started to leach from the surfaces. Therefore, the antimicrobial activity of the polymers containing more than 13 % cationic groups was additionally tested in aqueous solution and the same trend in antimicrobial activity as for the polymer coatings was observed. It was found that

among the polymers coated on surfaces, PVAm-EQ_{28}-$EA12_{11}$ showed the best antimicrobial activity (99.9 % - 100 % inhibition of bacterial growth) without leaching of material. Among the polymers tested in aqueous solution, PVAm-EQ_{30} showed the best antimicrobial activity (100 % inhibition of growth), which was even higher than the activity of the coated polymers. In the second part of this chapter, the ability of the polymer molecules to penetrate into a neutral lipid layer of dipalmitoylphosphatidylcholine (DPPC) was tested in Langmuir film experiments. The goal of these experiments was to investigate the influence of the hydrophilic/hydrophobic balance on the penetration ability of the novel polymers. The penetration ability was studied as a function of the concentration of cationic groups with and without introduced alkyl chains (EA12, 11 %). The thorough analysis showed that the penetration ability of the polymers reaches a maximum at a concentration of 17 % cationic groups in the polymer. The additional introduction of 11 % alkyl chains led in general to higher membrane affinities. In the next step, the penetration ability was studied as a function of the concentration of alkyl chains (EA12). This analysis revealed that the penetration ability increases with an increasing concentration of alkyl chains. This tendency stands in contrast to the trend in the antimicrobial activity, which decreases with increasing concentration of alkyl chains. This difference can be assigned to distinctions between the membrane polarity of the model system DPPC (neutral) and the natural bacterial membrane (negative), leading to differences in the interaction of the polymer and the membrane. In the neutral DPPC lipid layer system, hydrophobic interactions play the major role, whereas in the case of the negative bacterial membrane, ionic interactions play a crucial role in the polymer membrane interaction. It was found that among the tested polymers, PVAm-EQ_{17}-$EA12_{11}$ shows the highest membrane affinity with an increase in surface pressure ($\Delta\pi$) of 10.6 mN/m.

Since the antimicrobial mode of action of peptides containing cationic and hydrophobic amino acid residues is not completely understood to this date, the structure-properties

relations of the newly developed polymers were investigated. In Chapter 5, different microstructures were successfully introduced into the functional polymers. All polymers had the same chemical composition and molecular weight. The influence of the microstructures on different polymer properties was investigated for polymers in solution and for polymers coated on surfaces. The different microstructures were obtained by sequential and simultaneous addition of the functional epoxides EQ and EA12 to poly(vinyl amine) yielding three different polymers (PVAm-EQ_9-$EA12_{10}$, PVAm-1.EQ_{10}-2.$EA12_{10}$, and PVAm-1.$EA12_{10}$-2.EQ_9). It was found that the different microstructures lead to differences in the critical aggregation concentration, in the penetration ability into membranes (Langmuir monolayers of neutral and of charged lipids, and permeabilization of the outer/inner membrane of *E. coli*), and in the viscosity behavior of the polymers, which were all measured in solution. The antimicrobial effect and the hemolytic activity of the polymers which were measured on surfaces are not influenced by the polymers microstructures. The different polymer properties demonstrate that it was possible to introduce different three-dimensional microstructures into the polymers. These microstructures are, however not preserved when the material is coated onto a two-dimensional surface. Based on the differences in the properties, finally three different microstructures of the polymers are proposed. The first of these microstructures is obtained by first adding the cationic groups to PVAm, leading to an extended non-flexible conformation. The second microstructure can be realized by first adding the hydrophobic groups to PVAm, which leads to micelle-like segregated hydrophobic domains within the polymer. The resulting structure is more flexible than the first proposed structure, but still relatively inflexible. The most flexible microstructure is obtained by simultaneous addition of both functionalities. The flexibility is due to the contrary forces of the functional groups during the reaction (repulsive and attractive). This last microstructure builds micelles easier than the other two polymers.

APPENDIX A

SUPPLEMENTARY INFORMATION ON CHAPTER 4

This appendix gives supplementary information on Chapter 4. The proliferation curves of *E. coli* after exposure on surfaces coated (drop casting, different coating thicknesses) with the novel polymers (Table 1) are shown (Figure 1-Figure 6).

Table 1. Composition and assignment to different series of the prepared polymers.

Series[a)]	Name		degree of functionalization [%][b)]	
			EQ	EA12
1	**A170**	**PVAm-EQ$_7$-EA12$_{22}$**	7	22
1	**A172**	**PVAm-EQ$_7$-EA12$_{10}$**	7	10
2a	**A168**	**PVAm-EQ$_{14}$-EA12$_{11}$**	14	11
2a	**A172**	**PVAm-EQ$_7$-EA12$_{10}$**	7	10
2a	**A171**	**PVAm-EQ$_5$-EA12$_{10}$**	5	10
2a	**A174**	**PVAm-EA12$_{10}$**	-	10
3	**A174**	**PVAm-EA12$_{10}$**	-	10
3	**A175**	**PVAm-EA12$_{21}$**	-	21
3	**A176**	**PVAm-EA12$_{32}$**	-	32
3	**A177**	**PVAm-EA12$_{41}$**	-	41

[a)] Note that one polymer can belong to more than one series. This allows for a better comparison and investigation of structure properties relations. [b)] Degree of functionalization in [%] calculated from ^{1}H-NMR spectroscopy.

Substrates Coated (Drop Casting) with 1 wt% Polymer Solutions

Series 1: Influence of the concentration of EA12 at a constant concentration of EQ

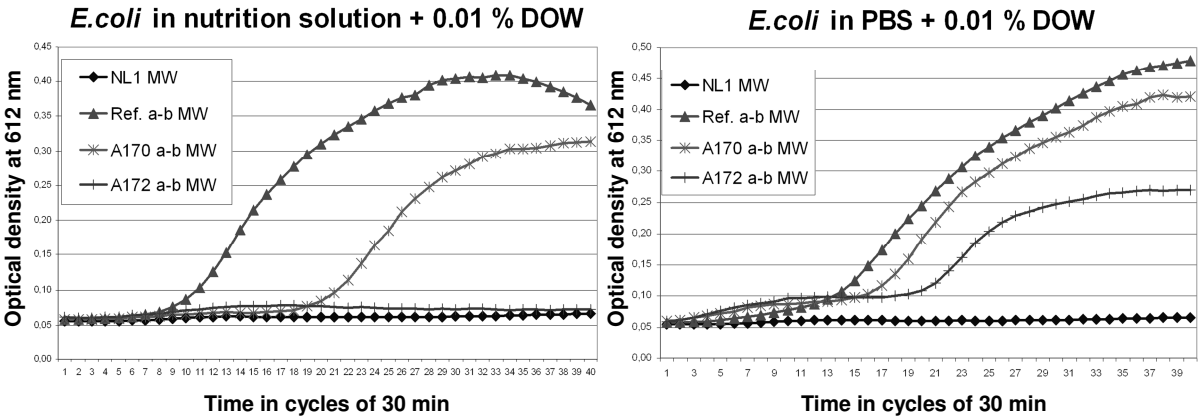

Figure 1. Proliferation curves of *E. coli* after exposure on differently coated glass surfaces (Series 1, 460 µg/cm²). NL1 = Sterility control; Ref. = growth control. All measuring points are the mean values of two measurements. Left: growth conditions, right: non-growth conditions.

Series 2a: Influence of the concentration of EQ at a constant concentration of EA12

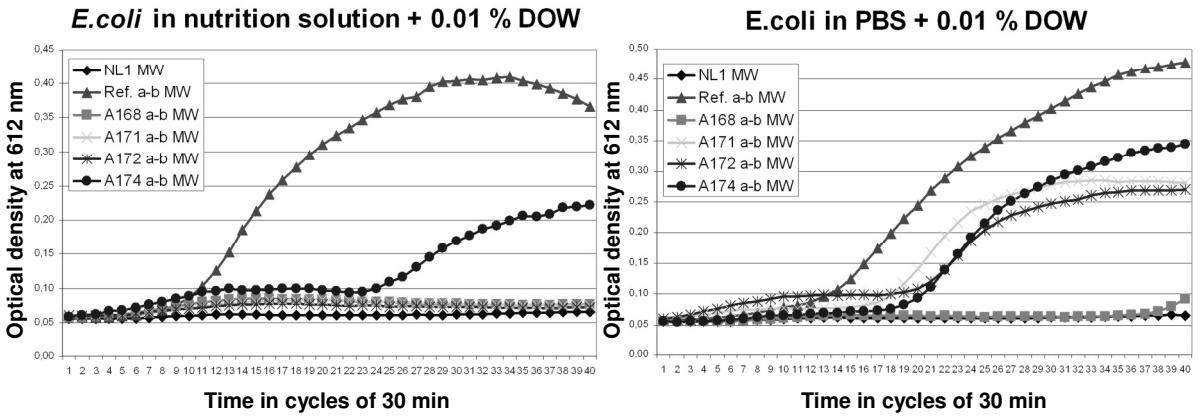

Figure 2. Proliferation curves of *E. coli* after 2.5 h exposure on differently coated glass surfaces (Series 2a, 460 µg/cm²). NL1 = Sterility control; Ref. = growth control. All measuring points are the mean values of two measurements. Left: growth conditions, right: non-growth conditions.

Series 3: Influence of different concentrations of EA12

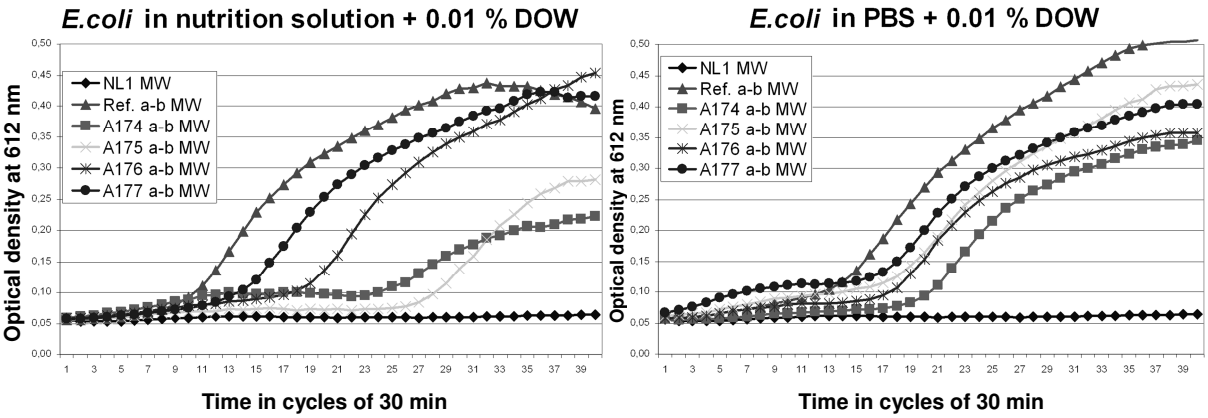

Figure 3. Proliferation curves of *E. coli* after 2.5 h exposure on differently coated glass surfaces (Series 3, 460 µg/cm²). NL1 = Sterility control; Ref. = growth control. All measuring points are the mean values of two measurements. Left: growth conditions, right: non-growth conditions.

Substrates Coated (Drop Casting) with 0.1 wt% Polymer Solutions

Series 3: Influence of different concentrations of EA12

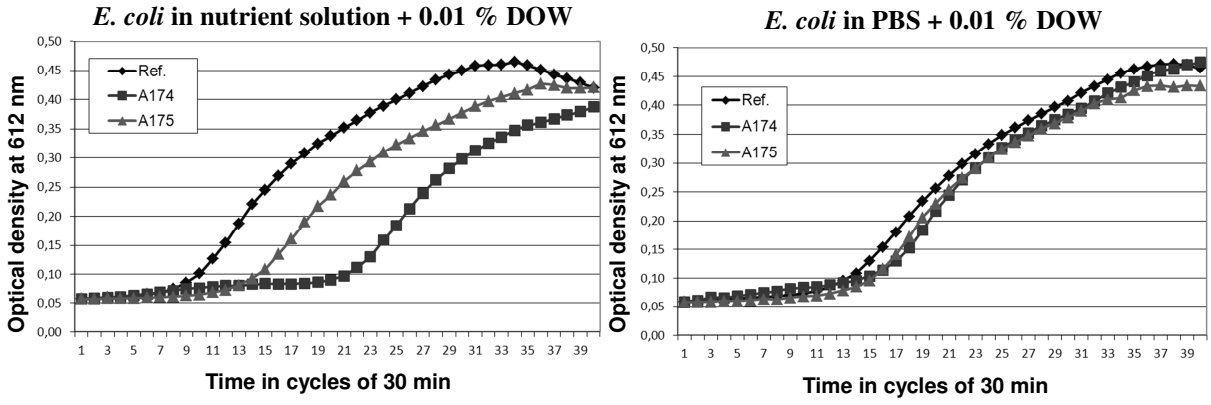

Figure 4. Proliferation curves of *E. coli* after exposure on differently coated glass surfaces (Series 3, 46 µg/cm^2). NL1 = Sterility control; Ref. = growth control. All measuring points are the mean values of two measurements. Left: growth conditions, right: non-growth conditions.

Substrates Coated (Drop Casting) with 0.05 wt% Polymer Solutions

Series 2a: Influence of the concentration of EQ at a constant concentration of EA12.

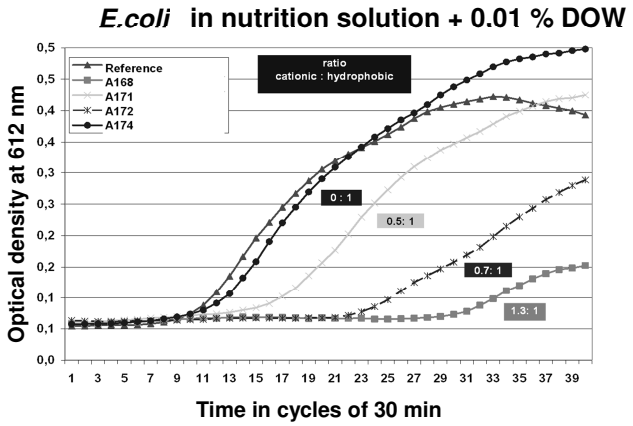

Figure 5. Proliferation curves of *E. coli* after exposure on differently coated glass surfaces (Series 2a, 23 µg/cm^2). Growth conditions; NL1 = Sterility control; Ref. = growth control. All measuring points are the mean values of two measurements.

Series 1: Influence of the concentration of EA12 at a constant concentration of EQ

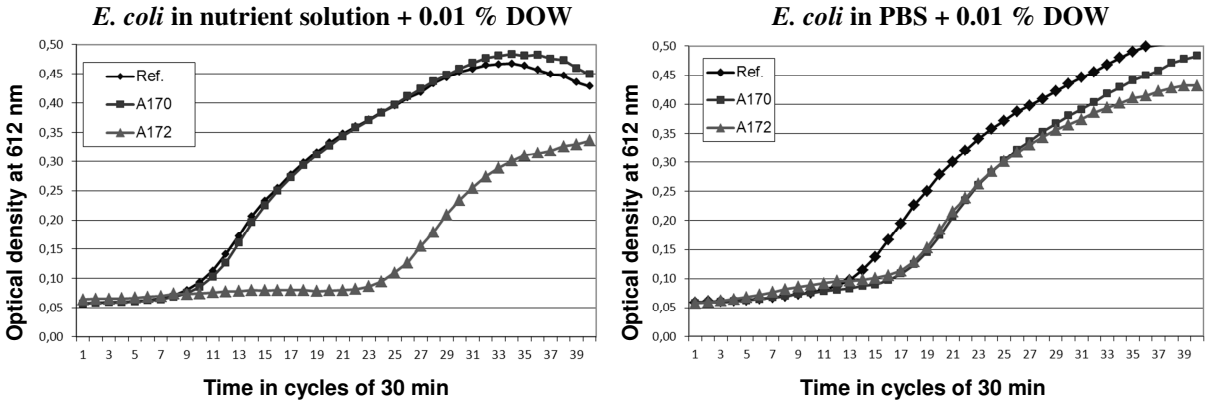

Figure 6. Proliferation curves of *E. coli* after exposure on differently coated glass surfaces (Series 1, 23 µg/cm^2). NL1 = Sterility control; Ref. = growth control. All measuring points are the mean values of two measurements. Left: growth conditions, right: non-growth conditions.

LIST OF PUBLICATIONS

A. Plum, H. Keul, E. Heine, M. Möller, "Multifunctional Polyvinylamine: Preparation and Antimicrobial Properties" (poster), *i-PolyMat*, Rolduc, Netherlands, **2010**.

A. Plum, E. Heine, H. Keul, M. Möller, "Amphiphilic Polymers for Antimicrobial Coatings" (poster), *8th Hellenic Polymer Society Symposium (H-POL8)*, Hersonissos, Greece, **2010**.

A. Plum, E. Heine, H. Keul, M. Möller, "Antimicrobial Polyvinylamine" (poster and oral presentation), *4. Aachen-Dresden International Textile Conference*, Dresden, Germany, **2010**.

A. Plum, E. Heine, H. Keul, M. Möller, "Antimicrobial Polyvinylamine", *Proceedings of the 4th Aachen-Dresden International Textile Conference*, November 25-26, **2010**, Dresden, ed. A. Doerfel, ITB/TU Dresden, Germany (ISSN 1867-6405), Poster P58.

A. Plum, E. Heine, H. Keul, M. Möller, „Preparation of Protein-like Amphipathic Polymers with Antimicrobial Activity" (poster), *European Polymer Congress*, Granada, Spain, **2011**.

CURRICULUM VITAE

Name	Angela Schmalen, geb. Plum
Date of birth	Mai 03, 1982
Place of birth	Aachen, Germany
Citizenship	German

08/1992 – 06/2001	Einhard-Gymnasium, Aachen, Germany
10/2001 – 12/2007	Studies in Chemistry (Diploma), RWTH Aachen University, Germany
10/2003	Intermediate Diploma
08/2005 - 10/2005	Internship under the supervision of Prof. Dr. Mark Lautens: *"MAD/n-Bu_4NI – Mediated Ring Expansion of Methylene-cyclopropyl Esters"*, University of Toronto, Canada
07/2007 – 12/2007	Diploma thesis under the supervision of Prof. Dr. Martin Möller: *"Amphiphilic Copolymers via Polymer-Analogous Reaction of Poly(vinyl amine) with Functional Carbonate Couplers"*, ITMC, RWTH Aachen University, Germany
02/2008 – 08/2012	PhD work under the supervision of Prof. Dr. Martin Möller: *"Post Polymerization Modification of Poly(vinyl amine)s with Functional Epoxides: Multifunctional, Antimicrobial, Protein-like Polymers"*, ITMC and DWI - Leibniz-Institut für Interaktive Materialien, RWTH Aachen University, Germany
04/2008 – 09/2013	Postgraduate studies in Business Administration (Diploma), RWTH Aachen University, Germany
05/2013 – 09/2013	Diploma thesis under the supervision of Prof. Dr. Frank T. Piller: *"The Not-Invented-Here Syndrome in Research and Development: Examination of the Construct Validity of a Measuring Scale"*, TIM, RWTH Aachen University, Germany
Since 06/2014	Development Engineer at Neenah Gessner GmbH, Bruckmühl, Germany